

UNIVERSITY OF GUANAJUATO

CAMPUS GUANAJUATO

DIVISION OF NATURAL AND EXACT SCIENCES

“REFINERY FOR THE PRODUCTION OF SOLAR GRADE SILICON AND
DIFFERENT PRODUCTS OF HIGH VALUE ADDED”

THESIS (PRE-DOCTORAL VERSION)

TO OBTAIN THE TITLE OF:

Doctor of Science degrees in Chemical Engineering

Presents:

M.S. César Ramírez Márquez

Guanajuato, Gto., February 2020

DECLARATION

I hereby take responsibility for the authenticity and originality of this work entitled:

“REFINERY FOR THE PRODUCTION OF SOLAR GRADE SILICON AND
DIFFERENT PRODUCTS OF HIGH VALUE ADDED”

PhD Juan Gabriel Segovia Hernández
Thesis Director

PhD Mariano Martín
Thesis Co-Director

PhD Erick Yair Miranda Galindo
Thesis Co-Director

Guanajuato, Gto., February 2020

Members of the Synodal Committee of the Professional Examination that to obtain the title of Doctor of Science degrees in Chemical Engineering presents the M. S. César Ramírez Márquez, with the work entitled:

“REFINERY FOR THE PRODUCTION OF SOLAR GRADE SILICON AND
DIFFERENT PRODUCTS OF HIGH VALUE ADDED”

PhD Salvador Hernández Castro
President

PhD Jorge A. Cervantes Jáuregui
Secretary

PhD Fernando Israel Gómez Castro
Vocal

PhD Zeferino Gamiño Arroyo
Vocal

PhD Nelly Ramírez Corona
Vocal

Guanajuato, Gto., February 2020

“REFINERY FOR THE PRODUCTION OF SOLAR GRADE SILICON AND DIFFERENT PRODUCTS OF HIGH VALUE ADDED”

Advised by: PhD Juan Gabriel Segovia Hernández
 PhD Mariano Martín
 PhD Erick Yair Miranda Galindo

Presents: César Ramírez Márquez

Abstract

Like other renewable energies, photovoltaic solar energy constitutes an inexhaustible resource in comparison to fossil resource. This contributes to a national and social energetic auto-supply with low environmental impact comparatively lower to traditional energy sources. In light of this, focus on the obtainment of products for the creation of solar panels becomes important. The obtention of solar-grade silicon is undoubtedly a process that calls for many inconveniences; mainly, the cost for its obtention on account of the need of high purity, the environmental impact this process represents, the setting up of the process, the health risk factors that existing components and conditions bring about and, worker's occupational health. In the present work, there is a description (design) and assessment of various indexes of the novel obtainment process of solar-grade silicon. One that obtains different high added value products, is cost-effective, has a low environmental impact and is safe at once. For that matter, throughout the text there is a compendium of a series of works done in a sequenced fashion that give an account of its design, the assessment of different indexes (financial, environmental impact, security and occupational health), and the improvement of a high performance process (under the proposed ideal operative guidelines). In those works, there is a comparison between the novel process with existing ones to produce solar-grade silicon (meaning the Siemens process and the Union Carbide process) to have a real reference of the range of the proposed process. The first part, results showed similar cost-effective between the Hybrid Process (15.21 %) and the Union Carbide process (15.38%). Overall, the high demand for the product of interest -under the precondition of a safe process-, the Hybrid Process can be deemed as an option for an industrial execution. When the novel process is improved to obtain a higher efficiency under operative guidelines, an OPEX of 6.46 M\$/y as a way of increasing the profit from that process. After the operative costs, the selling of solar-grade silicon and its by-products, the income is of 10 M\$/y (with a competitive price for polycrystalline silicone of 8.93 \$/kg., below the 11 \$/kg. estimated commercial price). In conclusion, the proposed process is capable of meeting future demand in a cost-effective, environmentally friendly and safe way. Likewise, the results show that with the refinery that produces tetraethoxysilane and chlorosilanes in addition to the production of polysilicon, the proposed design reduces the cost for polycrystalline silicon to 6.86 \$/kg, compared to a cost of polycrystalline silicon if the plant does not generate high value-added by-products, both below the commercial price.

“REFINERY FOR THE PRODUCTION OF SOLAR GRADE SILICON AND DIFFERENT PRODUCTS OF HIGH VALUE ADDED”

Direction of: PhD Juan Gabriel Segovia Hernández
 PhD Mariano Martín
 PhD Erick Yair Miranda Galindo

Presents: César Ramírez Márquez

Resumen

La energía solar fotovoltaica al igual que otras energías renovables, constituye frente a los combustibles fósiles, una fuente inagotable de energía, contribuyendo al autoabastecimiento energético nacional y por lo tanto social, con un impacto ambiental comparativamente mucho menor que las fuentes convencionales de energía. Por lo anterior, es importante centrar la atención en la obtención de productos para elaboración de celdas solares. La obtención del silicio grado solar es sin duda, un proceso que presenta muchos inconvenientes, principalmente, en el costo para su obtención debido a que se requieren purezas bastante elevadas, en el impacto ambiental que representa la operación y construcción del proceso, la seguridad inherente innata a la materia y condiciones de operación en dicho proceso, y la salud ocupacional de los trabajadores. Por lo anterior en el presente trabajo se muestra el diseño y evaluación bajo diferentes indicadores, de un proceso novedoso de obtención de silicio grado solar, capaz de obtener al mismo tiempo diferentes productos de alto valor agregado; que pretende ser más rentable, con menor impacto ambiental, y seguro. Por ende, a lo largo del documento se exhiben un compendio de trabajos elaborados de manera secuencial que justifican el diseño, la evaluación de diferentes indicadores (económico, impacto ambiental, seguridad inherente, salud ocupacional), y la optimización del proceso para obtener el mayor rendimiento bajo las condiciones de operación ideales del proceso propuesto. En dichos trabajos se compara el proceso novedoso con los procesos existentes para la obtención de silicio grado solar (Siemens y Union Carbide), para tener una referencia real del potencial del proceso propuesto. La primera parte de los resultados mostraron valores de rentabilidad similares entre el Proceso Híbrido (15.21%) y el Proceso Unión Carbide (15.38%). En general, debido a la alta demanda del producto de interés y bajo la premisa de un proceso seguro, el Proceso Híbrido se puede elegir como una opción para su implementación industrial. Al optimizar el proceso novedoso para obtener el mayor rendimiento bajo las condiciones de operación se muestra que para maximizar la ganancia del proceso novedoso, se requiere un costo operativo de 6.46 M\$/a. Las ganancias después de los gastos operativos, y considerando la venta de silicio grado solar y subproductos del proceso, son 10 M \$/a, presentando un precio competitivo de silicio policristalino de 8.93 \$/kg, por debajo del precio comercial estimado en 11 \$/kg. Se concluye que el proceso propuesto es capaz de satisfacer la demanda futura, de una manera rentable, amigable con el medio ambiente y segura. Asimismo, los resultados muestran que con la refinería que produce tetraetoxisilanos y clorosilanos, además de la producción de polisilicio, el diseño propuesto reduce el costo del silicio policristalino a 6.86 \$/kg, en comparación con el costo del silicio policristalino si la planta no genera subproductos de alto valor agregado, ambos por debajo del precio comercial.

DEDICATION

I dedicate this work to my dear mother, who with her demonstration of an exemplary mother taught me not to faint or surrender to anything and always persevere.

ACKNOWLEDGMENT

In life you realize what is really important and the value of the people around you. Your help has been fundamental, you have been with me even in the most turbulent moments. This project was not easy, but you were motivating me and helping me as far as your reach allowed. I thank you very much, Chaparra.

I also want to thank those people who in one way or another were pending throughout this process, providing all their unconditional support.

To my friends Eduardo, Gabriel, Edgar, Antonio, Lydia, Manuel, Julián, Ana Gaby, Heriberto, Evaristo, Juan José, because they always kept an eye on my progress day by day and gave me their support whenever I need it without asking me anything In return. You accompanied me throughout this process were pending that all things went well and that I did not make a bad decision, I thank you for the trust you placed in me to always be in good and bad together. Thank you for trusting and believing in me and having made this stage a journey of experience that I will never forget.

In a special and sincere way, I thank Dr. Juan Gabriel Segovia Hernández and Mariano Martín for their unconditional presence, their appreciated and relevant contributions, criticisms, comments and suggestions during the development of this research.

Content

1 Introduction	1
1.1 Solar industry around the world.....	1
1.2 Solar technology on a global scale.....	1
1.2.1 Photovoltaic systems.....	1
1.2.1 Technology costs.....	3
1.3 Manufacturing profile of photovoltaic technologies in the main global economies.....	4
1.3.1 Manufacturing of photovoltaic modules and cells.....	4
1.4 Photovoltaic solar energy.....	5
1.5 Solar silicon.....	5
1.5.1 Solar-grade silicon production.....	6
1.5.2 Solar-grade silicon status.....	7
1.6 Process Intensification.....	8
1.7 Perspective on the work done.....	8
1.8 Justification.....	10
1.9 Hypothesis.....	10
1.10 General Objective.....	10
1.11 Specific Objectives.....	10
1.12 References.....	10
2 Process design and intensification for the production of solar grade silicon ...	12
Abstract	12
2.1 Introduction.....	12
2.2 Methodology.....	14
2.2.1 Siemens Process.....	14
2.2.2 Intensified FBR Union Carbide Process.....	16
2.2.3 Hybrid Process.....	18
2.3 Optimization Problem.....	19
2.3.1 Optimization of the Siemens Process.....	21
2.3.2 Optimization of the Intensified FBR Union Carbide Process.....	21
2.3.3 Optimization of Hybrid Process.....	22
2.4 Results.....	23
2.5 Conclusions.....	29

2.6 Appendix A2	29
2.7 Acknowledgements.....	30
2.8 References	30
3 Safety, Economic and Environmental Optimization Applied to Three Processes for the production of solar grade silicon	33
Abstract	33
3.1 Introduction.....	33
3.2 Methodology	35
3.2.1 Process for obtaining solar grade silicon	35
3.2.1.1 Siemens Process	35
3.2.1.2 Intensified FBR Union Carbide Process	35
3.2.1.3 Hybrid Process.....	36
3.3 Optimization.....	36
3.3.1 Return on Investment (ROI)	36
3.3.3 Safety index	39
3.4 Multi-objective function.....	39
3.5 Methodology for Global Optimization	42
3.6 Results	42
3.7 Conclusions	51
3.8 Notation.....	51
3.9 Acknowledgements	52
3.10 References.....	52
4 Inherent Occupational Health Hazards In The Production Of Solar Grade Silicon	54
Abstract	54
4.1 Introduction	54
4.2 Methodology	56
4.3 Case Studies	56
4.3.1 Siemens Process	57
4.3.2 Intensified FBR Union Carbide Process	57
4.3.3 Hybrid Process	57
4.4 Assessment Method for Occupational Health Aspect.....	59
4.5 Results.....	59
4.6 Conclusions	64
4.7 Notation.....	64

4.8	Acknowledgements	64
4.9	References.....	64
	Appendix A4	66
5	Surrogate based optimization of a novel process of polycrystalline silicon production.....	76
	Abstract	76
5.1	Introduction	76
5.2	Methodology for process design.....	79
5.3	Modelling approach.....	82
5.3.1	Thermal carboreduction.....	82
5.3.2	Hydrochlorination Reactor.....	83
5.3.3	Separation and purification	85
5.3.4	Siemens Reactor	86
5.3.5	Auxiliary equipment.....	87
5.4	Solution Procedure	87
5.5	Results.....	88
5.5.1	Operating conditions.....	88
5.5.2	Economic evaluation.....	90
5.5.3	Scale-up study	93
5.6	Conclusions	95
5.7	Appendix A	95
5.7.1	Energy balances.....	95
5.8	Nomenclature	96
5.9	Acknowledgements	97
5.10	References.....	97
6	Optimal Portfolio of Products in a Polycrystalline Silicon Refinery.....	101
	Abstract	101
6.1	Introduction	101
6.2	Methodology	103
6.2.1	Process design	103
6.2.2	Modelling approach.....	106
6.2.2.1	Thermal carboreduction	106
6.2.2.2	Hydrochlorination Reactor.....	107
6.2.2.3	Separation and purification.....	107
6.2.2.4	RD technology to produce TEOS	108

6.2.2.5 RD technology to produce silane, monochlorosilane or dichlorosilane	110
6.2.2.6 Siemens Reactor	112
6.2.2.7 Auxiliary equipment.....	112
6.2.3 Solution procedure.....	113
6.3 Results.....	113
6.3.1 Main operating parameters	116
6.3.2 Polycrystalline Silicon Refinery and Other Value-Added Products Cost	118
6.3.3 Estimated Price of Polycrystalline Silicon	122
6.4 Conclusions	123
6.5 Nomenclature	123
6.6 Acknowledgements.....	124
6.7 References	124
7 Conclusions	126
8 Curriculum Vitae	129

TABLE INDEX

Table 2.1. Feeding of processes.....	14
Table 2.2. Kinetic parameters for the proportional decomposition of trichlorosilane in liquid phase.....	18
Table 2.3. Decision Variables Used in the Global Optimization of Process Routes for SiSG Production.....	22
Table 2.4. Results of the Optimization of TAC for the Siemens Process.....	25
Table 2.5. Results of the Optimization of TAC for the Intensified FBR Union Carbide Process.....	25
Table 2.6. Results of the Optimization of TAC for the Hybrid Process.....	27
Table 2.7. Comparative results for all process.....	28
Table 2.8. Prices of annualized products [Silicon solar grade (Sun&Wind Energy, 2017), hydrogen (Product Listing Policy a, 2017), dichlorosilane (Yaws et al., 1979), silicon tetrachloride (Product Listing Policy b, 2017), hydrogen chloride (Product Listing Policy c, 2017)].....	29
Table 3.1. Decision Variables Used in the Global Optimization of Process Routes for SiSG Production.....	41
Table 3.2. Results of the Optimization of ROI, Eco 99 and IR for the Siemens Process.....	48
Table 3.3. Results of the Optimization of ROI, Eco 99 and IR for the Intensified FBR Union Carbide Process.....	49
Table 3.4. Results of the Optimization of ROI, Eco 99 and IR for the Hybrid Process.....	51
Table 3.5. Results of ROI, Eco 99 and IR for all the processes.....	52
Table 4.1. Summary of Results.....	62
Table 4.2. Scaled Healthiness Index.....	63
Table 4.3. Results of the PRHI (Damage/kg Si), PRHI (Damage), ROI [%], Eco-99 [MP/y], IR [1/y] and Production of SiSG [kg/h].....	64
Table 4.4. Comparison of health, profitability, environmental impact, inherent safety and production of SiSG.....	64
Table A4.1. Conditions by process sections.....	68
Table A4.2. Summary of penalties for activities or operations (AP).....	70
Table A4.3. Summary of penalties for process conditions and material properties (CP).....	70
Table A4.4. Ranking matrix for occupational disease.....	72
Table A4.5. NFPA health rating criteria.....	72
Table A4.6. Fugitive Emissions for the entire process.....	74

<i>Table A4.7. Worker exposure concentration.....</i>	<i>74</i>
<i>Table A4.8. Estimated occupational exposure limit for the Intensified FRB Union Carbide Process.....</i>	<i>75</i>
<i>Table 5.1. Operating conditions of each stage of the process.....</i>	<i>89</i>
<i>Table 5.2. Energy requirements and temperatures of each objective function.....</i>	<i>90</i>
<i>Table 5.3. Profit [M\$/y], Operating costs [M\$/y], and kg of polycrystalline silicon/h of each objective function.....</i>	<i>92</i>
<i>Table 5.4. Costs per equipment.....</i>	<i>92</i>
<i>Table 5.5. Comparison of operating conditions.....</i>	<i>93</i>
<i>Table 5.6. Results of scaling study for the Hybrid Process.....</i>	<i>94</i>
<i>Table 6.1. Profit [M\$/y], Operating costs [M\$/y], kg of polycrystalline silicon/h, kg of TEOS, and kg of silane of the objective function.....</i>	<i>116</i>
<i>Table 6.2. Price of each Product for all scenarios.....</i>	<i>116</i>
<i>Table 6.3. Operating conditions of each stage of the process.....</i>	<i>120</i>
<i>Table 6.4. Energy requirements and temperatures of each scenario.....</i>	<i>120</i>
<i>Table 6.5. Costs per equipment.....</i>	<i>121</i>

LIST OF FIGURES

Figure 1.1. Evolution in the efficiency of solar cells.....	2
Figure 1.2. Decrease in photovoltaic generation costs.	3
Figure 1.3. Trade balance of photovoltaic modules, cells and polysilicon.	4
Figure 1.4. Evolution of the capacity and generation of photovoltaic electricity (SENER, 2016a).....	5
Figure 1.5 Process Intensification and their components (Ramshaw, 1995).....	9
Figure 2.1 Siemens process.....	16
Figure 2.2. Flowsheet Siemens Process.....	16
Figure 2.3. FBR Union Carbide with RD column process.	17
Figure 2.4. Flowsheet of Intensified FBR Union Carbide Process.....	18
Figure 2.5. Hybrid process FBR Union Carbide with Siemens.....	18
Figure 2.6. Flowsheet hybrid process FBR Union Carbide with Siemens.....	19
Figure 2.7. Hybrid platform to implement optimization.....	20
Figure 2.8. Optimization results of process sequences a) Siemens, b) Intensified FBR Union Carbide and c) Hybrid process.....	28
Figure 2.9. Results of capital cost, TAC, energy required, solar grade silicon, profit per sale, and Eco-Indicator of all configurations.....	29
Figure 3.1. Flowcharts of Siemens Process (— • —), Intensified FRB Union Carbide (*****) and Hybrid (———).....	38
Figure 3.2. Siemens Process, Intensified FRB Union Carbide and Hybrid.....	39
Figure 3.3. Possible accidents and frequencies that can happen in a process.....	40
Figure 3.4. Pareto front between ROI and EI99 for the three processes.....	44
Figure 3.5. Pareto front between IR and EI99 for the three processes.....	45
Figure 3.6. Pareto front between IR and ROI for the three processes.....	45
Figure 3.7. Pareto front between ROI and EI99 for: a) Siemens Process, b) Intensified FRB Union Carbide Process, and c) Hybrid Process.....	45
Figure 3.8. Pareto front between IR and EI99 for: a) Siemens Process, b) Intensified FRB Union Carbide Process, and c) Hybrid Process.....	46
Figure 3.9. Pareto front between IR and ROI for: a) Siemens Process, b) Intensified FRB Union Carbide Process, and c) Hybrid Process.....	48
Figure 4.1. Flowsheet Siemens Process.....	58
Figure 4.2. Flowsheet of Intensified FBR Union Carbide Process.....	59

<i>Figure 4.3. Flowsheet Hybrid Process FBR Union Carbide with Siemens.....</i>	<i>59</i>
<i>Figure 4.4. Diagram for calculating the PRHI (Hassim & Edwards, 2006).....</i>	<i>61</i>
<i>Figure 4.5. Results of the PRHI (Damage/kg SiSG).....</i>	<i>62</i>
<i>Figure 4.6. Results of the PRHI (Damage).....</i>	<i>63</i>
<i>Figure A4.1. Flowsheet of Intensified FBR Union Carbide Process for the evaluation of the PRHI.....</i>	<i>67</i>
<i>Figure 5.1. Flow chart of silicon manufacturing.....</i>	<i>78</i>
<i>Figure 5.2. Flowsheet of the Hybrid Process proposed.....</i>	<i>83</i>
<i>Figure 5.3. kg of polycrystalline silicon/h, operating cost, and profit of each objective function.....</i>	<i>92</i>
<i>Figure 5.4. Utility and raw material costs of each objective function.....</i>	<i>93</i>
<i>Figure 5.5. Effects of scaling study for the Hybrid Process.....</i>	<i>95</i>
<i>Figure 6.1. Flowsheet of Polycrystalline Silicon Refinery and Other Value-Added Products.....</i>	<i>105</i>
<i>Figure 6.2. Production of polycrystalline silicon and each one of the products of high added value in each proposed scenario.....</i>	<i>117</i>
<i>Figure 6.3. Costs of raw material, electricity, steam and refrigerant for each scenario.....</i>	<i>122</i>
<i>Figure 6.4. Estimated price of polycrystalline silicon in each scenario, without the generation of products with high added value (RS), and the market price according to PVInsights, (2019).....</i>	<i>123</i>

NOMENCLATURE

y_i	Molar fraction of
λ_i	Specific latent heat of component i
\hat{f}_i	Standard Gibbs free energy
$\hat{\phi}_i$	Fugacity coefficient
ΔE_C	Variation of kinetic energy
ΔE_P	Variation of potential energy
R_i	Mass rate of change in species i by chemical reaction
A_K	Total atomic mass of the k_{th} element in the system
$C_{p,i}$	Heat capacity
C_{pi}	Specific heat of the component i
G^T	Total Gibbs free energy
G_i^o	Standard Gibbs free energy
H_{fi}^{Tref}	Standard enthalpy for each element i
H_i^o	Standard enthalpy
I_F	Fixed annualized investment
$P_{inCompressor}$	Entry pressure [kPa]
p^o	Standard-state pressure (100 kPa);
$P_{outCompressor}$	Out pressure [kPa]
Q_{ConCol}	Condenser heat duty
Q_{RebCol}	Reboiler heat duty
S_i^o	Standard entropy
$S_{polycrystalline\ silicon}$	Profit from the sale of the polycrystalline silicon
T_{ConCol}	Top temperature
T_{RebCol}	Bottom temperature
$T_{inCompressor}$	Entry temperature [K];
$T_{outCompressor}$	Out temperature [K];
V_{SiMG}	Molar volume of silicon;
$W_{(Compressor)}$	Electrical energy [kW]
a_{ik}	Number of k_{th} atoms in each molecule of species i
$f_{c_{polycrystalline\ silicon}}$	Mass flow of polycrystalline silicon
f_i^o	Fugacity of species i
k_{ad}	Rate of $SiHCl_3$ chemisorption on the surface
k_r	Rate of decomposition.
n_c	Efficiency of the compressor
n_i	Number of moles
n_i	Amount of the component i
v_i	Stoichiometry coefficients of involved compounds
μ_i	Chemical potential
μ_i	Viscosity of the species i
ΔH	Enthalpy variation

AP	Penalties for activities
BLEVE	Boiling liquid expanding vapor explosion
C	Carbon
CO	Carbon monoxide
CP	Penalties for conditions
DDE	Dynamic Data Exchange
DE	Differential evolution
DETL	Differential Evolution with Tabu List
EI99	Eco-indicator 99
FBR	Fluidized Bed Reactor
FR	Feed Ratio
GAMS	General Algebraic Modeling System
H ₂	Hydrogen
HCl _(g)	Hydrogen chloride
HHI	Health Hazard Index
ICPHI	Inherent Chemical and Process Hazard Index
IR	Individual Risk
LC50	Lethal Concentration
LCA	Life-cycle assessment
MHI	Material Harm Index
N	Number of species in the reaction system
NLP	Nonlinear program
OEL _{min}	Minimum Occupational Exposure Limit
P	Pressure
PV	Photovoltaic
QRA	Quantitative Risk Analysis
R	Molar gas constant
Rel	H ₂ /SiCl ₄ molar feed ratio
ROI	Return on investment
RR	Reflux Ratio
Si	Silicon
Si ₂	Disilicon
Si ₂ C	Disilicon Carbide
SiC	Silicon Carbide
SiC ₂	Silicon dicarbide
SiCl ₄	Silicon tetrachloride
SiH ₂ Cl ₂	Dichlorosilane
SiH ₄	Silane
SiHCl ₃	Trichlorosilane
Si _{MG}	Metallurgical grade silicon
SiO	Silicon oxide
SiO ₂	Silicon dioxide
Si _{SG}	Solar grade silicon
T	Temperature
TAC	Total Annual Cost
TL	Tabu List
UVECE	Unconfined Vapor Cloud Explosion

WEC_{\max}	Maximum Worker Exposure Concentration
X	Amount of the specie [mass fraction]
x	Mole fraction
z	Polytropic coefficient
Q	Heat exchanged by the system
W	Work exchanged by the system.
a	Factor that considers annual expenses such as maintenance
b	The unit cost of each raw material RM
c	Cost of each utility E
$d MO$	Cost of manpower
k	Overall constant reaction
p	Price of each by-product SP
w	Total number of elements in the system

1 Introduction

1 Introduction

1.1 Solar industry around the world

Over the last few years, the use of sustainable energy has significantly increased all around the world. Some of the factors that have promoted this expansion are traditional fuel's price volatility, the fight against climate change and the search for new job opportunities. It is estimated that in 2015 the installed capacity for energy production, from sustainable energies, reached around 1,849 GW globally. However, investments in this field show a growing trend. About 285 million of dollars were invested to keep the growth of the electric generative capacity from sustainable resources (REN21, 2016).

Under these circumstances, solar energy has played an even greater role. By installed capacity, it is the third most important one within sustainable energy. In terms of the generation of electrical output, with 227 GW correspond to hydroelectric energy -which has been in development for several decades- and wind energy -which has a capacity of 435 GW-. During 2017, investments in solar energy for the production of electricity and heat surpassed investments in wind energy, they are only beneath hydroelectric energy - which has high capital expenses- (Rodríguez-Suárez et al., 2000).

In this chapter, an overview of the photovoltaic solar industry is presented identifying trends at an international level. There is also an analysis of several traits of available technologies to identify their main trends for display in the global market. Finally, there is a section on the evolution of costs and manufacturing capacities of solar technologies within the most important economies in the world.

1.2 Solar technology on a global scale

The Earth gather a great deal of energy from the Sun. Just with one-day of energy received from the Sun, the current energy demand could be covered for more than 20 years (GENI, 2011). Even when light is the main asset we have from the Sun, radiant energy directed to the planet can be transformed into heat or electricity. Transformed solar energy into heat can be used for heating and evaporating water, the drying of organic matter and space conditioning. Heat can also be turned into electricity and mechanical work, it can ease several physical and chemical conversions and, it has the potential to be used in industrial processes. However, the production of electricity, drawn from solar energy, widens the reach for consumption resulting from its employment for any sort of use.

1.2.1 Photovoltaic systems

For the last few decades, photovoltaic technologies have experienced considerable breakthroughs in both scientific and technological terms. The efficiency of several types of cells has increased 5 times (GENI, 2011); according to an innovative perspective, there are three generations of developed cells. The costs and energy quantity needed for manufacturing photovoltaic cells has decreased in such a way that investment can be recouped during the first two years of use; while reliability against defaults and adverse weather conditions enable warranties that surpass twenty years of lifespan (See Figure 1.1).

Thus, the electricity costs from these systems have decreased at a rapid pace. Decades ago, photovoltaic technology was only viable to charge telecommunication satellites. Nowadays, electric markets acquire large energy blocks through auctions where the

offered prices by sustainable sources -such as wind power and solar energy- have lower prices than those from traditional sources. Modern-day rate up to 3 kW for domestic use when connected to the network and up to 450 kW for utility plants when connected to electric transmission networks (Chen et al., 2012).

Photovoltaic solar energy is a technologic field that has favored a market but one that remains within a fast development to improve its efficiency and decrease its costs. Nowadays, crystalline silicon cells prevail in the photovoltaic market -with an 85% incidence within all of the conforming technologies- (Glunz et al., 2012). It is estimated that this material remains as a leader in the development of photovoltaic technologies for at least the next decade (MIT Energy Initiative, 2016). Multi-crystalline silicon panels show efficiencies between a 14 and 24.7 percentage; while monocrystalline silicon panels rate from 12% to 20.3% under normal conditions (the efficiency of silicon crystalline panels can decrease with temperature raising) (Rodríguez-Suárez et al., 2000).

Given their cost, modern-day silicon technologies could be used in escalated GW

installations with no considerable technological developments even though it is still not possible to bring about improvements in terms of its efficiency. These days, there are solar cells made by thin semiconductor films placed in layers over a low-cost bracket. The main thin-film categories are: amorphous (Si) -with efficiencies from 4% up to 11.1%- , multi-layer based tandem cells -with efficiencies up to 40%- , cadmium telluride (CdTe) -with a 16.5% efficiencies- , copper indium selenide (CIS) and copper indium gallium selenide (CIGS) -with efficiencies from 7% up to 19.5%- (Rodríguez-Suárez et al., 2000).

For some years now, solar cells are developed with organic materials that are divided into full organic cells and dye-sensitized hybrid solar cells. However, it still has not been proven if these panels can contribute to large electric systems along with advanced thin films; these are part of recently developed novel technologies (Glunz et al., 2012).

Recent research showcases the possibility of manufacturing panels with significantly higher efficiencies. One of the approaches consists of piling materials of different width in a multi-junction; for example, with the use of crystalline semiconductors with nanoscale measurements. Through this technique, it

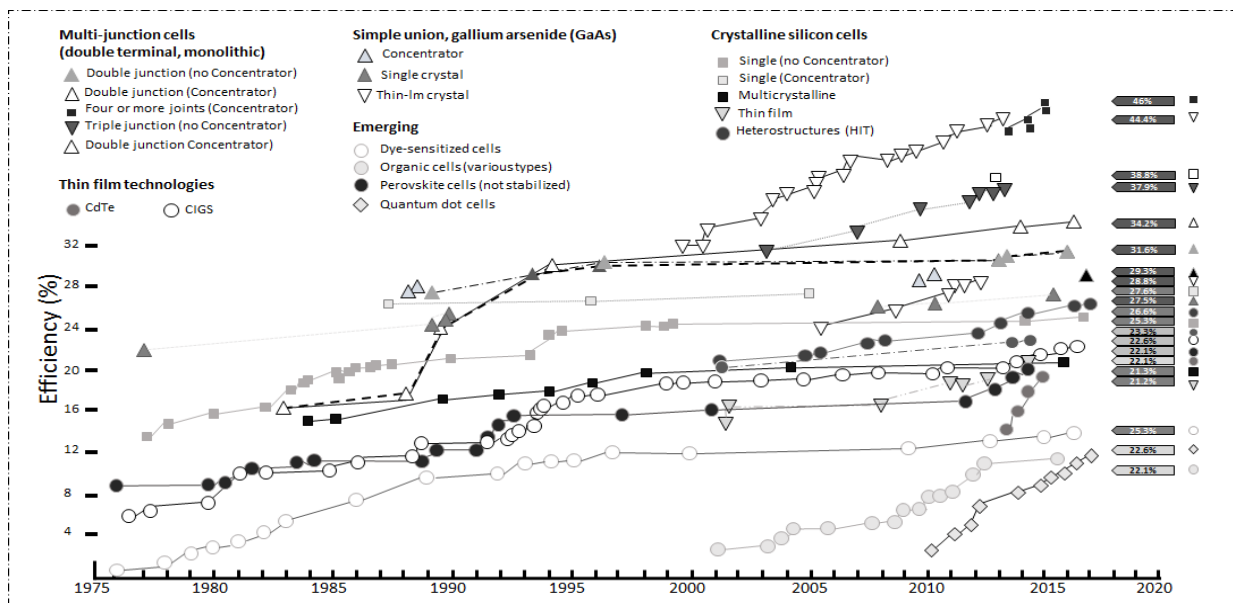


Figure 1.1. Evolution in the efficiency of solar cells (REN21, 2016)..

would be possible to reach more than 40% of efficiencies under a relatively low cost in spite of not having reached these results at a laboratory level (MIT Energy Initiative, 2016).

Photovoltaic modules are a group of interconnected cells with the capacity of giving a wide range of voltages that reach up to 100 W. A common photovoltaic silicon module has 60 to 90 (1.5 cm²) individual solar panels -with the capacity of producing four to five Watts at peak time-. Standard dimensions for commercial photovoltaic modules are 1 m. by 1.5 m. for 4 cm. -with a capacity of producing two hundred and sixty to three hundred and twenty Watts at peak time-. Now, there is the possibility of increasing the efficiency of commercial modules and reducing the cost and complexity of their manufacturing as well as the amount of required silicon to produce a Watt and the dependence of silver for the metallization of products (Glunz et al., 2012).

1.2.1 Technology costs

One of the factors that have favored the growth on photovoltaic investments has been the drop in the cost of this technology. The costs of photovoltaic modules have decreased over the last five years but they are

not as inexpensive to be massively implemented (including different technologies, such as crystalline silicon modules and thin-film panels).

In different sectors, there has been a large cost decrease of electricity production. Nowadays, there are lower costs in the solar sector with larger-scale projects -with installed capacities over 100 MW. The second sector is the commercial one -with installed capacities around 200 kW-. The last sector is the residential sector (also known as distributed generation) -with smaller scales of 5.6 kW systems- (See Figure 1.2). These differences result in economies of scale for each application of this technology (Rodríguez-Suárez et al., 2000).

In another perspective, the gap of capital expenses between photovoltaic solar projects and wind energy has reduced but it still has not reached the same level as global ones. The implementation of novel technologies will enable cost reduction in great-scale photovoltaic solar energy. This will allow for competition for wind installations which is the main growing sustainable energy for some years now.

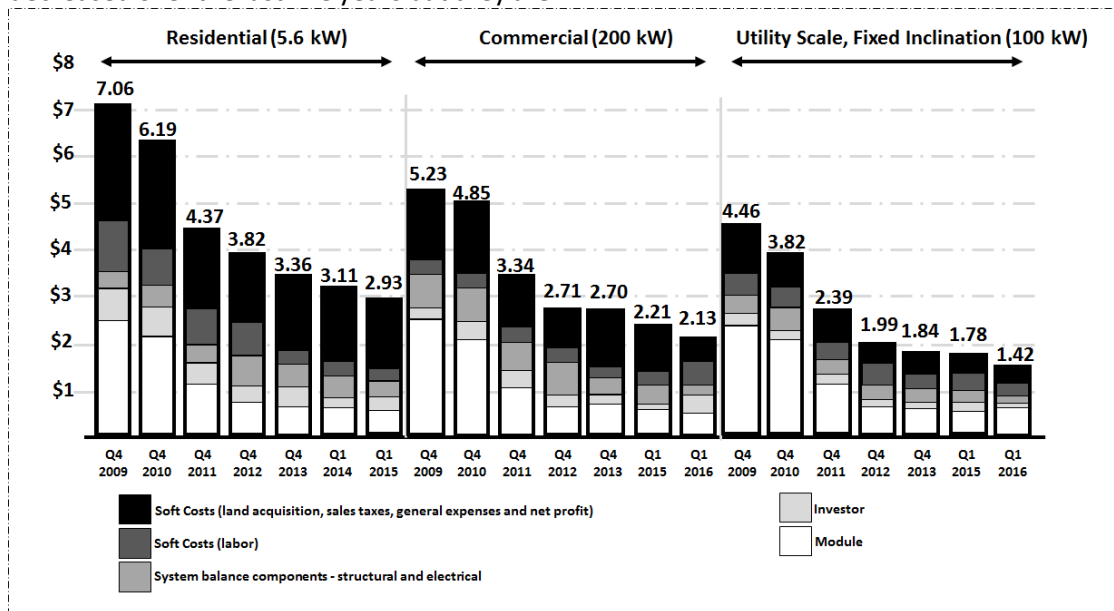


Figure 1.2. Decrease in photovoltaic generation costs (SENER, 2016a).

1.3 Manufacturing profile of photovoltaic technologies in the main global economies

1.3.1 Manufacturing of photovoltaic modules and cells

Clean energy technologies are rapidly expanding all around the world and are contributing more to global energy systems. Manufacturing for these technologies, including organic matter extraction and processing, the production of required by-products, or the assembly of the final product have become a global task (Rodríguez-Suárez et al., 2000). Recently, INEEL (National Institute of Electricity and Clean Energy) (in Spanish, the Instituto Nacional de Electricidad y Energías Limpias) published a comparative analysis of clean energy technology with support from the United State's EERE (in English, the Office of Energy Efficiency and

Renewable Energy) (Rodríguez-Suárez et al., 2000).

This analysis establishes a common framework as well as novel methodologies to assess and compare the manufacturing supply chain of clean energy technology. This aims to follow the manufacturing guidelines for costs provided by INEEL. For the analysis, there was an incorporation of market, manufacturing and trading data from the year 2014 to analyze photovoltaic technology modules (of crystalline silicon) (SENER, 2016a).

The impact of the manufacturing supply chain for these four technologies was assessed in terms of common reference frameworks for twelve chosen economies that constitute the main manufacturing centers of all four technologies: Brazil, Canada, China, Germany, India, Japan, Malaysia, Mexico, South Korea, the Republic of China (Taiwan), the United Kingdom, the United States. Results can be seen in Figure 1.3 (Rodríguez-Suárez et al., 2000).

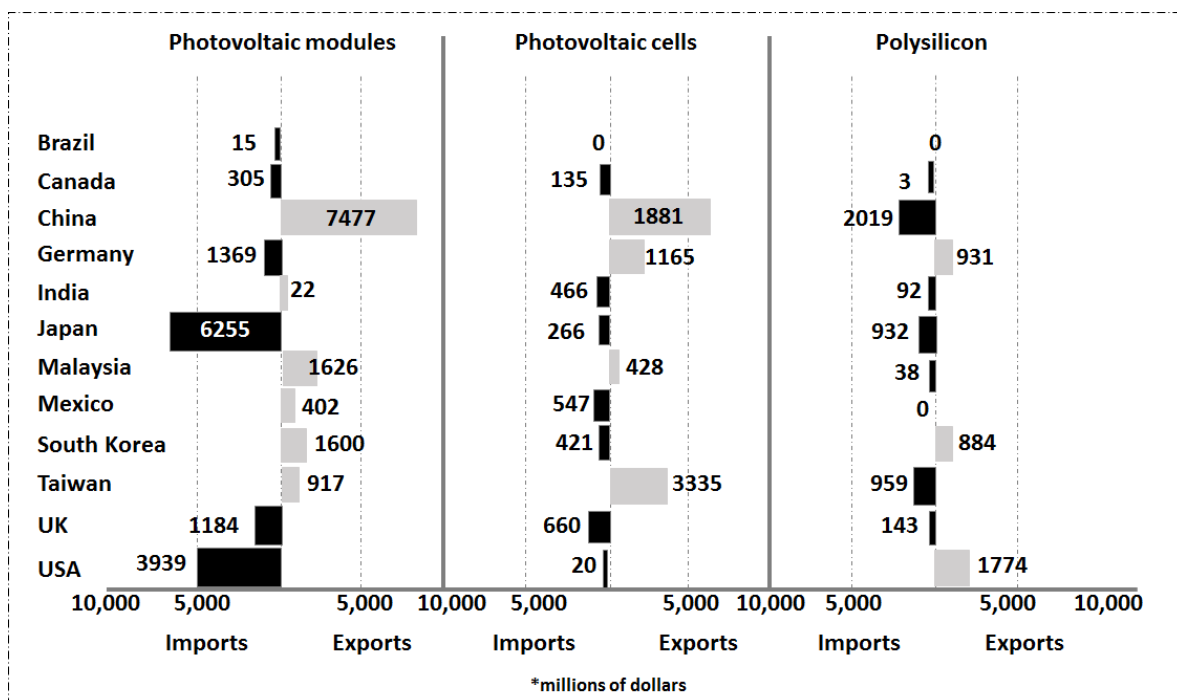


Figure 1.3. Trade balance of photovoltaic modules, cells and polysilicon (SENER, 2016a).

1.4 Photovoltaic solar energy

The use of solar energy to produce electricity through photovoltaic technology can be divided into two main realms: large-scale projects and small-scale and medium-scale photovoltaic systems, distributed in consumption places. Large-scale solar projects are mainly developed to deliver energy services required by energy enterprises and by great energy consumers. The development for these projects requires a larger financial period and it is necessary to consider them in the expansion of all national electric systems.

In other terms, there are lower-scale implementations set up in an end user sector such as residential and commercial sectors in a distributed generation. These lower-scale photovoltaic systems are principally though out to supply in-situ needs. They will eventually be available to sell energy to electric network, under national guidelines (Rodríguez-Suárez et al., 2000).

In 2016, 25% of the electricity generation capacity relied on clean energy sources while solar energy amounted to a small fraction of that percentage with an installed capacity of

270 MW (0.38% of the total national installed capacity). During 2018, electricity creation from photovoltaic systems reached 190 GWh (0.06% of all creation). See Figure 1.4 (SENER, 2016a).

1.5 Solar silicon

In 2018, more than 89% of photovoltaic generators production was made with crystalline silicon (Sinke, 2019). Therefore, crystalline silicon as inorganic matter turns out to be key to be essential in order to determine the volume and price for photovoltaic modules. This section aims to amplify knowledge of this matter and its impact in the final product, as well as its current place.

After oxygen, silicon is the most abundant and distributed element in our planet; although it is not isolated but combined with oxygen (SENER, 2016b). Silicon for industrial purposes comes from quartzite, with 90% silicon dioxide (SiO_2). Silicon comes off quartzite in a vacuum reduction metallurgic process by way of placing it in an electric arc furnace so as to enable a chemical bond

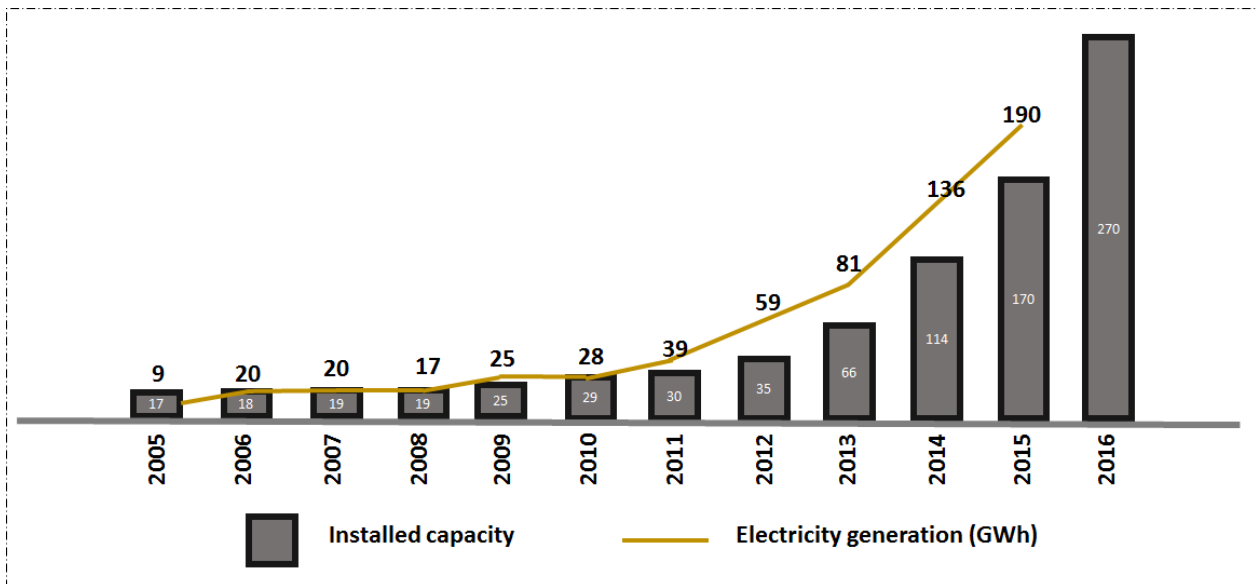


Figure 1.4. Evolution of the capacity and generation of photovoltaic electricity (SENER, 2016a).

breakdown of silicon and oxygen. This is how silicon -with a purity of more than 99% is obtained (1000 ppm). Silicon obtained follow this path is known as metallurgical-grade and it is appropriate for an industry that gets special alloys; however, it is not appropriate for the semi-conductor industry that requires high purity (some chips do not allow more than one impurity atom per million, 1 ppm) nor for the photovoltaic solar industry (which requires an intermediate purity of 10 ppm) (Anta and Asif, 2005).

1.5.1 Solar-grade silicon production

The creation of solar-grade silicon from quartzite has two large stages: the production of metallurgical-grade silicon and its purification so as to be transformed into solar-grade silicon. The production of metallurgical-grade silicon is done through quartzite reduction with coal. In this part of the process the equipment is an electric arc furnace that feeds a load made up of quartz (SiO_2), several forms of coal (like coke or, black coal) and wood splinters (which are used as fillers) (Søiland, 2005). The obtained silicon is known as metallurgical-grade silicon with a 98%-99% purity; it presents impurities of: iron, aluminum, titanium, phosphorus and boron (Brage, 2003).

The electric arc furnace reduces the tension current and lowers the intensity that reaches the low-tension plant that turns out to be appropriate for material heating using the Joule effect (in the heating and melting of the charge). Actually, it showcases a crucible where the feed is deposited with a 10 m diameter and 3 electrodes (three-phase electric arc furnace) placed within it that creates the necessary energy for the reaction to develop. A great energy input is needed to melt silicon oxide (it's melting point being 1986 K); 10-11 kWh are needed to produce a kilogram of silicon, reaching a temperature of almost 2300 K (Recamán-Payo, 2009).

After being refined, melted metallurgical-grade silicon is extracted from the inferior part of the furnace, then it is left to cool in a mold and after solidifying, it is grounded, and the silicon is cut depending on the size of the particle. Metallurgic-grade silicon does not have enough purity to be used in the manufacturing of photovoltaic cells, this being the reason behind a purification process. There are several technologies which objective is to obtain this purity. Said technologies are traditionally known as the Siemens process and the fluidized bed reactor (FBR) process.

The Siemens process is a developed and patented technology by the Siemens Corporation during the 50's. It uses trichlorosilane (SiHCl_3) as a silicon source. In the first stage, metallurgical-grade silicon reacts with the hydrogen chloride (HCl) in a fluidized bed reactor (between 273-673 K and 1-5 bar) (Pazzaglia et al., 2011). This is how a gas current made up by a series of chlorosilanes, the most important one in this process being trichlorosilane. The next stage of the process consists of a purifying process through distillation to obtain ultrapure trichlorosilane, this is possible because it has a boiling point of 304.8 K in normal conditions (Søiland, 2005).

Ultrapure trichlorosilane is deposited at 1373 K and it is diluted with H_2 by placing it inside a steam reforming reactor also known as bell jar reactor or Siemens Reactor where high-purity polysilicon (6N) is obtained, whereby it is placed over the baseline of a silicon rod and a gas steam of by-products that leaves the reactor (like hydrogen, hydrogen chloride (HCl), dichlorosilane (SiH_2Cl_2), trichlorosilane (SiHCl_3) and tetrachlorosilane (SiCl_4) (Erickson and Wagner, 1952).

For this reason, we must keep in mind that the Siemens Process is a complex process using a costly technology with costly technology, great energetic consumption and a high number of residual streams. Plus, we should

consider that the main parts of HCl have inorganic matter traces which results in a need for purifying processes so as to be circled.

On the other hand, the fluidized bed reactor (FBR) process developed by Union Carbide Corporation between 1970 and 1980 which uses silane as a source of silicon. The first stage of the process consists of the hydrogenation of metallurgical-grade silicon and tetrachlorosilane in an electric arc furnace (FBR) at 673-1073 K and 20-40 bar (Iya, 1986). After the separation processes through filtering and condensation to reduce solids and non-condensable gases (such as hydrogen); the effluent of such reaction essentially has trichlorosilane and tetrachlorosilane (Muller et al., 2002). This current goes under a new stage of separation and purification that can be undertaken by independent batch reactors or using a reactive distillation column. In this stage, trichlorosilane becomes in silicon through consecutive batch reactors where there is another product separation (such as silicon tetrachloride that is recirculated).

These batch reactions can be carried out simultaneously as the separation for distillation takes place because both are chemical balancing reactions that require ionic exchange resins with functional groups from the sorts of tertiary amines (:NR₃) or quaternary ammonium (NR₄⁺). As Ramírez-Márquez et al. (2016), suggest it can also be used for process intensification through reactive distilling for the creation of silane through a disproportioning reaction of trichlorosilane. Finally, the purity of the obtained silane, is taken through a chemical vapor deposition where it is broken to create polycrystalline silicon and hydrogen (at 973-1473 K) (Farrow, 1974).

For the Union Carbide process, it is thought that even though it has more efficiency in the polycrystalline obtainment than the Siemens Process. Given that the silane conversion is

greater than trichlorosilane because it runs under extreme operative conditions and has a high number of residual currents that can turn out to be unsafe and be a risk for the environment.

1.5.2 Solar-grade silicon status

For the first decades of photovoltaic industry development, the solar industry has not needed to go through the previously mentioned complex processes. On account of their needs, it has had enough with the created remnants of the electronic industry. The superior and inferior part of the ingot - that is not cylindrical but conic-, the ingots that do not reach the required guidelines by the electronic industry, the silicon that remains in the crucible, the testing wafers are ones that the electronic industry rejects and that the solar industry recycles, etc. This rejection is of about 10 % of the silicon that the electronic industry consumes; by being refused, the solar industry could benefit from the obtainment of solar-grade polysilicon (Anta and Asif, 2005).

Prices remained low when working at variable cost expenses was done. At the end of the last century, the growing need for solar-grade silicon has grown at a rapid pace and it was thought that it could be higher than the amount of refuse from the electronic industry and its capacity to create silicon; although the issue did not appear to be discouraging, no other investments were made so as to obtain an extra capacity of silicon.

It should be noted that there was a requirement for significant investments with zero profits (there was a need for competition of disposable products or without fixed costs). These investments were aimed to handle the issue of the lack of inorganic matter that had no set date for production. This dilemma occurred after years when the silicon industry had done considerable investments (in the 90's) waiting for a substantial growth for the demand that did not succeed (meaning, the

bubble of telecommunications and the Internet) whereby the silicon industry was affected. The status of solar silicon has rapidly changed in a matter of a couple of years, due to a high and sustained world growth of photovoltaic installations that has overlapped with the electronic market's recovery (Anta and Asif, 2005).

1.6 Process Intensification

In the early 90's, while opening the 1st International Conference on Process Intensification in the Chemical Industry, Ramshaw, one of the pioneers of the field, defined process intensification as a strategy for making dramatic reductions in the size of the chemical plant so as to reach a given product objective. These reductions can come from shrinking the size of individual pieces of equipment and also from cutting the number of unit operations or apparatuses involved. In any case, the degree of reduction must be significant (Ramshaw, 1995).

Ramshaw's definition is quite narrow, describing process intensification exclusively in terms of the reduction in plant or equipment size. In fact, this is merely one of several possible desired effects. Clearly, a dramatic increase in the production capacity within a given equipment volume, a step decreases in energy consumption per ton of product, or even a marked cut in wastes or by-products formation also qualify as process intensification (Ramshaw, 1995).

Not surprisingly, process intensification, being driven by the need for breakthrough changes in operations, focuses mainly on novel methods and equipment. Under this idea the process of production of solar-grade silicon is subject to intensification in order to have the previously mentioned benefits.

Process intensification consists of the development of novel apparatuses and techniques that, compared to those

commonly used today, are expected to bring improvements in manufacturing and processing, substantially decreasing equipment-size/production-capacity ratio, energy consumption, or waste production, and ultimately resulting in cheaper, sustainable technologies; as shown in Figure 1.5. The field can be divided into two areas:

- Process-intensifying equipment, such as novel reactors, and intensive mixing, heat-transfer and mass-transfer devices; and
- Process-intensifying methods, such as new or hybrid separations, integration of reaction and separation, heat exchange, or phase transition (in so-called multifunctional reactors), techniques using alternative energy sources (light, ultrasound, etc.), and new process-control methods (like intentional unsteady-state operation) (Ramshaw, 1995).

1.7 Perspective on the work done

In the present work, there is a description of the procedures and results of the simulation and improvement of the processes of production of solar-grade silicon for the manufacturing of photovoltaic cells. Although the current state of the art of the technology includes other types of material and hardware, due to the establishment of silicon technologies, it is possible to have a cost-effective, safe and environmental process. Observations on the limits of today's obtainment technologies of solar-grade silicon stated that in order to have a global overview of the current state of technology (and the different applied solutions adopted for the obtainment of a lower-cost solar-grade silicon) it is necessary to include a plant which is capable of producing high added value elements that can be obtained at

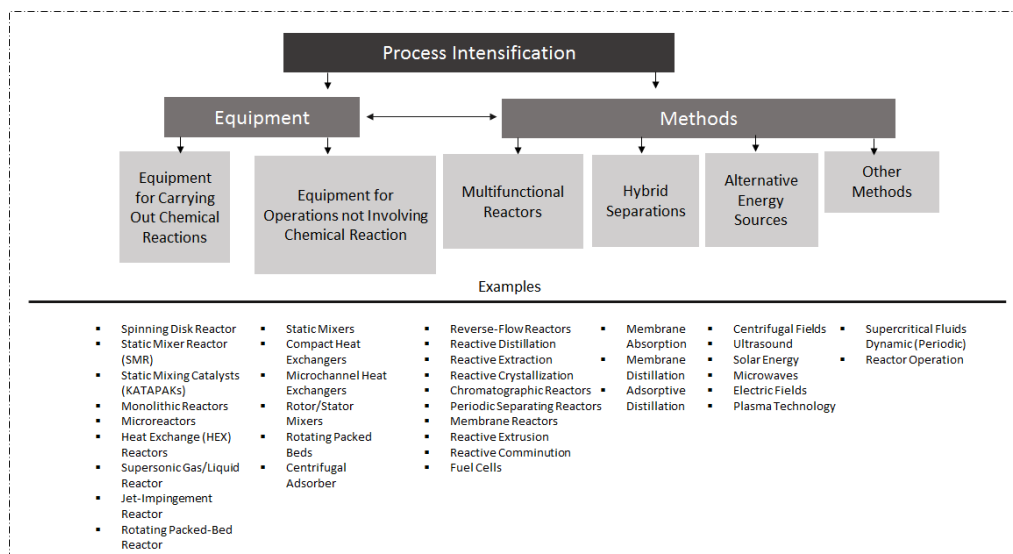


Figure 1.5 Process Intensification and their components (Ramshaw, 1995).

the same time that the process is made cost-effective and to have achieved on the ideal operative conditions for an industrial implementation.

In the first chapter, there is an analysis of security, environmental, and occupational health traits, related to solar-grade silicon (beyond the ones included for their manufacturing cost). The objective is to make a diagnose of the current development of this material not only in its economic scope but in its environmental and security guidelines for the worker that labors in the plants.

In the second chapter, there is a detailed financial comparison of existing technologies and the proposed innovative process to produce solar-grade silicon. This option will enable a comprehensive overview of solar-grade silicon technology and an understanding of the recently proposed production diagrams with solar-grade silicon.

In the third chapter, there is a revision of what the evolution of novel processes constitutes. Most importantly, the advancements represented in the silicon market by novel technologies. Whereby the premise of having a process that meets both design guidelines and operating conditions; which guarantees

profits, a low environmental impact, and security.

In the fourth chapter, there is a reference to the in-demand devising of novel designs which of course refers to guaranteeing the occupational health of workers in any sort of plant. This issue unfolds as mandatory for processes that have raw material, intermediate products or final products that constitute a health risk issue for employees; particularly, in existing processes such as solar-grade silicon production. Therefore, research on this matter emerges as a need to guarantee -from an industrial perspective- the setting up of such process under working guidelines.

In the fifth chapter, there is an analysis of the novel process for the obtainment of solar-grade silicon with an ideal design that guarantees the highest quality production efficiency. This analysis will allow for a clear notion on the scope that solar-grade silicon obtention processes have and its constraints in terms of its development for industrial and commercial scales.

In the final version of this work, the sixth chapter will address the issue of solar-grade silicon plants. The purpose is to show that the

design of a plant of this kind allows the existing processes to be more cost-effective as it downscales produced refuse, makes the process safer and its environmentally friendly.

The presentation of each of the tasks throughout all chapters is an attempt to extensively, to a great extent, the design of a multi-product solar-grade silicon plant. On account of an overview of the main features of solar-grade silicon in its different application and approaches. To conclude, there are some preliminary conclusions.

1.8 Justification

The increasing market of silicon as a raw material for solar cells has considerably escalated in the last few decades with an even greater rise of its demand. While numbers show a noticeable growth, the fixed energetic capacity is but a fraction of the total energy created by all energy sources; this shows the extensive field of growth for its immediate future.

Nowadays, silicon cells compete with polycrystalline cells and other types of sophisticated cells. Polycrystalline silicon's high cost is due to its creation process as well as silane's production process. This explains the idea behind the innovative design of a solar-grade silicon multi-product plant; one that is cost-effective, safe and has a low environmental impact while it reduces the cost of silicon production and makes it more accessible for the market.

1.9 Hypothesis

- The production cost of solar cells, from silicon oxide, will decrease with a minimal environmental impact and a minimal risk index; through a solar-grade silicon production plant and the parallel creation of high added value products for each element of the process, along with the harnessing of the remnant energy currents and the

standardized operation conditions for each element of the process.

1.10 General Objective

- To design a production process of solar-grade silicone as well as the production of a series of high added value components which reach a cost-effective, safe and environmentally low process; where the production cost of solar-grade silicon is reduced in terms of the manufacture of solar cells drawn from silicon oxide through the standardized design of each element.

1.11 Specific Objectives

- To simulate two known processes and the innovative process for the production of solar-grade silicon, and develop a novel one.
- To optimize designs under the cost's objectives, security and environmental indicators.
- To attain optimal conditions of operation for each element of the process that pan out better economic, security and environmental indicators within a larger frame of production matter.

1.12 References

REN21. 2016. Energías Renovables 2016. Reporte de la situación mundial.

J. S. Rodríguez-Suárez, E. Espinoza-Navarrete, J. Rosenbusch, H. O. Ortega Navarro, M. Martínez Fernández, K. G. Cedano Villavicencio, M.M. Armenta. (2000). La Industria Solar Fotovoltaica Y Fototérmica En México. <https://www.promexico.mx/documentos/biblioteca/industria-solar.pdf>

Global Energy Network Institute (GENI, 2011). Review and Comparison of Different Solar Energy Technologies. www.geni.org

Chen, H., Cong, T. N., Yang, W., Tan, C., Li, Y., & Ding, Y. (2009). Progress in electrical energy

- storage system: A critical review. *Progress in natural science*, 19(3), 291-312.
- Glunz, S. W., Preu, R., & Biro, D. (2012). 16: Crystalline silicon solar cells—state-of-the-art and future developments. *Comprehensive renewable energy*, 1, 353-387.
- Massachusetts Institute of Technology (MIT, Energy Initiative, 2016). *The Future of Solar Energy. An Interdisciplinary MIT Study*. Agosto, 2016. <http://energy.mit.edu/wp-content/uploads/2015/05/MITEI-The-Future-of-Solar-Energy.pdf>
- International Energy Agency (IEA), (2011). *Solar Energy Perspectives. Renewable Energy Technologies*. http://www.iea.org/publications/freepublications/publication/solar_energy_perspectives2011.pdf
- Secretaría de Energía (SENER, 2016a). *Reporte de Avance de Energías Limpias 2016*.
- Sinke, W. C. (2019). Development of photovoltaic technologies for global impact. *Renewable energy*, 138, 911-914.
- Secretaría de Energía (SENER, 2016b). *Balance Nacional de Energía 2016*.
- Anta, J., & Asif, I. F. (2005). El silicio solar. *Revista Energética XXI. Asociación de la industria fotovoltaica*. Mayo. [29] NEWS SOLICLIMA. *Energía solar fotovoltaica*. <http://news.soliclima.com>
- Søiland, A. K. (2005). *Silicon for solar cells*.
- Brage, F. J. P. (2003). *Contribución al modelado matemático de algunos problemas en la metalurgia del silicio* (Doctoral dissertation, Universidade de Santiago de Compostela).
- Recamán-Payo, M. J. (2009). *Purificación de triclorosilano por destilación en el proceso de obtención de silicio de grado solar* (Doctoral dissertation, Universidad Complutense de Madrid, Servicio de Publicaciones).
- Pazzaglia, G., Fumagalli, M., & Kulkarni, M. (2011). U.S. Patent Application No. 13/084,243.
- Erickson, C. E., & Wagner, G. H. (1952). U.S. Patent No. 2,595,620. Washington, DC: U.S. Patent and Trademark Office.
- Iya, S. K. (1986). Production of ultra-high-purity polycrystalline silicon. *Journal of Crystal Growth*, 75(1), 88-90.
- Muller, D., Ronge, G., Fer, J. S., & Leimkuhler, H. J. (2002). Development and economic evaluation of a reactive distillation process for silane production. In *Proceedings of the International Conference on Distillation and Absorption* (pp. 4-1).
- Ramírez-Márquez, C., Sánchez-Ramírez, E., Quiroz-Ramírez, J. J., Gómez-Castro, F. I., Ramírez-Corona, N., Cervantes-Jauregui, J. A., & Segovia-Hernández, J. G. (2016). Dynamic behavior of a multi-tasking reactive distillation column for production of silane, dichlorosilane and monochlorosilane. *Chemical Engineering and Processing: Process Intensification*, 108, 125-138.
- Farrow, R. F. C. (1974). The Kinetics of Silicon Deposition on Silicon by Pyrolysis of Silane A Mass Spectrometric Investigation by Molecular Beam Sampling. *Journal of The*
- Ramshaw, C., (1995). The Incentive for Process Intensification, *Proceedings, 1st Intl. Conf. Proc. Intensif. for Chem. Ind.*, 18, BHR Group, London, p. 1.

2 Process design and intensification for the production of solar grade silicon



Process design and intensification for the production of solar grade silicon



César Ramírez-Márquez ^a, Marta Vidal Otero ^b, José Antonio Vázquez-Castillo ^c,
Mariano Martín ^{b,*}, Juan Gabriel Segovia-Hernández ^a

^a Universidad de Guanajuato, Campus Guanajuato, División de Ciencias Naturales y Exactas, Departamento de Ingeniería Química, Norte Alta S/N, 20256 Guanajuato, Gto., México

^b Universidad de Salamanca, Departamento de Ingeniería Química, Pza. Caldas 1-5, 37008, Salamanca, Spain

^c Universidad Autónoma de Chihuahua, Facultad de Ciencias Químicas, Circuito Universitario 8, Campus UACH II, 31125, Chihuahua, Chih., México

2 Process design and intensification for the production of solar grade silicon

Abstract

Solar grade silicon (Si_{SG}) is typically used in photovoltaic applications, and it is commercially manufactured via Siemens process. Despite the fact that current levels of demand are satisfied, there may be a shortage of Si_{SG} in the near future. To improve the low yield of the Siemens process, two alternative types of Si_{SG} production processes have been developed and analyzed using a stochastic optimization scheme within ASPEN PLUS. The first one is an intensified Fluidized Bed Reactor (FBR) process using a reactive distillation column. The second process is a hybrid process combining both the Siemens and the conventional FBR processes. In addition to supplying future demand, these processes are intended to reduce the use of raw materials. The results show the great value of optimizing the processes, since it achieves savings in the TAC of 53.28%, 67.65% and 62.58% (Siemens, Intensified FBR and Hybrid process, respectively). Siemens process shows the lowest TAC (\$0.50 M/y), but this does not mean that it is the process with the highest potential, since it has the lowest silicon production rate, 0.47 kt/y. The Intensified FBR Union Carbide Process turns out to be the most expensive of the three (\$2.57 M/y), with a large production of Si_{SG} , 1.49 kt/y. However, it turns out that the hybrid process shows the larger yield by far, with a production of 1.89 kt/y of Si_{SG} and TAC of \$1.95 M/y, showing the highest profit from sales, \$40.47 M/y. However, from the environmental point of view, the Siemens process shows the lowest environmental impact based on the eco-indicator 99, while the Hybrid process is the second best.

2.1 Introduction

Solar photovoltaics, PV solar, is gaining attention as a technology to make use of the largest energy source available, up to 162,000 TW that the Earth's receives annually (Bououdina, 2014). Its market share among renewable energy increases and currently it is the most newly installed renewable source of power (Solar Market Insight Report, 2016), in the race to replace fossil based power and fuel sources. Furthermore, current volatility in crude prices is another driver towards the

goal of self sufficient supply of energy (Ginley et al., 2008). However, renewable technologies are not yet competitive with their fossil based counterparts. Therefore, there is a research opportunity to improve their yields and efficiencies. In particular, PV panels have improved their performance reducing the cost. For instance, in the southwest of the United States, in order to meet the cost goal of \$0.33/W or \$0.05–0.06/kWh for utility-scale production, these modules with 15% efficiency, needed to be

manufactured at a cost of \$50/m² or less (Ginley et al., 2008). Further penetration of this technology into the market will make possible to reduce costs even further. So far, the basic raw material for the production of these panels is polysilicon.

For years, microelectronic industry has been an important source of polysilicon. In that industry, ultrapure Si, 9N or Si_(EG), is required. The waste of Si remaining in the melting units as well as the pieces of waffles that do not reach the proper purity are typical sources of solar grade Si (Braga et al., 2008). However, the development of the solar sector has increased the demand for solar grade Silicon and the scraps from microelectronic industry are no longer enough to meet the needs as raw material. Therefore, there is a need to improve the production processes from polysilicon to reduce their cost. The cost shares per Watt Peak of polysilicon solar systems are roughly as follows: Solar grade silicon (Si_(SG)): 20%; ingot and wafer production: 28%; solar cell processing: 13%; solar module processing: 9%; installation of the PV-system including converter costs: 30% (Sadique, 2010). There are two main possibilities to achieve the cost reduction since approximately half of the costs are caused by feedstock, bulk silicon production and wafer manufacturing (Müller et al., 2006). Thus, the development of optimized processes for production of cheap Si_(SG) feedstock material can allow better competitiveness.

Solar grade silicon can be produced from quartz following a two-stage process consisting of the production of metallurgic silicon and its further purification up to solar grade quality. The two most used processes are Siemens and Fluidized Bed Reactor, FBR, from Union Carbide. Siemens process was patented by Siemens Corporation in the

1950's. Its main feature is the Siemens or Bell reactor where 6N silicon is produced by Si deposition on a silicon pole (Payo, 2009). However, this alternative shows a large energy consumption and a number of waste streams. On the other hand, Union Carbide's process uses Silane as a raw material for the production of Si. It was developed in the 1970-1980 (Erickson and Wagner, 1952). Even though the yield of this alternative is larger than the one provided by Siemens process, the conversion from silane is larger than that from trichlorosilane and the operating conditions are more difficult to achieve.

Due to the high production cost of PV panels, the aim of this work is to reduce the production costs of Si_(SG) by developing more efficient processes. In particular two novel processes have been proposed in this paper. The first one corresponds with an intensified FBR's process by substituting the conventional reactors and separation zone with a reactive distillation column. In this case, a reactive distillation column (RD) is used to overcome the traditional process since fewer distillation columns and no reactors are required. Essentially, the idea of employing a reactive distillation column is to improve the chemical conversion, because products alone are withdrawn from the reactive zone while reactants remain inside the reactive zone for further reaction. This reactive distillation process is reported previously in the work of Ramírez-Márquez et al. (2016). The second alternative process is a novel process that is based on both, the Siemens and the FBR attempting to reduce the use of raw material (Vidal and Martín, 2014).

It is important to note that the three simulated processes were optimized to make a comparison in their Total Annual Cost (TAC) and in their production of solar grade silicon.

Since scale is an advantage for any of these processes we target an annual production similar to the ones reported by major competitors (Nitol Chem Group [1.500 t/y], PV Crystalox [2.250 t/y], SolarWorld [3.200 t/y] (SOLAR PV INVESTOR) (List of World's Polysilicon Producers According to Country for Last 3, 2013)).

The rest of the work is organized as follows. Section two presents the description of each one of the three alternatives compared, Siemens as a base case, intensified FBR and hybrid process, discussing the modelling effort and the assumptions. The section ends with the description of the optimization method used, an evolutionary hybrid method based on tabu list using the total annualized cost as objective function. Section three presents the results comparing the operation and the economics of the three processes. Finally we draw some conclusions in section four.

2.2 Methodology

We first simulate the all three processes rigorously in Aspen Plus V8.4. To predict the thermodynamic of the system, we used the thermodynamic package Peng-Robinson, and 'Solids' property method for solids components. All the sequences presented were obtained considering the complete set of mass and energy balances, equilibrium relationships, and summation constraints along with the phase equilibrium calculations. Over sections 2.1 to 2.3 all three alternatives are described in terms of the chemical reactions and separations taking place and the assumptions to model the various units in Aspen Plus. The production capacity selected, 2,000 t/y is based on the average production of major companies (List of World's Polysilicon Producers According to Country for Last 3, 2013). The standard feed can be seen in Table 2.1. Next, we perform a

stochastic based optimization to decide on the column design and the operating conditions for each process.

Furthermore in this work we have added the calculation of the environmental impact which is measured through the Eco-indicator 99, a cradle to gate methodology, which reflects the advances in the damage-oriented method recently developed for Life Cycle Impact Assessment, as show Guillén-Gosálbez et al., (2008). With regard to the environmental impact, three damage categories are considered: human health, ecosystem quality, and resources. The process data are used to compute to environmental performance information. The human health damages are quantified in terms of disability adjusted life years (DALYs). The ecosystem quality damages are defined in terms of possible disappearance of species m^2/y . Finally, regarding the damages to resources, these are specified in terms of megajoules (MJ) of surplus energy (Guillén-Gosálbez et al., 2008). The data associated with the three categories above mentioned, will be taken from standard databases, i.e. TEAM and DEAM, (1998). Finally, the damages of each category are normalized and aggregated into a single impact factor (Eco-indicator 99). By normalizing categories with different units as described above, a single unit of P/y is given, where one point per year is the one-thousandth of the impact of one European citizen per year.

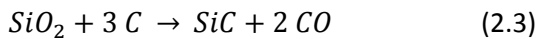
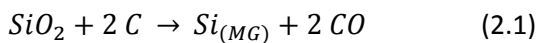
Table 2.1. Feeding of processes.

Component	kg/h
SiO ₂	532,32
C	369,84

2.2.1 Siemens Process

This process uses quartz as raw material. It is cheap and readily available, as it can be seen in Figures 2.1 and 2.2. The first stage is to

produce metallurgic silicon via quartz reduction with coal. An electric arc furnace is the unit used for this transformation (Ranjan et al., 2011). The purity obtained for metallurgic grade silicon, $Si_{(MG)}$ is around 98-99%. The typical impurities remaining are Fe, Al, Ti, P and B (Søiland, 2005). In this work it is considered a base feed of pure SiO_2 . This furnace transforms high voltage and low intensity current into high intensity and low voltage to make use of Joule's heating effect to melt the feed. The unit consists of a crucible of 10 m diameter and three electrodes where the feed is loaded. Triphasic current is made through the feed to carry on the reaction. Large amount of energy is required to melt silicon, 1986 K. The furnace performance must be in the order of 45-50% so that the energy consumption matches the experimental results from Brage, (2003). Thus, we model this unit in Aspen Plus 8.4v using a mixer module (Mixers/Splitters-Mixer) to feed coal and Si, a furnace (Exchangers-Heater-Furnace module) to heat up the mixture from standard conditions, 298 K and 1 bar up to 2273K and 1 bar. We use a stoichiometric reactor (Reactors-RStoic module) to evaluate the product of the reactions taking place in equations (2.1)-(2.3) (Schei et al., 1998).



The conversion of silicon dioxide (SiO_2) to metallurgical grade silicon ($Si_{(MG)}$) is 85 %. The rest is slag. To compute the slag, we assume that the rest of the SiO_2 reacts equally through each of the reactions (2.2) and (2.3). Since the stoichiometric reactor (Reactor-RStoic module) in Aspen only has one exit stream, we use a component separator (Separator-Sep module) so that we separate

the slag and gases from the $Si_{(MG)}$ (Barbouche et al., 2016). Gas processing is out of the scope of this work.

The $Si_{(MG)}$ is fed to the fluidized bed for the production of chlorosilanes. The target is trichlorosilane (Payo, 2009). It operates at 273-673 K and 1.5 bar. In the reactor the following reactions take place:

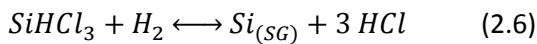


Both reactions are quick and exothermic so that there is no need for catalyst and the use of a fluidized bed is justified. This unit is modeled within Aspen as a stoichiometric reactor (Reactors-RStoic module). To target trichlorosilane ($SiHCl_3$), a temperature of 533K is recommended reaching 90% of selectivity to $SiHCl_3$ and the rest to tetrachlorosilane ($SiCl_4$) (Kotzsch et al., 1977). This selectivity is achieved by adding 10% excess of HCl with respect to the stoichiometric one (Jain et al., 2011).

The exit stream is fractionated. First, hydrogen (H_2) and hydrochloric acid (HCl) are removed when chlorosilanes condense. A flash (Separators-Flash2 module) is used to recover the chlorosilane gases, before that, a compressor (Pressure Changers-Comp-Icon2 module) is required to drive all the gases generated. The components (H_2 , HCl) pass through a separator (Separators-Sep module) to leave the pure hydrogen, then to be transported by a compressor (Pressure Changers-Comp-Icon2 module) and be stored as a by-product of high added value. Next, a distillation column is used to split the liquid stream of $SiHCl_3$ and $SiCl_4$ (List of World's Polysilicon Producers According to Country for Last 3, 2013). "RadFrac" module is used to model the column (Columns-RadFrac-Fract1). The bottoms, $SiCl_4$, is a byproduct of the process while from the top a stream 99.99%

SiHCl_3 is obtained (Díez et al., 2013). This purity is good enough to feed the stream to the chemical vapor deposition reactor of the Siemens process. Auxiliary equipment is required, such as pumps (Pressure Changers-Pump module) to give the necessary force to transport the liquid from the dome liquid streams and bottom of the column.

The production of solar grade silicon uses the SiHCl_3 and hydrogen via chemical vapor deposition. The typical composition of the stream is 5% SiHCl_3 and 95% H_2 (Del Coso et al., 2007). U shape bars of ultrapure silicon are used as seed. These bars are heated up using electric current. To model this unit, we consider the use of a furnace (Exchangers-Heater-Furnace module) to heat up the stream to 1373 K at 1 bar (Pazzaglia et al., 2011), and a stoichiometric reactor (Reactors-RStoic module). This is the temperature of the silicon deposition. However, the gases are expected to be at 673 K (Díez et al., 2013). The main reactions taking place are (2.6) and (2.7). The conversion to polysilicon is 30%, the rest goes to SiCl_4 (Jain et al., 2011).



After silicon deposition, by products of HCl , H_2 and SiCl_4 are obtained. A component separator (Separators-Sep module) is used to recover the solar grade silicon ($\text{Si}_{(\text{SG})}$) and the gases. We cool down the silicon with an exchanger (Exchangers-Heater-Heater module) to ambient temperature and the gases are separated by a set of equipment (Separators-Sep module), to be recycled to the process. Specially, hydrogen, see Figures 2.1 and 2.2.

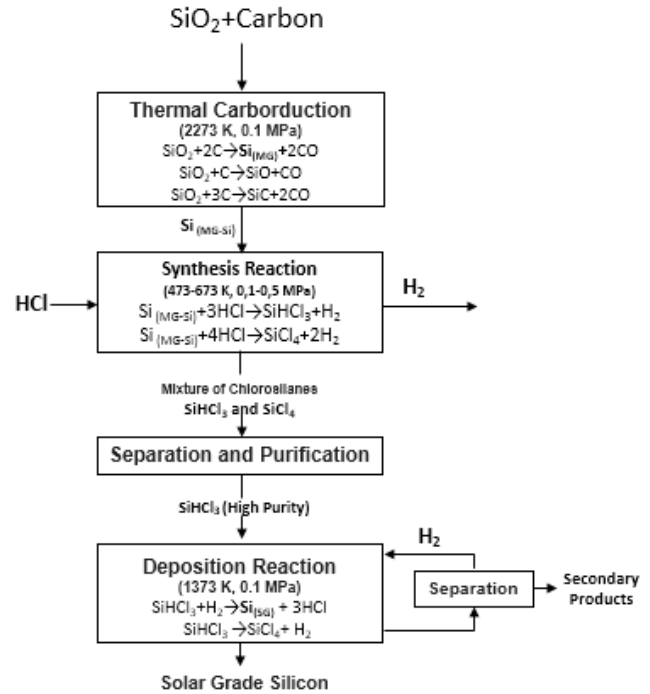


Figure.2.1 Siemens process.

2.2.2 Intensified FBR Union Carbide Process

FBR process uses silane as a source for $\text{Si}_{(\text{SG})}$ (Erickson and Wagner, 1952), see Figure 2.3 for a scheme of the process.

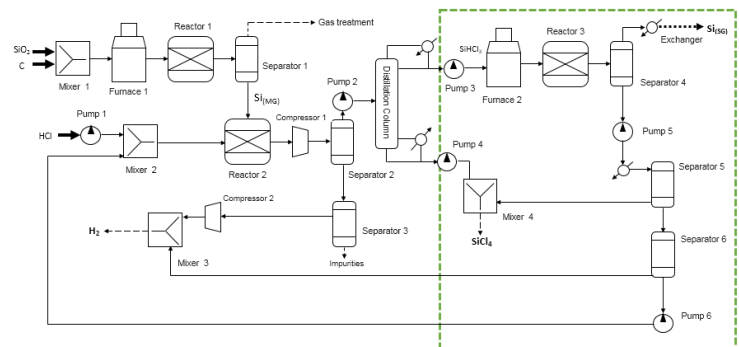
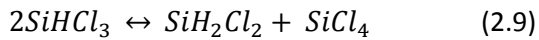
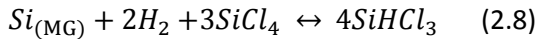


Figure 2.2. Flowsheet for the Siemens Process.

This process shares the production of metallurgic grade silicon, $\text{Si}_{(\text{MG})}$, with Siemens process. From that point on $\text{Si}_{(\text{MG})}$ is hydrogenated together with SiCl_4 in a fluidized bed reactor at 774 K and 36 bar (Erickson and Wagner, 1952). This reactor is modelled as a stoichiometric one (Reactors-

RStoic module) where the following reactions take place:

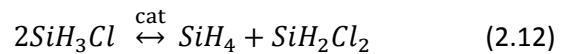
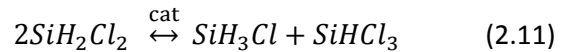
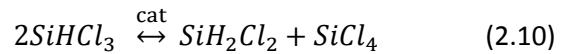


The yield of the first reaction reaches 25%. Typically, redistribution reaction may also take place (see equation 2.9). The conversion from $SiHCl_3$ to SiH_2Cl_2 is 10.5% (Pazzaglia et al., 2011). The stream of products is processed by a flash module (Separators-Flash2) to separate the chlorosilanes and others gases, such as the hydrogen. Now the other gases pass through a separator (Separators-Sep module) to leave the pure hydrogen, then to be transported by a compressor (Pressure Changers-Comp-Icon2 module) and be stored as a by-product.

Next, the stream consisting mainly of trichlorosilane and tetrachlorosilane, is fed to

column we obtain a high purity $SiCl_4$ stream that is recycled. In the last column we obtain high purity trichlorosilane bottom product that will be fed to the reactive distillation column. Auxiliary equipment is required, such as pumps (Pressure Changers-Pump module) to give the necessary force to transport the liquid from the dome liquid streams and bottom of the column. However, trichlorosilane disproportionation reactions (see equations 2.10 to 2.12) are carried out in a reactive distillation column. Thus, $SiCl_4$ is fed to the reactor with a 10% excess (Yaws et al., 1986)

High purity trichlorosilane is fed to the new intensified process, the reactive distillation system, that it was previously reported by Ramírez-Márquez et al., (2016). The reaction takes place following a three step mechanism, eqs. (2.10)-(2.12). Apart from silane, intermediates such as dichlorosilane (SiH_2Cl_2) and monochlorosilane (SiH_3Cl) are produced together with $SiCl_4$ (Ramírez-Márquez et al., 2016).



The catalyst selected for the reaction is “Amberlyst” (A-21) that shows good reaction rates from 30 to 80 °C and it is resistant up to 100°C. The temperature profile of the reaction zone shows that the maximum temperature achieved at the catalyst was 71.80°C, and the pressure reached is 2.54 atm. Table 2.2 shows the kinetic parameters (Ramírez-Márquez et al., 2016). The reactive distillation column was modelled using the “RadFrac” module (Columns-RadFrac-Fract1). The column produces high purity silane over the top that is fed to the chemical vapor deposition reactor to produce high purity

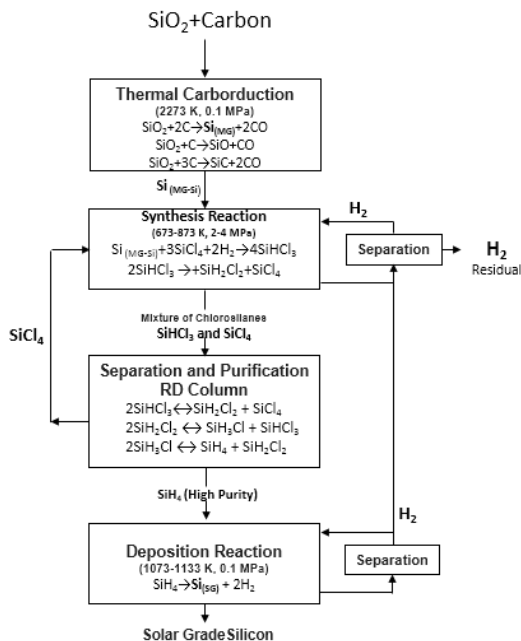


Figure 2.3. FBR Union Carbide with RD column process.

a regular system of two distillation columns modelled using “RadFrac” module (Columns-RadFrac-Fract1). From the bottoms of the first

silicon and hydrogen at 973 K, see eq. (2.13) (Farrow, 1974). The dome and bottom streams are carried by pumps (Pressure Changers-Pump module). We model this reactor as a furnace (Exchangers-Heater-Furnace module) and a stoichiometric reactor

(Reactors-RStoic module). Where the following reaction takes place:

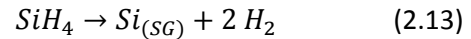
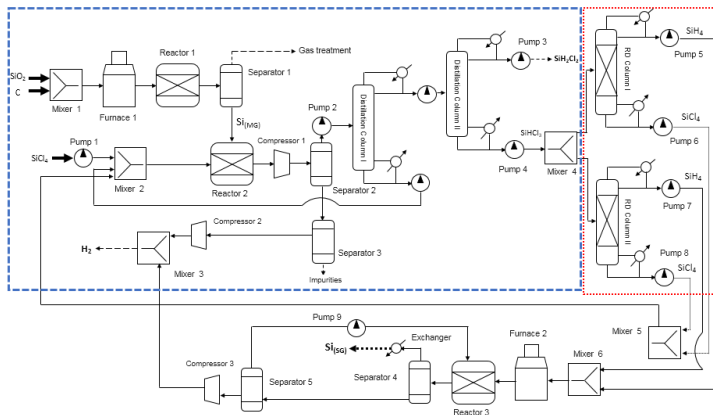


Table 2.2. Kinetic parameters for the proportional decomposition of trichlorosilane in liquid phase.

	k_0 [s ⁻¹]	E [J/mol]	K_0	ΔH [J/mol]
r_1		73.5	30045	0.1856
r_2	949466.4		51083	0.7669
r_3	1176.9		26320	0.6890



this box refers to the FBR Union Carbide Process area, and a dotted green line box surrounds the Siemens section. The whole of the two zones is what generates the process the so-called hybrid process.

Figure 2.4. Flowsheet of Intensified FBR Union Carbide Process.

Silane conversion reaches 80% (Tejero-Ezpeleta et al., 2004). The product stream is separated to isolate the polysilicon from the gases. Both streams are cooled down in two different heat exchangers (Exchangers-Heater-Furnace module). Polysilicon is solidified while the gases, mainly H₂ and HCl, are recycled. Figure 2.3 shows a scheme of the process and Figure 2.4 for the complete flowsheet.

2.2.3 Hybrid Process

This process, see Figure 2.5 for a scheme, aims at combining Siemens and FBR processes to make the most of the advantages of both. In Figure 2.6, a blue dashed line box is identified;

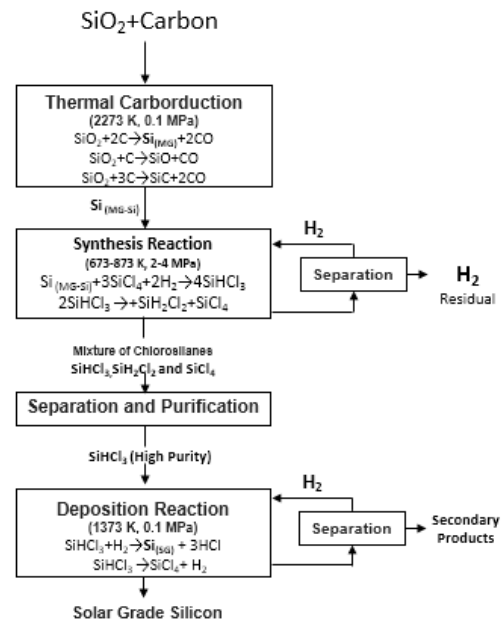


Figure 2.5. Hybrid process FBR Union Carbide with Siemens.

method, called differential evolution with tabu list (DETL) (Srinivas and Rangaiah, 2007a). This method is based on the theory of natural selection proposed by Darwin (Srinivas and Rangaiah, 2007a). It is very similar to the methods of genetic optimization, although with some differences in its coding. The description of the DETL algorithm can be reviewed in the work by Srinivas and Rangaiah, (2007a). That work shows that using the tabu list helps improve the performance of the evolutionary differential algorithm. In general, the DETL hybrid method, which contains parts of the evolutionary differential method and parts of the tabu list. The tabu list is used to follow up the evaluated points, helping to not to be subjects of search in the optimization again.

Srinivas, and Rangaiah (2007b) compared the performance of various algorithms using two types of problems, moderate and difficult ones and classifying the response into two categories: reliability and computational efficiency. The results of Srinivas, and Rangaiah (2007b), showed that the number of function evaluations of DETL is less for both moderate and difficult functions compared to differential evolution algorithm, tabu search algorithm, and modified differential evolution algorithm. Furthermore they also showed that on average, DETL took less CPU time compared to the others methods for the parameter estimation problems due to the computationally intensive objective function. With the significant reductions in the number of function evaluations, it was shown that DETL is attractive for engineering applications where the objective function evaluation requires considerable computational time, as is the case of this work.

The implementation of this optimization approach was made using a hybrid platform including Microsoft Excel, Aspen Plus and

Matlab. The vector of decision variables (i.e., the design variables) are sent to Microsoft Excel to Aspen Plus using DDE (Dynamic Data Exchange) through a COM technology. In Microsoft Excel, these values are attributed to the process variables that Aspen Plus needs. After the simulation, Aspen Plus returns to Microsoft Excel the resulting vector. Those values are sent from Microsoft Excel to Matlab where the objective functions are calculated. Finally, Microsoft Excel suggests new values of decision variables according to the used stochastic optimization method. Figure 2.7 illustrates the optimization process involving the software aforementioned.

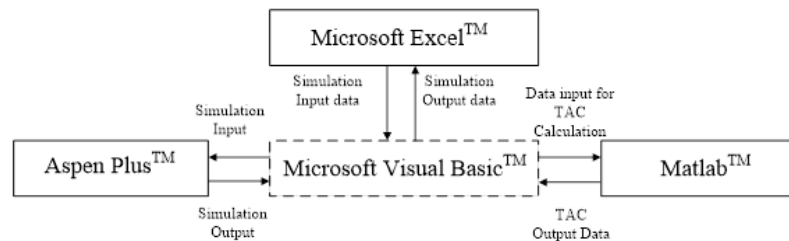


Figure 2.7. Hybrid platform to implement optimization.

For this study, the following parameters have been used for the DETL method: 200 generations, 200 individuals, a tabu list size of 100 individuals, a tabu radius of 2.5×10^{-6} , Crossover fractions (Cr): 0.8, Mutation fractions (F): 0.6, respectively. The parameters were obtained via preliminary calculations, as shown in the methodology of Srinivas and Rangaiah, (2007a).

The objective function for this work is the total annual cost (TAC), based on Guthrie's, (1969) method modified by Ulrich, (1984). The objective function estimates the lowest annual cost of the process, considering both the units and the plant's utilities. For the estimating the cost of the units, the correlations published by Turton et al., (2009)

are used. The objective function used is shown in equation (2.14).

$$TAC = \frac{\text{Capital Cost}}{\text{Payback time}} + \text{Operating cost} \quad (2.14)$$

The payback time of the plant is considered to be five years, and 8400 hours of yearly operation for each process are assumed. The design variables are presented in Table 2.3.

In each of the iterations we calculate the TAC of units such as the vessel of the reactor, furnaces, separators, mixers, heat exchangers, pumps and compressors. The units cost depend on their size and operating cost.

2.3.1 Optimization of the Siemens Process

The Siemens process is optimized using as objective function, the TAC which is directly proportional to the heat duty of the units (reactors, columns, and separators), services, and size of the units. The minimization of this objective is subject to the required recoveries and purities in each product stream, as shown in equation (2.15).

$$(Min)TAC f(N_{tn,i}, N_{fn,i}, R_{rn,i}, F_{tn,i}, D_{tn,i}, P_{tn,i})$$

$$\text{Subject to } \vec{y}_m \geq \vec{x}_m \quad (2.15)$$

where $N_{tn,i}$ are total stages of column i , $N_{fn,i}$ is the feed stages in column i , $R_{rn,i}$ is the reflux ratio of column i , $F_{rn,i}$ is the distillate fluxes of each of the columns, $D_{cn,i}$ is the column diameter, $P_{tn,i}$ is the top pressure, y_m and x_m are vectors of obtained and required purities for the m components, respectively. The results must satisfy each restriction of purity, $Si_{(SG)}$ 99.999% (wt %), $SiCl_4$ 99.999% (wt %), $SiHCl_3$ 99.99% (wt %), HCl 99.99% (wt %), and H_2 99.9999% (wt %) for Siemens Process.

The minimization infers the manipulation of 7 decision variables among continuous and

discrete variables for each route process, where 6 variables are used for the design of the column.

2.3.2 Optimization of the Intensified FBR Union Carbide Process

The objective function for the intensified process is again the minimization of TAC. The minimization of this objective is shown in equation (2.16). The major difference is the inclusion of the reactive distillation column, which have an additional constraint, the reactive zone should not exceed 100 °C so that the catalyst does not deactivate, as describes in section 2.2.

$$(Min) TAC f(N_{tn}, N_{fn}, R_{rn}, F_{tn}, D_{tn}, P_{tn}, R_{tn}, H_R)$$

$$\text{subject to } \vec{y}_m \geq \vec{x}_m \quad (2.16)$$

where N_{tn} are total column stages, N_{fn} is the feed stages in column, R_{rn} is the reflux ratio, F_{rn} is the distillate fluxes, D_{cn} is the column diameter, P_{tn} is the top pressure, R_{tn} are the reactive stages, H_R is the holdup, y_m and x_m are vectors of obtained and required purities for the m components, respectively. The results must satisfy each restriction of purity $Si_{(SG)}$ 99.999% (wt %), SiH_2Cl_2 99.999% (wt %), SiH_2Cl_2 99.99% (wt %) , $SiHCl_3$ 99.99% (wt %), SiH_4 99.999% (wt %) and H_2 99.9999% (wt %) for Intensified FBR Union Carbide Process.

The minimization implies the manipulation of 29 variables among continuous and discrete variables for each route process, where 6 variables are used for the design of each conventional column and 8 variables are used for the design of each reactive distillation column. The design variables can be seen in Table 2.3.

2.3.3 Optimization of Hybrid Process

The hybrid process is a combination of the two processes described before. As in the Intensified FBR Union Carbide Process, it includes a reactive distillation column for the disproportion of trichlorosilane. Therefore, the equation that governs this optimization is (2.17).

$$(Min)TAC = f(N_{tn,i}, N_{fn,i}, R_{rn,i}, F_{tn,i}, D_{tn,i}, P_{tn,i})$$

$$\text{subject to } \overrightarrow{y_m} \geq \overrightarrow{x_m} \quad (2.17)$$

The minimization infers the manipulation of 13 continuous and discrete variables for each route process, where 6 variables are used for the design of each column. All design variables for the cases of study are described in Table 2.3. The results must satisfy each restriction of purity $Si_{(SG)}$ 99.999% (wt %), SiH_2Cl_2 99.999 % (wt %), $SiHCl_3$ 99.99 % (wt %), $SiCl_4$ 99.999 % (wt %), HCl 99.99% (wt %), and H_2 99.9999% (wt %).

Table 2.3. Decision Variables Used in the Global Optimization of Process Routes for SISG Production.

Decision Variables	Siemens Process		Intensified FBR Union Carbide Process		Hybrid Process	
	Continuous	Discrete	Continuous	Discrete	Continuous	Discrete
Number of stages COLCONV1	N/A	X	N/A	X	N/A	X
Number of stages COLCONV2	N/A	N/A	N/A	X	N/A	X
Number of stages RDC 1	N/A	N/A	N/A	X	N/A	N/A
Number of stages RDC 2	N/A	N/A	N/A	X	N/A	N/A
Feed stages COLCONV1	N/A	X	N/A	X	N/A	X
Feed stages COLCONV2	N/A	N/A	N/A	X	N/A	X
Feed stages RDC 1	N/A	N/A	N/A	X	N/A	N/A
Feed stages RDC 2	N/A	N/A	N/A	X	N/A	N/A
Reflux ratio COLCONV1	X	N/A	X	N/A	X	N/A
Reflux ratio COLCONV2	N/A	N/A	X	N/A	X	N/A
Reflux ratio RDC 1	N/A	N/A	X	N/A	N/A	N/A
Reflux ratio RDC 2	N/A	N/A	X	N/A	N/A	N/A
Distillate rate COLCONV1	X	N/A	X	N/A	X	N/A
Distillate rate COLCONV2	N/A	N/A	X	N/A	X	N/A
Distillate rate RDC 1	N/A	N/A	X	N/A		N/A
Distillate rate RDC 2	N/A	N/A	X	N/A		N/A
Diameter COLCONV1	X	N/A	X	N/A	X	N/A
Diameter COLCONV2	N/A	N/A	X	N/A	X	N/A
Diameter RDC 1	N/A	N/A	X	N/A	X	N/A
Diameter RDC 2	N/A	N/A	X	N/A	X	N/A
Top Pressure COLCONV1	X	N/A	X	N/A	N/A	N/A
Top Pressure COLCONV2	N/A	N/A	X	N/A	N/A	N/A
Top Pressure RDC 1	N/A	N/A	X	N/A	N/A	N/A
Top Pressure RDC 2	N/A	N/A	X	N/A	N/A	N/A
Feed $SiCl_4$	N/A	N/A	X	N/A	X	N/A
Feed HCl	X	N/A	N/A	N/A	N/A	N/A
Reactive Distillation Stages RC1	N/A	N/A	N/A	X	N/A	N/A
Reactive Distillation Stages RC2	N/A	N/A	N/A	X	N/A	N/A
Holdup 1	N/A	N/A	X	N/A	N/A	N/A
Holdup 2	N/A	N/A	X	N/A	N/A	N/A
Total	7		29		13	

The sequences shown in Figures 2.2, 2.4, and 2.6 are the initial designs, these comply with the above-mentioned purities and will be sought to reduce their TAC.

2.4 Results

In this section we present the results of the optimization of each of the processes including the iteration results to show that a plateau is reached and the operating and design variables. Thus, we first show a Figure of the iterations vs TAC obtained for each case will be shown.

In order to illustrate what has been done in the optimization, the graphs of the iterations vs the TAC are presented (See Figure 2.8). We can see that the TAC decreases over the iterations and a good value is achieved for 40,000 iterations. This is taken to be a valid solution since there is not a significant decrease in the last evaluations. This demonstrates the robustness of the DETL method, showing the convergence and results corresponding to good solutions.

All the runs to carry out the optimization were performed on an Intel (R) Core™ i7-4790 CPU @ 3.6 GHz, 16 GB computer, the computing time for obtaining the optimal solutions was different according to the complexity of each process: The Siemens process required 28.2 hours, the FBR Union Carbide Process required 125.6 hours, and the Hybrid process required 127.2 hours. Tables 2.4-2.6 show the optimized variables for the units.

In the case of the Siemens configuration, it is possible to observe that only the optimization

of a single conventional column and the fresh feed of HCl to initiate the reaction of the reactor producing the silanes are performed. These parameters represent a substantial economic saving in the process, since the separation section always represents a high cost in any chemical process, and that the right amount of reactant represent large savings in the actual operation of the process. This can be seen in Figure 2.8a, where the initial configuration has a TAC of \$1.08 M/y, ending with a TAC of \$0.50 M/y, representing a saving of 53.28%.

The Intensified FBR Union Carbide Process has the highest number of decision variables to optimize. The optimization was carried out in two conventional columns, two reactive distillation columns, and the fresh feed stream of SiCl₄. In Figure 2.8b it can be seen that the TAC of the initial configuration is \$7.95 M/y and ending with \$2.57 M/y, saving 67.65%. The Hybrid Process shows the optimization of two conventional columns, and the fresh SiCl₄ feed. The initial configuration has a TAC of \$5.21 M/y, ending with \$1.95 M/y, saving 62.58% (see Figure 2.8c).

Since all three sequences are optimized, and with the same feed as mentioned in Table 2.1, a comparison can be made to find the best sequence for the production of Si_(SG). Table 2.7 shows, for all sequences, the capital cost, the TAC, the energy required and the products. Note the comparison between the TAC and the amount of products, mainly with the produced Si_(SG).

Table 2.4. Results of the Optimization of TAC for the Siemens Process.

	COLCONV1	REACTOR 1	REACTOR 2	REACTOR 3
Feed Stream flow (kg/h)	123.805 (SiCl ₄) 888.34 (SiHCl ₃) 0.0006 (SiH ₂ Cl ₂)	369.84 (C) 532.32 (SiO ₂)	204.66 (SiMG) 887.92 (HCl)	888.24 (SiHCl ₃)
Feed Stream temperature (K)	323.15	298.15	491.79	350.44
Output stream (kg/h)	Top 8.60e-6 (SiCl ₄) 888.24 (SiHCl ₃) 0.0006 (SiH ₂ Cl ₂) Bottom 123.805 (SiCl ₄) 0.09 (SiHCl ₃) 4.32 e-11 (SiH ₂ Cl ₂)	204.66 (SiMG) 76.23 (CO)	16.16 (H ₂) 123.81 (SiCl ₄) 888.34 (SiHCl ₃) 0.0006 (SiH ₂ Cl ₂) 64.28 (HCl)	55.25 (SiSG) 5.29 (H ₂) 779.886 (SiCl ₄) 47.82(HCl)
Output Stream temperature (K)	N/A	2273	533	1373
Number of stages	43	N/A	N/A	N/A
Feed stage	33	N/A	N/A	N/A
Reflux ratio	39.69	N/A	N/A	N/A
Distillate rate (kmol/h)	6.55	N/A	N/A	N/A
Reboiler heat duty (kW)	1630.76	N/A	N/A	N/A
Condenser heat duty (kW)	-1709.59	N/A	N/A	N/A
Diameter (m)	1.00	N/A	N/A	N/A
Top pressure (atm)	3.88	N/A	N/A	N/A
Bottom pressure (atm)	4.58	N/A	N/A	N/A
Top temperature (K)	350.44	N/A	N/A	N/A
Bottom temperature (K)	386.62	N/A	N/A	N/A
Fresh feed				
HCl (kg/h)		840.103		

Table 2.5. Results of the Optimization of TAC for the Intensified FBR Union Carbide Process.

	COLCONV1	COLCONV2	RDC1	RDC2	REACTOR 1	REACTOR 2	REACTOR 3	REACTOR 4	
Feed Stream flow (kg/h)	12,672.1 (SiCl ₄)	0.0054 (SiCl ₄)					151.27 (H ₂)		
	3,533.64 (SiHCl ₃)	3533.63 (SiHCl ₃)	1766.75 (SiHCl ₃)	1766.75 (SiHCl ₃)	369.84 (C) 532.32 (SiO ₂)	204.66 (Si _{MG}) 16,126.3 (SiCl ₄)	12,412.1(SiCl ₄)	200.53 (SiH ₄)	
	154.57 (SiH ₂ Cl ₂)	154.57 (SiH ₂ Cl ₂)					3,948.2 (SiHCl ₃)		
	Feed Stream temperature (K)	323.15	335.29	323.15	323.15	298.15	491.79	773	333
Output stream (kg/h)	Top	Top	Top	Top					
	0.0054 (SiCl ₄)	1.14e-3 (SiHCl ₃)	100.26 (SiH ₄)	100.27 (SiH ₄)					
	3533.63 (SiHCl ₃)	154.56 (SiH ₂ Cl ₂)				151.27 (H ₂)	151.27 (H ₂)	173.15 (Si _{5G})	
	154.57 (SiH ₂ Cl ₂)				204.66 (Si _{MG})	12,412.1(Si Cl ₄)	12,672.1(SiCl ₄)	24.86 (H ₂)	
	Bottom	Bottom	Bottom	Bottom	76.23 (CO)	3948.2 (SiHCl ₃)	3533.64 (SiHCl ₃)	49.50 (SiH ₄)	
	12,672 (SiCl ₄)	0.0054 (SiCl ₄)					154.57 (SiH ₂ Cl ₂)		
	0.01 (SiHCl ₃)	3533.49 (SiHCl ₃)	1674.45.1 (SiCl ₄)	1765.8.(SiCl ₄)					
	7.99e-6 (SiH ₂ Cl ₂)	0.01 (SiH ₂ Cl ₂)							
	Output Stream temperature (K)	N/A	N/A	N/A	N/A	2273	773	773	1273
	Number of stages	41	40	63	62	N/A	N/A	N/A	N/A
Feed stage	21	27	49	50	N/A	N/A	N/A	N/A	
Reflux ratio	12.82	47.73	85.56	86.23	N/A	N/A	N/A	N/A	
Distillate rate (kmol/h)	29.63	1.42	3.125	3.125	N/A	N/A	N/A	N/A	
Reboiler heat duty (kW)	950.77	241.69	949.42	951.34	N/A	N/A	N/A	N/A	
Condenser heat duty (kW)	-2751.04	-396.59	-928.23	-925.78	N/A	N/A	N/A	N/A	
Diameter (m)	1.02	1.06	1.00	1.00	N/A	N/A	N/A	N/A	
Top pressure (atm)	2.63	4.86	2.33	2.34	N/A	N/A	N/A	N/A	
Bottom pressure (atm)	3.32	5.55	2.65	2.65	N/A	N/A	N/A	N/A	
Top temperature (K)	335.29	332.22	177.84	177.65	N/A	N/A	N/A	N/A	
Bottom temperature (K)	372.85	365.04	364.56	363.59	N/A	N/A	N/A	N/A	
Reactive Stages	N/A	N/A	21-48	21-49	N/A	N/A	N/A	N/A	
Holdup (cum)	N/A	N/A	0.13	0.14	N/A	N/A	N/A	N/A	
Fresh feed									
SiCl ₄ (kg/h)	1123								

Table 2.6. Results of the Optimization of TAC for the Hybrid Process.

	COLCONV1	COLCONV2	REACTOR 1	REACTOR 2	REACTOR 3	REACTOR 4
Feed Stream flow (kg/h)	31,549.2 (SiCl ₄) 3533.64 (SiHCl ₃) 154.57 (SiH ₂ Cl ₂)	3.53 e-3 (SiCl ₄) 3532.65 (SiHCl ₃) 154.57 (SiH ₂ Cl ₂)	369.84 (C) 532.32 (SiO ₂)	204.66 (SiMG) 35,004.3(SiCl ₄)	151.27 (H ₂) 31,289.3 (SiCl ₄) 3948.2 (SiHCl ₃)	3533.43 (SiHCl ₃)
Feed Stream temperature (K)	323.15	357.23	298.15	491.79	773	359.93
Output stream (kg/h)	Top	Top				
	3.53 e-3(SiCl ₄)	0.2 (SiHCl ₃)		151.27 (H ₂)	151.27 (H ₂)	219.79 (Si ₆ G)
	3532.65(SiHCl ₃)	154.52 (SiH ₂ Cl ₂)	204.66 (SiMG)	31,289.3 (SiCl ₄)	31,549.2 (SiCl ₄)	21.03 (H ₂)
	154.57 (SiH ₂ Cl ₂)		76.23 (CO)	3948.2 (SiHCl ₃)	154.57 (SiH ₂ Cl ₂)	3,102.38 (SiCl ₄)
	Bottom	Bottom				
31,289 (SiCl ₄)	3533.43 (SiHCl ₃)			3533.64 (SiHCl ₃)	190.23 (HCl)	
0.95 (SiHCl ₃)	0.5 (SiH ₂ Cl ₂)					
4.79 e-6 (SiH ₂ Cl ₂)						
Output Stream temperature (K)	N/A	N/A	2273	773	773	1373
Number of stages	42	81	N/A	N/A	N/A	N/A
Feed stage	16	41	N/A	N/A	N/A	N/A
Reflux ratio	27.69	55.70	N/A	N/A	N/A	N/A
Reboiler heat duty (kW)	2141.79	335.21	N/A	N/A	N/A	N/A
Distillate rate (kmol/h)	31.24	1.53	N/A	N/A	N/A	N/A
Condenser heat duty (kW)	-5750.24	-505.63	N/A	N/A	N/A	N/A
Diameter (m)	1.02	1.00	N/A	N/A	N/A	N/A
Top pressure (atm)	4.49	4.21	N/A	N/A	N/A	N/A
Bottom pressure (atm)	5.18	4.90	N/A	N/A	N/A	N/A
Top temperature (K)	357.23	326.72	N/A	N/A	N/A	N/A
Bottom temperature (K)	392.25	359.93	N/A	N/A	N/A	N/A
Fresh feed						
SiCl ₄ (kg/h)			994.445			

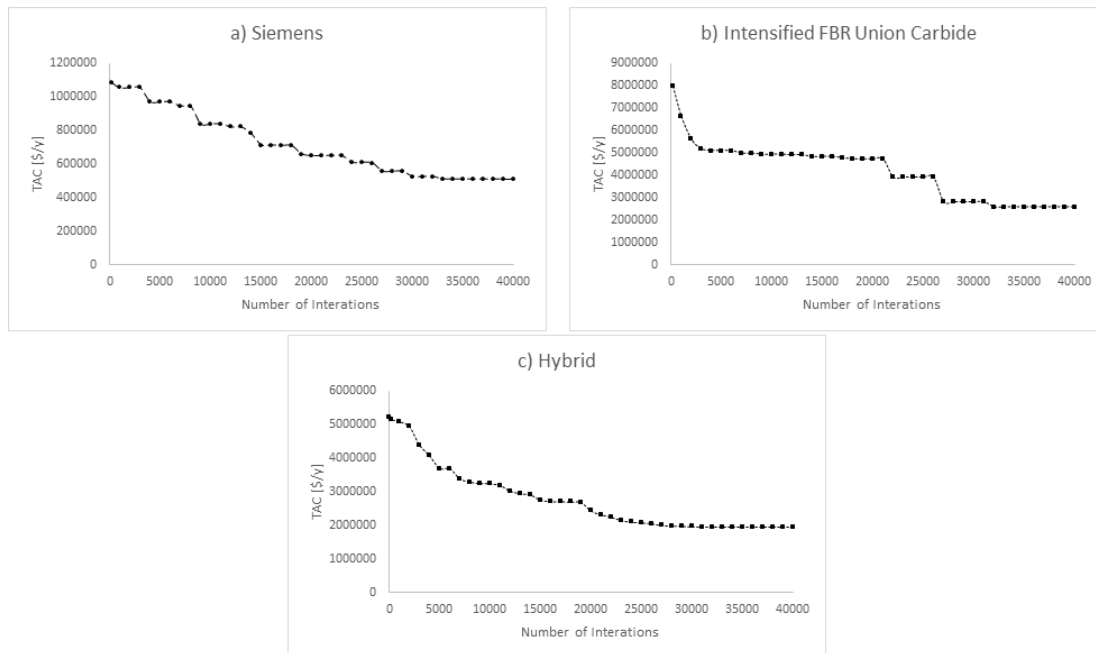


Figure 2.8. Optimization results of process sequences a) Siemens, b) Intensified FBR Union Carbide and c) Hybrid process.

Table 2.7. Comparative results for all process.

	Capital Cost			Products				
	[\$]	TAC [\$/y]	Q [kW]	Si _{s-g} [ton/y]	H ₂ [ton/y]	SiH ₂ Cl ₂ [ton/y]	SiCl ₄ [ton/y]	HCl [ton/y]
Siemens FBR	2,025,253.25	506,790.12	58,963.48	477.36	185.24	N/A	7807.88	N/A
Union Carbide	11,992,503.8	2,573,400.30	63,042.65	1,495.93	221.01	1,237.16	N/A	N/A
Hybrid	9,741,229.2	1,951,075.43	64,344.18	1,899.02	260.15	1,335.13	5762.88	1643.50

It can be observed that the optimized designs for the distillation columns and the reactive distillation columns, the number of stages and their heights are in concordance with the mechanical considerations in the design of distillation columns built so far (Górak and Olujic, 2014).

The least expensive process is the Siemens process. However, it also has the minimum annual production of Si_(SG) of 0.47 kt/y. The Intensified FBR Union Carbide process turns out to be the most expensive of the three proposed, with a large production of Si_(SG) of 1.49 kt/y, but it is not the best in this way. The Hybrid Process shows the highest production

of Si_(SG) of 1.89 kt/y, at a higher cost compared to the Siemens process, but lower than the Intensified FBR Union Carbide process. The final column of Table 2.8 shows the annual profits that are obtained by selling all products from each process, these benefits were considered before taxes. In this table we can see the profitability of the Hybrid Process, providing the largest benefits of all three processes. It is necessary to take into account that the Hybrid Process is the one that obtains larger amount of byproducts, which makes it to have larger profits. Figure 2.9 is very illustrative, it shows the potential of the hybrid process with the most important items.

Performing the analysis of the results the potential of the Hybrid Process could be observed, which could represent an incentive for the silicon industry. It is known that the processes Siemens and FBR Union Carbide, are technologies that have matured over time and are the ones usually used in the production of $Si_{(SG)}$, but the $Si_{(SG)}$ industry could benefit from novel alternatives such as the Hybrid Process.

Considering the environmental impact measured by the Eco-Indicator 99, Siemens process showed the lowest impact, 3.43 [MP/y], followed by the Hybrid process, 5.55 [MP/y]. Finally the intensified process shows an impact almost twice that of the Siemens process, see Figure 2.9. The reason for the difference in the environmental impact among the processes is due to the number of

units, in particular, the difference in the number of distillation columns. The index is directly related to the amount of steel required in construction. Thus, the smaller the number of units the less the steel used. Furthermore, distillation also involves large cooling and energy needs. Therefore, reducing the distillation columns, we reduce utilities consumption too.

Table 2.8. Prices of annualized products [Silicon solar grade (Sun&Wind Energy, 2017), hydrogen (Product Listing Policy a, 2017), dichlorosilane (Yaws et al., 1979), silicon tetrachloride (Product Listing Policy b, 2017), hydrogen chloride (Product Listing Policy c, 2017)].

	(a) $Si_{(SG)}$ [\$/y]	(b) H_2 [\$/y]	(c) SiH_2Cl_2 [\$/y]	(d) $SiCl_4$ [\$/y]	(e) HCl [\$/y]	Profit per sale [\$/y]
Siemens	6,172,264.80	2,060,511.68	N/A	19,519,704.00	N/A	27,245,690.36
FBR Union Carbide	19,342,369.73	2,458,398.22	184.71	N/A	N/A	19,227,552.36
Hybrid	24,554,330.67	2,893,770.85	199.342	14,407,200.00	575,225.00	40,479,650.43

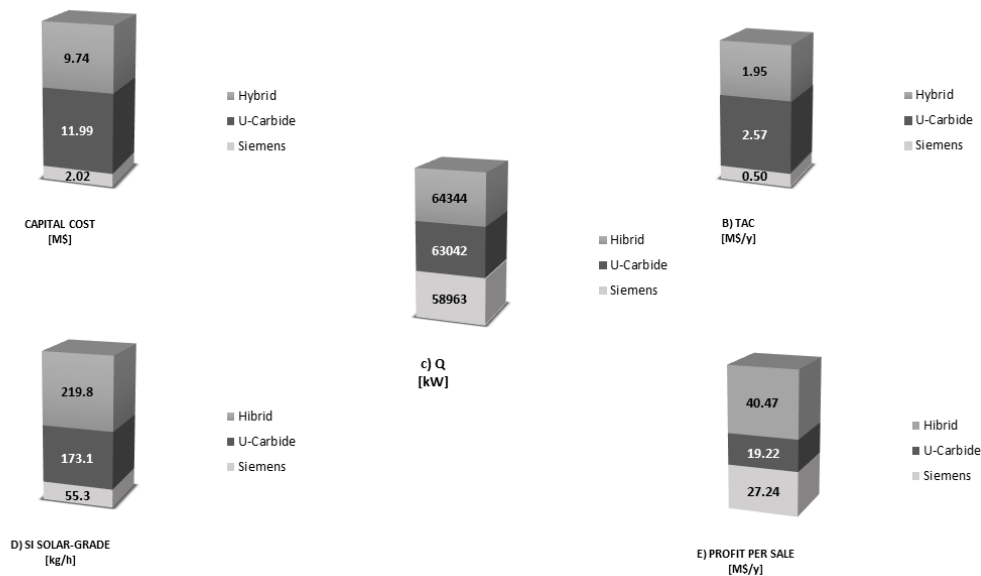


Figure 2.9. Results of capital cost, TAC, energy required, solar grade silicon, profit per sale, and Eco-Indicator of all configurations.

2.5 Conclusions

In this work, we performed a stochastic global optimization for the design of processes for $\text{Si}_{(\text{SG})}$ production to improve and compare their cost. The Siemens process is the base case, but it has been optimized, and two novel processes have been developed and optimized, an intensified process based on the one Union Carbide is using, where we substitute the distillation columns by a reaction distillation column and a Hybrid one combining Siemens and Union Carbide processes.

The results shows than the Siemens process presented the smallest TAC, but with the lowest production of $\text{Si}_{(\text{SG})}$. The Intensified FBR Union Carbide Process, showed the largest TAC due to the capital cost of the equipment and the heat duty for $\text{Si}_{(\text{SG})}$ purification. Finally the Hybrid Process exhibited a large production of $\text{Si}_{(\text{SG})}$, with a TAC between the one of the Siemens process and that of the Intensified FBR Union Carbide. Evaluating the TAC vs production of $\text{Si}_{(\text{SG})}$, it turned out that the Hybrid Process was the best of the three from the economic point of view. The Hybrid Process shows the largest profit from the sale of the multiple products resulting, with earnings of \$40.47 M/y. However, the environmental impact measured by the Eco-Indicator 99 showed that the Siemens process is the one with the lowest impact. The Hybrid process is the second best. It is expected that with this type of research can be made more competitive the technology based on $\text{Si}_{(\text{SG})}$, lowering the costs of the process and generating new research routes to be carried out for the industry of solar panels.

2.6 Appendix A2

The reactive distillation MESH equations are very similar to conventional distillation MESH equations. The main difference is the addition

of the reaction rate term in the total material balance and component material balance as well as the addition of the heat of reaction to total heat balance (Al-Arfaj, 1999). The reactive MESH equation are:

Total material balance

Total condenser

$$V_{NT} = D(1 + RR) \quad (2.18)$$

Tray j

$$V_{j-1} + L_{j+1} + F_j + \sum_i r_{i,j} = (L_j + U_j) + (V_j + W_j) \quad (2.19)$$

Reboiler

$$L_1 = B + V_B \quad (2.20)$$

Component material balance (Component i)

Total condenser

$$V_{NT}y_{i,NT} = D(1 + RR)x_{i,D} \quad (2.21)$$

Tray j

$$V_{j-1}y_{i,j-1} + L_{j+1}x_{i,j+1} + F_{i,j} + r_{i,j} = (L_j + U_j)x_{i,j} + (V_j + W_j)y_{i,j} \quad (2.22)$$

Reboiler

$$L_1x_{i,1} = Bx_{i,B} + V_By_{i,B} \quad (2.23)$$

Total energy balance

Total condenser

$$V_{NT}H_{NT} = D(1 + RR)h_D + Q_D \quad (2.24)$$

Tray j

$$V_{j-1}H_{j-1} + L_{j+1}h_{j+1} + F_{i,j}H_j^F + Q_j + \sum_i r_{i,j}H_j^R = (L_j + U_j)h_j + (V_j + W_j)H \quad (2.25)$$

Reboiler

$$L_1h_1 + Q_B = Bh_B + V_BH_B \quad (2.26)$$

Vapor Liquid Equilibrium equation

$$y_{i,j} = K_{i,j} x_{i,j} = \frac{\gamma_{i,j} P_{i,j}^{vap}}{P} x_{i,j} \quad (2.27)$$

Summation equation

$$\sum_i y_{i,j} = 1 \quad (2.28)$$

$$\sum_i x_{i,j} = 1 \quad (2.29)$$

where,

L_j = liquid flowrate of tray j

V_j = vapor flowrate of tray j

F_j = feed flowrate to tray j

U_j = liquid side stream flowrate of tray j

W_j = vapor side stream flow rate of tray j

$x_{i,j}$ = liquid mole fraction of component i in tray j

$y_{i,j}$ = vapor mole fraction of component i in tray j

$x_{F,i}$ = feed mole fraction of component i in tray j

h_j = liquid enthalpy of tray j

H_j = vapor enthalpy of tray j

H^F = feed enthalpy

Q_j = side heating or cooling rate of tray j

$\gamma_{i,j}$ = activity coefficient of component i in tray j

$P_{i,j}^{vap}$ = vapor pressure of component, i in tray j

P = total pressure

$r_{i,j}$ = reaction rate of component i in tray j

H_j^R = heat of reaction in tray j.

2.7 Acknowledgements

The authors acknowledge CONACyT (Mexico), Universidad de Guanajuato and Salamanca Research for software licenses and the project DPI2015-67341-C2-1-R.

2.8 References

- Al-Arfaj, M., 1999. Quantitative heuristic design of reactive distillation. MSc Thesis. Lehigh University.
- Barbouche, M., Hajji, M., Ezzaouia, H., 2016. Electric arc furnace design and construction for metallurgical and semiconductor research. Int. J. Adv. Manuf. Technol., 82(5-8), 997-1006.
- Bououdina, M., 2014. Handbook of research on nanoscience, nanotechnology, and advanced materials. IGI Global, 119-126.
- Braga, A. F. B., Moreira, S. P., Zampieri, P. R., Bacchin, J. M. G., Mei, P. R., 2008. New processes for the production of solar-grade polycrystalline silicon: A review. Sol. Energ. Mat. Sol. C, 92(4), 418-424.
- Brage, F. J. P., 2003. Contribución al modelado matemático de algunos problemas en la metalurgia del silicio. PhD Thesis. Universidad de Santiago de Compostela.
- Del Coso, G., Tobias, I., Canizo, C., Luque, A., 2007. Temperature homogeneity of polysilicon rods in a Siemens reactor. J. Cryst. Growth, 299(1), 165-170.
- Díez, E., Rodríguez, A., Gómez, J. M., Olmos, M., 2013. Distillation assisted heat pump in a trichlorosilane purification process. Chem. Eng. Process., 69, 70-76.
- Erickson, C. E., and Wagner, G. H., 1952. U.S. Patent No. 2,595,620. Washington, DC: U.S. Patent and Trademark Office.
- Farrow, R. F. C., 1974. The Kinetics of Silicon Deposition on Silicon by Pyrolysis of Silane A Mass Spectrometric Investigation by Molecular Beam Sampling. J. Electr. Soc., 121(7), 899-907.

- Ginley D., M.A. Green, R. Collins, 2008. Solar energy conversion toward 1 terawatt. *Mrs Bulletin*, 33(04), 355-364.
- Górák, A., Olujic, Z., 2014. *Distillation: equipment and processes*, first ed. Elsevier, Oxford.
- Guillen-Gosalbez, G., Caballero, J. A., Jimenez, L., 2008. Application of life cycle assessment to the structural optimization of process flowsheets. *Industrial & Engineering Chemistry Research*, 47(3), 777-789.
- Guthrie, K. M., 1969. Capital cost estimating. *Chemical Engineering*, 24, 114.
- Jain, M. P., Sathiyamoorthy, D., Rao, V. G., 2011. Studies on hydrochlorination of silicon in a fixed bed reactor. *Indian Chemical Engineer*, 53(2), 61-67.
- Kotzsch, H. J., Vahlensieck, H. J., Josten, W., 1977. U.S. Patent No. 4,044,109. Washington, DC: U.S. Patent and Trademark Office.
- List of World's Polysilicon Producers According to Country for Last 3, 2013. <http://studylib.net/doc/8255119/list-of-world-s-polysilicon-producers-according-to-countr>.
- Müller, A., Ghosh, M., Sonnenschein, R., Woditsch, P., 2006. Silicon for photovoltaic applications. *Mat. Sci. Eng. B*, 134(2), 257-262.
- Payo, M. J. R., 2009. Purificación de triclorosilano por destilación en el proceso de obtención de silicio de grado solar. PhD Thesis. Universidad Complutense de Madrid
- Pazzaglia, G., Fumagalli, M., Kulkarni, M., 2011. U.S. Patent Application No. 13/084,243. Washington, DC: U.S. Patent and Trademark Office.
- Product Listing Policy (a), 2017. https://www.alibaba.com/product-detail/High-purity-Hydrogen-GasArgonGas_60005508312.html?spm=a2700.7724838.0.0.OBxkVL&s=p.
- Product Listing Policy (b), 2017. https://www.alibaba.com/product-detail/Tetrachlorosilane_1301683533.html.
- Product Listing Policy (c), 2017. https://www.alibaba.com/product-detail/Low-Price-Hydrochloric-Acid-For-Organic_60350455133.html
- Ramírez-Márquez, C., Sánchez-Ramírez, E., Quiroz-Ramírez, J. J., Gómez-Castro, F. I., Ramírez-Corona, N., Cervantes-Jauregui, J. A., Segovia-Hernández, J. G., 2016. Dynamic behavior of a multi-tasking reactive distillation column for production of silane, dichlorosilane and monochlorosilane. *Chem. Eng. Process.*, 108, 125-138.
- Ranjan, S., Balaji, S., Panella, R. A., Ydstie, B. E., 2011. Silicon solar cell production. *Comp. Chem. Eng.*, 35(8), 1439-1453.
- Sadique, S. E., 2010. Production and Purification of Silicon by Magnesiothermic Reduction of Silica Fume. MSc Thesis. University of Toronto.
- Schei, A., Tuset, J. K., Tveit, H., 1998. Production of high silicon alloys. Tapir. Trondheim, Norway.
- Søiland, A. K., 2005. Silicon for solar cells. PhD Thesis NTNU
- Solar Market Insight Report, 2016. <http://www.seia.org/research-resources/solar-market-insight-report-2016-q2>.
- Srinivas, M., Rangaiah, G. P., 2007a. Differential Evolution with Tabu List for Solving Nonlinear and Mixed-Integer Nonlinear Programming Problems. *Ind. Eng. Chem. Res.*, 46, 7126–7135.
- Srinivas, M., Rangaiah, G. P., 2007b. Differential evolution with tabu list for global optimization and its application to phase equilibrium and parameter estimation problems. *Ind. Eng. Chem. Res.* 46(10), 3410-3421.

- Sun&Wind Energy, 2017. <http://www.sunwindenergy.com/photovoltaics/polysilicon-market-2020>.
- TEAM and DEAM, 1998. http://www.ecobalance.com/uk_team.php
- Tejero-Ezpeleta, M. P., Buchholz, S., Mleczko, L., 2004. Optimization of Reaction Conditions in a Fluidized-Bed for Silane Pyrolysis. *Can. J. Chem. Eng.*, 82 (3), 520-529.
- Turton, R. Bailie, R. C.; Whiting, W. B.; Shaeiwitz, J. A., 2009. *Analysis, Synthesis and Design of Chemical Process*, 3rd ed. Prentice Hall, USA.
- Ulrich, G. D., 1984. *A guide to chemical engineering process design and economics*; first ed. Wiley: New York.
- Vidal, M., Martín, M., 2014. Planta de producción de silicio para módulos fotovoltaicos. *Era Solar. Fototérmica y Fotovoltaica*. 180, Año XXXII. 24-35.
- Yaws, C. L., Jelen, F. C., Li, K. Y., Patel, P. M., Fang, C. S., 1979. New technologies for solar energy silicon: cost analysis of UCC silane process. *Solar Energy*, 22(6), 547-553.
- Yaws, C. L., Li, K. Y., Chou, S. M., 1986. Economics of polysilicon processes. Lamar University, Beaumont, Texas 77710, U.S.A., N86-26683, 79-122.

3

Safety, Economic and Environmental Optimization Applied to Three Processes for the production of solar grade silicon

ACS
Sustainable
Chemistry & Engineering

Research Article

Cite This: *ACS Sustainable Chem. Eng.* 2019, 7, 5355–5366

pubs.acs.org/journal/ascecg

Safety, Economic, and Environmental Optimization Applied to Three Processes for the Production of Solar-Grade Silicon

César Ramírez-Márquez,[†] Gabriel Contreras-Zarazúa,[†] Mariano Martín,^{‡,§} and Juan Gabriel Segovia-Hernández^{*,†,§}

[†]Universidad de Guanajuato, Campus Guanajuato, División de Ciencias Naturales y Exactas, Departamento de Ingeniería Química, Noria Alta S/N, 20256 Guanajuato Gto., México

[‡]Universidad de Salamanca, Departamento de Ingeniería Química, Pza. Caldos 1-5, 37008 Salamanca, España

 Supporting Information

3 Safety, Economic and Environmental Optimization Applied to Three Processes for the production of solar grade silicon

Abstract

In this work, we present the optimization of three different processes to obtain solar grade silicon, including considerations of safety, economic and environmental impact in the design stage of the process. Safety is involved through the individual risk index (IR), the economy with the return on investment (ROI), and the environmental impact with the eco-indicator 99 (EI99). The design of the Siemens Process turned out to be the one that obtained the best safety, profitability and environmental indexes, despite having the lowest solar-grade silicon production, being four times lower than the Hybrid Process. The results shown a similar profitability values between the Hybrid Process (15.21%) and the Intensified FBR Union Carbide Process (15.38%). In general, due to the high demand of the product of interest and under the premise of a safe process, the Hybrid Process can be chosen as an option for its industrial implementation.

3.1 Introduction

There is a growing awareness of the importance of including safety and environmental impact issues in industrial process design (Guillen-Cuevas et al., 2017). This is due to the fact that the greatest challenges that presents today society, they go together with pollution issues, scarcity of resources, and global warming issues (Huang and Peng, 2014). Consequently the safety risks in the industrial process and the derivations that represent a fault in this, as well as the environmental impact generated an industrial process, becomes a focal point to the industrial development long-term.

In last decade, have been achieved significant advances in recognition and understanding in the problems related with the safety and environmental impact in industries. Nowadays, the manufacturing process safety and environmental impact of most products are widely studied and practiced. Nevertheless, there is much to do, since the safe and clean engineering practice has shown its potential for being applied more broadly, deep and systematic (Huang and Peng, 2014).

One of the main objectives of the incorporation of safety, environmental and profitability criteria of any process, is closing the gap between research and

technological development; i.e. the strengthening between the academic and industrial world. An investigation key area is the energy renewable industry and the challenges that represents.

The increase of the global energy demand served as a driver to find an alternative and renewable energy sources. Therefore the photovoltaic solar energy has inverted its penetration in the market following an issue in the efficiency and reduction in the costs.

The solar silicon production is a key step in the photovoltaic industry. The solar grade silicon (Si_{SG}) production should care besides an economic aspect, the process safety as well as the environmental aspect. The Si_{SG} production can be carried mainly through two routes. The first route following a metallurgic approach, which combines a series of refining stages, as well as a solidification stage (Safarian et al., 2012). This approach involves several stages in batches which causes difficulties in the operation, the process dynamics, the reduction of energy costs and also several issues with the environmental normative. The second route is the solar grade silicon production following chemical methods, which have the advantage of producing better quality solar grade silicon (Chigondo, 2018). The Chemical methods essentially involve two known ways. The Siemens process, where the metallurgical silicon treated with hydrochloric acid (HCl) to produce trichlorosilane (SiHCl_3). Then a hydrogenated reduction helps obtain solar grade silicon. Similarly is the Union Carbide process, consisting of the production of the metallurgical silicon using the silicon tetrachloride (SiCl_4) reaction to produce trichlorosilane, which by a series of redistribution reactions produce Silane (SiH_4), which is carried to a vapor deposition reactor where it decomposes to produce solar grade silicon (Ramírez-Márquez et al., 2018). The main problems of the chemical routes are the high consumption of energy,

the safety risk presented by the processes while the chlorosilanes production implies an environmental hazard. These compounds are toxic and corrosive, therefore represent safety and environmental problems (Chigondo, 2018).

In the production of good quality silicon the chemical routes are mostly used worldwide, because of the operational advantages that deliver (Braga et al., 2008). However the chemical routes for the production of solar grade silicon are subjected to several safety and environmental issues. The silicon production requires high temperatures that constitutes a hazard and results extremely expensive and need a lot of energy and further produce large amounts of waste (Coalition, 2009).

The safety environment likewise plays an important role in this kind of process, such is the case of silane gas (SiH_4) that represents a significant risk in solar grade silicon production on Union Carbide process because is extremely explosive and is dangerous to workers and communities. It is known that accidental releases of silane explode spontaneously and semiconductor industry reports several silane incidents every year (Coalition, 2009).

Another substances that represents a risk are silicon tetrachloride (SiCl_4) and hydrochloric acid (HCl), as they are extremely toxic, corrosive and the first one reacts violently with water. Nevertheless, the HCl can be easily recovered and reused as inputs for the silane production, to not constitute an extreme safety and environmental hazard. Washington Post reported in 2008, the silicon manufacture is increasing rapidly in China but the infrastructure to recycle the silicon tetrachloride and other toxic products do not follow the rhythm (Coalition, 2009).

Building on the description above, it is extremely important to consider environmental and safety issues in the

design of the solar grade silicon production plants. In this work, the inherent safety is a fundamental part for select a design. The inherent safety has become a valuable concept in process design the last years, since it provides necessary information to avoid and prevent possible incidents (Medina-Herrera et al., 2014). The objective of this work is the optimization of three process to obtain solar grade silicon, considering safety (IR), profitability (ROI) and environmental (EI99) aspects in order to provide the current industrial needs. This procedure results in a multiobjective optimization problem, in which safety, profitability and environmental metrics are conflicting factors that must be minimized and maximized in the case of profitability.

3.2 Methodology

The present section shows the multiobjective optimization methodology of the three process to obtain solar grade silicon, developed in Ramírez-Márquez et al., (2018) In general terms it will show a briefly explanation of the process, how the optimization is done and the description of each objective function.

3.2.1 Process for obtaining solar grade silicon

The process shown by Ramírez-Márquez et al., (2018) are: Siemens, Intensified FBR Union Carbide Process and Hybrid (See Figures 3.1 and 3.2). The procedure to elaborate diagrams of process it is described in Ramírez-Márquez et al., (2018), there it is shown the modules used in Aspen Plus V8.4, the amount of raw material, as well as the considerations used for the assembly of each process.

In general, the processes are described as follows:

3.2.1.1 Siemens Process

This process uses SiO_2 as raw material. The first stage is to produce metallurgic silicon

via SiO_2 reduction with coal. An electric arc furnace is the unit used for this transformation (Ranjan et al., 2011). The purity achieved for metallurgic grade silicon, $\text{Si}_{(\text{MG})}$ is around 98-99%. The $\text{Si}_{(\text{MG})}$, H_2 and HCl are fed to the fluidized bed for the production of chlorosilanes. The exit stream is fractionated. The hydrogen (H_2) and hydrochloric acid (HCl) are removed when chlorosilanes condense. Then, a distillation column is used to split the liquid stream of SiHCl_3 and SiCl_4 . The bottoms, SiCl_4 , is a byproduct of the process while from the top a stream 99.99% SiHCl_3 is obtained (Díez et al., 2013). This purity is good enough to feed the stream to the chemical vapor deposition reactor of the Siemens process. The production of solar grade silicon uses the SiHCl_3 and hydrogen via chemical vapor deposition. U shape bars of ultrapure silicon are used as seed. These bars are heated up using electric current. After silicon deposition, by products of HCl , H_2 and SiCl_4 are obtained. We cool down the silicon with an exchanger to ambient temperature and the gases are separated by a set of equipment, to be recycled to the process.

3.2.1.2 Intensified FBR Union Carbide Process

The stage to obtain the $\text{Si}_{(\text{MG})}$ is the same as for the Siemens Process. The $\text{Si}_{(\text{MG})}$ is hydrogenated together with SiCl_4 in a fluidized bed reactor. The stream of products is treated by a flash module to separate the chlorosilanes and others gases, such as the hydrogen. Afterward, the stream consisting mainly of trichlorosilane and tetrachlorosilane, is fed to a two distillation columns. We obtain a high purity SiCl_4 from the bottoms of the first column stream, which is recycled. In the other column we obtain high purity trichlorosilane bottom product that will be fed to the reactive distillation column. Nevertheless, trichlorosilane disproportion reactions are carried out in a reactive

distillation column. High purity trichlorosilane is fed to the new intensified process, the reactive distillation system. The column produces high purity silane over the top that is fed to the chemical vapor deposition reactor to produce high purity silicon and hydrogen (Farrow, 1974). We model a stoichiometric reactor when the silane conversion reaches 80% (Tejero-Ezpeleta et al., 2004). The product stream is separated to isolate the polysilicon from the gases. Polysilicon is solidified while the gases, mainly H_2 and HCl , are recycled.

3.2.1.3 Hybrid Process

The production of $Si_{(MG)}$ is carried out as in previous cases, by means of the carboreduction of SiO_2 . Then, an FBR is used for the hydrogenation of $Si_{(MG)}$ and $SiCl_4$. The process in the beginning requires a fresh feed of $SiCl_4$ for its operation. We obtained and separated a solids, non-condensables and a mixture of di, tri and tetrachlorosilane. Two distillation columns are used to separate the mixture of chlorosilanes. From the top of the first column we obtain di and trichloro silane while from the bottoms we use tetrachlorosilane with traces of $SiHCl_3$ that will be removed, so that it is recycled to the process. The second column, separates the mixture of $SiHCl_2$ and $SiHCl_3$, and we obtaining from the bottom $SiHCl_3$ of high purity. After that, we uses the $SiHCl_3$ as feed for the chemical Siemens vapor deposition reactor. Next of the deposition, HCl and hydrogen are separated from the $Si_{(SG)}$. Both streams are cooled down.

3.3 Optimization

The process shown above were optimized by an hybrid algorithm called differential evolution with Taboo List (DETL). Generally, to evaluate a process are use an economic indicators, although in recent years, has been done a big effort to incorporate environmental impact and safety indicators in an evaluation, thus increasing the depth

of the analyzes. In particular, the silicon photovoltaic industry needs to be evaluated in the three items to continue growing and it is thought of sustainable systems. Simply, said objective functions are required to industry acquire practices that supports a profitable, clean and safe process.

Unlike the economic aspect, the environmental and safety indicators are hindered due to problems related with the lack of availability and reliability of data. It is therefore that the objective functions were chosen: ROI, Eco-indicator 99 and IR, since they result suitable and reliable indicators for the three aspects analysis.

This optimization methodology allows incorporated conflicting objective functions, trying to obtain more profitable design, respectful with the environment and good in safety terms.

Below the optimization indexes are described and the multiobjective optimization. The adequate conditions obtained in each process optimization must consider several aspects such as profitability, the environmental impact, and the incorporating a safety factor, which entail an important optimization issue.

3.3.1 Return on Investment (ROI)

The use of the return on investment (ROI) as economic objective allows observe the economic performance of the process since shows the investment planning problems.

The most simplify equation of ROI is the following:

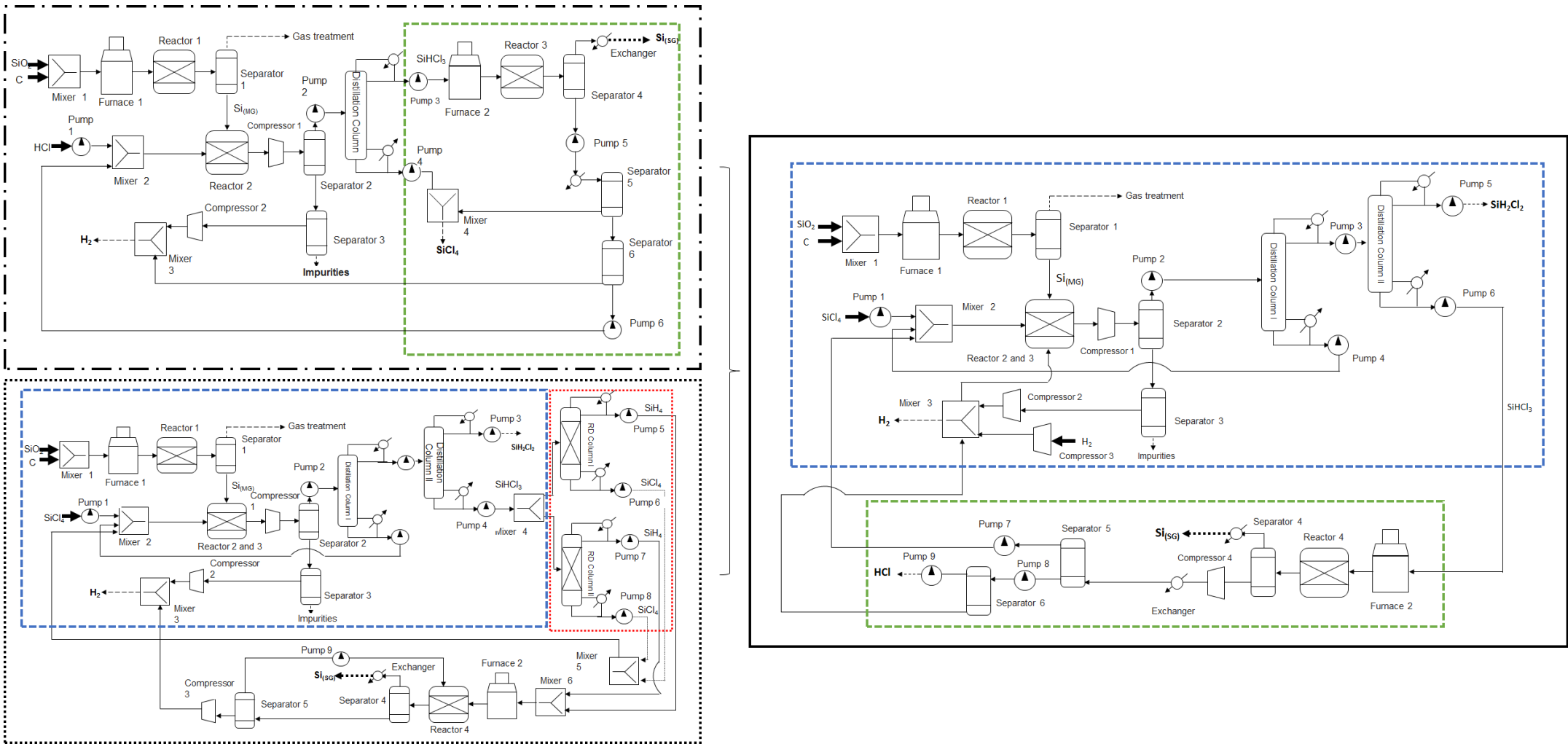


Figure 3.1. Flowcharts of Siemens Process (— · —), Intensified FRB Union Carbide (·····) and Hybrid (——).

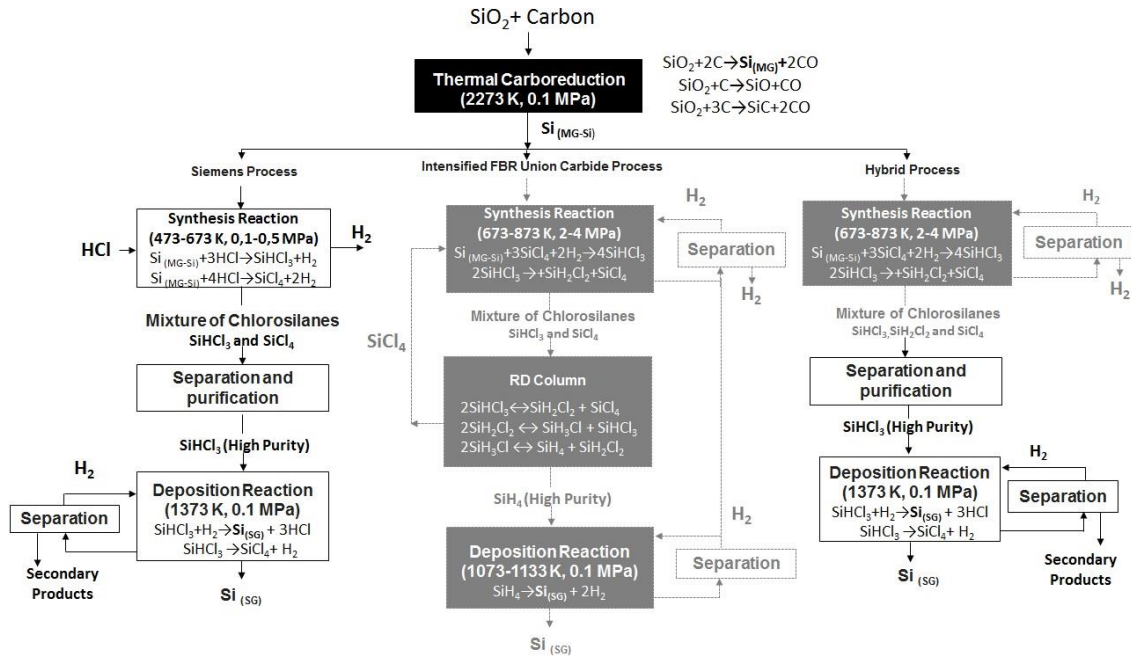


Figure 3.2. Siemens Process, Intensified FRB Union Carbide and Hybrid.

$$ROI = \frac{\sum_{i=1}^N CF_i / N}{I}, \quad (3.1)$$

where, CF_i is the after taxes cash flow, I is the capital investment, N is the number of years of the project, is used an average value of the after taxes revenues (Sánchez-Ramírez et al., 2016).

3.3.2 Environmental index

In this work, an eco-indicator 99 (EI99) was used to evaluate the environmental impact. The EI99 is a methodology based on the life cycle assessment (LCA), where the hierarchical weighting in the relative evaluation of the damage is reasoned.

The EI99 makes possible the environmental load evaluation associated with: a process, a product or an activity, that identifies and quantifies the material and the energy used. This methodology have been used by many authors in recent years (Gebreslassie et al., 2009; Errico et al., 2017).

The EI99 methodology consider three mains categories of impact: (1) human health, (2) ecosystem quality, and (3) resources depletion. The following elements are elect to compute EI99: steel to build equipment and important accessories, the steam used to produce heat and pumping electricity. The associated data with these activities were taken from the standard databases (Goedkoop and Spriensma, 2018).

The EI99 is define in the following equation:

$$EI99 = \sum_b \sum_d \sum_{k \in K} \delta_d \omega_d \beta_b \alpha_{b,k} \quad (3.2)$$

Where, δ_d is the normalization factor for damage of category d , ω_d is the weighting factor for the damage of category d , β_b represents the total amount of chemical product b released per unit of reference flow due to direct emissions, $\alpha_{b,k}$ is the damage caused in category k per unit of chemical product b released to the environment.

One point on the EI99 scale represents one thousandth part of the annual environmental loads of an average European citizen (Goedkoop and Spriensma, 2018).

3.3.3 Safety index

In this work the individual risk (IR) index was used for the process safety quantification. The IR defines the risk that has a person

depending on its position, implicate frequency occurrence and a probability of death or injuries that could be caused by an accident. The IR is defined as follows:

$$IR = \sum f_i P_{x,y} \quad (3.3)$$

Where, f_i is the frequency in which the accident can happen; $P_{x,y}$ is the affection probability in a specific area.

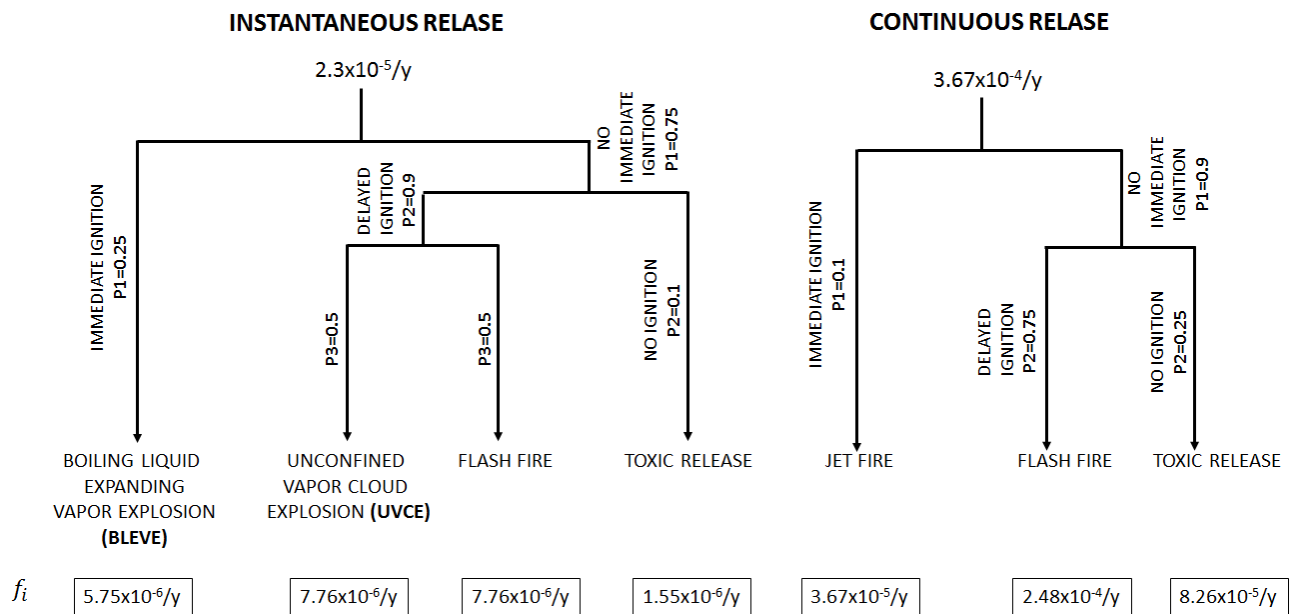


Figure 3.3. Possible accidents and frequencies that can happen in a process.

The use of a qualitative risk analysis (QRA) allows identifying the affection frequency and probability of the potential incidents and accidents, as well as possible consequences that may have. The first step of the QRA methodology is to identify the incidents. Incident is defined as any material or energy release in the process (Kumar, 1996). The Figure 3.3 displays the possible accidents and the frequencies that can happen in a process. Once identified possible accidents, we proceed to variable identification that causes this. Kumar, (1996) tell us that the BLEVE, Jet Fire, and Flash Fire, have like causative variable the thermal radiation (E_r). For UVCE, the overpressure (P_o) is the reason; and finally

for the Toxic Release the release concentration de la is the cause.

The probable accidents and causative variables calculations of each accident are shown in Appendix A.

3.4 Multi-objective function

Taking into account the profitability, environmental and safety indexes described above, the objective function can be written like the following:

$$\begin{aligned} \text{Min}(-ROI, EI99, IR) = \\ f(N_{tn}, N_{fn}, R_{rn}, F_{tn}, D_{tn}, P_{tn}, R_{tn}^*, H_R^*) \\ \text{Subject to } x_m^{\rightarrow} > y_m^{\rightarrow} \end{aligned} \quad (3.4)$$

where N_{tn} are total column stages, N_{fn} is the feed stages in column, R_{rn} is the reflux ratio, F_{rn} is the distillate fluxes, D_{cn} is the column diameter, P_{tn} is the top pressure, R_{tn} are the reactive stages, HR is the holdup (these last two in the case of reactive distillation), y_m^{\rightarrow} and x_m^{\rightarrow} are vectors of obtained and required purities for the m components, respectively. The results must satisfy each restriction of purity of at least 99.999% of each output component. All design

variables for the cases of study are described in Table 3.1. From Górak and Olujić (2014), it can be observed that the boundaries of the values of the design variables in the optimization for the distillation columns and the reactive distillation columns, the number of stages and their heights are in concordance with the mechanical considerations in the design of distillation columns built so far.

Table 3.1. Decision Variables Used in the Global Optimization of Process Routes for SiSG Production.

Decision Variables	Siemens Process		Intensified FBR Union Carbide Process		Hybrid Process	
	Continuous	Discrete	Continuous	Discrete	Continuous	Discrete
Number of stages COLCONV1	N/A	X	N/A	X	N/A	X
Number of stages COLCONV2	N/A	N/A	N/A	X	N/A	X
Number of stages RDC 1	N/A	N/A	N/A	X	N/A	N/A
Number of stages RDC 2	N/A	N/A	N/A	X	N/A	N/A
Feed stages COLCONV1	N/A	X	N/A	X	N/A	X
Feed stages COLCONV2	N/A	N/A	N/A	X	N/A	X
Feed stages RDC 1	N/A	N/A	N/A	X	N/A	N/A
Feed stages RDC 2	N/A	N/A	N/A	X	N/A	N/A
Reflux ratio COLCONV1	X	N/A	X	N/A	X	N/A
Reflux ratio COLCONV2	N/A	N/A	X	N/A	X	N/A

Reflux ratio RDC 1	N/A	N/A	X	N/A	N/A	N/A
Reflux ratio RDC 2	N/A	N/A	X	N/A	N/A	N/A
Distillate rate COLCONV1	X	N/A	X	N/A	X	N/A
Distillate rate COLCONV2	N/A	N/A	X	N/A	X	N/A
Distillate rate RDC 1	N/A	N/A	X	N/A		N/A
Distillate rate RDC 2	N/A	N/A	X	N/A		N/A
Diameter COLCONV1	X	N/A	X	N/A	X	N/A
Diameter COLCONV2	N/A	N/A	X	N/A	X	N/A
Diameter RDC 1	N/A	N/A	X	N/A	X	N/A
Diameter RDC 2	N/A	N/A	X	N/A	X	N/A
Top Pressure COLCONV1	X	N/A	X	N/A	N/A	N/A
Top Pressure COLCONV2	N/A	N/A	X	N/A	N/A	N/A
Top Pressure RDC 1	N/A	N/A	X	N/A	N/A	N/A
Top Pressure RDC 2	N/A	N/A	X	N/A	N/A	N/A
Feed SiCl ₄	N/A	N/A	X	N/A	X	N/A
Feed HCl	X	N/A	N/A	N/A	N/A	N/A
Reactive Distillation Stages RC1	N/A	N/A	N/A	X	N/A	N/A
Reactive Distillation Stages RC2	N/A	N/A	N/A	X	N/A	N/A
Holdup 1	N/A	N/A	X	N/A	N/A	N/A
Holdup 2	N/A	N/A	X	N/A	N/A	N/A
Total	7		29		13	

3.5 Methodology for Global Optimization

All the processes were optimized individually using the stochastic hybrid optimization method called Differential Evolution with Tabu List (DETL). The stochastic methods are attractive for the optimization complex problems, high non-linear and potentially non-convex (Ramírez-Márquez et al., 2018). For the reason that of the complexity of the problem, DETL was used as the optimization algorithm. The DETL method was recently used in similar works (Errico et al., 2017; Sánchez-Ramírez et al., 2017; Contreras-Zarazúa et al., 2017). It is a method based on the natural selection theory (Ramírez-Márquez et al., 2018; Srinivas and Rangaiah, 2007). Although initially the differential evolution (DE) methods were only suited to solve one unique objective function, over time they adapted to solve multiobjective problems (Madavan and Biegel, 2002). Glover et al., (1989) gave us the Tabu List (TL) concept, which permit us have a register of the search area and avoid that repeats search spaces.

The optimization with the DETL method was carried out by means of a hybrid platform that includes Microsoft Excel and Aspen Plus. Where basically the vector of variables of decision is sent from Microsoft Excel to Aspen Plus through DDE (Dynamic Data Exchange) through COM technology.

There the values are assigned to the process variables in Aspen Plus Modeler, to perform the simulation. Once the simulation is done, Aspen Plus return the exit values to Microsoft Excel like a result vector that contains the exit data. Finally, Microsoft Excel analyze the objective function values and propose new values of variables of decision according to DETL methodology.

For this study, the following parameters have been used for the DETL method: 834

generations, 120 individuals, a Tabu list size of 60 individuals, a Tabu radius of 0.01, Crossover fractions (Cr): 0.8, Mutation fractions (F): 0.3, respectively. The parameters were obtained via preliminary calculations, as shown in the methodology of Srinivas and Rangaiah, (2007).

In each of the iterations is calculated the three indexes for each of the units such as the reactor vessel, ovens, separators, mixers, heat exchangers, bombs (pumps) and compressors. The unit's indexes depends of their size and operating cost.

3.6 Results

This section shows the optimization results performed by the three processes mentioned above. The Pareto fronts were obtained after 100,000 evaluations, observing that there are no significant improvements after this number of evaluations. The optimization executions were carried out in a computer equipment with the following specifications: AMD Ryzen™ 5-1600 @3.2GHz, and 16GB of RAM computer, the computing time for obtaining the optimal solutions was different according to the complexity of each process: The Siemens process required 168 hours, the FBR Union Carbide Process required 432 hours, and the Hybrid process required 260 hours.

In Figure 3.4 can be compare the three processes around the profitability with the ROI indicator and environmental impact with the EI99 indicator. For the case of Siemens Process, it can be observed that the higher profitability, the less is the environmental indicator. In the other two processes Intensified FRB Union Carbide and Hybrid, can be seen that even though the ROI is the same, and the EI99 increases considerably for the hybrid process case. It can be observed that the Hybrid Process would be a process with less environmental impact than the FRB Union Carbide Process due to the amount of equipment required

by each process. However, the Hybrid Process has more EI99 points, due to the amount of by-products (SiCl_4 and HCl) that are generated in final reactor. Affecting the human health and ecosystem quality factors in the calculation of EI99.

Figure 3.5 shows the Pareto between IR and EI99 objectives. Similarly, the Siemens Process shows a desired behavior. It presents a better safety, and lower environmental risk. For the Intensified FRB Union Carbide process, something different occurs. The lower the environmental index, the larger the risk in terms of process safety. The increase in the IR index in the FRB Union Carbide is due to the incorporation of the SiH_4 compound, which increases the frequency and the affectation probability of some accident in the process. Being a gas that ignites spontaneously in the air and that in case of blow up cannot be extinguished according to the data of the safety sheet. A different behavior can be observed for the Hybrid Process. Since while present the worst environmental index, it is the second best process in safety terms. The worst EI99 is due to the steel amount to

build, and electricity consumption for pumping the high flows of raw material to get the adequate Si_{SG} amount. The Hybrid Process has an adequate safety behavior, due to the avoidance of the use of SiH_4 in the de Si_{SG} production, since this turns out to be a pretty dangerous and toxic material, which together with the reactive distillation processes, increase the danger of the Intensified FRB Union Carbide process.

In Figure 3.6 it can be observed the Pareto Front of IR versus the ROI. As in previous results, the Siemens Process are shows a desirable behavior. Larger profitability and less danger in safety terms. The Hybrid and Intensified FRB Union Carbide Processes practically present the same ROI with a considerable difference of security. So that the IR for Intensified FRB Union Carbide process is twice as high as the Hybrid process, considering as mentioned earlier, the affectation of SiH_4 compound in the reactive distillation as the main reason, that increases greatly the frequency and the affectation probability of some accident in the process.

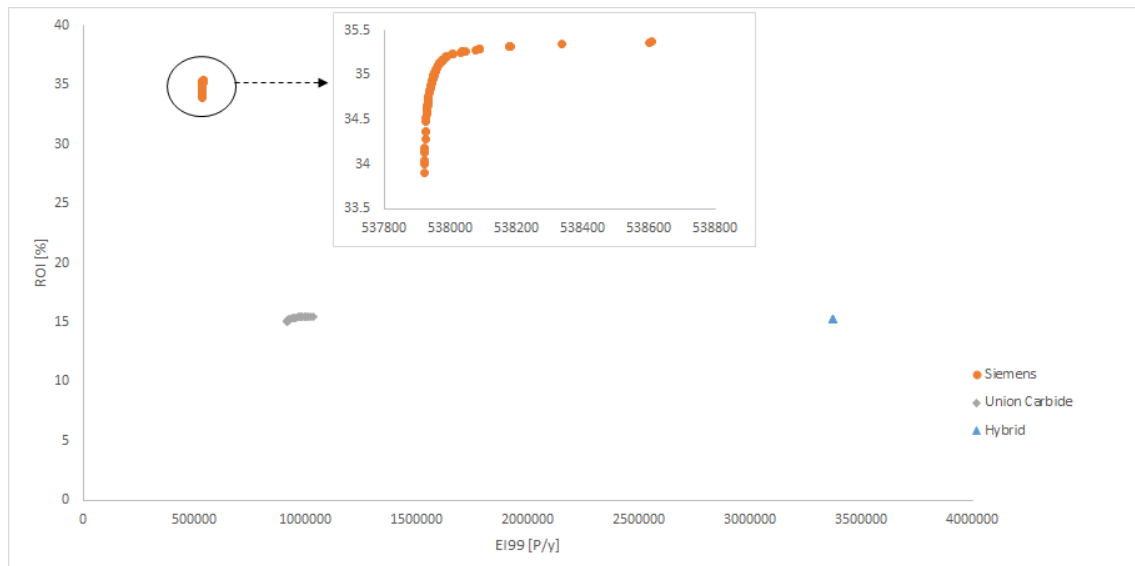


Figure 3.4. Pareto front between ROI and EI99 for the three processes.

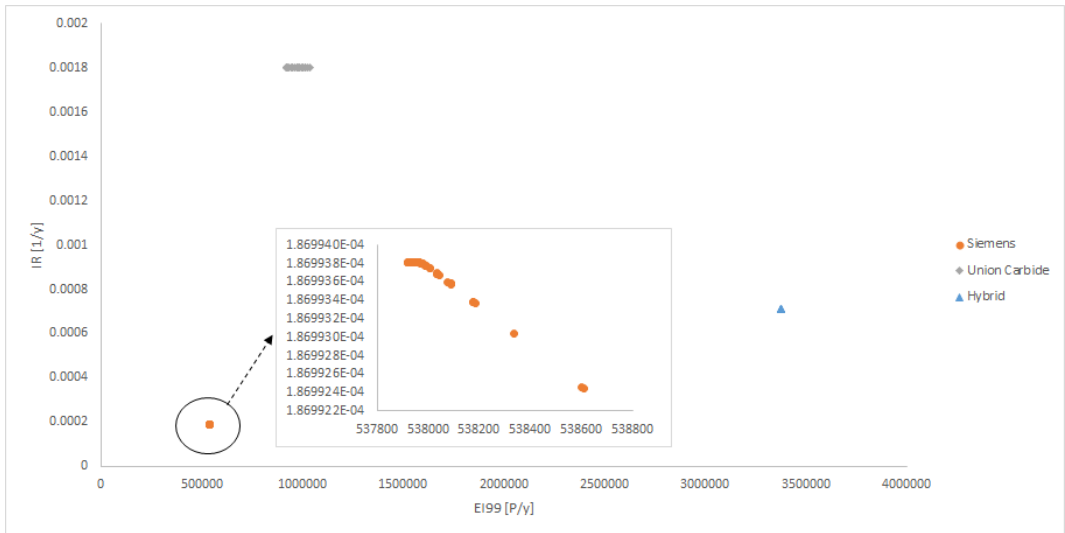


Figure 3.5. Pareto front between IR and EI99 for the three processes.

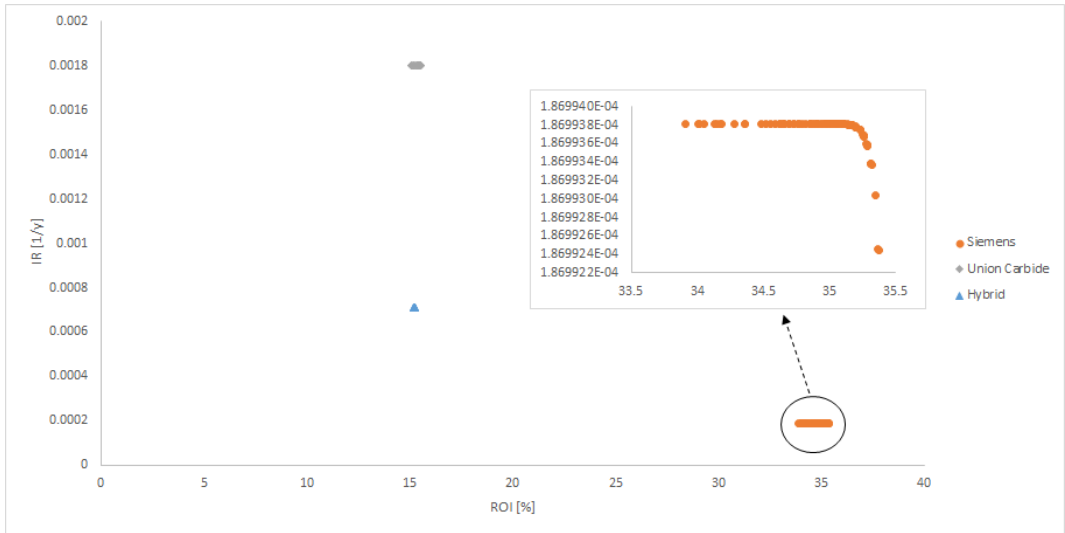


Figure 3.6. Pareto front between IR and ROI for the three processes.

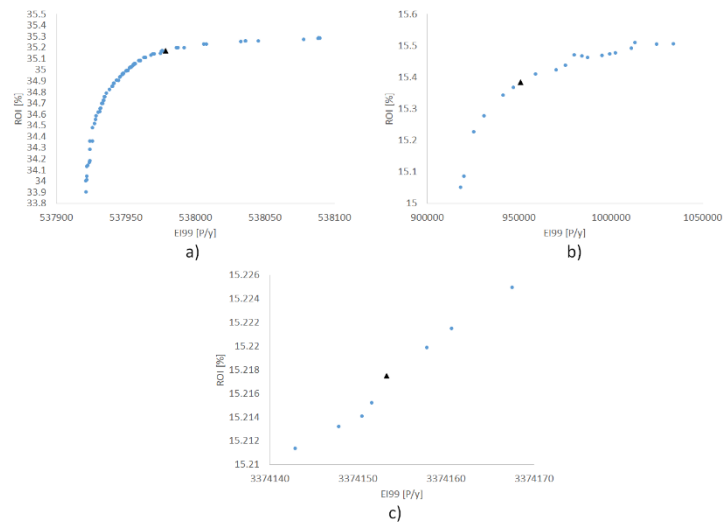


Figure 3.7. Pareto front between ROI and EI99 for: a) Siemens Process, b) Intensified FRB Union Carbide Process, and c) Hybrid Process.

Figures 3.7-3.9 present more clearly each one of the Pareto Fronts for each process. It is important to note that in each process has an optimal one, and in this case is marked with a triangle. The choice of optimal sequence of non-dominated points set was carried out selecting one point of the inflection area where the objectives values find a minimum value without compromise the other one. There are several methodologies for the utopian point choice as is shown in Wang and Rangaiah (2017) work, are exposed 10 methodologies where are observed the election area coincidence of the utopian point with the selected for this work, so it turns out be a good indicator of the choice made. For these cases the Tables 3.3-3.5 provide the optimal obtained parameters of each case.

The results shown in Figures 3.4-3.6 provide a brief view of the performance of the processes with respect to the three objectives. However, to evaluate the processes a more detail study is needed. The ROI resulting of Siemens process optimization is more than twice as large as Intensified FRB Union Carbide and Hybrid processes, and it would turn out to be the more profitable process, but it is the one with the smaller production of Si_{SG} , see

Tables 3.2 to 3.4 (55.25kg/h, 183.26 kg/h y 219.80 kg/h, respectively). It is assumed that the high profitability of 35.17%, the environmental index of 0.53 (MP/y) and better safety index of $1.86E-04$ (1/y) of Siemens Process is given by the small number of pieces of equipment and little amount of material required in comparison to the other processes, and that in the case of the profitability index ROI is not enough to notice the improvement in Si_{SG} production and others byproduct that are sell.

The Intensified FRB Union Carbide and Hybrid processes exhibit practically the same profitability 15.39% vs 15.22% respectively. It can be seen a notorious difference in the case of EI99, in favor of the Intensified FRB Union Carbide Process of 0.95 (MP/y) with respect to 3.37 (MP/y) of the Hybrid Process. In addition, we can also see a large difference in the IR in favor to Hybrid Process with $7.13E-04$ (1/y), being an order of magnitude smaller than Intensified FBR Union Carbide Process, for the reasons explained above. Can be say that the three processes are profitable, although with a significant difference in the others indexes (EI99 and IR), all the results can be observe in Table 3.5.

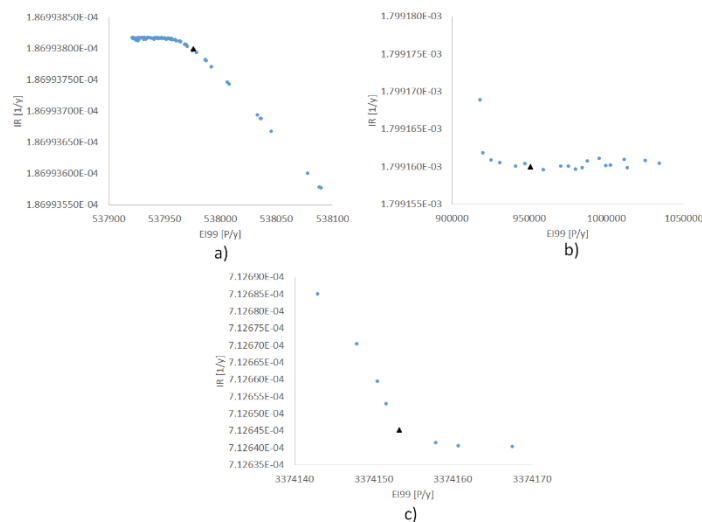


Figure 3.8. Pareto front between IR and EI99 for: a) Siemens Process, b) Intensified FRB Union Carbide Process, and c) Hybrid Process.

As in the work shown by Ramírez-Márquez et al., (2018) it can be considered that Hybrid Process is attractive for being the process with the higher production, being the second best in inherent safety terms with respect to the other two processes. However, with the worst EI99 index.

In the present work also planned to do a parameters quick comparative analysis of each optimized unit with respect to the work shown by Ramírez-Márquez et al., (2018) where only have as an objective function the minimizing of Total Annual Cost (TAC).

Substantial changes can be observe in the parameters of each process, as is the case of: number of stages, feed stage, reflux ratio, etc. The parameter of greatest change in the Siemens Process case is the reboiler heat duty where with the optimized sequence with the three objectives (ROI, EI99 and IR; see Table 3.2), manages to bring down 410.82 kW. Besides the change in the number of stages of 43 for the TAC optimization to 40 for the optimization of the three objectives, decreasing the column height. We can also observe a radical change in the diameter of the column going from 1 m (TAC optimization) to 0.3646 m. The temperatures and pressures remain almost the same in both works.

In the Intensified FRB Union Carbide Process there are structural alterations in the distillation columns changing substantially in: the number of stages, the reboiler heat duty and the diameter of all the columns, noticing more in the second conventional column which happens to have 40 stages for TAC optimization to 93 for ROI, EI99 and IR optimization and a diameter almost three times greater for the ROI, EI99 and IR optimization case (see Table 3.3).

The Hybrid Process also presents important changes in its parameters. The reboiler heat duty of the first column more significant. Going from 2141.79 kW for TAC optimization to 1674.72 kW for ROI, EI99 and IR optimization, see Table 3.4. As well as the columns diameters that are a third and the half the presented diameters in the TAC optimization.

It is important to present a comparison of both works, it is observed than exist important changes in the parameters on each unit depending of the objectives that are intended to achieve. This work is required to show the new parameters of each process with better safety, environmental and profitability indexes.

In general terms, there is a certain convenience in the Hybrid Process election based on the production and process safety, a relevant factor to design a process is the not election of highly toxic and flammable substance. However, if the scope in the production of a Si_{5G} production plant pretend to be short, the Siemens Process shows clear advantage in economic, environmental and safety terms.

Likewise, as it can be inferred from the present work, the IR value reduction for any process can be explained mainly in two ways. The process size reduction will generate an IR value reduction, in addition to the presence of toxic and dangerous substances through it will increase the IR values. For EI99, the steel for built equipment and accessories, the utilized vapor for produce heat, and electricity; increase the index value considerably. And finally the ROI allows to visualize generally the process profitability, but can leave aside aspects that determine the selling capacity and production of any process.

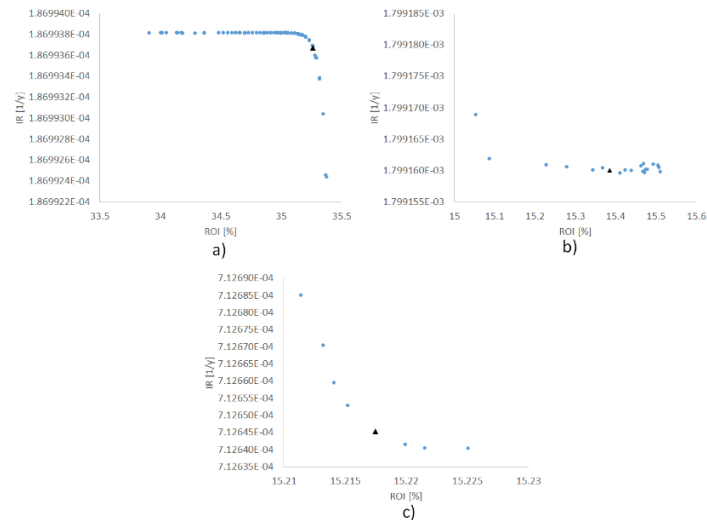


Figure 3.9. Pareto front between IR and ROI for: a) Siemens Process, b) Intensified FRB Union Carbide Process, and c) Hybrid Process.

Table 3.2. Results of the Optimization of ROI, Eco 99 and IR for the Siemens Process.

	COLCONV1	REACTOR 1	REACTOR 2	REACTOR 3
Feed Stream flow (kg/h)	123.805 (SiCl ₄) 888.344 (SiHCl ₃)	369.84 (C) 532.32 (SiO ₂)	204.6619 (SiMG) 901.4546 (HCl)	888.3438 (SiHCl ₃)
Feed Stream temperature (K)	533	298.15	492.56	351.578
Output stream (kg/h)	Top 0.0262963 (SiCl ₄) 888.3438 (SiHCl ₃) Bottom 123.7789 (SiCl ₄) 0.000421111 (SiHCl ₃)	204.66 (SiMG) 76.23 (CO)	16.15892 (H ₂) 123.8052 (SiCl ₄) 888.3443 (SiHCl ₃) 74.17817 (HCl)	55.2587 (SiSG) 5.2884 (H ₂) 779.9985 (SiCl ₄) 47.82461 (HCl)
Output Stream temperature (K)	N/A	2273	533	1373
Number of stages	40	N/A	N/A	N/A
Feed stage	13	N/A	N/A	N/A
Reflux ratio	30.43	N/A	N/A	N/A
Distillate rate (kmol/h)	6.5585	N/A	N/A	N/A
Reboiler heat duty (kW)	1219.9413	N/A	N/A	N/A
Condenser heat duty (kW)	-1298.4807	N/A	N/A	N/A
Diameter (m)	0.3646	N/A	N/A	N/A
Top pressure (atm)	3.9477	N/A	N/A	N/A
Bottom pressure (atm)	4.6282	N/A	N/A	N/A
Top temperature (K)	351.5783	N/A	N/A	N/A
Bottom temperature (K)	387.7451	N/A	N/A	N/A
Fresh Feed				
HCl (kg/h)	853.69			
ROI [%]	35.17123185			
Eco-99[MP/y]	0.537975844			
IR [1/y]	1.869937994E-04			

Table 3.3. Results of the Optimization of ROI, Eco 99 and IR for the Intensified FBR Union Carbide Process.

		COLCONV1	COLCONV2	RDC1	RDC2	REACTOR 1	REACTOR 2	REACTOR 3	REACTOR 4
Feed Stream flow (kg/h)		15874.04 (SiCl ₄) 3547.766 (SiHCl ₃) 155.1895 (SiH ₂ Cl ₂)	0.0053 (SiCl ₄) 3547.765 (SiHCl ₃) 155.1139 (SiH ₂ Cl ₂)	1773.883 (SiHCl ₃)	1773.883 (SiHCl ₃)	369.84 (C) 532.32 (SiO ₂)	204.66 (Si _{M6}) 19327.17 (SiCl ₄)	151.27 (H ₂) 15613.01 (SiCl ₄) 3963.984 (SiHCl ₃)	209.567 (SiH ₄)
Feed	Stream	323.15	349.5433	357.9455	357.9455	298.15	491.79	773	333
Feed temperature (K)									
Output stream (kg/h)		Top 0.0053 (SiCl ₄) 3547.765 (SiHCl ₃) 155.1139 (SiH ₂ Cl ₂)	Top 2.9714E-10 (SiHCl ₃) 155.1021 (SiH ₂ Cl ₂)	Top 104.695 (SiH ₄)	Top 104.872 (SiH ₄)				
		Bottom 15874.0347 (SiCl ₄) 0.001 (SiHCl ₃) 0.0756281 (SiH ₂ Cl ₂)	Bottom 0.0053 (SiCl ₄) 3547.765 (SiHCl ₃) 0.0118 (SiH ₂ Cl ₂)	Bottom 1663.111 (SiCl ₄)	Bottom 1664.058 (SiCl ₄)	204.66 (Si _{M6}) 76.23 (CO)	151.27 (H ₂) 15613.01 (SiCl ₄) 3963.984 (SiHCl ₃)	151.2701 (H ₂) 15874.04 (SiCl ₄) 3547.766 (SiHCl ₃) 155.1895 (SiH ₂ Cl ₂)	183.2604 (Si _{SG}) 26.3076 (H ₂) 52.39201 (SiH ₄)
Output	Stream	N/A	N/A	N/A	N/A	2273	773	773	1273
Output temperature (K)									
Number of stages		29	93	71	71	N/A	N/A	N/A	N/A
Feed stage		21	45	11	11	N/A	N/A	N/A	N/A
Reflux ratio		19.5022	41.5206	41.8717	42.2522	N/A	N/A	N/A	N/A
Distillate rate (kmol/h)		26.3536	1.4617	3.2833	3.2833	N/A	N/A	N/A	N/A
Reboiler heat duty (kW)		1384.2761	370.0256	515.5398	517.1288	N/A	N/A	N/A	N/A
Condenser heat duty (kW)		-3448.8243	-363.811	-494.614	-496.1694	N/A	N/A	N/A	N/A
Diameter (m)		0.5050	2.8794	0.63563	0.63563		N/A	N/A	N/A
Top pressure (atm)		3.9476	3.94769	2.3	2.3	N/A	N/A	N/A	N/A
Bottom pressure (atm)		4.6281	4.628153	2.6454	2.6454	N/A	N/A	N/A	N/A
Top temperature (K)		349.5587	324.711	177.9741	177.9388	N/A	N/A	N/A	N/A
Bottom temperature (K)		387.1773	357.9368	364.0261	364.0478	N/A	N/A	N/A	N/A
Reactive Stages		N/A	N/A	2-70	2-70	N/A	N/A	N/A	N/A

Holdup (cum)	N/A	N/A	0.175	0.175	N/A	N/A	N/A	N/A
Fresh Feed								
SiCl4 (kg/h)	16,000							
ROI [%]	15.38502548							
Eco-99[MP/y]	0.950797681							
IR [1/y]	1.799160029E-03							

Table 3.4. Results of the Optimization of ROI, Eco 99 and IR for the Hybrid Process.

		COLCONV1	COLCONV2	REACTOR 1	REACTOR 2	REACTOR 3	REACTOR 4
Feed Stream flow (kg/h)		9023.468	9.87 E-04		204.66	151.2709	
		(SiCl ₄)	(SiCl ₄)	369.84 (C)	(SiMG)	(H ₂)	
		3533.549	3533.548	532.32	12477.27	8763.483	3533.549
		(SiHCl ₃)	(SiHCl ₃)	(SiO ₂)	(SiCl ₄)	(SiCl ₄)	(SiHCl ₃)
		154.566	154.566		180.65 (H ₂)	3948.1	
	(SiH ₂ Cl ₂)	(SiH ₂ Cl ₂)			(SiHCl ₃)		
Feed Stream temperature (K)		323.15	350.1238	298.15	491.79	773	359.93
Output stream (kg/h)	Top	9.87 E-04	5.70971E-07				
		(SiCl ₄)	(SiHCl ₃)				
		3533.548	154.5479			151.2709	219.8015
		(SiHCl ₃)	(SiH ₂ Cl ₂)		151.2709	(H ₂)	(Si ₅ G)
		154.566		204.66	(H ₂)	9023.468	21.03545
		(SiH ₂ Cl ₂)		(SiMG)	8763.483	(SiCl ₄)	(H ₂)
	Bottom	3533.548	76.23 (CO)		(SiCl ₄)	154.566	3102.481
		(SiCl ₄)	(SiHCl ₃)		(SiHCl ₃)	(SiH ₂ Cl ₂)	(SiCl ₄)
		0.00146201	0.0181421			3533.549	190.2311
		(SiHCl ₃)	(SiH ₂ Cl ₂)			(SiHCl ₃)	(HCl)
	3.7154E-13	9.87 E-04					
	(SiH ₂ Cl ₂)	(SiCl ₄)					
Output Stream temperature (K)	N/A	N/A	2273	773	773	1373	
Number of stages	47	81	N/A	N/A	N/A	N/A	
Feed stage	11	31	N/A	N/A	N/A	N/A	
Reflux ratio	15.8689	67.6217	N/A	N/A	N/A	N/A	
Reboiler heat duty (kW)	1674.7221	544.8967	N/A	N/A	N/A	N/A	
Distillate rate (kmol/h)	28.1982	1.5301	N/A	N/A	N/A	N/A	
Condenser heat duty (kW)	-3045.6752	-619.2744	N/A	N/A	N/A	N/A	
Diameter (m)	0.3506	0.6022	N/A	N/A	N/A	N/A	
Top pressure (atm)	3.9476	3.6516	N/A	N/A	N/A	N/A	
Bottom pressure (atm)	4.6281	4.3320	N/A	N/A	N/A	N/A	
Top temperature (K)	350.1238	321.8233	N/A	N/A	N/A	N/A	
Bottom temperature (K)	387.7453	355.3240	N/A	N/A	N/A	N/A	
Fresh feed							
SiCl ₄ (kg/h)	451.56						
ROI [%]							
15.2174847046739							
Eco-99 [P/y]							
3.374153250							
IR [1/y]							
7.126452555E-04							

Table 3.5. Results of ROI, Eco 99 and IR for all the processes.

	ROI [%]	Eco-99[MP/y]	IR [1/y]
Siemens Process	35.17123	0.53797	1.86993E-04
Intensified FBR Union Carbide Process	15.38502	0.95079	1.79916E-03
Hybrid Process	15.21748	3.37415	7.12645E-04

3.7 Conclusions

The work presents the evaluation of three processes for obtaining Si_{SG} , according to properties of safety, profitability and environmental impact. The optimal parameters of each process were obtained by means of multiobjective optimization by the DETL method. Through the Pareto Fronts, the solutions with the best values of each objective function were found. The inclusion of safety principles in the design of the three processes leads to the development of one of the main approaches that must be taken into account in the birth of any process. The results show the Siemens Process as the best process in terms of the three objectives. However, it has to be considered that Si_{SG} production is very low (25% of that obtained from the Hybrid Process) and that current markets demand higher production, so the choice of ROI as an economic index did not turn out to be the adequate. Taking into account the above and considering that the Hybrid Process results with a safety index very similar to that of the Siemens Process, it can be the best option for its industrial implementation. The Intensified FBR Union Carbide Process proved to be the least safe process of the three, although with better performance in environmental terms than the Hybrid Process. It was concluded that one of the factors that most affect safety in the Intensified FBR Union Carbide Process is the inclusion of SiH_4 in the production of Si_{SG} , that increases greatly the frequency and the

affectation probability of some accident in the process. The approach presented here is an effort to include safety as part of process design, and in particular it can be extended to other systems that also present substances which may represent a hazard.

3.8 Notation

Si_{MG}	Metallurgical grade silicon
Si_{SG}	Solar grade silicon
$SiHCl_3$	Trichlorosilane
$SiCl_4$	Silicon tetrachloride
SiH_4	Silane
ROI	Return on investment
EI99	Eco-indicator 99
IR	Individual Risk
LCA	Life-cycle assessment
QRA	Quantitative Risk Analysis
TAC	Total Annual Cost
BLEVE	Boiling liquid expanding vapor explosion
UVECE	Unconfined Vapor Cloud Explosion
LC50	Lethal Concentration
DETL	Differential Evolution with Tabu List
DE	Differential evolution
TL	Tabu List

DDE Dynamic Data Exchange

3.9 Acknowledgements

Authors acknowledge the economic support provided by CONACYT and Universidad de Guanajuato.

3.10 References

Braga, A. F. B.; Moreira, S. P.; Zampieri, P. R.; Bacchin, J. M. G.; Mei, P. R., 2008. New processes for the production of solar-grade polycrystalline silicon: A review. *Solar energy materials and solar cells*, 92(4), 418-424.

Chigondo, F., 2018. From metallurgical-grade to solar-grade silicon: an overview. *Silicon*, 10(3), 789-798.

Coalition, S. V. T., 2009. *Toward a Just and Sustainable Solar Energy Industry*. San Jose: Silicon Valley Toxics Coalition.

Contreras-Zarazúa, G.; Vázquez-Castillo, J. A.; Ramírez-Márquez, C.; Segovia-Hernández, J. G.; Alcántara-Ávila, J. R., 2017. Multi-objective optimization involving cost and control properties in reactive distillation processes to produce diphenyl carbonate. *Computers & Chemical Engineering*, 105, 185-196.

Díez, E.; Rodríguez, A.; Gómez, J. M.; Olmos, M., 2013. Distillation assisted heat pump in a trichlorosilane purification process. *Chem. Eng. Process*, 69, 70-76.

Errico, M.; Sanchez-Ramirez, E.; Quiroz-Ramírez, J. J.; Rong, B. G.; Segovia-Hernandez, J. G., 2017. Multiobjective Optimal Acetone–Butanol–Ethanol Separation Systems Using Liquid–Liquid Extraction-Assisted Divided Wall Columns. *Industrial & Engineering Chemistry Research*, 56(40), 11575-11583.

Farrow, R. F. C., 1974. The Kinetics of Silicon Deposition on Silicon by Pyrolysis of Silane A Mass Spectrometric Investigation by

Molecular Beam Sampling. *J. Electr. Soc*, 121(7), 899-907.

Gebreslassie, B. H.; Guillén-Gosálbez, G.; Jiménez, L.; Boer, D., 2009. Design of environmentally conscious absorption cooling systems via multi-objective optimization and life cycle assessment. *Applied Energy*, 86(9), 1712-1722.

Glover, F., 1989. Tabu search—part I. *ORSA Journal on computing*, 1(3), 190-206.

Goedkoop, M.; Spriensma, R., 2018. *The Eco-indicator 99: A Damage Oriented Method for Life Cycle Impact Assessment-Methodology Report*. www.pre.nl (accessed January 2018).

Górak, A.; Olujić, Z., 2014. *Distillation: equipment and processes*, first ed; Elsevier, Oxford.

Guillen-Cuevas, K.; Ortiz-Espinoza, A. P.; Ozinan, E.; Jiménez-Gutiérrez, A.; Kazantzis, N. K.; El-Halwagi, M. M., 2017. Incorporation of safety and sustainability in conceptual design via a return on investment metric. *ACS Sustainable Chemistry & Engineering*, 6(1), 1411-1416.

Huang, Y.; Peng, X., 2014. Sustainable chemical product and process engineering. *ACS Sustainable Chemistry & Engineering*, 2,1-2.

Kumar, A., 1996. *Guidelines for evaluating the characteristics of vapor cloud explosions, flash fires, and bleves*. Center for Chemical Process Safety (CCPS) of the AIChE, Published by the American Institute of Chemical Engineers, New York, NY (1994), 387 pages, [ISBN: 0-8169-0474-X], US List Price: \$150. *Environmental Progress*, 15(1), S11-S12.

Madavan, N. K.; Biegel, B. A., 2002. Multiobjective optimization using a Pareto differential evolution approach.

Medina-Herrera, N.; Grossmann, I. E.; Mannan, M. S.; Jiménez-Gutiérrez, A., 2014. An approach for solvent selection in extractive distillation systems including safety considerations. *Industrial & Engineering Chemistry Research*, 53(30), 12023-12031.

Ramírez-Márquez, C.; Otero, M. V.; Vázquez-Castillo, J. A.; Martín, M.; Segovia-Hernández, J. G., 2018. Process design and intensification for the production of solar grade silicon. *Journal of Cleaner Production*, 170, 1579-1593.

Ranjan, S.; Balaji, S.; Panella, R. A.; Ydstie, B. E., 2011. Silicon solar cell production. *Comp. Chem. Eng*, 35(8), 1439-1453.

Safarian, J.; Tranell, G.; Tangstad, M., 2012. Processes for upgrading metallurgical grade silicon to solar grade silicon. *Energy Procedia*, 20, 88-97.

Sánchez-Ramírez, E.; Quiroz-Ramírez, J. J.; Hernández, S.; Segovia-Hernández, J. G.; Kiss, A. A., 2017. Optimal hybrid separations for intensified downstream processing of biobutanol. *Separation and purification technology*, 185, 149-159.

Sánchez-Ramírez, E.; Quiroz-Ramírez, J. J.; Segovia-Hernández, J. G.; Hernández, S.; Ponce-Ortega, J. M. Economic and environmental optimization of the biobutanol purification process. *Clean Technologies and Environmental Policy*. 2016, 18(2), 395-411.

Srinivas, M.; Rangaiah, G. P., 2007. Differential Evolution with Tabu List for Solving Nonlinear and Mixed-Integer Nonlinear Programming Problems. *Ind. Eng. Chem. Res*, 46, 7126-7135.

Tejero-Ezpeleta, M. P.; Buchholz, S.; Mleczko, L., 2004. Optimization of Reaction Conditions in a Fluidized-Bed for Silane Pyrolysis. *Can. J. Chem. Eng*, 82 (3), 520-529.

Wang, Z.; Rangaiah, G. P., 2017. Application and analysis of methods for selecting an optimal solution from the Pareto-optimal front obtained by multiobjective optimization. *Industrial & Engineering Chemistry Research*, 56(2), 560-574.

4 Inherent Occupational Health Hazards In The Production Of Solar Grade Silicon

Process Safety and Environmental Protection

Official journal of the European Federation of Chemical Engineering: Part B



4 Inherent Occupational Health Hazards In The Production Of Solar Grade Silicon

Abstract

Solar energy has become one of the most developed renewable energy sources in recent years. As with any energy source or product, there are health risks associated with the manufacturing of solar cells. And even though the photovoltaic industry uses far lesser amounts of toxic and flammable substances than many other industries, the use of hazardous chemicals can present occupational and environmental hazards. One of the most important aspects in the selection of new processes lies in the protection of workers' health. Health risks can be reduced if a process is chosen properly and in preliminary phases. Since we have found it necessary to carry out an evaluation of the health risks to workers in the production of polycrystalline silicon for the manufacturing of photovoltaic cells, in this work we will use the Process Route Healthiness Index to quantify the health risk that each silicon production process represents (the higher the index, the higher the hazards). The polycrystalline silicon production processes evaluated with the healthiness index are: Siemens Process, Intensified Fluidized Bed Reactor Union Carbide Process, and Hybrid Process. Our results show that the Siemens Process is the healthiest process, but with the Process Route Healthiness Index values are closer to the Hybrid Process.

4.1 Introduction

In recent years, the energy industry has paid special attention to productivity improvement, to waste reduction and to quality control, all in the areas of research, development, and manufacturing. This is due not only to the consideration of cost reduction, but also to the awareness of sustainability increase in the manufacturing process (Cave and Edwards, 1997). Although it is known that the processes of obtaining non-renewable energy impacts the

environment in various ways. The processes of non-renewable energy production by their nature turn out to be potentially dangerous for human and environmental health (Owusu and Asumadu-Sarkodie, 2016).

To achieve this, there are two approaches to make these processes healthier, safer and more environmentally friendly, called internal and external means (Hassim and Edwards, 2006). However, the use of internal media, commonly known as an inherent approach, turns out to be better, since it is based on the

fundamental properties of the process, on the nature of the chemicals required by the process and on the conditions of the process (Adu et al., 2008; Warnasooriya and Gunasekera, 2017). If, in the inherent approach a chemical does not exist, it does not represent any danger. Therefore, the inherent approach requires less protection systems, which will make them more manageable (Edwards and Lawrence, 1993).

However, there are not many studies that assess the principles of inherent occupational health hazards in energy production processes from renewable sources. It is believed that renewable energy and its obtaining process turn out to be harmless. In spite of this, each one of the parameters or principles of health hazards has to be evaluated in order to compare and to decide which process is more appropriate under this approach.

Inside the renewable energies, the energy from the sun is the most abundant. It is estimated that it could cover around 35% of the total energy that the United States will require by 2050 (Fthenakis et al., 2009). Presently, research on the potential of solar energy continues on the economic, social and technical aspects, as well as being compared to the potential of fossil fuels. Contrary to fossil fuels, solar energy is based on cost per kilowatt and in recent years, the United States, China and countries in the European Union, have implemented initiatives to reduce the cost of solar energy per watt. In some cases, as in a project developed by *First Solar*, it has managed to reduce the cost as far as one U.S. dollar per watt (United States Department of Energy, 2012).

Renewable sources have been steadily pairing up to fossil fuels in economic value; and, despite the idea that these are “clean resources”, they also represent a continuous struggle with the environmental and health risks that they themselves may cause. Solar industry is no exception. Nowadays, the

massive production of solar panels has resulted in a problem that needs special attention due to the use of toxic compounds that are harmful for both humans and the environment.

Despite the aforementioned, there exist evidence that solar panel production is much safer for the environment and workers than fossil fuel energy production (Galland, 2012). However, this raises the question to the evaluation problem in health and environmental aspects in solar panel production. Even if the photovoltaic industry uses far fewer amounts of toxic and flammable substances than many other industries, the use of hazardous chemicals can represent occupational and environmental hazards. Nowadays, there are reports that consider health, environmental impact and industrial hygiene in the photovoltaic industry (Briggs and Owens, 1980; Taylor, 2010; Fthenakis and Moskowitz, 2000). These reports display discussions about aspects among the various technologies of photovoltaic cells production: monocrystalline and polycrystalline silicon cells, gallium arsenide cells, cadmium sulfide cells. However, none of these reports show in detail the health aspects that represent each of the processes for raw material production in the manufacture of cells.

There is a great array of materials for solar panel production, the leading technologies at a commercial level are silicon-based, whether it be monocrystalline or polycrystalline (Briggs and Owens, 1980). In 2010, silicon represented 88% in all the photovoltaic cells (Price et al., 2010). A key point in the manufacture of silicon based solar cells is the acquisition of raw material. The literature shows two industrial consolidated processes for the acquisition of silicon polycrystalline, the first one is the Siemens Process, which is the most widely used (Bye and Ceccaroli, 2014). The second one is the Fluidized Bed Reactor (FBR) from Union Carbide (Erickson and Wagner, 1952). Moreover, Ramírez-

Márquez et al. (2018) proposed an improved FBR process, called Hybrid, which conceptually results in higher production of silicon polycrystalline, in addition to being suitable in economic, safety and environmental aspects (Ramírez-Márquez et al., 2019).

Even though in the work by Ramírez-Márquez et al. (2019) aspects such as economy, environmental impact and safety are addressed, it is important to make a detailed study of the evaluation of inherent occupational health hazards of the three processes; this, due to the nature of said processes, since these represent a real potential hazard to the operator's health, and they require the use of raw materials (in liquid, solid and gas state) with inherent toxicological properties which can represent a health risk (Warnasooriya and Gunasekera, 2017).

That is why a polycrystalline silicon production health risk evaluation must be a determining factor for selecting the best route. Although there is research that evaluates the inherent occupational health hazards issues in the early stages of design and help to choose the appropriate process route (Koller et al., 2000; Adu et al., 2008; Sugiyama, 2007).

In this work we use the methodology of inherent occupational health hazards of Hassim and Edwards (2006) to assess the occupational health problems related in production of silicon polycrystalline in the three processes mentioned above. The Hassim and Edwards methodology (2006) is used because the technique takes into account both the hazard from the chemicals present, and the potential damage caused by the exposure of workers to chemicals. Assessing occupational health in all processes is of great importance since workers are exposed to dangerous chemical substances which can cause chronic diseases in the long run. With this in mind, it is necessary to

identify hazardous substances and how to detect which parts of the processes cause the most damage in order to make improvements and prevent any type of incidents.

4.2 Methodology

The objective of this work is to estimate the risks for the occupational health in the three process designs for polycrystalline silicon production following the Hassim & Edwards methodology (Hassim and Edwards, 2006). This methodology was designed and developed to take into account the possible factors that could be a potential health risk in the workplace. To achieve this, certain factors that represent the Process Route Healthiness Index (PRHI) were estimated in a quantitative manner. The PRHI includes all the factors that contribute to the risks in the occupational health (Hassim and Edwards, 2006). A higher value of PRHI means that the process represents a greater risk in occupational health terms. Methodologies like the PRHI are very useful when comparing different processes to determine which process might represent the greatest damage to the health of workers and to identify possible solutions.

4.3 Case Studies

The data obtained in the optimization performed by Ramírez-Márquez et al. (2019) have been considered; in it, the three processes for the silicon production under a multi-objective framework were optimized to account for safety, profitability and environmental impact. The indexes used were: Individual Risk (IR), Return on Investment (ROI) and Eco-indicator 99 (EI99), respectively. The modeling of the processes was carried out in Aspen Plus V8.4. The optimization was carried out by a hybrid algorithm called Differential Evolution with Taboo List (DETL). The considered processes are briefly described in next sections.

condensed so that they may pass into several distillation columns. From the second column and all through the bottom, the trichlorosilane is removed, which is

introduced into the Siemens vapor deposition reactor. Lastly, the HCl and H₂ are separated from the Si₃SG (See Figure 4.3).

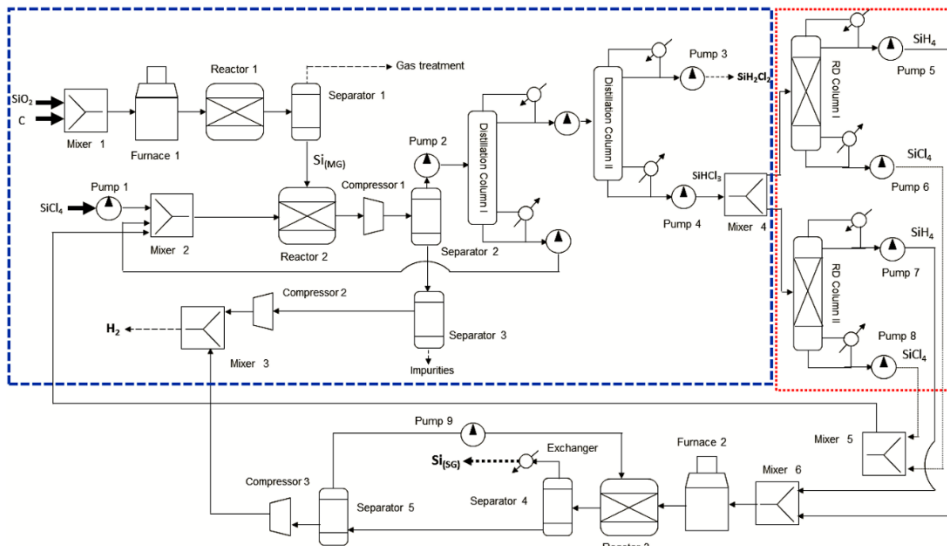


Figure 4.2. Flowsheet of Intensified FBR Union Carbide Process.

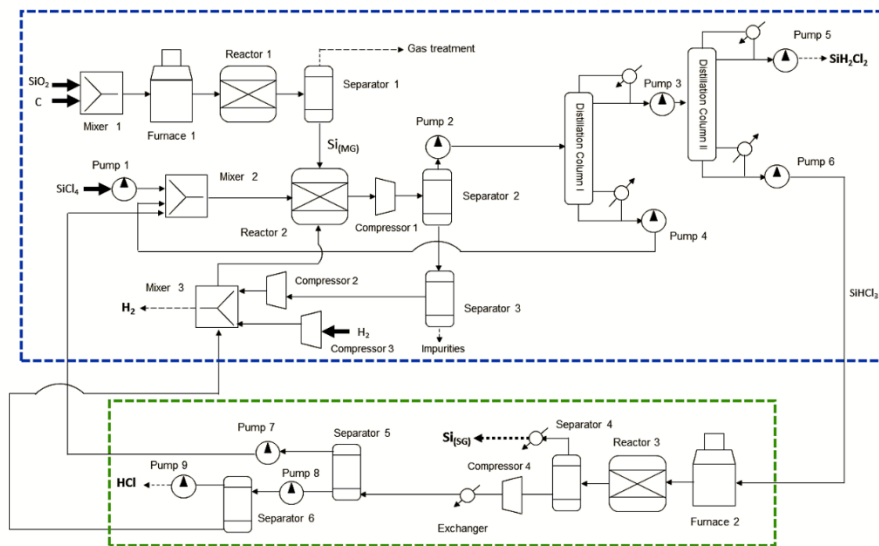


Figure 4.3. Flowsheet Hybrid Process FBR Union Carbide with Siemens.

For more information on the models used for the three processes, consult the work of Ramírez-Márquez et al. (2018) (Chapter 2).

4.4 Assessment Method for Occupational Health Aspect

To evaluate the inherent occupational health hazards, an approach that quantifies and provides an index about the health hazard for a given process is necessary. As mentioned above, the three evaluated processes related to inherent occupational health hazards are: the Siemens Process, the Intensified FBR Union Carbide Process, and the Hybrid Process. Specifically, the parameters of each process were taken from the work by Ramírez-Márquez et al. (2019), which carried out the optimization of the processes contemplating aspects such as safety, environmental impact, and the profitability of the three processes. The parameters resulting from each process can be observed in the work of Ramírez-Márquez et al. (2019).

This work aims to perform an analysis of inherent occupational health hazards on the results of multiobjective optimization to include another primordial aspect in determining the most convenient process. In this project, an index called the Process Route Healthiness Index (PRHI) is used, this describes the inherent occupational health hazard in the processes.

The PRHI for each process is calculated by the following relationship:

$$PRHI = ICPHI \times MHI \times HHI \times \frac{WEC_{max}}{OEL_{min}} \quad (4.1)$$

where, ICPHI stands for Inherent Chemical and Process Hazard Index and evaluates the operating conditions, the conditions of the process and the properties of the materials involved that are potentially harmful to health; MHI represents the Material Harm Index and takes into account the limits of

exposure, as well as the possible damages and/or effects that each of the substances can cause, the penalization of the substances is according to the criteria of the NFPA; HHI symbolizes the Health Hazard Index and determines the ability of substances to cause occupational diseases, whether through irritation, sensitivity or cancer (this information is obtained from the OSHA database). WEC_{max} represents the maximum Worker Exposure Concentration and is the maximum concentration to which a worker is exposed to in the worst case and takes into account the quantity of substance that can be released to the work environment through emissions or small leaks and considers the relation between the estimated time of exposure of (6 hours) and the average (8 hours) of a normal working day; and lastly, OEL_{min} indicates the minimum Occupational Exposure Limit and represents the maximum concentration to which a worker will be exposed without any cause of damage.

The elements for calculating the PRHI are listed in Figure 4.4.

Described above is an adequate methodology for the evaluation of occupational health in the silicon processes. Since some of the information was not available in the early process design stage. Hassim & Edwards (2006) presented a detailed methodology for calculating the PRHI.

4.5 Results

This section presents the results of the evaluation of inherent occupational health hazards in the production of solar grade silicon, for three processes: Siemens, Intensified FBR Union Carbide and Hybrid. A summary of the healthiness index for each process is presented in Table 4.1, where all the results of the aspects considered by the PRHI are shown. The whole procedure of the evaluation of the PRHI for the Intensified FBR

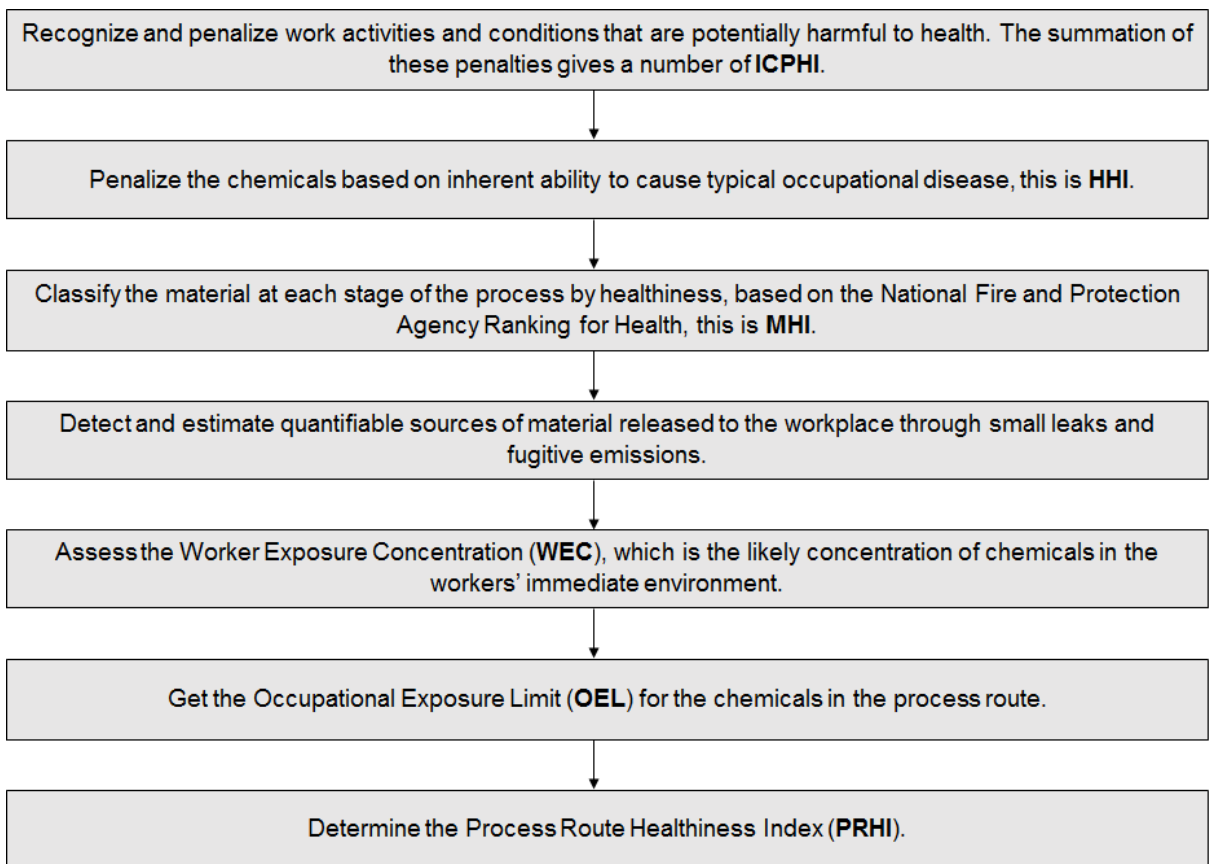


Figure 4.4. Diagram for calculating the PRHI (Hassim & Edwards, 2006).

Union Carbide Process is presented in Appendix 4A.

The PRHI is then scaled to make it clearer and to facilitate the comparison of the results. The scaled healthiness index values are listed in Table 4.2. This is done by dividing the index by the highest index value calculated by the three silicon production process routes that are being compared. The highest value of PRHI is presented in the Intensified FBR Union Carbide Process.

There are many reasons that raise the PRHI in the Intensified FBR Union Carbide Process. This is partly due to the Intensified FBR Union Carbide Process having the major number of reaction steps and the use of various compounds in the process. It has the highest penalty for activities and conditions, the highest HHI and MHI values and the uppermost OEL. The conversion of

trichlorosilane to silane is necessary for the deposition of polycrystalline silicon. In the reaction of disproportionation of trichlorosilane to silane, intermediate products (SiH_2Cl_2 and SiH_3Cl) are generated. These compounds are harmful to health, with a high value (of 4, where 5 is the maximum value) in the category of limited exposure-death/major residual injury. This according to the NFPA health rating criteria.

A different important aspect is generated in the chemical vapor deposition reactor in the Intensified FBR Union Carbide Process. Both, the high operating pressure of chemical deposition reactor and the boiling point of silane in the reactor is less than -112°C , which result in a very high value of airborne material generated from flashing liquid. On the one hand, it can be determined that the Intensified FBR Union Carbide Process presents the highest potential hazard to

human health in producing polycrystalline silicon (See Figure 4.5).

Table 4.1. Summary of Results

	AP	CP	ICPHI=AP+CP	HHI	MHI	WEC _{MAX}	OEL _{min} (kg/m ³) 10 ⁶	PRHI 10 ⁻¹⁴
Siemens	42	30	72	29	15	2510	2.48	0.316141562
Intensified FBR Union	51	40	91	38.6	21	61279	4.98	9.085718795
Hybrid	42	30	72	33.3	19	4282	2.49	0.784304839

AP, Penalties for Activities; CP, Penalties for Conditions; ICPHI, Inherent Chemical and Process Hazard Index; HHI, Health Hazard Index; MHI, Material Harm Index; WECmax, Worker Exposure Concentration; OELmin, Minimum Occupational Exposure Limit.

PRHI (Damage/kg Si_{SG})

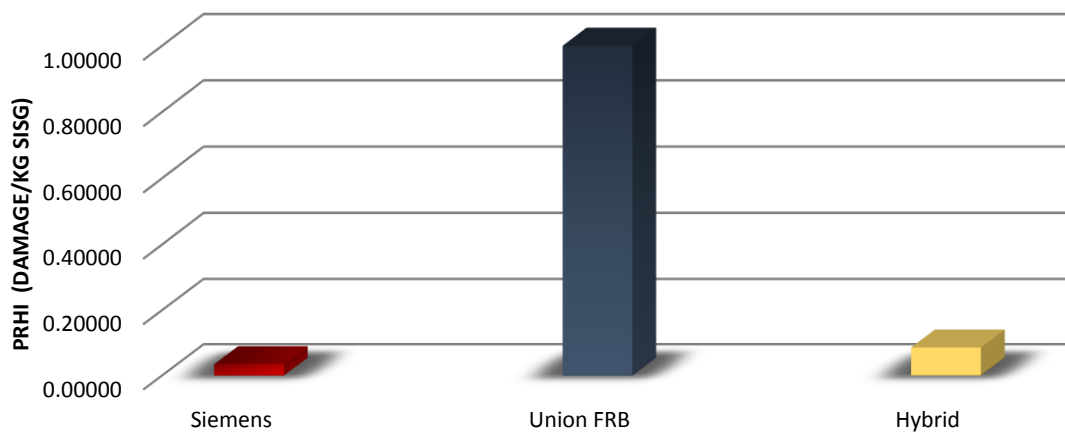


Figure 4.5. Results of the PRHI (Damage/kg Si_{SG}).

Table 4.2. Scaled Healthiness Index.

	PRHI _{SCALED} (Damage/kg Si)	PRHI _{SCALED} (Damage)	Ranking
Siemens	0.03480	1.92275	1
Intensified FBR Union	1.00000	183.26040	3
Hybrid	0.08632	18.97388	2

1–Posses the best case.

On the other hand, the PRHI value calculated for the Siemens Process does not demonstrate much difference from the Hybrid Process. Nevertheless, the PRHI for the Siemens Process is low compared to the other two processes. This is a repercussion of the process conditions and the unit operations involved in the Siemens Process.

The Siemens Process is similar to the Hybrid Process in terms of the involved compounds. The difference is the usage of SiCl₄ as a raw material in the Hybrid Process and HCl in the

Siemens Process, which presents a similar health hazard to humans. An interesting fact can be seen in Figure 4.6, where the difference between PRHI values of the Siemens Process and Hybrid Process tends to rise if the production of Si₅G is not considered.

The same three processes have been assessed by Ramírez-Márquez et al. (2019) in terms of their economic profitability (ROI), environmental impact (EI99) and inherent safety (IR). The Hybrid Process ranks as the second worse process in almost all aspects,

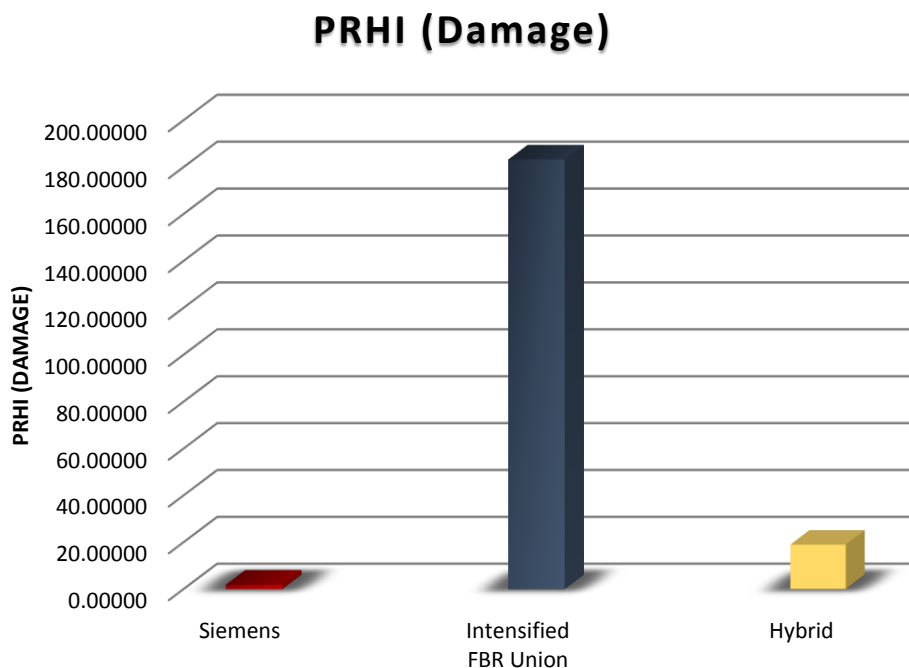


Figure 4.6. Results of the PRHI (Damage).

however, as mentioned before, the difference between the Si_{SG} production for the Siemens Process and the Hybrid Process is four times higher, as Table 4.3 shows.

The comparison of the processes by these five aspects are tabulated in Table 4.4. Based on this comparison, the Intensified FBR Union Carbide is the route that should not be

considered when looking for the best process for producing Si_{SG}. From the comparison shown in Table 4.4, the Siemens Process is potentially the healthiest, most profitable, safest and most environmentally friendly, but also with the lowest production of Si_{SG}. For greater Si_{SG} production, the Hybrid Process is an appropriate option.

Table 4.3. Results of the PRHI (Damage/kg Si), PRHI (Damage), ROI [%], Eco-99 [MP/y], IR [1/y] and Production of Si_{SG} [kg/h].

	PRHI _{SCALED} (Damage/kg Si)	PRHI _{SCALED} (Damage)	ROI [%]	Eco-99 [MP/y]	IR [1/y]	Production of Si _{SG} [kg/h]
Siemens	0.03480	1.92275	35.17123	0.53797	0.00019	55.2587
Intensified FBR Union	1.00000	183.26040	15.38502	0.95079	0.00180	183.2604
Hybrid	0.08632	18.97388	15.21748	3.37415	0.00071	219.8015

Table 4.4. Comparison of health, profitability, environmental impact, inherent safety and production of Si_{SG}.

	PRHI _{SCALED} (Damage)	ROI [%]	Eco-99 [MP/y]	IR [1/y]	Production of Si _{SG} [kg/h]
Best Process	Siemens	Siemens	Siemens	Siemens	Hybrid
↓	Hybrid	Hybrid/ Intensified FBR Union	Intensified FBR Union	Hybrid	Intensified FBR Union
Worst Process	Intensified FBR Union	---	Hybrid	Intensified FBR Union	Siemens

4.6 Conclusions

The PRHI has been tested on three processes for Si_{SG} production, in accordance to the case study results, type of compounds, and the several operating conditions that play a key role in determining the level of inherent occupational health hazards. The compound boiling points and the equipment operating conditions (Temperature and Pressure) are two parameters that disrupt the value of the index. Moreover, the number of reactions involved in the processes also have a huge impact on the PRHI values. The index assessed in the three processes for polycrystalline silicon production proves that it is possible to attempt a quantification of inherent occupational health hazards in the initial stages of process design. According to the presented comparison of the different processes, the Siemens Process is hypothetically the healthiest, most profitable, safest and most environmentally friendly. That is, the process that best follows the concept of inherent occupational health hazards, but it is also the least productive. For superior Si_{SG} production, the Hybrid Process is the best suitable option.

4.7 Notation

AP	Penalties for activities
C	Carbon
CP	Penalties for conditions
EI99	Eco-indicator 99
H ₂	Hydrogen
HCl _(g)	Hydrogen chloride
HHI	Health Hazard Index
ICPHI	Inherent Chemical and Process Hazard Index
IR	Individual risk
MHI	Material Harm Index
OEL _{min}	Minimum Occupational Exposure Limit
ROI	Return on investment
Si _{MG}	Metallurgical grade silicon
Si _{SG}	Solar grade silicon
SiCl ₄	Silicon tetrachloride

SiH ₄	Silane
SiHCl ₃	Trichlorosilane
SiH ₂ Cl ₂	Dichlorosilane
SiO ₂	Silicon dioxide

WEC_{max} Maximum Worker Exposure Concentration

4.8 Acknowledgements

Authors acknowledge the economic support provided by CONACYT, Universidad de Guanajuato and Universidad Michoacana de San Nicolas de Hidalgo.

4.9 References

- Adu, I. K., Sugiyama, H., Fischer, U., & Hungerbühler, K., 2008. Comparison of methods for assessing environmental, health and safety (EHS) hazards in early phases of chemical process design. *Process Saf Environ*, 86(2), 77-93. <https://doi.org/10.1016/j.psep.2007.10.005>
- Briggs, T. M., & Owens, T. W., 1980. Industrial hygiene characterization of the photovoltaic solar cell industry (No. DHEW (NIOSH)-80-112). National Inst. for Occupational Safety and Health, Cincinnati, OH (USA). Div. of Surveillance, Hazard Evaluation and Field Studies. OSTI ID: 5265468
- Bye, G., & Ceccaroli, B., 2014. Solar grade silicon: Technology status and industrial trends. *Solar Energy Materials and Solar Cells*. 130, 634-646. <https://doi.org/10.1016/j.solmat.2014.06.019>
- Cave, S. R., & Edwards, D. W. (1997). Chemical process route selection based on assessment of inherent environmental hazard. *Computers & Chemical Engineering*, 21, S965-S970. [https://doi.org/10.1016/S0098-1354\(97\)87627-2](https://doi.org/10.1016/S0098-1354(97)87627-2)
- Edwards, D. W., & Lawrence, D., 1993. Assessing the inherent safety of chemical process routes: is there a relation between plant costs and inherent safety?. *Process Saf Environ*, 71(B4), 252-258.

- Erickson, C. E., & Wagner, G. H., 1952. U.S. Patent No. 2,595,620. Washington, DC: U.S. Patent and Trademark Office.
- Fthenakis, V. M., & Moskowitz, P. D., 2000. Photovoltaics: environmental, health and safety issues and perspectives. *Prog Photovoltaics: research and applications*. 8(1), 27-38. [https://doi.org/10.1002/\(SICI\)1099-159X\(200001/02\)8:1<27::AID-PIP296>3.0.CO;2-8](https://doi.org/10.1002/(SICI)1099-159X(200001/02)8:1<27::AID-PIP296>3.0.CO;2-8)
- Fthenakis, V., Mason, J. E., & Zweibel, K., 2009. The technical, geographical, and economic feasibility for solar energy to supply the energy needs of the US. *Energy Policy*.37(2), 387-399. <https://doi.org/10.1016/j.enpol.2008.08.011>
- Galland, A., 2012. Best Practices in Photovoltaics Manufacturing. In 2012 38th IEEE Photovoltaic Specialists Conference. 001639-001642. DOI: 10.1109/PVSC.2012.6317910
- Hassim, M. H., & Edwards, D. W., 2006. Development of a methodology for assessing inherent occupational health hazards. *Process Saf Environ*. 84(5), 378-390. <https://doi.org/10.1205/psep.04412>
- Koller, G., Fischer, U., Hungerbühler, K., 2000. Assessing safety health, and environmental impact early during process development. *Ind. Eng. Chem. Res*. 39 (4), 960–972. <https://doi.org/10.1021/ie990669i>
- Owusu, P. A., & Asumadu-Sarkodie, S., 2016. A review of renewable energy sources, sustainability issues and climate change mitigation. *Cogent Engineering*, 3(1), 1167990. <https://doi.org/10.1080/23311916.2016.1167990>
- Price, S., Margolis, R., Barbose, G., Bartlett, J., Cory, K., Couture, T. & Hemmeline, C., 2010. 2008 solar technologies market report (No. LBNL-3490E). Lawrence Berkeley National Lab. (LBNL), Berkeley, CA (United States). <https://www.nrel.gov/docs/fy10osti/46025.pdf>
- Ramírez-Márquez, C., Contreras-Zarazua, G., Martín, M., & Segovia-Hernández, J. G., 2019. Safety, economic and environmental optimization applied to three processes for the production of solar grade silicon. *ACS Sustain Chem Eng*. <https://doi.org/10.1021/acssuschemeng.8b06375>
- Ramírez-Márquez, C., Otero, M. V., Vázquez-Castillo, J. A., Martín, M., & Segovia-Hernández, J. G., 2018. Process design and intensification for the production of solar grade silicon. *J. Clean. Prod*. 170, 1579-1593. <https://doi.org/10.1016/j.jclepro.2017.09.126>
- Sugiyama, H., 2007. Decision-making framework for chemical process design including different stages of environmental, health and safety (EHS) assessment. *ETH Zurich*. <https://doi.org/10.3929/ethz-a-0005398654>
- Taylor, D. A., 2010. Occupational Health: On the Job with Solar PV. DOI: 10.1289/ehp.118-a19
- Tong, R., Cheng, M., Yang, X., Yang, Y., & Shi, M., 2019. Exposure levels and health damage assessment of dust in a coal mine of Shanxi Province, China. *Process Saf Environ*. <https://doi.org/10.1016/j.psep.2019.05.022>
- United States Department of Energy, “SunShot Initiative”, 2012. <http://www1.eere.energy.gov/solar/sunshot/>. Additional savings could be realized by addressing the costs of permitting solar installations, last modified February 9.
- Warnasooriya, S., & Gunasekera, M. Y., 2017. Assessing inherent environmental, health and safety hazards in chemical process route selection. *Process Saf Environ*, 105, 224-236. <https://doi.org/10.1016/j.psep.2016.11.010>

Appendix A4 Procedure of the evaluation of the PRHI for the Intensified FBR Union Carbide Process

The Solar grade Silicon production based on the Intensified FBR Union Carbide Process can be seen in Figure A1.

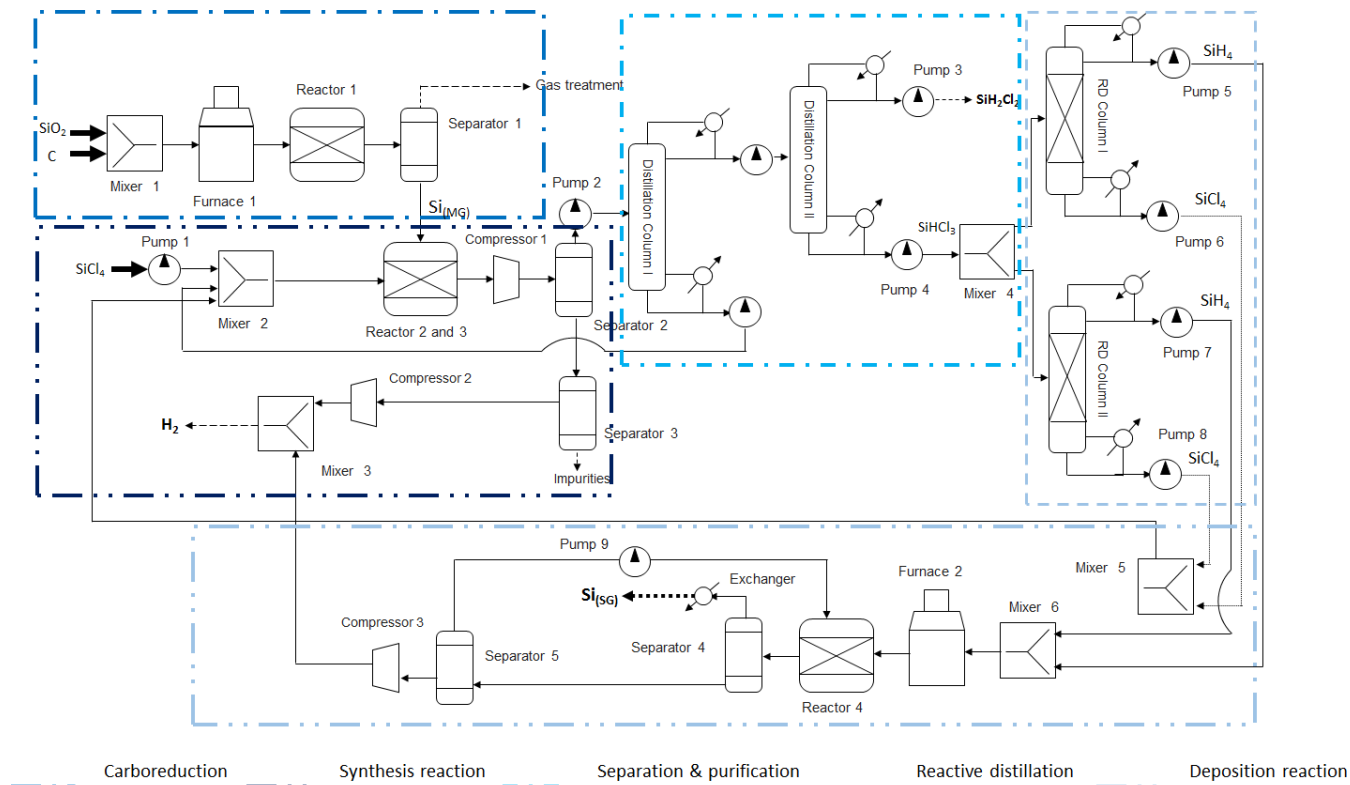


Figure A4.1. Flowsheet of Intensified FBR Union Carbide Process for the evaluation of the PRHI.

PRHI estimation for the Intensified FRB Union Carbide Process

Potentially Harmful Activities and Process Conditions: Inherent Chemical and Process Hazard Index

Table A4.1. Conditions by process sections.

Carboreduction								
		MW	Mass Flow [kmol/h]	Mole Fraction	Mass Flow [kg/h]	Mass Fraction	Temperature [C]	Pressure [atm]
In	C (s)	12.01	30.792	0.777	369.840	0.410	19.850	1.000
	SiO ₂ (s)	60.08	8.860	0.223	532.320	0.590		
Out	Si (s) _{MG}	28.09	7.287	0.728	204.662	0.729	1999.850	1.000
	CO (g)	28.01	2.719	0.272	76.146	0.271		
Synthesis reaction								
In	Si(s) _{MG}	28.09	7.287	0.037	204.662	0.010	20.915	1.000
	SiCl ₄ (g)	169.90	113.756	0.580	19327.170	0.982		
	H ₂ (g)	2.02	75.039	0.383	151.270	0.008		
Out	H ₂ (g)	2.02	75.039	0.379	151.270	0.008	499.850	35.529
	SiCl ₄ (g)	169.90	91.895	0.465	15613.010	0.785		
	SiHCl ₃ (g)	135.45	29.265	0.148	3963.984	0.199		
	SiH ₂ Cl ₂ (g)	101.10	1.535	0.008	155.190	0.008		
Separation and purification								
In	SiCl ₄ (l)	169.90	93.432	0.771	15874.040	0.811	124.440	6.908
	SiHCl ₃ (l)	135.45	26.192	0.216	3547.766	0.181		
	SiH ₂ Cl ₂ (l)	101.10	1.535	0.013	155.190	0.008		
Out	Dome							

	SiH ₂ Cl ₂ (l) - Column 2	101.10	1.533	0.999	155.034	0.999	51.563	3.948
	Bottom							
	SiCl ₄ (l) - Column 1	169.90	93.33823402	0.999	15858.16596	0.999	114.594	4.689
	SiHCl ₃ (l) - Column 2	135.45	26.16624757	0.999	3544.218234	0.999	84.888	4.628
Reactive distillation								
In	SiHCl ₃ (l) - RDC-1	135.45	13.15958	1	1782.485	1	84.888	4.628
	SiHCl ₃ (l) - RDC-2	135.45	13.00667	1	1761.733	1		
Out	Dome							
	SiH ₄ (l) - RDC-1	32.12	3.259	1	104.695	0.999	-94.653	2.300
	SiH ₃ Cl (l) - RDC-1	66.56	0.002	0	0.105	0.001		
	SiH ₄ (l) - RDC-2	32.12	3.265	1	104.872	0.999	-94.653	2.300
	SiH ₃ Cl (l) - RDC-2	66.56	0.002	0	0.105	0.001		
	Bottom							
	SiCl ₄ (l) - RDC-1	169.90	9.789	0.999	1663.11	0.999	90.475	2.631
	SiCl ₄ (l) - RDC-2	169.90	9.794	0.999	1664.058	0.999	90.214	2.631
Deposition reaction								
In	SiH ₄ (l)	32.12	6.525	1.000	209.567	1.000	-94.653	2.300
Out	Si (s) _{GS}	28.09	6.525	0.328	183.260	0.700	699.850	39.477
	H ₂ (g)	2.02	13.050	0.656	26.308	0.100		
	SiH ₄ (l)	169.90	0.308	0.016	52.392	0.200		

According to the work of Hassim & Edwards (2006) the penalty tables are as follows:

Table A4.2. Summary of penalties for activities or operations (AP).

	Carboreduction		Synthesis reaction		Separation and purification		Reactive distillation		Deposition reaction	
<i>Transport</i>	Vibration	4	Pipe	1	Pipe	1	Pipe	1	Pipe	1
<i>Mode of process</i>	Semi-continuos	2	Continuous	1	Continuous	1	Continuous	1	Batch	3
<i>Venting or flaring</i>	Occupiable platform level	3	Above occupiable level	2	Above occupiable level	2	Above occupiable platform level	2	Above occupiable level	2
<i>Mantaince works</i>	Yes	1	Yes	1	Yes	1	Yes	1	Yes	1
<i>Noise level</i>	Hazardous	2	Hazardous	2	Hazardous	2	Hazardous	2	Hazardous	2
<i>Others</i>	Size reduction, solid handling	3	Size reduction	2	Size reduction	2	Size reduction	2	---	---

Table A4.3. Summary of penalties for process conditions and material properties (CP).

	Carboreduction		Synthesis reaction		Separation and purification		Reactive distillation		Deposition reaction	
<i>Temperature (°C)</i>	High	1	High	1	High	1	High	1	High	1
<i>Pressure (atm)</i>	Low	0	Low	0	Low	0	Low	0	Low	0
<i>Viscosity (cp)</i>	---	---	Low	1	Medium	2	Medium	2	Low	1
<i>Ability to precipitate</i>	Yes	1	No	0	No	0	No	0	Yes	1
<i>Density difference (sg)</i>	Low	1	Low	1	Low	1	Low	1	Low	1
<i>Ability to cause corrosion</i>	No	0	Yes	1	Yes	1	Yes	1	Yes	1
<i>Volume changes (%)</i>	---	---	High	3	High	3	High	3	---	---
<i>Solubility</i>	No	0	Yes	1	Yes	1	Yes	1	Yes	1
<i>Material state</i>	Granules	3	Gas	0	Liquid	1	Liquid	1	Gas	0

The total sum of the ICPHI is: **91**.

Ability to Cause Typical Occupational Diseases: Health Hazard Index (HHI)

Table A4.4. Ranking matrix for occupational disease.

	<i>SI</i>	<i>H₂</i>	<i>SiCl₄</i>	<i>SiHCl₃</i>	<i>SiH₂Cl₂</i>	<i>C</i>	<i>CO</i>	<i>SiH₄</i>	<i>SiH₃Cl</i>	<i>SiO₂</i>
CANCER	---	---	---	---	---	---	---	---	---	---
CHRONIC (CUMULATIVE) TOXICITY	---	---	---	---	---	---	---	---	---	---
CHRONIC (CUMULATIVE) TOXICITY- LONG TERM	---	---	---	---	---	---	---	---	4.5	---
ACUTE TOXICITY	---	---	---	---	---	---	---	4.3	---	---
REPRODUCTIVE HAZARDS	---	---	---	---	---	---	---	---	---	---
NERVOUS SYSTEM DISTURBANCES- CHOLINESTERASE	---	---	---	---	---	---	---	---	---	---
NERVOUS SYSTEM DISTURBANCES-NERVOUS SYSTEM	---	---	---	---	---	---	---	---	3.5	---
NERVOUS SYSTEM DISTURBANCES-NARCOSIS	---	---	---	---	---	---	---	---	---	---
RESPIRATORY EFFECTS OTHER THAN IRRITATION (ASTHMA)	---	---	---	3	---	---	---	---	---	---
RESPIRATORY EFFECTS OTHER THAN IRRITATION (LUNG DAMAGE)	---	---	---	---	---	---	---	---	---	---
RESPIRATORY EFFECTS	---	---	2.5	---	2.5	2.5	---	---	2.5	---
HEMATOLOGIC (BLOOD) DISTURBANCES ANEMIAS	---	---	---	---	---	---	---	---	---	---
HEMATOLOGIC (BLOOD) DISTURBANCES METHEMOGLOBINEMIA	---	---	---	---	---	---	---	---	---	---
IRRITATION: EYES, NOSE, THROAT, SKIN-MARKED	---	---	1.8	1.8	1.8	---	---	---	1.8	---
IRRITATION: EYES, NOSE, THROAT, SKIN- MODERATE	---	---	---	---	---	---	---	---	---	1.5
IRRITATION: EYES, NOSE, THROAT, SKIN-MILD	---	---	---	---	---	1.3	---	---	---	---
ASPHYXIANTS, ANOXIANTS	---	---	---	---	---	---	1	---	1	---
EXPLOSIVE, FLAMMABLE, SAFETY	---	---	---	---	---	---	---	---	0.8	---
GENERALLY LOW RISK HEALTH EFFECTS-NUISANCE PARTICULATES, VAPOURS OR GASES	0.5	---	---	---	---	---	---	---	---	---

GENERALLY LOW RISK HEALTH EFFECTS-ODOUR

--- | --- | --- | --- | --- | --- | --- | --- | --- | ---

The total sum of the HHI is: **38.6**.

Material Harm Index (MHI)

Table A4.5. NFPA health rating criteria.

	SI	H ₂	SiCl ₄	SiHCl ₃	SiH ₂ Cl ₂	C	CO	SiH ₄	SiH ₃ Cl	SiO ₂
LIMITED EXPOSURE - DEATH/MAJOR RESIDUAL INJURY	---	---	---	---	4	---	---	---	4	---
SHORT TERM EXPOSURE - SERIOUS TEMPORARY/RESIDUAL INJURY	---	---	3	3	---	---	3	---	---	---
INTENSE/CONTINUED EXPOSURE - TEMPORARY INCAPACITATION/POSSIBLE RESIDUAL INJURY	---	---	---	---	---	---	---	---	---	---
EXPOSURE - IRRITATION/MINOR RESIDUAL INJURY	1	---	---	---	---	1	---	1	---	1
EXPOSURE UNDER FIRE CONDITIONS - NO HAZARD	---	---	---	---	---	---	---	---	---	---

The total sum of the MHI is: **21**.

Determining the Airbone Quantity Resulting from Small Leaks

Table A4.5. The Airbone Quantity Resulting from Small Leaks.

	CARBOREDUCTION		SYNTHESIS REACTION		SEPARATION AND PURIFICATION			REACTIVE DISTILLATION				DEPOSITION REACTION			
	In	Out	In	Out	In	Dome	Bottom SiCl ₄	Bottom SiHCl ₃	In	Domo RD1	Domo RD2	Bottom RD1	Bottom RD2	In	Out
MW AVG	0	28	161	161	161	101	170	134	134	33	34	170	169	32	170
PG, KPA	---	---	---	---	599	299	374	368	368	132	132	165	165	132	3899

<i>PA, KPA</i>	101	101	101	3600	700	400	475	469	469	233	233	267	267	233	4000
<i>T, °C</i>	20	2000	21	500	124	52	115	85	85	-95	-95	90	90	-95	700
<i>TB, °C</i>	---	---	---	---	53	8	58	32	32	-106	-103	58	57	-112	58
<i>L, KG/S</i>	---	---	---	---	1	1	1	1	1	0	0	1	1	0	3
<i>WP, KG/S</i>	---	---	---	---	---	---	---	---	---	---	---	---	---	---	---
<i>AP, M²</i>	---	---	---	---	---	---	---	---	---	---	---	---	---	---	---
AIRBORNE MATERIAL FROM GASEOUS RELEASE	---	0	0	0	---	---	---	---	---	---	---	---	---	---	---
AIRBORNE MATERIAL FROM FLASHING LIQUIDS	---	---	---	---	311	0	240	0	0	0	0	92	91	0	6075
AIRBORNE MATERIAL EVAPORATION FROM THE SURFACE OF A POOL	---	---	---	---	---	---	---	---	---	---	---	---	---	---	---

The total sum of the SM (kg/h) x (1 h / 3600s) is: 24'511,810.86.

D of the hole, mm: 6.35

The estimation of workplace concentration is according to the Hassim & Edwards,⁵¹ equations

WC_{MAX} (KG/M³) 12'255,905.4
 WC_{MIN} (KG/M³) **81,706.0**

Fugitive Emissions

Table A4.6. Fugitive Emissions for the entire process.

	FE (KG/H)
CARBOREDUCTION	0.28896
SYNTHESIS REACTION	1.398432
SEPARATION AND PURIFICATION	0.804648
REACTIVE DISTILLATION	0.804648
DEPOSITION REACTION	0.700504
	3.997192

Determining worker exposure concentration (WEC)

Table A4.7. Worker exposure concentration.

	min	max
Estimated exposure time EET _j (h)	4	6
Normal average work time AWD (h)	8	8
WEC (kg/m ³)	6'127,952.71	61,280

Estimating occupational exposure limit (OEL)

Table A4.8. Estimated occupational exposure limit for the Intensified FRB Union Carbide Process.

	STREAM	SUBSTANCE	OEL(KG/M ₃)	OEL AVG (KG/M ³) 10 ⁶
CARBOREDUCTION	In	C (s)	1.4348	4.98
		SiO ₂ (s)	3.540	---
	Out	Si (s) MG	10.932	25.8
		CO (g)	14.914	---
SYNTHESIS REACTION	In	Si (s) MG	0.161	34.5
		SiCl ₄ (g)	34.369	---
		H ₂ (g)	0	---
	Out	H ₂ (g)	0	33.3
		SiCl ₄ (g)	28.141	---
		SiHCl ₃ (g)	5.203	---
		SiH ₂ Cl ₂ (g)	0	---
SEPARATION AND PURIFICATION	In	SiCl ₄ (l)	28.141	33.3
		SiHCl ₃ (l)	5.203	---
		SiH ₂ Cl ₂ (l)	0	---
	Dome	SiH ₂ Cl ₂ (l)	0	---
	Bottom SiCl ₄	SiCl ₄ (l)	34.744	34.7
	Bottom SiHCl ₃	SiHCl ₃ (l)	27.380	27.7
		In	SiHCl ₃ (l)	27.380
Dome RD1		SiH ₄ (l)	7	7
		SiH ₃ Cl (l)	0	---
Dome RD2		SiH ₄ (l)	7	7
		SiH ₃ Cl (l)	0	---
Bottom RD1		SiCl ₄ (l)	34.440	34.7
		SiHCl ₃ (l)	0.239	---

DEPOSITION REACTION

Bottom Rd2	SiCl ₄ (l)	34.250	34.6
	SiHCl ₃ (l)	0.389	---
In	SiH ₄ (l)	7	7
	Si (s) _{GS}	11.665	19.4
Out	H ₂ (g)	0	---
	SiH ₄ (l)	7.724	---

OEL_{min} (kg/m³) **4.98 x10⁻⁶**

Then:

$$PRHI = ICPHI \times MHI \times HHI \times \frac{WEC_{max}}{OEL_{min}} \quad (S1)$$

The final result of the PRHI for the Intensified FRB Union Carbide Process is:

PRHI= **9.09x10¹⁴**

5

Surrogate based optimization of a novel process of polycrystalline silicon
production

**Computers
& Chemical
Engineering**

An International Journal

5 Surrogate based optimization of a novel process of polycrystalline silicon production

Abstract

In this work, the optimal operating conditions for a route for polycrystalline silicon production are determined. The design and optimization of the process follows a two stage procedure to pay attention to the reactors. Surrogate models for the major units are developed following different techniques depending on the operating information, either experimental or based on rigorous models. Next, the optimization of the entire process flowsheet allows determining the optimal tradeoff between yield and energy consumption of the process. For the three scenarios evaluated, maximum silicon production, minimum operating costs and maximum total profit, and a production capacity of 2000 t/y of polycrystalline silicon, an investment of 9.97 M\$ is required. The optimization shows that to maximize the profit of the process, an operating cost adds up to 6.48 M\$/y. The profit after operating expenses, and considering the sale of polycrystalline silicon and the byproducts generated by the process (SiC, SiH₂Cl₂, SiCl₄, HCl, and H₂), are 10 M\$/y, presenting a competitive price of polycrystalline silicon of 8.93 \$/kg, below the commercial price, estimated at 10 \$/kg. Furthermore, a plant scale-up study was performed, observing a decrease in the price of polycrystalline silicon if the production size of the polycrystalline silicon plant is increased, resulting in a reduction of 1.03 \$/kgSiPoly when increasing production 10 times.

5.1 Introduction

As result of the constant increase in the worldwide energy requirements to meet the demand of the modern society, together with the effects of the climate change as consequence of the anthropogenic emissions of greenhouse gases, the renewable sources of energy have become a paramount pillar to achieve sustainable development. The aim is

to produce power following an environmentally friendly and sustainable path. One of the alternatives with the potential to meet these requirements is solar energy. Among the different solar-based technologies for energy production, silicon based solar cells have been consolidated as one of the most promising technologies (Green, 2009).

Although silicon-based photovoltaic panels can be built using both polycrystalline and monocrystalline silicon, the scope of the present work is focused on the first of the technologies. Traditionally, polycrystalline silicon (also called polysilicon) was mainly used in the microelectronic industry (Pizzini, S., 2010). Over the last decade the rise of the solar power sector has converted the photovoltaic industry (PV) into the main consumer of polysilicon, as shown in Figure 5.1 (Hesse et al., 2009). As a result, the polysilicon production capacity is overcome by the demand from the photovoltaic industry generating a shortage (Chigondo, 2018).

The growth of the experimented in PV industry over the last decade, has allowed a decrease in the production cost of electricity, to the extent that some countries have reached the socket parity point (Polman, et al., 2016). In spite of this fact, a further reduction of the photovoltaic cells cost and an increase in the electricity production efficiency are necessary to achieve more competitive electricity generation costs, ensuring its long-term sustainability and penetrating new markets across the world (Wang et al., 2013; Morita & Yoshikawa, 2011). To reach these objectives, one of the keys is to reduce the manufacturing costs of

polycrystalline silicon. Approximately one half of the finished module costs corresponds to the production of polycrystalline silicon (Weber et al., 2004). Therefore, lowering the polycrystalline silicon production costs is expected to reduce the manufacturing costs of the solar panels. Hence both, the shortage of silicon in the photovoltaic industry, and the need to reduce its manufacturing cost, have led the research for the development of new polycrystalline silicon production processes to improve their economics and environmental sustainability.

Currently, two paths for polycrystalline silicon production are known: the metallurgical, and the chemical routes (Ranjan, et al., 2011). The chemical route is the one which focus the research efforts because of the high purity of the silicon produced. Thus, it is the one used at industrial scale (Zadde et al., 2002), see Figure 5.1. Within the chemical route two processes can be distinguished: the Siemens process, based on the decomposition of trichlorosilane at high temperature in hydrogen atmosphere (SiHCl_3) (O'Mara et al., 2007; Nie & Hou, 2018), and the process developed by Union Carbide Co., based on the disproportionation of trichlorosilane to produce silane, SiH_4 , as high purity silicon precursor of polysilicon (Union Carbide, 1981).

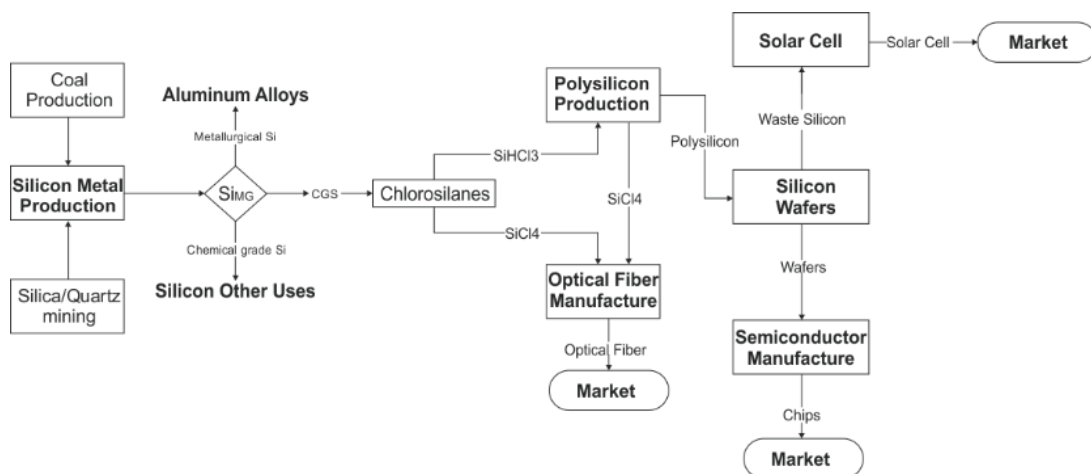


Fig 5.1. Flow chart of silicon manufacturing.

To achieve the targets of lower cost and higher production capacity, novel processes are needed. In the works developed by Ramírez-Márquez et al., (2018, 2019), a process with a high production capacity of polycrystalline silicon was developed and optimized using different objective functions: economic, (total annual cost (TAC) and the return on investment (ROI)), safety,(the individual risk index (IR)), and environmental, (the eco-indicator 99 (EI99)). However, one of the observed drawbacks of the methodology used in the aforementioned works is the null possibility of evaluating the operating conditions of the reaction systems. The optimization, basically, only exists in the separation systems. This result is due to the fact that the optimization was carried out using a stochastic optimization scheme within the Aspen Plus® software. Although Aspen Plus® contains several modules for reactors simulation, it is difficult to introduce detailed customized models. Therefore, the models for reaction systems are accurate only in a limited range of operating conditions. In addition, the information about the distribution of the reaction products, and their variation as a function of the operating conditions in the reactor is generally not detailed enough and difficult to obtain. Usually, the data provided in the literature is circumscribed to a narrow range of operating conditions where, for example, the catalyst performance is optimal. Additionally, these conditions are generally not the most economically favorable. There are a number of works that describe individually each unit in the process. For instance, the work of Yadav et al., (2017) reviewed numerical models incorporating thermodynamics, reaction kinetics, fluid dynamics, heat and mass transfer calculations to examine the refinement of metallurgical silicon to polycrystalline silicon production for each unit independently. In addition, researchers such as Sugiura et al., (1992) showed in their work the solution of the partial differential mass balance equations to model the

hydrogenation of trichlorosilane in a fixed bed reactor under the assumption that the reactions are in a fixed state. Similarly, authors such as Kato and Wen (1969), tested models for gas-solid fluidized beds; the models are based on three-phase theory involving bubble, emulsion and cloud phases. Wang (2011), conducted a study of 2-D cylindrical fluidized bed reactor model for hydrochlorination of silicon. Ni et al., (2014) showed studies of gas velocity distribution in bell-jar reactor with 12 rods of three different diameters from 3-D CFD simulations. Although, there are a number of works that describe independently the units of the polycrystalline silicon production process, there is no study that captures the features of all the major units within a process model.

In this work the major units of the process, not only distillation columns but specially the reactors, involved in the production of silicon polycrystalline are modeled based on experimental and industrial data. Different surrogate modeling approaches are used depending on the data available to develop a framework for the entire process for polycrystalline silicon production in Ramírez-Márquez et al., (2018) that will allow evaluating the operating conditions at each of the units toward minimizing the production cost of the polycrystalline silicon. The process proposed can be divided into four main sections. The first section is the carboreduction of SiO_2 using C to obtain metallurgical silicon. The second section corresponds to the production of chlorosilanes through the reactions system formed by the hydrogenation of silicon tetrachloride and the hydrochlorination of metallurgical silicon with HCl. The third section consists in the purification of the chlorosilanes obtained from the previous reactor using distillation columns. Finally, the fourth section is the conversion of trichlorosilane into polysilicon in a Siemens deposition reactor. The entire process is modeled using the algebraic language GAMS

as an NLP model. The rest of the paper is organized as follows. Section 5.2 presents the process description. Section 5.3 shows the development of surrogate models for all the units. In section 5.4 the solution procedure presenting the various objective functions is discussed. Section 5.5 comments on the results and finally conclusions are drawn.

5.2 Methodology for process design

To guarantee that the proposed process has a similar production capacity to some polycrystalline silicon production companies (Nitol Chem Group 1,500 ton/year, PV Crystalox 2,250 ton/year, SolarWorld 3,200 ton/year) (List of World's Polysilicon Producers, 2013), an average production capacity of the plant of 2,000 annual metric tons of polycrystalline silicon is considered.

It is important to present some previous knowledge of the existing conventional processes to justify the use of the process developed in previous work (Ramirez-Marquez et al 2018). The Siemens process is a technology based on the use of trichlorosilane (SiHCl_3) as a silicon source. Initially, a metallurgical reduction of quartz is carried for the production of metallurgical grade silicon, Si_{MG} . The Si_{MG} produced reacts with hydrogen chloride (HCl) in a fluidized bed reactor to produce a gas stream composed by a mix of chlorosilanes. Among them, the most important is trichlorosilane, which will be the used as precursor in the final polysilicon production stage (Pazzaglia et al., 2011). Subsequently, the purification process consists in a distillation column sequence to obtain ultrapure trichlorosilane. Finally, for polycrystalline silicon production, the ultrapure trichlorosilane is decomposed in a chemical vapor deposition reactor known as Bell reactor or Siemens reactor (Erickson & Wagner, 1952). It should be mentioned that the Siemens process is a complicated process that has as a drawback the use of extremely

pure HCl for the synthesis of chlorosilanes, with the associated risks for the safety and environment inherent to use of this compound.

However, the process developed by Union Carbide Co, uses silane (SiH_4) as a source of polycrystalline silicon. Similarly to the Siemens process, Si_{MG} is produced via metallurgical reduction of SiO_2 and C. Then, Si_{MG} and silicon tetrachloride, which is recirculated from the next step, are hydrogenated in a fluidized bed reactor (FBR) to produce chlorosilanes: SiCl_4 , SiH_2Cl_2 , and SiHCl_3 . (Iya, 1986). Subsequently, the chlorosilanes obtained are subjected to a separation and purification stage. This process has the characteristic of transforming the trichlorosilane in silane through successive redistribution reactions (Iya, 1986), or through the use of reactive distillation columns (Muller et al., 2002; Ramírez-Márquez et al., 2016). Finally, the high purity silane obtained is introduced in a vapor deposition reactor where it is decomposed to produce the polycrystalline silicon. One of the advantages of the process developed by the Union Carbide Co. is the high efficiency in obtaining polycrystalline silicon, since the conversion of silane to silicon is larger than that from trichlorosilane. However, this process operates in more extreme operating conditions than the ones used in the Siemens process.

From the processes descriptions above, it can be observed that the conventional processes for polycrystalline silicon production can be divided into four main stages: a) thermal carboreduction stage, where a metallurgical reduction process is carried out. This process consists of melting the silica in presence of carbon in an electric arc furnace at a temperature above of the boiling point of SiO_2 $>2500^\circ\text{C}$, to produce Si_{MG} ; b) chlorosilanes production from Si_{MG} ; c) the purification stage, that separates different chlorosilanes originated from the previous process; and finally d) polycrystalline silicon production

through chemical vapor deposition. Taking into account every stage of the conventional processes, a process for polycrystalline silicon was developed by the Ramírez-Márquez et al., (2018 & 2019), see Figure 5.2. In those works, the conceptual design of the process, named as Hybrid Process, is presented from the strategic combination of stages of the Siemens process and the Union Carbide process. The conceptual design was originated by the idea of taking advantage of the maximum productivity of each of the stages, combining them in the optimal arrangement, and verifying the feasibility of the final integration of stages.

The first stage, for the Si_{MG} production, is carried out similarly in both conventional processes, through the metallurgical reduction of SiO_2 with C. The works of Ramírez-Márquez et al., (2018 & 2019) used the global reaction operating at the common operating conditions, where basically the oxygen detached from the SiO_2 is caught by C to form carbon monoxide (CO). However, in practice, this reaction is usually more complicated, generating also other by-products, such as $\text{SiC}_{(\text{s})}$, $\text{Si}_2\text{C}_{(\text{g})}$, $\text{Si}_{2(\text{g})}$, $\text{SiC}_{2(\text{g})}$, $\text{Si}_{(\text{g})}$ and $\text{SiO}_{(\text{g})}$. Therefore, in this work a more detailed model for the reaction considering the distribution of species of the system Si-O-C is developed. The reaction is carried out in an electric arc furnace whose product distribution is a function of the temperature (above SiO_2 boiling point $>2500^\circ\text{C}$) (Wai & Hutchison, 1989).

Once the reaction is completed, the gases are extracted from the furnace, leaving the liquid silicon in the bottom of the furnace. The liquid silicon is collected at the melting pot, which is filled by the top and it is emptied from the bottom on the casting where it is solidified. The temperature at which silicon is extracted from the furnace is above the silicon melting temperature (Berciano et al, 2009), being a critical parameter in the Si_{MG} production. If the temperature of the silicon is too high it can cause a premature wear of the refractory

materials and increase the risk of dissolution of gases in the liquid silicon. On the contrary, a low temperature results in low silicon fluidity (573 K). During the time that silicon remains in the melting pot, the refining of silicon is carried out by an oxidative process, eliminating a large part of the impurities through the formation of slag, obtaining silicon with a purity of 98%-99%. The slag is eliminated mechanically or by gravity, and it is stored in a tank. Meanwhile the silicon remains in the melting pot until it reaches a temperature between 318 K and 348 K. Usually, several melting pots work following the method denominated sequential casting, where successive melting pots are operated in a sequential mode, continuously feeding the vessel of the continuous casting system.

The melting pot discharges molten silicon into a distribution vessel. When the silicon quantity contained on the vessel is enough to maintain a steady feeding flow, this is opened and the liquid silicon is allowed to fall into the ingot mold. This is cooled by water that runs through a pipe located in the internal part, reducing the silicon temperature until it solidifies. Later, solid silicon undergoes a secondary cooling by water showers to adjust the temperature to an adequate value, around 298 K, for the subsequent grinding in a roller crusher (Ceccaroli & Lohne, 2003). The small pieces of Si_{MG} obtained after grinding are stored at environmental conditions in a covered silo which feeds the chlorosilane synthesis reactor.

For the second stage recycled SiCl_4 is hydrogenated in a fluidized bed reactor in the presence of metallurgical grade Si. A simplified model of the $\text{SiCl}_4\text{-H}_2\text{-Si}_{\text{MG}}$ is used by Ramírez-Márquez et al., (2018, 2019) to estimate the products obtained with fixed operating conditions based on literature data. The rigorous $\text{SiCl}_4\text{-H}_2\text{-Si}_{\text{MG}}$ model was chosen for this stage because of the advantages associated with this kind of reactor for the chlorosilanes production, which include

relatively low operation temperatures, typically between 673 and 873 K, and larger silicon tetrachloride conversion (Ding, et al., 2014). During this reaction, impurities such as Fe, Al, and B react to form their halides (e.g. FeCl_3 , AlCl_3 , and BCl_3). The SiHCl_3 has a low boiling point of 31.8 °C and distillation is used to purify the SiHCl_3 from impurity halides. The resulting SiHCl_3 now has electrically active impurities (such as Al, P, B, Fe, Cu or Au) of less than 1 ppba. These reactions are omitted for the represented process, since at this point a conceptual stage model is developed. According to the experimental observations of Ding et al., (2014), it is assumed that in the $\text{SiCl}_4\text{-H}_2\text{-Si}_{\text{MG}}$ system the following species are involved: SiCl_4 , H_2 , Si_{MG} , SiHCl_3 , SiH_2Cl_2 , and HCl . Therefore, the operating conditions of this system are susceptible to be modified, affecting the distribution of the products formed. In the present work a more detail model is developed to evaluate the effect of the operating conditions on the distribution of the products.

The reactor outlet stream contains a mixture of SiCl_4 , SiHCl_3 , SiH_2Cl_2 , together with HCl and H_2 . This stream is fed into a condensation stage that separates the reactor effluent in a gas phase stream and a liquid phase. The gas phase stream is formed by the most volatile compounds, H_2 and HCl , while the liquid stream is formed mainly by SiH_2Cl_2 , SiHCl_3 and SiCl_4 . Due to the large difference of volatility between the hydrogen, hydrogen chloride, and the chlorosilanes, a 100% separation efficiency in this stage is considered (Payo, 2008). Therefore, the gaseous stream, is cooled in the condenser until 298 K. The chlorosilanes condense forming a liquid phase. Next, the stream is introduced into a phase separator where the gaseous hydrogen and hydrogen chloride are separated and stored in a tank, while the liquid stream consisting of the chlorosilanes are sent to the third stage.

The third step is a purification stage where two conventional distillation columns are used to separate the chlorosilanes mix. The SiCl_4 is separated first, due to the large quantity that it represents. From the top of the first column a $\text{SiH}_2\text{Cl}_2\text{-SiHCl}_3$ mix is recovered, while from the bottoms high purity SiCl_4 is obtained. The second column separates the $\text{SiH}_2\text{Cl}_2\text{-SiHCl}_3$ mix obtained from the dome of the previous distillation column, obtaining a high purity stream of SiH_2Cl_2 at the top, and a high purity stream of SiHCl_3 at the bottom (Ramírez-Márquez et al., 2018).

In the last stage SiHCl_3 is fed to the Siemens vapor deposition reactor. The Siemens reactor consists of a chamber where several thin high purity silicon rods are heated up by an electric current that flows through them. In the reactor, the thermal decomposition of trichlorosilane in a hydrogen atmosphere is carried out at temperatures of 373-873 K, leading to the silicon deposition on the rods, where the solar grade polysilicon is obtained. Similar to the models of the reactors presented in the work of Ramírez-Márquez et al., (2018 and 2019), it was also modelled assuming a stoichiometric reactor. In the present work, the optimization of reaction conditions, particularly gas flow and temperature, is pursued with the aim of finding an optimal trade-off between polycrystalline silicon growth and operation costs due to energy consumption.

The process diagram for polycrystalline silicon production that was used in the present work is showed in Figure 5.2. It shows all process sequence and the products generated in each stage.

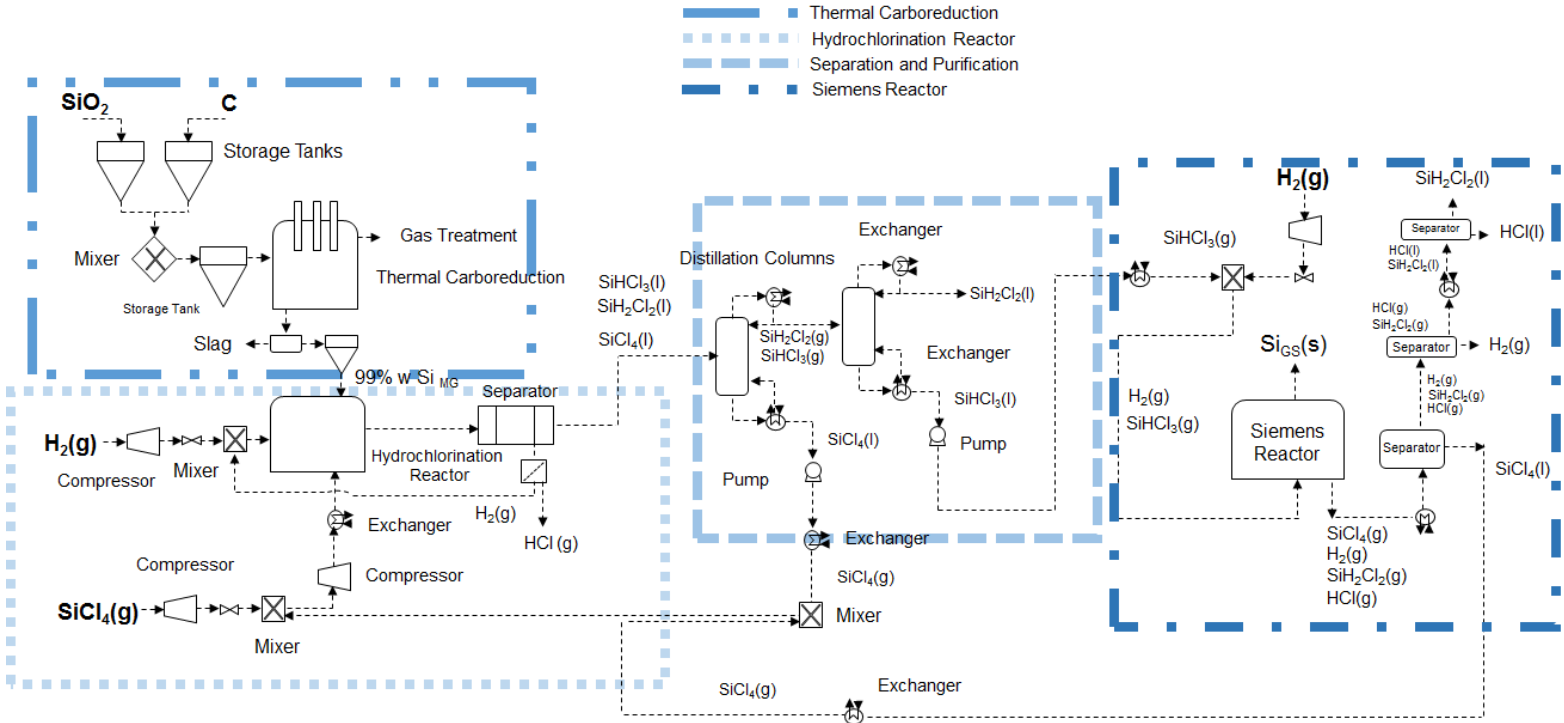


Fig 5.2. Flowsheet of the Hybrid Process proposed.

5.3 Modelling approach

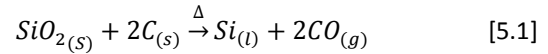
In this section the description of the surrogate model development is presented for the three main reactors and the two distillation columns. The rest of the units, compressors, heat exchangers, mixers and splitters are modelled based on first principles and thermodynamics (Martin, 2016)

5.3.1 Thermal carboreduction

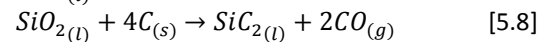
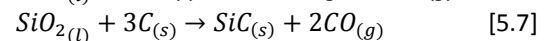
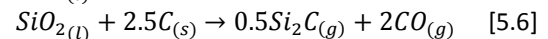
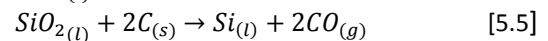
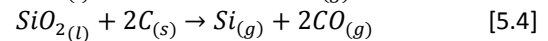
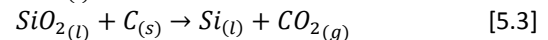
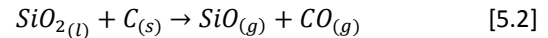
The process starts at a carboreduction process. The raw materials used are quartz (SiO₂) and carbon (C). The raw materials are stored in storage tanks, to be further blended in a mixer, and finally they are fed into the carboreduction reactor. The storage tanks and mixers have been modeled through material balances (Martin, 2016).

The model for the carboreduction reactor is based on the work reported by Wai and Hutchison (1989). That work showed that the

reaction among SiO₂ and C, Eq. 5.1, actually consists of a number of stages



The detailed model proposed by Wai and Hutchison considers the multiple silicon dioxide reactions with carbon at high temperatures to form several products. The possible reactions that may take place during the silicon dioxide carboreduction process are shown in Eqs. 5.2 to 5.8.



Wai and Hutchison (1989) computed the products distribution for a C/SiO₂ feeding

molar ratio of 2:1, a total pressure of 1 atm, and a temperature range of 2500-3500 K. to achieve the production capacity of typical industrial plants, in the present work a feed of 15kmol/h of SiO₂ and 30 kmol/h of C is considered. To model the carboreduction process, the distribution diagram of gaseous and condensed species in the system Si-O-C at different temperatures obtained by Wai and Hutchison (1989) is used. Based on that work, correlations are developed to estimate the distribution of the products obtained at the reactor (mol fraction) as a function of the reaction temperature (K).

In some cases, it is necessary to extract values from figures and graphics since some scientific publications only show the graphs, but the data values are not published. The PlotDigitizer software was used to data extraction. The data extraction process by this software is straightforward: 1) Import the graphic from a file, 2) the axes system is defined, and 3) it is digitized either automatically or manually. The data values are copied in Excel for their manipulation. Once numerical data are obtained from the plot, to check the accuracy of the extraction process the data are plot and compared with the original diagram. The temperature interval considered ranges from 2600 to 3100 K. Therefore, the fit of numerical data obtained for each species was carried out as a function of the temperature, obtaining the following correlations for the distribution of the carboreduction products, Eqs. 5.9 to 5.16. Note that not all the correlations present the same mathematical shape. This is due to the complex shape of the profiles:

$$x_{Si(l)} = -2.48131 \times 10^{-9} T^3 + 1.90239 \times 10^{-5} T^2 - 4.79395 \times 10^{-2} T + 39.71359 \quad [5.9]$$

$$x_{CO(g)} = 9.82689 \times 10^{-5} T^3 + 1.90239 \times 10^{-5} T + 3.74066 \times 10^{-1} \quad [5.10]$$

$$x_{Si(g)} = 5.93093 \times 10^{-10} e^{6.31510 \times 10^{-3} T} \quad [5.11]$$

$$x_{SiC(s)} = 7.14539 \times 10^{-7} T^2 - 4.50044 \times 10^{-3} T + 7.08465 \quad [5.12]$$

$$x_{Si2C(g)} = 1.72881 \times 10^{-7} T^2 - 9.13915 \times 10^{-4} T + 1.20759 \quad [5.13]$$

$$x_{SiC2(g)} = -1.19611 \times 10^{-14} T^5 + 1.65491 \times 10^{-10} T^4 - 9.14807 \times 10^{-7} T^3 + 2.52572 \times 10^{-3} T^2 - 3.48320 T + 1919.64937 \quad [5.14]$$

$$x_{SiO(g)} = 7.58739 \times 10^{-7} T^2 - 4.47932 \times 10^{-3} T + 6.69671 \quad [5.15]$$

$$x_{Si2(g)} = 4.76996 \times 10^{-13} e^{7.68303 \times 10^{-3} T} \quad [5.16]$$

Where, x_i is the molar fraction of each specie i , and T in the temperature between the range of 2600 a 3100 K in Kelvin. Likewise, an energy balance to the reactor is performed to calculate the utilities required. The process requires electrodes, which provide the necessary energy for the reaction. A large consumption of power is required to melt the silica, around 10-11 kWh to produce a kilogram of silicon, reaching temperatures over 2600 K (Brage, 2003).

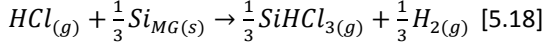
Regarding the post processing of the liquid product obtained, mainly melted silicon, the modeling of the discharge to the melting pot, the distribution pipe, the secondary cooling, and the roller crusher was carried out by material and energy balances. The second exit stream consisting of the gaseous components is sent to gas treatment. The solid SiC is extracted in the melting pot as slag, whereas the metallurgical silicon is sent to the solidification stage by cooling for its subsequent use in the chlorosilane synthesis reactor.

5.3.2 Hydrochlorination Reactor

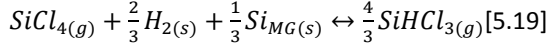
In this reactor recycled SiCl₄ is hydrogenated in the presence of Si_{MG}. In the present work, the thermodynamic analysis of the system SiCl₄-H₂-Si_{MG} performed by Ding, et al., (2014) was considered to model the hydrochlorination reactor, where chlorosilanes are produced as intermediate products. Ding, et al., (2014) studied the SiCl₄ hydrogenation in presence of Si_{MG}, from both thermodynamic and experimental perspectives. The series of reactions that the proposed system includes are the SiCl₄ hydrogenation in the gas phase, Eq. 5.17:



And the hydrochlorination of Si_{MG} with HCl, Eq. 5.18:



Combining 5.17 and 5.18 yields the SiCl₄-H₂-Si_{MG} process, Eq. 5.19:



The total Gibbs free energy minimization model is used to determinate the equilibrium reaction system compositions. Next surrogate models are developed to estimate the composition as a function of the operating conditions

The total Gibbs free energy of the system is given the Eq. 5.20:

$$G^T = \sum_{i=1}^N n_i \mu_i = \sum_{i=1}^N n_i \left(G_i^o + RT \ln \frac{\hat{f}_i}{f_i^o} \right) \quad [5.20]$$

Furthermore, considering the constraint defined by Eq. 5.21:

$$\sum_i n_i a_{ik} = A_k \quad (k = 1, 2, \dots, w) \quad [5.21]$$

The following equations are indicated for the gas-phase, defining the standard Gibbs free energy \hat{f}_i^o , fugacity, f_i^o , and molar fraction, y_i , given by Eqs. 5.22, 5.23 and 5.24, respectively.

$$\hat{f}_i = y_i \hat{\phi}_i P, \quad f_i^o = P^o, \quad y_i = \frac{n_i}{\sum_i^N n_i} \quad [5.22]$$

For solid silicon:

$$RT \ln \frac{\hat{f}_i}{f_i^o} = \int_{P^o}^P V_{SiMG} (P - P^o) \quad [5.23]$$

which, as V_{SiMG} changes little with pressure, can be approximated by Eq 5.24:

$$RT \ln \frac{\hat{f}_i}{f_i^o} = V_{SiMG} (P - P^o) \quad [5.24]$$

Therefore, combining Eqs. 5.20 to 5.24, we obtain Eq. 25 to describe the total Gibbs free energy of the system:

$$G^T = \sum_{i=1}^N n_i \left(G_i^o + RT \ln \frac{y_i P}{P^o} \right) + n_{Si} G_{Si}^o + V_{SiMG} (P - P^o) \quad [5.25]$$

Where the Gibbs–Helmholtz relationship is defined by Eq. 5.26:

$$G_i^o = H_i^o + TS_i^o \quad [5.26]$$

being the standard enthalpy and standard entropy defined by Eqs. 5.27 and 5.28,

$$H_i^o = H_{i,298}^o + \int_{298}^T C_{p,i} dt \quad [5.27]$$

$$S_i^o = S_{i,298}^o + \int_{298}^T \frac{C_{p,i}}{T} dt \quad [5.28]$$

In these expressions, G^T is the total Gibbs free energy; N is the number of species in the reaction system; n_i is the number of moles; μ_i is the chemical potential; G_i^o is the standard Gibbs free energy; \hat{f}_i^o is the standard Gibbs free energy; f_i^o is the fugacity of species i; R is the molar gas constant; T is the temperature; a_{ik} is the number of kth atoms in each molecule of species i; A_k is the total atomic mass of the kth element in the system; w is the total number of elements in the system; P is the total pressure. $\hat{\phi}_i$ is the fugacity coefficient; y_i is the molar fraction of species i; P^o is the standard-state pressure (100 kPa); V_{SiMG} is the molar volume of silicon; and H_i^o , S_i^o , and $C_{p,i}$ are the standard enthalpy, standard entropy, and heat capacity, respectively, of species i. Thermodynamic data for the chemical species involved is taken from Ding, et al., (2014).

Using the model given by the Gibbs free energy minimization, it is possible to determine the species distribution when the reaction system reaches the equilibrium at different conditions of temperature, pressure and H₂/SiCl₄ molar feeding ratio. For convenience, the reaction system SiCl₄-H₂-Si_{MG} was treated as ideal, and the following variables ranges were studied: temperature (T), 373–873 K; pressure (P), 1–20 atm; y molar feeding ratio (Rel) H₂/SiCl₄, 1-5. The total Gibbs free energy minimization

was performed offline using GAMS. This model was used to develop surrogate models to be incorporated into the flowsheet optimization framework. Surrogates for each one of the species involved in the reactions presented in Eqs. 5.17 and 5.18 as a function of the three variables, temperature, pressure and H₂/SiCl₄ ratio are presented in Eqs. 5.29-5.33:

$$x_{SiCl_4(g)} = 5.345 \times 10^{-1} - 4.0 \times 10^{-6} P - 1.6805 \times 10^{-1} Rel + 1.7367 \times 10^{-2} Rel^2 + 1.0 \times 10^{-6} P * Rel \quad [5.29]$$

$$x_{SiHCl_3(g)} = 2.3454 \times 10^{-1} + 4.0 \times 10^{-6} P - 7.369 \times 10^{-2} Rel - 8.0 \times 10^{-6} T + 7.633 \times 10^{-3} Rel^2 + 1.0 \times 10^{-6} T Rel * T \quad [5.30]$$

$$x_{SiH_2Cl_2(g)} = 2.781 \times 10^{-2} + 1.0 \times 10^{-6} P - 9.358 \times 10^{-3} Rel + 4.0 \times 10^{-6} T + 1.031 \times 10^{-3} Rel^2 \quad [5.31]$$

$$x_{HCl(g)} = 1.60 \times 10^{-3} + 6.0 \times 10^{-6} P - 1.594 \times 10^{-3} Rel + 2.73 \times 10^{-4} Rel^2 - 1 \times 10^{-6} P * Rel \quad [5.32]$$

$$x_{H_2(g)} = 2.048 \times 10^{-1} - 6.0 \times 10^{-6} P + 2.505 \times 10^{-1} Rel + 2.0 \times 10^{-6} T - 2.6166 \times 10^{-2} Rel^2 + 1.0 \times 10^{-6} P * Rel \quad [5.33]$$

where, x is the equilibrium amount of the specie (mol fraction); P is the pressure (atm); T is the temperature (K); and Rel is the H₂/SiCl₄ molar feed ratio.

The condensation step was modelled based on material and energy balances considering complete separation of the effluent in a gas phase stream and the liquid phase stream. Likewise, the phase separator in which the hydrogen and hydrogen chloride gaseous are separated from the liquid chlorosilanes stream was modeled through material balances and their respective energy balance assuming perfect separation based on experimental results (Payo, 2008).

5.3.3 Separation and purification

For the separation of the chlorosilanes two conventional distillation columns are used. The rigorous modeling and sizing of the columns was performed using the Aspen Plus

software based on previous work (Ramírez-Márquez et al., 2019). The product purity and size of the distillation columns are fixed in the simulations while the effect of the feed and the reflux ratios on the energy and operating temperatures of each column were evaluated. The variables were evaluated in the following ranges: feeding molar ratio SiCl₄-(SiH₂Cl₂-SiHCl₃) values from 1 to 2.1698 for the first column; SiH₂Cl₂ - SiHCl₃ molar ratio from 2.99 to 7.5678 for the second column; and reflux ratio from 10 to 80 for the first column and from 60 to 90 for the second column. Surrogate models were developed from the data obtained in the simulations. Eqs. 5.34 to 5.41 present the computed variables including the reboiler and condenser thermal duties, as well as the top and bottom temperatures.

$$Q_{ConCol1} = -497.162 + 150.215 FR - 495.071 RR - 2.17 \times 10^{-4} RR^2 + 150.191 FR * RR \quad [5.34]$$

$$Q_{RebCol1} = 909.868 - 209.970 FR + 495.071 RR + 2.14 \times 10^{-4} RR^2 - 150.191 FR * RR \quad [5.35]$$

$$T_{ConCol1} = 351.296 - 4.93 \times 10^{-4} RR - 1.70050 FR + 6 \times 10^{-6} RR^2 - 1.0 \times 10^{-4} RR * FR \quad [5.36]$$

$$T_{RebCol1} = 387.695 - 9.0 \times 10^{-6} FR \quad [5.37]$$

$$Q_{ConCol2} = -15.777 - 1.1074 FR - 18.3726 RR + 1.0438 \times 10^{-1} FR^2 + 1.0 \times 10^{-6} RR^2 + 3.632 \times 10^{-3} FR * RR \quad [5.38]$$

$$Q_{RebCol2} = 19.968 + 9.4538 FR + 18.3726 RR - 1.0427 \times 10^{-1} FR^2 - 1.0 \times 10^{-6} RR^2 - 3.632 \times 10^{-3} FR * RR \quad [5.39]$$

$$T_{ConCol2} = 321.8 - 1 \times 10^{-6} FR \quad [5.40]$$

$$T_{RebCol2} = 346.2 + 1.714 FR - 1.057 \times 10^{-1} FR^2 \quad [5.41]$$

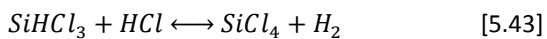
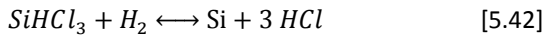
where, $Q_{ConCol1}$ is the condenser heat duty of the column 1 (kW); $Q_{RebCol1}$ is the reboiler heat duty of the column 1 (kW); $T_{ConCol1}$ is the top temperature of the column 1 (K); $T_{RebCol1}$ is the bottom temperature of the column 1 (K); $Q_{ConCol2}$ is the condenser heat duty of the column 2 (kW); $Q_{RebCol2}$ is the reboiler heat duty of the column 2

(kW); $T_{ConCol2}$ is the top temperature of the column 2 (K); $T_{RebCol2}$ is the bottom temperature of the column 2 (K); FR is the Feed Ratio; RR is the Reflux Ratio.

The mass balances were considered as follows: in the first column dome a SiH_2Cl_2 - SiHCl_3 mix is recovered, whose composition depends on the operating conditions of the hydrochlorination reactor, while in the bottom of the column high purity SiCl_4 (99.999% wt.) is obtained. The second distillation column separates the SiH_2Cl_2 - SiHCl_3 mix, obtaining high purity SiH_2Cl_2 in the dome (99.999% wt.), while for the bottoms high purity SiHCl_3 (99.999% wt.) is recovered (Ramírez-Márquez et al., 2018).

5.3.4 Siemens Reactor

The deposition of polycrystalline silicon was modeled according to the work by Del Coso and Luque, (2008). In that work, the operating conditions required for polycrystalline silicon deposition in the traditional Siemens reactor are provided. They present analytic solutions for the deposition process, based on the approach of splitting the second-order reaction rate into two systems of first-order reaction rate. The growth rate, the deposition efficiency, the power-loss dependence on the gas velocity, the composition of the mixture of gas, the reactor pressure, and the surface temperature have been analyzed, providing information regarding the deposition velocity and the polycrystalline silicon quantity obtained. The variables analyzed were the polysilicon growth rate, the deposition efficiency and the system temperature. The U shape bars of ultrapure silicon present in the Siemens reactor are heated up using electric current. The variables described above are studied in the reaction system formed by the reactions showed in Eqs. 5.42 and 5.43 (Del Coso and Luque, 2008; Jain et al., 2011).



It is assumed that silicon deposition follows a second order kinetics, where the consumption or generation mass rate of the species i in the surface of the rods can be expressed as Eq. 5.44:

$$R_i = v_i \mu_i k [\text{SiHCl}_3] [\text{H}_2] \quad [5.44]$$

where, R_i is the mass rate of change in species i by chemical reaction, $[\text{kg}/\text{m}^2\text{s}]$; μ_i is the viscosity of the species i , $[\text{kg}/\text{m s}]$; v_i corresponds the stoichiometry coefficients of the compounds involved in the reactions (-1 for SiHCl_3 and H_2 and 3 for HCl); k is the overall reaction coefficient; and $[i]$ is the mole concentration of species i on the surface.

The global deposition reaction coefficient can be expressed as:

$$\frac{1}{k} = \frac{[\text{SiHCl}_3]}{k_r} + \frac{[\text{H}_2]}{k_{ad}} \quad [5.45]$$

where, k_{ad} is the rate of SiHCl_3 chemisorption on the surface; and k_r is the trichlorosilane decomposition rate. The kinetic coefficients are temperature dependent. Therefore, the Arrhenius's law applied at atmospheric pressure is considered, as shown in Eqs. 5.46 and 5.47:

$$k_{ad}(T) = 2.72 \times 10^6 \exp\left(\frac{-1.72 \times 10^5}{RT}\right) \quad [5.46]$$

$$k_r(T) = 5.63 \times 10^3 \exp\left(\frac{-1.80 \times 10^5}{RT}\right) \quad [5.47]$$

where, T is the temperature (K); and R is the constant of ideal gases in SI units.

The model defined by the Eqs. 5.44-5.47 was solved with the data reported by Del Coso and Luque, (2008) for a temperature range from 1372 to 1500 K. As in the previous cases, a surrogate model is developed to estimate the species distribution as a function of the temperature in the range studied, eq. 5.48-5.51. It should be noted that the reaction coefficients estimated through Eqs. 5.46 and 5.47 are validated at atmospheric pressure, and consequently, they should not be used to

calculate the effect of pressure inside the reactor.

$$X_{Si(s)} = -6.220 \times 10^{-7} T^2 + 1.8580059 \times 10^{-3} T - 1.3159371763 \quad [5.48]$$

$$X_{H_2(g)} = 3.9 \times 10^{-9} T^2 - 1.17934 \times 10^{-5} T + 1.47006954 \times 10^{-2} \quad [5.49]$$

$$X_{HCl(g)} = 3.57 \times 10^{-8} T^2 - 1.066805 \times 10^{-4} T + 1.329638743 \times 10^{-1} \quad [5.50]$$

$$X_{SiCl_4(g)} = 1 - X_{Si(s)} - X_{H_2(g)} - X_{HCl(g)} \quad [5.51]$$

where, X_i is the concentration of the specie i (mass fraction) and T is the temperature (K). The polycrystalline silicon deposition itself, is the largest contributor to the energy consumption of the overall process is assumed to be 60 kWh per kg (Ramos et al., 2015).

The silicon rods grow continuously to a thickness of 150 mm–80 mm per rod (Ramos et al., 2015). Electrical power is used to heat the rods. The deposition process takes about 3 to 5 days (Ramos et al., 2015). For this reason it is necessary to use several deposition reactors for the required production.

5.3.5 Auxiliary equipment

Pumps, separators and heat exchangers were modeled according to mass and energy balances in steady state. Regarding compressor modeling, polytropic behavior for all compressors was considered, as well as an efficiency, n_c , of 0.85 (Walas, 1990). The polytropic coefficient, z , was obtained from Aspen Plus offline simulations, having a value of 1.4. Energy balance for compressors was estimated considering Eqs. 5.52 and 5.53.

$$T_{outCompressor} = T_{inCompressor} + T_{inCompressor} \left(\left(\frac{P_{outCompressor}}{P_{inCompressor}} \right)^{\frac{z-1}{z}} - 1 \right) \frac{1}{n_c} \quad [5.52]$$

$$W_{(Compressor)} = F \cdot \left(\frac{R \cdot z \cdot (T_{inCompressor})}{(M_w) \cdot (z-1)} \right) \cdot \frac{1}{n_c} \cdot \left(\left(\frac{P_{outCompressor}}{P_{inCompressor}} \right)^{\frac{z-1}{z}} - 1 \right) \quad [5.53]$$

where, $T_{outCompressor}$ is the out temperature (K); $T_{inCompressor}$ is the entry temperature (K); $P_{outCompressor}$ is the out pressure (kPa); $P_{inCompressor}$ is the entry pressure (kPa); z is a polytropic coefficient; n_c is the efficiency of the compressor; $W_{(Compressor)}$ is the electrical energy (kW); and R is the constant of ideal gases in SI units.

5.4 Solution Procedure

The process was formulated as a nonlinear programming (NLP) problem. The model consists of 1,281 equations and 1,695 variables, which are solved to optimize the operating conditions of the Hybrid Process for polycrystalline silicon production process proposed in Ramirez-Marquez et al. (2018, 2019) using three different objective functions. Hence, the main variables of decision are: the temperature of the thermal carboreduction reactor; the temperature, pressure, and $H_2/SiCl_4$ feeding molar ratio of the hydrochlorination reactor, the feeding ratio and the reflux ratio of each distillation column, and the operating temperature of the Siemens Reactor. For the present work, the superstructure was optimized under three different independent objective functions, Eqs. 5.54 to 5.56:

The first objective function, Eq. 5.54, seeks to maximize the polycrystalline silicon production.

$$\text{OF 1) } \max z = f_{C_{polycrystalline\ silicon}} \quad [5.54]$$

where, $f_{C_{polycrystalline\ silicon}}$ is the mass flow of polycrystalline silicon.

The second objective function, Eq. 5.55, seeks to minimize the process operation cost according to the methodology presented by Gutiérrez (2003).

$$\text{OF 2) } \min z = a I_F + b RM + c E + d MO - p SP \quad [5.55]$$

where, a is a factor that considers annual expenses such as maintenance; I_F is the fixed

annualized investment ; b is the unit cost of each raw material RM ; c is the cost of each utility E ; d MO is the cost of manpower; p is the price of each by-product SP . The raw material, vapor, cooling and electricity costs are taken from the report of Intratec Solutions (2019).

Finally, the third objective function, Eq 5.56, aims to maximize the process total profit, considering not only the production of the main product (polysilicon), but also the income from byproducts (chlorosilanes), deducting the manufacturing cost.

$$\text{OF 3) } \max z = S_{\text{polycrystalline silicon}} + p SP - b RM - c E \quad [5.56]$$

where, $S_{\text{polycrystalline silicon}}$ is profit from the sale of the polycrystalline silicon.

Also, a detailed economic evaluation based on Turton et al. (2012) procedure was carried out, estimating the equipment cost, production cost, maintenance, administration and manpower. The problem is formulated as an NLP, solved using a multistart initialization approach with CONOPT as the preferred solver.

5.5 Results

5.5.1 Operating conditions

The optimization of the polycrystalline silicon production plant is evaluated under three different optimization criteria described in the section "Solution procedure". In the first case, OF 1, the polycrystalline silicon production is maximized, in the second case,

OF 2 is minimized of the operating costs of the facility, while, in the third case, OF 3 is maximized the profits of the process. The optimization of each objective functions results in the operational characteristics shown in Table 5.1.

The first objective function maximizes the polycrystalline silicon production and presents two particularities. The first one is that, for a large silicon production, the hydrochlorination reactor temperature is low using a $H_2/SiCl_4$ molar ratio of 1.92. However, despite the low energy requirement of the reactor (see Table 5.2), high production costs of $SiHCl_3$ are obtained due to the use of considerable amounts of $SiCl_4$. The second particularity is that the process requires a high energy consumption in the distillation columns due to the high values of the reflux ratios (see Table 5.2). This guarantees a high polycrystalline silicon production capacity although the operating cost is high.

The first objective function maximizes the polycrystalline silicon production and presents two particularities. The first one is that, for a large silicon production, the hydrochlorination reactor temperature is low using a $H_2/SiCl_4$ molar ratio of 1.92. However, despite the low energy requirement of the reactor (see Table 5.2), high production costs of $SiHCl_3$ are obtained due to the use of considerable amounts of $SiCl_4$. The second particularity is that the process requires a high energy consumption in the distillation columns due to the high values of the reflux ratios (see Table 5.2)

Table 5.1. Operating conditions of each stage of the process.

OF	TCarb	Hydro			Separation				Siemens
	T [K]	T [K]	P [kPa]	$H_2/SiCl_4$	Column 1 FR	Column 1 RR	Column 2 FR	Column 2 RR	T [K]
1	2859.65	673.15	2026.00	1.92	2.17	80.00	6.82	90.01	1493.57
2	2776.91	873.25	2026.00	5.00	2.09	13.89	5.06	59.99	1372.50
3	2868.71	873.25	2026.00	4.56	2.09	13.92	5.15	59.99	1500.50

* OF= Objective function; TCarb=Thermal Carbo-reduction; Hydro=Hydrochlorination Reactor; T= Temperature; P=Pressure; FR= Feed Ratio; RR= Reflux Ratio.

This guarantees a high polycrystalline silicon production capacity although the operating cost is high.

Regarding the second objective function, the one that minimizes of the operating cost, the carboreduction reactor presents a lower operating temperature, involving a moderate metallurgical silicon production. However, this guarantees lower energy consumption as it can be observed in Table 5.2. In the hydrochlorination reactor, the operating temperature of 873.25 K and the H₂/SiCl₄ feeding ratio of 5, guarantee a high SiHCl₃ production. Finally, the distillation columns and the Siemens reactor present low thermal load (see Table 5.2). This results in a process with a minimum operation cost, although, it is translated in a lower polycrystalline silicon production.

Finally, the third scenario corresponds to the profit maximization. It maintains reflux ratios similar to the case of optimizing OF2 but reduces the feed ratio to the hydrogenation reactor to 4.56. The temperature at the Siemens reactor is slightly higher than in the previous cases. The results of the optimization are summarized in Tables 5.1 and 5.2. These operating conditions of the process result in the production of the amount of polycrystalline silicon required, and the obtaining of high added value by-products which improves the profitability of the process, achieving an adequate overall operating cost.

There are many improvements and optimizations yet to be undertaken, but with these production conditions and the cost effectiveness, even more at this state of high conversion efficiency, the approach has a practical utility. For this reason, making a comparison with the operating conditions with the existing industrial silicon polycrystalline process gives a real picture of the optimized process.

The most widely used process, which is the Siemens Process, begins by producing metallurgic silicon in the first stage via quartz reduction with coal. An electric arc furnace is the unit used for this transformation. The unit consists of a crucible of 10 m in diameter and three electrodes where the feed is loaded. Triphasic current is made through the feed to carry on the reaction. Large amount of energy is required to melt silicon, 1986 K. The furnace conditions must be in the order of 2300-3500K and 1 bar these conditions match the experimental results from Brage, (2003). The Si_{MG} is fed to the fluidized bed for the production of chlorosilanes. The target is trichlorosilane (Payo, 2009). It operates at 573 K and 1.5 bar. Then, a distillation column is used to split the liquid stream of chlorosilanes. For the production of silicon polycrystalline the SiHCl₃ and hydrogen via chemical vapor deposition is used. The typical conditions to heat up the stream to 1300-1500 K at 1 bar (Pazzaglia et al., 2011). After silicon deposition, by products of HCl, H₂ and SiCl₄ are obtained

Table 5.2. Energy requirements and temperatures of each objective function.

OF	TCarb	Hydro	Separation				Siemens	Comp	Exchanger	
	Q [kW]	Q [kW]	Column 1		Column 2		Q [kW]	W [kW]	St	Co
			Q _{Con} /Q _{Reb} [kW]	T _{Con} /T _{Reb} [K]	Q _{Con} /Q _{Reb} [kW]	T _{Con} /T _{Reb} [K]			Q [kW]	Q [kW]
1	4308.24	568.809	-13710/ 13989	347.60/ 387.695	-1669.95/ 1731.09	321.80/ 352.97	14,560.00	334.34	1040.36	-3242.90
2	4028.80	2140.52	-2700.00/ 2987.78	347.73/ 387.69	-1119.77/ 1166.26	321.80/ 352.17	11,571.86	708.83	1086.77	-6623.58
3	4345.68	2363.79	-2700.00/ 2987.65	347.73/ 387.69	-1119.75/ /1166.96	321.80/ 352.22	15,755.12	781.54	1183.3	-7123.78

*Comp=Compressors; Exch= Exchanger; St= Steam; Co=Coolant; Q= Heat Duty; Con=Condenser; Reb=Reboiler; W=Work.

Now, for the industrial Union Carbide process, the production of metallurgic grade silicon, Si_{MG} , is similar to that of the Siemens process. Therefore the operating conditions at this stage are the same. Afterwards, the Si_{MG} is hydrogenated together with $SiCl_4$ in a fluidized bed reactor at 500-900 K and 20-36 bar (Erickson and Wagner, 1952). Which then, the stream consisting mainly of trichlorosilane and tetrachlorosilane is fed to a regular system of two distillation columns. High purity trichlorosilane is fed to the intensified process, the reactive distillation system to produce SiH_4 . The column produces high purity silane over the top that is fed to the chemical vapor deposition reactor to produce high purity silicon and hydrogen at 973 K, (Farrow, 1974). The product stream is separated to isolate the polysilicon from the gases.

The comparison of the optimized process conditions is a mixture of the aforementioned processes. In Table 5.1 it can be seen that in all optimized units the operating conditions of the industrial processes are very similar to the ones obtained in the optimization, and that these conditions obtained guarantee that the objective function is being evaluated.

In the specific case of carboreduction, the value in all objective functions (2700-2800K) is within the industrially reported range (2300-3500 K). For the production of chlorosilanes via $SiCl_4$, the range reported in the industry is 500-900K and 20-36 bar, and the values obtained in the optimization are around 600-900K and 20 bar. In the case of separation-purification, the data obtained from the industrial separation were taken. The values of the industrial operating conditions of the Siemens deposition reactors are 1300-1500 K at 1 bar, and the values of

those obtained in the optimizations are similar. For the capacity of 2000 ton/y of polycrystalline silicon, 25 Siemens Reactor units are required to complete the production.

5.5.2 Economic evaluation

The results shown in Table 5.3 summarize the economic parameters of the process. It can be seen that the larger the polycrystalline silicon production obtained optimizing OF1 does not result in a larger profit. The adequate arrangement of the operation conditions of each unit, the by-products generation, the raw material consumption, and the services consumption, are the ones that give a maximum profit in the process of 10 M\$/y, see Figure 5.3. This is an interesting result that can lead to the development of a silicon multiproduct refinery rather than the production of Si_{SG} alone. Figure 5.4 shows the consumption of each one of the utilities and raw materials for each one of the objective functions evaluated, showing that the maximum polycrystalline silicon production is associated with high costs in raw material.

Maximizing the process total profit, a lowest production price of polycrystalline silicon of 8.93 \$/kg is obtained. The above compares positively with the commercial price of 10 \$/kg (PVinsights, 2019), making the Hybrid Process a profitable and competitive process in the PV industry.

The investment cost of the polycrystalline silicon plant results in \$9.97 M. The investment cost is disaggregated in Table 5.4. It can be seen that the distillation columns are the most expensive, followed by the Siemens Reactor and the thermal Carboreduction Reactor. Only these equipment represent 77% of the total cost of the process.

Table 5.3. Profit [M\$/y], Operating costs [M\$/y], and kg of polycrystalline silicon/h of each objective function.

OF	1	2	3
Profit [M\$/y]	6.34	9.09	10.1
Operating costs [M\$/y]	11.64	6.32	6.48
kg of polycrystalline silicon/h	236.71	173.641	217.752

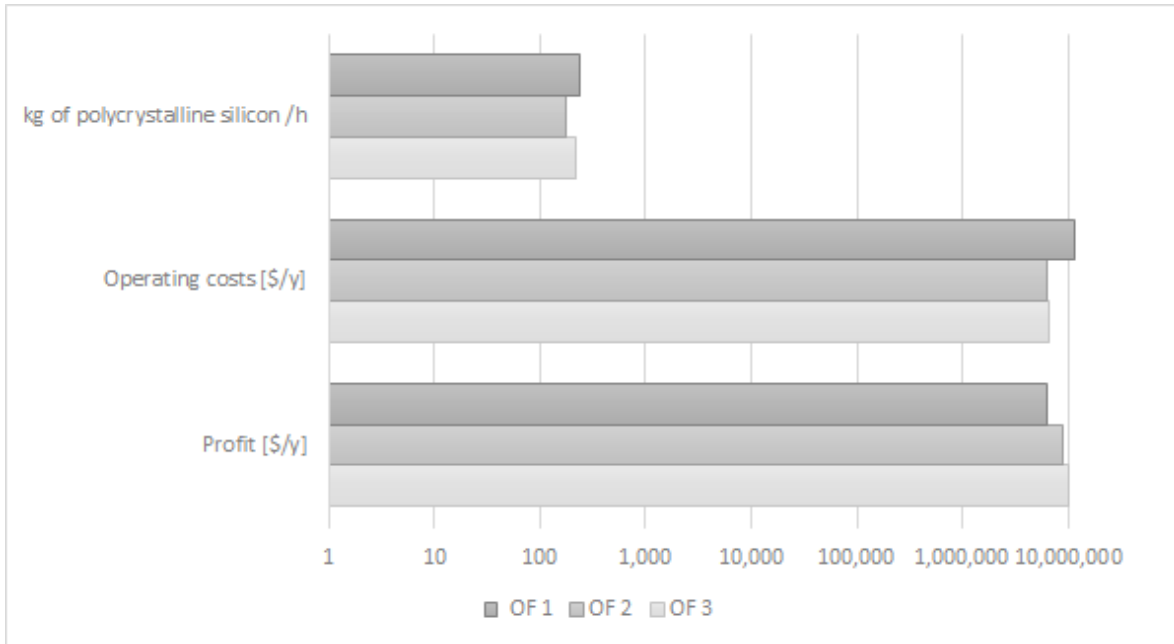


Figure 5.3. kg of polycrystalline silicon/h, operating cost, and profit of each objective function.

Table 5.4. Costs per equipment.

Equipment	Number of equipment	Total Cost (\$USD)	Total Annualized Cost (\$USD/y)
Tanks	4	\$49,120.99	\$9,824.20
Mixers	3	\$262,601.81	\$52,520.36
Thermal Carbo-reduction Reactor	1	\$1,488,607.01	\$297,721.40
Melting pot	1	\$78,798.85	\$15,759.77
Conveyor belt	1	\$358,000.00	\$71,600.00
Hydrochlorination Reactor	1	\$265,252.64	\$53,050.53
Chlorosilanes separator	1	\$238,587.79	\$47,717.56
Compressors	4	\$928,308.52	\$185,661.70
Heat exchanger	4	\$112,678.95	\$22,535.79
Distillation Columns	2	\$3,915,626.17	\$783,125.23
Siemens Reactor	25	\$2,272,813.21	\$454,562.64
Total		\$9,970,395.94	\$1,994,079.18

* 5 years for the annualization.

A fundamental part of the development of a robust model for the production of silicon, consists of performing of the comparison between the results of the current developed model, and the results of the process modeled in Aspen Plus software by Ramírez-Márquez et al., (2019). It should be reminded that the model evaluated using the Aspen Plus software shows limitations in the operating conditions within the reactor models. However, for the present work we take advantage of the rigorous Aspen simulations to model the distillation columns while developing detail surrogate models for the reactors involved. Table 5.5 summarizes the results of the comparisons between both models. The benefits of being able to find the optimal operation conditions of each unit

individually can be observed. It can be seen that since in the previous optimizations performed in Aspen Plus (Ramírez-Márquez et al., (2019), the energy required by each stage is greater, higher operation costs are shown compared to this work. Furthermore, the production capacity is only similar in case of optimizing it, using OF1 as objective function, otherwise the system adjusts the production capacity to reduce the manufacturing costs to reach an optimal production cost. It can be seen the improvement in the results obtained optimizing the process under the methodology shown in the present work combining the best of rigorous column modeling and details surrogate models for the reactors.

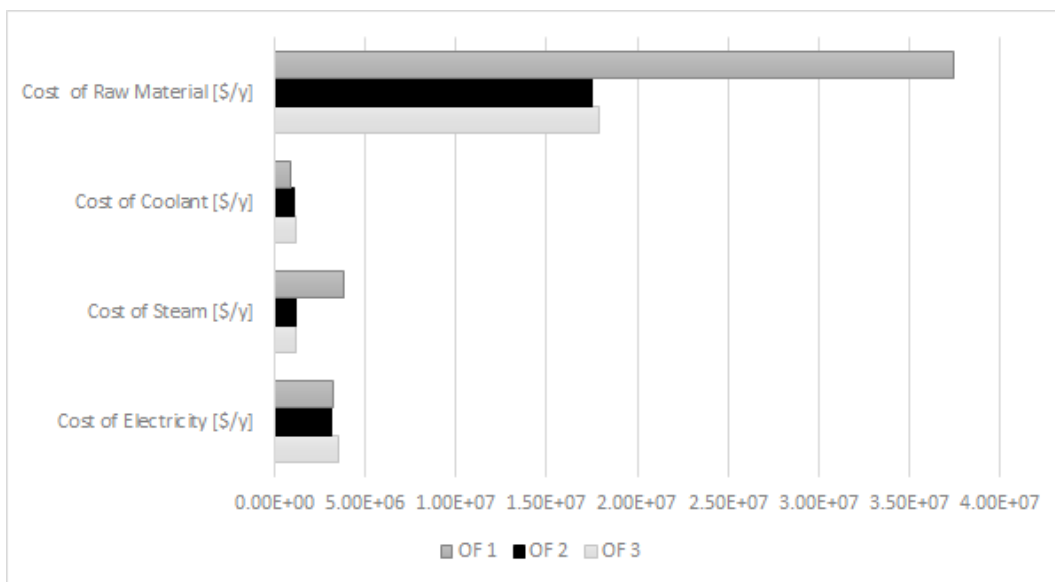


Figure 5.4. Utility and raw material costs of each objective function.

Table 5.5. Comparison of operating conditions.

	TCarb			Hydro				Siemens			SiPoly
	T [K]	P [kPa]	Q [kW]	T [K]	P [kPa]	H ₂ /SiCl ₄	Q [kW]	T [K]	P [kPa]	Q [kW]	[ton/y]
1	2859.65	100	4308.24	673.15	2026.00	1.92	568.80	1493.57	100	14,560.00	2012.04
2	2776.91	100	4028.80	873.25	2026.00	5.00	2140.52	1372.50	100	9,571.86	1475.94
3	2868.71	100	4345.68	873.25	2026.00	4.56	2363.79	1500.50	100	12,755.12	1850.89
AS	2273.00	100	6798.00	773.00	3600.00	0.01	2551.96	1373.00	100	1871.93	1899.07

* Si_{Poly}= Polycrystalline silicon

5.5.3 Scale-up study

Polycrystalline silicon technology, relies on processes that have been mainly borrowed from the semiconductor industry. Consequently, unitary equipment, machines and accessories essential for the industrial process are widely available. In the past couple of decades the manufacture of the equipment, machines and accessories has increased (Ranjan, et al., 2011). The replacement pieces can be acquired with ease. There exists a critical experience of maintenance and operation, knowledge and heuristics for such equipment are extensive and easily manageable. Therefore, by employing processes for which the equipment and supporting infrastructure are predominant, researchers may be able to ensure a degree of scalability in their technologies.

As a result, when transitioning to higher production volumes or larger product scales, it becomes a challenge to consistently produce large quantities of polycrystalline silicon with the same quality. The successful reproduction of these process conditions at scale can be managed by process factors that are not considered at lower scales and will impact the final price of polycrystalline silicon, as well as the profit of the process.

In this work, the capacity of the facility is chosen to be 2.000 ton/y. Although a decrease in the price of silicon was observed, this capacity is not big enough to have low manufacturing costs derived from scale economies. Today, the accepted value for minimum capacity of a green-field polysilicon

plant is around 15,000 ton/y. For this reason, a scaling study was carried out with values of around 5,000, 10,000, 15,000 and 20,000 ton/y of polycrystalline silicon. It is evident that while increasing the size of the polycrystalline silicon production plant, the cost of plant investment increases, since larger equipment is required or additional equipment is used to carry out the production, this can be corroborated in the increase in investment shown in Table 5.6. The scaling study was carried out in the same way as the study for 2000 ton/y, the feed of each of the raw materials was increased, and with the same methodology the operating costs and the costs of each process unit were recalculated. In other words, to determine the scaling study, the surrogate model is used at different raw material feed values to obtain a final production capacity of the plant, similar to the methodology followed by Sánchez & Martín, (2018). It is important to mention that the scaling study was carried out with the only objective function to maximize profits.

Table 5.6 shows the results of the scaling of the polycrystalline silicon plant. In this table we can observe the increase in investment costs, in production and in profits. The most relevant data to note is the increase in the earnings of the process, from a scale of 2000 ton/y to 20,000 ton/y a 100% improvement in the profit is observed. Likewise, a decrease in the price of polycrystalline silicon is observed if the production size of the polycrystalline silicon plant is increased; of plant of 2000 ton/y to 20,000 ton/y and a decrease of \$ 1.03/kg_{SiPoly}.

Table 5.6. Results of scaling study for the Hybrid Process.

SiO ₂ [kmol/h]-C [kmol/h]	Si _{Poly} [kg/h]	Si _{Poly} [ton/y]	Price estimated [\$/kg]	Investment [M\$]	Operational Cost [M\$/y]	Profit [M\$/y]
15-30	217.752	1850.892	8.94	9.97	6.48	10.1
40-80	591.183	5025.0555	8.71	24.96	8.01	38.25
80-160	1168.78	9934.63	8.49	50.3	8.86	81.19
120-240	1825.284	15514.914	8.07	75.68	14.37	118.41
160-320	2369.137	20137.6645	7.91	99.16	15.98	157.11

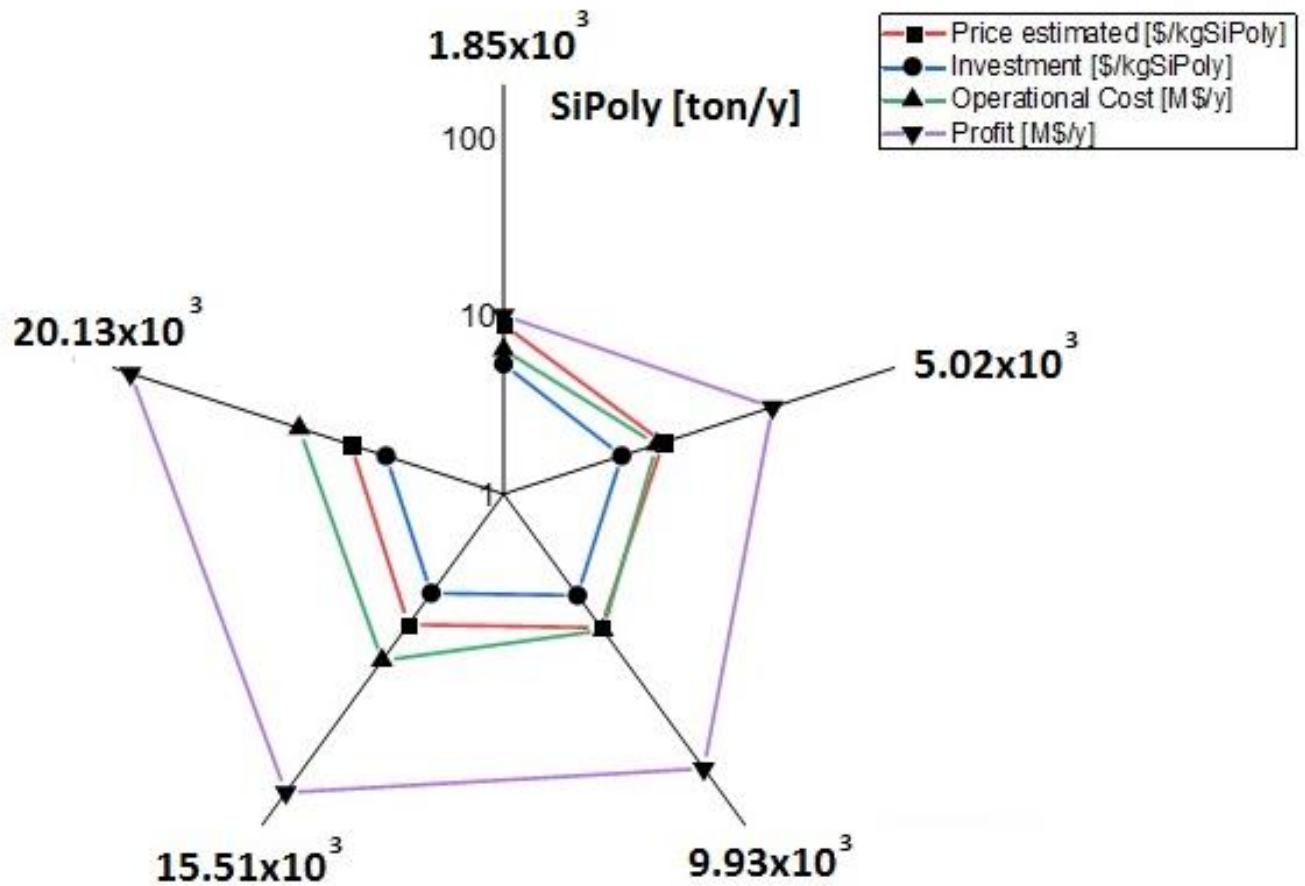


Figure 5.5. Effects of scaling study for the Hybrid Process.

Figure 5.5 shows the behavior of the increase in polycrystalline silicon production in areas such as: estimated price, investment, operational cost and profit. It is straightforward that while the production of polycrystalline silicon is increased, the operation and investment costs also increase, and in the same manner the profits of the process increases considerably and the price of the kilogram of polycrystalline silicon is reduced.

Responsiveness of these disparities presents an opportunity for the research and the industry. By understanding the characteristics of production processes and equipment and how they diverge from those used in low scale, we may be able to anticipate how the process factors that drive them will change upon scaling up. In fact, by studying the attributes, constraints, and practical limitations of large-scale processes, we may learn how to control the conditions necessary to produce the desired product amount at scale.

5.6 Conclusions

In this work the surrogate based optimization of a polycrystalline silicon production process based on the hybridization of the Siemens and the Union Carbide processes developed in previous works (Ramirez-Marquez et al., 2018 & 2019) is performed. Each unit has been modeled in detail. The entire process, and therefore the operating conditions of each unit of the process were optimized under three objective functions: the maximization of the production of polycrystalline silicon, the maximization profit of the process, and the minimization of operating costs. The advantage of evaluating the process under the three objective functions is to determine the effect of the operating conditions under each objective function showing that the maximum production of the target compound does not always guarantee a lower selling price. The optimal operating conditions of the facility that guarantee a lower energetic consumption, meeting with the required production of polycrystalline silicon require the production of high valuable by-products which aid in the economic sustainability of the process. The results of each objective function present advantages and disadvantages. For a large production of polycrystalline silicon, operating costs increase. If operating costs are minimized, the production of polycrystalline silicon is low. By maximizing the profit of the process, a trade-off between the last two objective functions is achieved. For this last scenario, the results after operating expenses, and considering the sale of polycrystalline silicon and the byproducts of the process, are an operational cost of 6.48 M\$/y. The investment for the process is 9.97M\$. Obtaining a competitive production cost for polycrystalline silicon of 8.93 \$/kg, below the commercial price estimated at 10 \$/kg. Also, a decrease in the price of polycrystalline silicon is observed if the production size of the polycrystalline

silicon plant is increased, the price was reduced by 1.03 \$/kgSi_{Poly}, increasing production 10 times. Additionally, the advantages of optimizing the development of customize optimization methods, in contrast with the use of generic equipment models in the previous works developed in the Aspen Plus software has been shown.

5.7 Appendix A

5.7.1 Energy balances

The energy balance to an open system in steady state is described by the Eq. 57 (Doran, 2013).

$$\Delta E_C + \Delta E_P + \Delta H = Q + W \quad [5.57]$$

where, ΔE_C is the variation of kinetic energy; ΔE_P is the variation of potential energy; ΔH is the enthalpy variation; Q is the heat exchanged by the system; and W is the work exchanged by the system.

In the present work, the mechanic energy contributions (kinetic and potential energy) to the system total energy were considered negligible compared with the other terms. Thus, the energy balance is simplify, obtaining the Eq. 58:

$$\Delta H = Q + W \quad [5.58]$$

The enthalpy variation respect to a reference state is defined according to the Eq. 59:

$$\Delta H = \sum_i n_i \cdot \int_{T_{Ref}}^T C_{pi} \cdot dt + \sum_i n_i \cdot \lambda_i + \sum_i n_i \cdot H_{fi}^{T_{ref}} \quad [5.59]$$

where, n_i is the amount of the component i ; T is the temperature [K]; C_{pi} is the specific heat of the component i ; λ_i is the specific latent heat for each element i ; $H_{fi}^{T_{ref}}$ is the standard enthalpy for each element i .

The first term of Eq. 59 refers to the energy exchanged due to a temperature change

(called sensible heat), and it's represented by Q_s . The second term, called sensible heat, represents the heat involve if a change of phase of the considered substance occurs, and it's represented by Q_L . Finally, the third term represents the energy associated with the substance formation through a chemical reaction (called reaction heat), and it's represented by Q_R . The thermodynamic data required in the modelling of the different processes was taken from National Institute of Standards and Technology (2018).

5.8 Nomenclature

w	Total number of elements in the system
p	Price of each by-product SP
k	Overall constant reaction
$d MO$	Cost of manpower
c	Cost of each utility E
b	The unit cost of each raw material RM
a	Factor that considers annual expenses such as maintenance
W	Work exchanged by the system.
Q	Heat exchanged by the system
z	Polytropic coefficient
x	Mole fraction
X	Amount of the specie [mass fraction]
TAC	Total Annual Cost
T	Temperature [K]
SiO ₂	Silicon dioxide
SiO	Silicon oxide
Si _{MG}	Metallurgical grade silicon

SiHCl ₃	Trichlorosilane
SiH ₄	Silane
SiH ₂ Cl ₂	Dichlorosilane
SiCl ₄	Silicon tetrachloride
SiC ₂	Silicon dicarbide
SiC	Silicon Carbide
Si ₂ C	Disilicon Carbide
Si ₂	Disilicon
Si	Silicon
RR	Reflux Ratio
ROI	Return on investment
Rel	H ₂ /SiCl ₄ molar feed ratio
R	Molar gas constant
PV	Photovoltaic
P	Pressure [kPa]
NLP	Nonlinear program
N	Number of species in the reaction system
IR	Individual Risk
HCl	Hydrogen chloride
H ₂	Hydrogen
GAMS	General Algebraic Modeling System
FR	Feed Ratio
FBR	Fluidized Bed Reactor
EI99	Eco-indicator 99
CO	Carbon monoxide
C	Carbon
ΔH	Enthalpy variation
μ_i	Viscosity of the species i
μ_i	Chemical potential
v_i	Stoichiometry coefficients of involved compounds
n_i	Amount of the component i
n_i	Number of moles
n_c	Efficiency of the compressor
k_r	Rate of decomposition.

k_{ad}	Rate of SiHCl_3 chemisorption on the surface	H_i^o	Standard enthalpy
f_i^o	Fugacity of species i	H_{fi}^{Tref}	Standard enthalpy for each element i
$f_{C_{polycrystalline\ silicon}}$	Mass flow of polycrystalline silicon	G_i^o	Standard Gibbs free energy
a_{ik}	Number of k_{th} atoms in each molecule of species i	G^T	Total Gibbs free energy
$W_{(Compressor)}$	Electrical energy [kW]	C_{pi}	Specific heat of the component i
V_{SiMG}	Molar volume of silicon;	$C_{p,i}$	Heat capacity
$T_{outCompressor}$	Out temperature [K];	A_K	Total atomic mass of the k_{th} element in the system
$T_{inCompressor}$	Entry temperature [K];	R_i	Mass rate of change in species i by chemical reaction
T_{RebCol}	Bottom temperature	ΔE_P	Variation of potential energy
T_{ConCol}	Top temperature	ΔE_C	Variation of kinetic energy
$S_{polycrystalline\ silico}$	Profit from the sale of the polycrystalline silicon	$\hat{\varphi}_i$	Fugacity coefficient
S_i^o	Standard entropy	\hat{f}_i	Standard Gibbs free energy
Q_{RebCol}	Reboiler heat duty	λ_i	Specific latent heat for each element i
Q_{ConCol}	Condenser heat duty	y_i	Molar fraction of species i
$P_{outCompressor}$	Out pressure [kPa]		
p^o	Standard-state pressure (100 kPa);		
$P_{inCompressor}$	Entry pressure [kPa]		
I_F	Fixed annualized investment		

5.9 Acknowledgements

The authors acknowledge CONACyT (Mexico), Universidad de Guanajuato and PSEM3 at Universidad de Salamanca.

5.10 References

Brage, F. J. P., 2003. Contribución al modelado matemático de algunos problemas en la metalurgia del silicio (Doctoral dissertation, Universidade de Santiago de Compostela).

Ceccaroli, B., & Lohne, O. (2003). Solar grade silicon feedstock. *Handbook of photovoltaic science and engineering*, 153-204.

Chigondo, F., 2018. From metallurgical-grade to solar-grade silicon: an overview. *Silicon*, 10(3), 789-798.

- Del Coso, G., Del Canizo, C., & Luque, A., 2008. Chemical vapor deposition model of polysilicon in a trichlorosilane and hydrogen system. *Journal of the Electrochemical Society*, 155(6), D485-D491.
- Ding, W. J., Yan, J. M., & Xiao, W. D., 2014. Hydrogenation of silicon tetrachloride in the presence of silicon: thermodynamic and experimental investigation. *Industrial & Engineering Chemistry Research*, 53(27), 10943-10953.
- Doran, P. M., 2013. Bioprocess engineering principles, Chapter 5 - Energy Balances. Elsevier, 139-176.
- Enríquez-Berciano, J.L., Tremps-Guerra, E., Fernández-Segovia, D. and de Elío de Bengy, S., 2009. Monografías sobre Tecnología del Acero. Parte III: Colada del acero. *Universidad Politécnica de Madrid*.
- Erickson, C. E., & Wagner, G. H., 1952. U.S. Patent No. 2,595,620. Washington, DC: U.S. *Patent and Trademark Office*.
- Farrow, R. F. C., 1974. The Kinetics of Silicon Deposition on Silicon by Pyrolysis of Silane A Mass Spectrometric Investigation by Molecular Beam Sampling. *J. Electr. Soc.*, 121(7), 899-907.
- Green, M. A., 2009. The path to 25% silicon solar cell efficiency: history of silicon cell evolution. *Progress in Photovoltaics: Research and Applications*, 17(3), 183-189.
- Gutiérrez, A. J., 2003. Diseño de procesos en ingeniería química. *Reverté*, 8-27.
- Hesse K., Schindlbeck E., Dornberger E., Fischer M., 2009. Status and development of solar-grade silicon feedstock. *In 24th European Photovoltaic Solar Energy Conference*, 883-885.
- Intratec Solutions., 2019. Examine Production Costs of Chemicals. San Antonio, TX. United States of America Publishing. Recovered from <https://www.intratec.us/>
- Iya, S. K., 1986. Production of ultra-high-purity polycrystalline silicon. *Journal of Crystal Growth*, 75(1), 88-90.
- Jain, M. P., Sathiyamoorthy, D., & Rao, V. G., 2011. Studies on hydrochlorination of silicon in a fixed bed reactor. *Indian Chemical Engineer*, 53(2), 61-67.
- Kato, K., & Wen, C. Y., 1969. Bubble assemblage model for fluidized bed catalytic reactors. *Chemical engineering science*, 24(8), 1351-1369.
- List Of World's Polysilicon Producers According To Country For Last 3., 2013. [en línea] < <http://studylib.net/doc/8255119/list-of-world-s-polysilicon-producers-according-to-countr...>>
- Martín, M (2016) Industrial Chemical process. Analysis and Design. Elsevier Oxford.
- Morita, K., & Yoshikawa, T., 2011. Thermodynamic evaluation of new metallurgical refining processes for SOG-silicon production. *Transactions of Nonferrous Metals Society of China*, 21(3), 685-690.
- Muller, D., Ronge, G., Fer, J. S., & Leimkuhler, H. J., 2002. Development and economic evaluation of a reactive distillation process for silane production. *In Proceedings of the International Conference on Distillation and Absorption* (pp. 4-1).
- National Institute of Standards and Technology (NIST), 2018. Libro del Web de Química del NIST. U.S. Department of Commerce. Recovered from <https://webbook.nist.gov/chemistry/>.
- Ni, H., Lu, S., & Chen, C., 2014. Modeling and simulation of silicon epitaxial growth in

- Siemens CVD reactor. *Journal of Crystal Growth*, 404, 89-99.
- Nie, Z., Ramachandran, P. A., & Hou, Y., 2018. Optimization of effective parameters on Siemens reactor to achieve potential maximum deposition radius: An energy consumption analysis and numerical simulation. *International Journal of Heat and Mass Transfer*, 117, 1083-1098.
- O'Mara, W., Herring, R. B., & Hunt, L. P., 2007. *Handbook of semiconductor silicon technology*. Crest Publishing House.
- Papoulias, S. A., & Grossmann, I. E., 1983. A structural optimization approach in process synthesis—I: utility systems. *Computers & Chemical Engineering*, 7(6), 695-706.
- Payo, M. J. R., 2008. Purificación de triclorosilano por destilación en el proceso de obtención de silicio de grado solar (*Doctoral dissertation, Universidad Complutense de Madrid*).
- Pazzaglia, G., Fumagalli, M., & Kulkarni, M., 2011. *U.S. Patent Application* No. 13/084,243.
- Pizzini, S., 2010. Towards solar grade silicon: Challenges and benefits for low cost photovoltaics. *Solar energy materials and solar cells*, 94(9), 1528-1533.
- Polman, A., Knight, M., Garnett, E. C., Ehrler, B., & Sinke, W. C., 2016. Photovoltaic materials: Present efficiencies and future challenges. *Science*, 352(6283), aad4424.
- PVinsights, 2019. PVinsights Grid the world. United States of America Publishing. *Recovered from* <http://pvinsights.com/>
- Ramírez-Márquez, C., Contreras-Zarazúa, G., Martín, M., & Segovia-Hernández, J. G., 2019. Safety, Economic, and Environmental Optimization Applied to Three Processes for the Production of Solar-Grade Silicon. *ACS Sustainable Chemistry & Engineering*, 7(5), 5355-5366.
- Ramírez-Márquez, C., Otero, M. V., Vázquez-Castillo, J. A., Martín, M., & Segovia-Hernández, J. G., 2018. Process design and intensification for the production of solar grade silicon. *Journal of cleaner production*, 170, 1579-1593.
- Ramírez-Márquez, C., Sánchez-Ramírez, E., Quiroz-Ramírez, J. J., Gómez-Castro, F. I., Ramírez-Corona, N., Cervantes-Jauregui, J. A., & Segovia-Hernández, J. G., 2016. Dynamic behavior of a multi-tasking reactive distillation column for production of silane, dichlorosilane and monochlorosilane. *Chemical Engineering and Processing: Process Intensification*, 108, 125-138.
- Ramos, A., Filtvedt, W. O., Lindholm, D., Ramachandran, P. A., Rodríguez, A., & Del Cañizo, C., 2015. Deposition reactors for solar grade silicon: A comparative thermal analysis of a Siemens reactor and a fluidized bed reactor. *Journal of Crystal Growth*, 431, 1-9.
- Ranjan, S., Balaji, S., Panella, R. A., & Ydstie, B. E., 2011. Silicon solar cell production. *Computers & Chemical Engineering*, 35(8), 1439-1453.
- Sánchez, A., & Martín, M., 2018. Scale up and scale down issues of renewable ammonia plants: Towards modular design. *Sustainable Production and Consumption*, 16, 176-192.
- Sugiura, M., Kurita, H., Nisida, T., & Fuwa, A. (1992). Hydrogenation Reactions and Their Kinetics for SiCl₄ (g)–H₂ (g) and SiCl₄ (g)–Si (s)–H₂ (g) Systems Using a Fixed Bed Type Reactor. *Materials Transactions, JIM*, 33(12), 1138-1148.
- Turton R., Bailie R. C., Whiting W.B., Shaeiwitz J.A., Bhattacharyya D. 2012. *Analysis, Synthesis and Design of Chemical Processes*. Pearson Education.

Union Carbide. Base Gas Condition for use Silane Process, 1981. *Report DOE/JPL-954343-21, Nat. Tech. Inform. Center, Springfield, VA.*

Wai C. M. & Hutchison S. G., 1989. Free energy minimization calculation of complex chemical equilibria: Reduction of silicon dioxide with carbon at high temperature. *Journal of Chemical Education*, 66 (7), 546.

Walas, S. M., 1988. Chemical process equipment; selection and design (No. 660.28 W3).

Wang, C., Wang, T., Li, P., & Wang, Z., 2013. Recycling of SiCl₄ in the manufacture of granular polysilicon in a fluidized bed reactor. *Chemical engineering journal*, 220, 81-88.

Wang, X., 2011. Two-Dimensional Temperature Distribution in Fluidized Bed Reactors for Synthesizing Trichlorosilane (Doctoral dissertation, Hong Kong University of Science and Technology).

Weber, K. J., Blakers, A. W., Stocks, M. J., Babaei, J. H., Everett, V. A., Neuendorf, A. J., & Verlinden, P. J., 2004. A novel low-cost, high-efficiency micromachined silicon solar cell. *IEEE Electron Device Letters*, 25(1), 37-39.

Yadav, S., Chattopadhyay, K., & Singh, C. V., 2017. Solar grade silicon production: A review of kinetic, thermodynamic and fluid dynamics based continuum scale modeling. *Renewable and Sustainable Energy Reviews*, 78, 1288-1314.

Zadde, V. V., Pinov, A. B., Strebkov, D. S., Belov, E. P., Efimov, N. K., Lebedev, E. N., ... & Touryan, K., 2002. New method of solar grade silicon production. *In 12th Workshop on Crystalline Silicon Solar Cell Materials and Processes: Extended Abstracts and Papers from the workshop held 11-14 August 2002, Breckenridge, Colorado (No. NREL/CP-520-35650)*. National Renewable Energy Lab., Golden, CO.(US).

6 Optimal Portfolio of Products in a Polycrystalline Silicon Refinery

I&EC research
Industrial & Engineering Chemistry Research

ACS Publications
Most Trusted. Most Cited. Most Read.

At the Forefront of Chemical Engineering Research Since 1909

selectivity

GSE
Grape Seeds Extract (GSE)

6 Optimal Portfolio of Products in a Polycrystalline Silicon Refinery

Abstract

The silicon industry is a source of various types of products, including materials for the implementation of renewable energy systems, with a comparatively lower environmental impact than conventional fossil energy sources and high added value by-products. In this context, the exploitation of the different by-products generated in the production of polycrystalline silicon (polysilicon) offers opportunities to increase the economic efficiency of the polycrystalline silicon production process. In this work, a silicon based refinery is conceptually designed using surrogate models for the major units to evaluate the portfolio of products. Although the main product is polysilicon, there are a number of products that might be generated in the process to increase its profitability, such as tetraethoxysilane (at different purities) as well as chlorosilanes, including SiH_4 , SiH_2Cl_2 , and SiH_3Cl . Next, an economic evaluation of the facility is carried out to determine its economic feasibility. The results show that the refinery produces tetraethoxysilane and chlorosilanes in addition to the production of polysilicon. The proposed design reduces the cost for polycrystalline silicon to 6.86 \$/kg, compared to a cost of 8.93 \$/kg of polycrystalline silicon if the plant does not generate high value-added by-products, both below the commercial price, which is estimated at 10 \$/kg. Therefore, the refinery is not only capable of meeting the market share requirements, but in a way the generation of different high added value by-products increases the plant profit compared to that of the net income earned by traditional polysilicon mono-product plants.

6.1 Introduction

Phenomena such as climate change, resource depletion and waste pollution have prompted the industrial and academic sector to seek new and more sustainable approaches to energy supply. While there are numerous sustainable alternatives (biofuels, wind, geothermal, etc.), photovoltaic (PV) energy is considered one of the best sustainable energy solutions (Darling, et al., 2011). The abundant

solar radiation found within the Earth allow PV systems meeting the yearly worldwide energy needs (EPIA, 2011). Likewise, PV systems produce electricity without the need to emit pollutants during their operation, in addition to having a low carbon footprint during their life cycle, building the PV panels is superior in environmental performance compared to power generation from fossil fuels (Yue et al., 2014). Currently, silicon-based photovoltaic technologies is receiving

more attention, this is because they have the largest share in the market, as well as being the first renewable based power technology to be commercialized on a large scale (IEA, 2012).

For years the PV industry's was highly dependent on the availability of polycrystalline silicon as scraps from the production of integrated circuits, power devices and discrete semiconductor devices. In most cases, the photovoltaic industry used refined silicon rejections from the semiconductor device industry, which are of a slightly lower grade and, therefore, less expensive. The increased demand for PV panels has driven the development of processes for refining polycrystalline silicon (Ciftja, 2008).

The refining of polycrystalline silicon is rather intensive in energy and in the generation of residual products. However, detailed technical studies on lower cost replacement methods to produce polycrystalline silicon in recent years have failed to identify a new alternative process. There are currently two industrial processes used in the production of polycrystalline silicon. The first and former method, the Siemens process, was the only commercial route to polycrystalline silicon before 1980. It remains the main technology used in the production of high quality polycrystalline silicon. The second or recent method was established in the late 1970s by Union Carbide, and it is called the monosilane process (Chamness and Tracy, 2011). Searching for an improvement in the costs of polycrystalline silicon and, therefore, a greater application of polycrystalline silicon, current studies have focused on technological innovation, equipment upgrades and process improvements. This will help improve the profitability of silicon-based photovoltaic energy.

Lately, the polycrystalline silicon photovoltaic (PV) industry has thrived, developing a truly global chain of supply. In this decade alone,

polycrystalline silicon based solar panels have come to represent more than 90% of photovoltaic production, accounting for more than 95% of its production in 2018 (Mints, 2018). This development was caused by the increase in the demand of photovoltaic (PV) energy, as well as by the technical progress in the performance of PV cells, and the improvement in the manufacturing processes of polycrystalline silicon, allowing drastic cost reductions in PV modules cost. Nevertheless, the polysilicon production costs (the cost per kilogram of polycrystalline silicon) can be further improved valorizing the by-products generated in the process, which would otherwise be considered as waste.

In the case of the polycrystalline silicon industry, the main by-product of polycrystalline silicon manufacturing is tetrachlorosilane, which currently is fed back into the production cycle. Tetrachlorosilane can also be extracted and post-processed to obtain added value products. However, the processing of tetrachlorosilane to obtain high added value by-products can be integrated with the main polycrystalline silicon production process, avoiding the discharge of waste streams and increasing the economic and environmental efficiencies of the process; which has been demonstrated by the polycrystalline silicon company Wacker™, who integrated the production of pyrogenic silica from tetrachlorosilane to the polycrystalline silicon process in different facilities, such as Charleston in the USA, and Burghausen and Nuenchritz in Germany.⁸ Pyrogenic silica is a valuable product used as a filler in silicone elastomers and as an archaeological restoration, additive in paints, adhesives, and unsaturated polyester resins (Rubber & Plastics News Report, 2016). However, pyrogenic silica is not the only product that can be generated from tetrachlorosilane.

The present work develops a superstructure optimization approach for the selection of the portfolio of products from quartz including

the production tetraethoxysilane (TEOS), which is the most prominent derivative of the family of silicon compounds. Tetraethoxysilane is mainly used in the manufacture of chemical and heat resistant coatings, organic silicon solvents, and precision casting adhesives. Additionally, the production of a series of chlorosilanes with high added value (silane, dichlorosilane and monochlorosilane) also derives from trichlorosilane. The major units of the process involved in the refinement of silicon polycrystalline and other value-added products are modeled based on experimental and industrial information. Diverse surrogate modeling approaches are used depending on the data that will place together a framework for the entire process of polycrystalline silicon production in Ramírez-Márquez et al., (2018) together with equipment for the production of high value-added products (in the waste streams of the main process) will allow for the evaluation of the operating conditions at each of the units toward minimizing the production cost of the polycrystalline silicon and the generation of high added value products. The latter part of the paper is organized as follows. Section 2 presents the Methodology which shows the development of surrogate models for all the units and the solution procedure by presenting the objective function. Section 3 touches upon the results, and then, conclusions are drawn.

6.2 Methodology

6.2.1 Process design

To design a polycrystalline silicon process with an analogous production capacity to more modern polycrystalline silicon production companies as Wacker Co., an average production capacity of the plant of 15,000 annual metric tons of polycrystalline silicon is considered (Rubber & Plastics News Report, 2016). The polycrystalline silicon production process is an extension of the one

proposed by Ramírez-Márquez et al., (2018). In this work, the conceptual design of the process, named as Hybrid Process, is presented. The Hybrid Process is the result of a strategic combination of the stages of the Siemens and the Union Carbide process. The Hybrid Process is extended using a couple of reactive distillation columns for the production of high added value products such as: TEOS 98.5, TEOS 99.0, TEOS 99.5, silane, dichlorosilane and monochlorosilane. The process diagram for multi-product polycrystalline silicon refinery that was used in the present work is showed in Figure 6.1.

The proposed process consists of six stages: In the first stage, the Si_{MG} production (which is alike in all conventional processes) is performed through the carbothermic reduction of quartz with coal. Here, a detailed model for the reaction considering the allocation of species of the system Si-O-C was developed. This reaction is executed in an electric arc furnace whose product distribution is a function of the temperature (above quartz boiling point $>2500^{\circ}C$) (Wai and Hutchison, 1989). Once this process is concluded the gases are extracted, leaving the liquid silicon at the lowermost part of the furnace. The liquid silicon is then collected, poured into the melting pot, and emptied from the bottom part of the melting pot onto the casting belt where it is solidified. The temperature at which silicon is extracted (a critical parameter in the Si_{MG} production) from the furnace is above the silicon melting temperature (Enríquez-Berciano et al., 2008). Were the temperature of silicon too high, a premature deterioration of the refractory materials might take place and increase the possibility of dissolution of gases in the liquid silicon. Contrarily, lower temperatures can result in low silicon fluidity (573K) (Enríquez-Berciano et al., 2008). It is here, while silicon sits in the melting pot that the refining process takes place by an oxidative process, eliminating a large part of impurities through the formation of slag; thus, obtaining silicon

In the second stage, recycled SiCl_4 is hydrogenated in a fluidized bed reactor in the presence of metallurgical grade Si. The $\text{SiCl}_4\text{-H}_2\text{-Si}_{\text{MG}}$ model is chosen for this second stage due to the advantages linked with the chlorosilane production that include rather low operation temperatures (anywhere between 673 K and 873 K) and larger silicon tetrachloride conversion (Ding et al., 2014). It is in this part of the process that impurities such as Fe, Al, and B react to form their halides (e.g. FeCl_3 , AlCl_3 , and BCl_3). The SiHCl_3 has a low boiling point of 31.8 °C and distillation is used to purify the SiHCl_3 from the impurity halides. The resulting SiHCl_3 now has electrically active impurities (such as Al, P, B, Fe, Cu or Au) below 1 ppba. At conceptual design level the reactions involving them are omitted. In relation to the experimental observations of Ding et al., (2014) it is assumed that in the $\text{SiCl}_4\text{-H}_2\text{-Si}_{\text{MG}}$ system the subsequent set of species is involved: SiCl_4 , H_2 , Si_{MG} , SiHCl_3 , SiH_2Cl_2 , and HCl. Hence, the operating conditions of this system are liable to be altered, disturbing the distribution of the created products. In this work, a detailed model was developed to calculate the effect of the operating conditions on the distribution of products.

The reactor outlet stream which contains a mixture of SiCl_4 , SiHCl_3 , SiH_2Cl_2 ; along with HCl and H_2 , is fed into a condensation stage that separates the reactor effluent into a gas and a liquid phase. The gas phase stream is formed by the most volatile compounds, H_2 and HCl, while the liquid phase stream is formed primarily by SiH_2Cl_2 , SiHCl_3 and SiCl_4 . Due to the great variance of volatility between hydrogen, hydrogen chloride, and the chlorosilanes a 100% separation efficacy in this stage is considered (Payo, 2008). Thus, the gaseous stream is cooled in the condenser until it reaches a temperature of 298 K, where the chlorosilanes condense. Following this, the stream is introduced into a phase separator where the gaseous hydrogen and hydrogen chloride are separated and

deposited in a tank. The liquid stream containing the chlorosilanes is sent to the third stage.

In the third stage, a purification process occurs where convectional distillation columns are used to separate the chlorosilane mix. First, and due to the large quantity that it represents, the SiCl_4 is separated. From the top of the first distillation column, a $\text{SiH}_2\text{Cl}_2\text{-SiHCl}_3$ mix is recovered; while from the bottom of the same distillation column, high purity SiCl_4 is obtained. The second distillation column separates the $\text{SiH}_2\text{Cl}_2\text{-SiHCl}_3$ mix that was obtained from the previous distillation column obtaining a high purity stream of SiH_2Cl_2 at the top, and a high purity stream of SiHCl_3 at the bottom (Ramírez-Márquez et al., 2018).

In the fourth stage, the bottom stream of the first column which contains highly pure SiCl_4 is divided to feed a reactive distillation column that generates TEOS. The remaining part of the stream is recirculated to the hydrochlorination reactor.

In the fifth stage, the trichlorosilane stream is divided to feed a reactive distillation column that performs the disproportion of trichlorosilane to silane, dichlorosilane, and monochlorosilane. These may also feed the Siemens reactor.

In the last stage, SiHCl_3 is fed into the Siemens vapor deposition reactor that consists of a chamber where various high purity silicon rods are heated by an electric current which flows through it. The thermal decomposition of trichlorosilane in a hydrogen atmosphere is carried out at temperatures of 373-873 K within the reactor that leads to the deposition of silicon on the rods. It is here that solar grade polysilicon is obtained. In this work, the optimization of reaction conditions (gas flow and temperature) is sought after with the aim to find an optimal compensation between

polycrystalline silicon growth and operational costs due to energy consumption.

The process diagram for polycrystalline silicon refinery and other value-added products that were used in this work are showed in Figure 1, as well as all process sequence and the products generated in each stage.

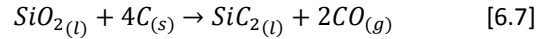
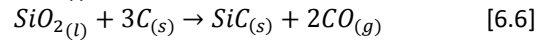
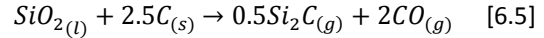
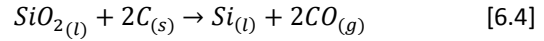
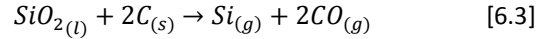
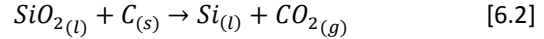
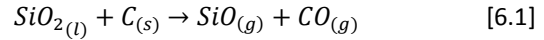
6.2.2 Modelling approach

In this section, the explanation of the surrogate development model for the main reactors, for the distillation columns and for the distillation reactive columns are presented. The other units: compressors, heat exchangers, mixers and splitters are modelled based on first principles and thermodynamics (Martín, 2016). To achieve the production capacity of typical industrial plants of 15,000 ton/y, in the present work a feed of 120 kmol/h of SiO₂ and 240 kmol/h of C is considered. The models of the thermal carboreduction, the hydrochlorination reactor, separation and purification, and deposition reactor were taken from the work of Ramírez-Márquez, (2019).

6.2.2.1 Thermal carboreduction

The complete model proposed by Wai and Hutchison, (1989) for the carboreduction of quartz has been considered for the carboreduction furnace. This model considers the different reactions between silicon dioxide with carbon, leading the formation of multiple products. The assumptions of the model consider a C/SiO₂ feeding molar ratio of 2:1, a total pressure of 1 atm, and a temperature range of 2500-3500 K to assess the reactions carried out in the furnace and the distribution of products obtained. The evaluation of the different phases exist as a result of the different reactions, the distribution diagram of gaseous and condensed species in the system Si-O-C at different temperatures obtained by Wai and

Hutchison, (1989) are also considered to develop correlations to estimate the distribution of the products obtained at the reactor (mol fraction) as a function of the reaction temperature in a range from 2600 to 3100 K. The reactions that may take place during the silicon dioxide carboreduction process are shown in Eqs. 6.1 to 6.7.



The fit of numerical data obtained for each species was carried out as a function of the temperature, obtaining the following correlations for the distribution of the carboreduction products, Eqs. 6.8 to 6.15, where, x_i is the molar fraction of each specie i , and T in the temperature between the range of 2600 a 3100 K in Kelvin.

$$x_{\text{Si}_{(l)}} = -2.48131 \times 10^{-9} T^3 + 1.90239 \times 10^{-5} T^2 - 4.79395 \times 10^{-2} T + 39.71359 \quad [6.8]$$

$$x_{\text{CO}_{(g)}} = 9.82689 \times 10^{-5} T^3 + 1.90239 \times 10^{-5} T + 3.74066 \times 10^{-1} \quad [6.9]$$

$$x_{\text{Si}_{(g)}} = 5.93093 \times 10^{-10} e^{6.31510 \times 10^{-3} T} \quad [6.10]$$

$$x_{\text{SiC}_{(s)}} = 7.14539 \times 10^{-7} T^2 - 4.50044 \times 10^{-3} T + 7.08465 \quad [6.11]$$

$$x_{\text{Si}_2\text{C}_{(g)}} = 1.72881 \times 10^{-7} T^2 - 9.13915 \times 10^{-4} T + 1.20759 \quad [6.12]$$

$$x_{\text{SiC}_2(g)} = -1.19611 \times 10^{-14} T^5 + 1.65491 \times 10^{-10} T^4 - 9.14807 \times 10^{-7} T^3 + 2.52572 \times 10^{-3} T^2 - 3.48320 T + 1919.64937 \quad [6.13]$$

$$x_{\text{SiO}_{(g)}} = 7.58739 \times 10^{-7} T^2 - 4.47932 \times 10^{-3} T + 6.69671 \quad [6.14]$$

$$x_{\text{Si}_2(g)} = 4.76996 \times 10^{-13} e^{7.68303 \times 10^{-3} T} \quad [6.15]$$

To estimate the operation costs, electricity consumption of electrodes (which provide the necessary energy for the reaction) is calculated through energy balance. A large consumption of power is required to melt the silica, around 10-11 kWh to produce a kilogram of silicon (Brage, 2003).

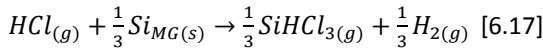
The post processing of the liquid product obtained, mainly melted silicon, is carried out in a solidification train composed by the discharge of the melted silicon to the melting pot, the distribution pipe, the secondary cooling, and the roller crusher. The gaseous exit containing the gaseous effluents of the quartz carboreduction process is sent to a gas treatment. The solid SiC is extracted in the melting pot as slag, whereas the metallurgical silicon is sent to the solidification stage by cooling for its subsequent use in the chlorosilane synthesis reactor.

6.2.2.2 Hydrochlorination Reactor

In these reactors the hydrogenation of the recycled SiCl₄, together with the Si_{MG} is carried out, resulting in the production of chlorosilanes. The modeling of the hydrochlorination reactor is performed through the thermodynamic analysis of the SiCl₄-H₂-Si_{MG} system accomplished by Ding et al., (2014) including both thermodynamic and experimental perspectives. The series of reactions that the proposed system includes are the SiCl₄ hydrogenation in the gas phase, Eq. 6.16:



and the hydrochlorination of Si_{MG} with HCl, Eq. 6.17:



Joining 17 and 18 yields the SiCl₄-H₂-Si_{MG} process, Eq. 6.18:



Considering the minimization of Gibbs free energy for the reactions of the SiCl₄-H₂-Si_{MG} system, it is possible to determine the species distribution when the reaction system reaches the equilibrium as a function of temperature, pressure and H₂/SiCl₄ molar feeding ratio. In the model developed it is

assumed that the chemical system SiCl₄-H₂-Si_{MG} is ideal. The range of operating variables for the correlation is the following: temperature (T), 373–873 K; pressure (P), 1–20 atm; and H₂/SiCl₄ molar feeding ratio (Rel), 1-5. The minimization of the total Gibbs free energy was modeled using GAMS and computed offline. The results obtained were used to develop surrogate models to be incorporated into the flowsheet optimization framework, Eqs (6.19) to (6.23), where, x_i concentration of specie I at equilibrium; P is referred to the pressure (atm); T is the temperature (K); and Rel is referred to the H₂/SiCl₄ molar feed ratio.

$$x_{SiCl_{4(g)}} = 5.345 \times 10^{-1} - 4.0 \times 10^{-6} P - 1.6805 \times 10^{-1} Rel + 1.7367 \times 10^{-2} Rel^2 + 1.0 \times 10^{-6} P * Rel \quad [6.19]$$

$$x_{SiHCl_{3(g)}} = 2.3454 \times 10^{-1} + 4.0 \times 10^{-6} P - 7.369 \times 10^{-2} Rel - 8.0 \times 10^{-6} T + 7.633 \times 10^{-3} Rel^2 + 1.0 \times 10^{-6} T Rel * T \quad [6.20]$$

$$x_{SiH_2Cl_2(g)} = 2.781 \times 10^{-2} + 1.0 \times 10^{-6} P - 9.358 \times 10^{-3} Rel + 4.0 \times 10^{-6} T + 1.031 \times 10^{-3} Rel^2 \quad [6.21]$$

$$x_{HCl(g)} = 1.60 \times 10^{-3} + 6.0 \times 10^{-6} P - 1.594 \times 10^{-3} Rel + 2.73 \times 10^{-4} Rel^2 - 1 \times 10^{-6} P * Rel \quad [6.22]$$

$$x_{H_2(g)} = 2.048 \times 10^{-1} - 6.0 \times 10^{-6} P + 2.505 \times 10^{-1} Rel + 2.0 \times 10^{-6} T - 2.6166 \times 10^{-2} Rel^2 + 1.0 \times 10^{-6} P * Rel \quad [6.23]$$

The different chlorosilanes contained in gas effluents from the hydrochlorination reactor are separated from the hydrogen and hydrogen chloride in condensation. The modeling of the condensation process is based on material and energy balances, assuming the complete separation of the condensed phase containing the chlorosilanes from the hydrogen and hydrogen chloride gas phase, based on experimental results (Payo, 2008).

6.2.2.3 Separation and purification

Chlorosilanes are separated through conventional distillation. The process is

carried out in a set of two conventional distillation columns. In the first column dome a SiH_2Cl_2 - SiHCl_3 mix is recovered, whose composition depends on the operating conditions of the hydrochlorination reactor, while in the bottom of the column high purity SiCl_4 (99.999% wt.) is obtained. The second distillation column separates the SiH_2Cl_2 - SiHCl_3 mix to obtain high purity SiH_2Cl_2 in the dome (99.999% wt.), while for the bottom high purity SiHCl_3 (99.999% wt.) is recovered (Ramírez-Márquez et al., 2018).

Based on a previous work of Ramírez-Márquez et al., (2019) the distillation columns were rigorously modeled using Aspen Plus. To develop surrogate models for the chlorosilanes distillation, the product purity and size of the distillation columns were fixed in the simulations while the effect of the feed and the reflux ratios on the energy and operating temperatures of each column were assessed. The ranges evaluated for these variables are the following:

- Feeding molar ratio SiCl_4 - (SiH_2Cl_2 - SiHCl_3): values from 1 to 2.1698 for the first column; SiH_2Cl_2 - SiHCl_3 molar ratio from 2.99 to 7.5678 for the second column
- Reflux ratio from 10 to 80 for the first column and from 60 to 90 for the second column.

Surrogate models were developed considering the main variables affecting the distillation process, including the reboiler and condenser thermal duties, as well as the top and bottom temperatures Eqs. (6.24) to (6.31).

$$Q_{ConCol1} = -497.162 + 150.215 FR - 495.071 RR - 2.17 \times 10^{-4} RR^2 + 150.191 FR * RR \quad [6.24]$$

$$Q_{RebCol1} = 909.868 - 209.970 FR + 495.071 RR + 2.14 \times 10^{-4} RR^2 - 150.191 FR * RR \quad [6.25]$$

$$T_{ConCol1} = 351.296 - 4.93 \times 10^{-4} RR - 1.70050 FR + 6 \times 10^{-6} RR^2 - 1.0 \times 10^{-4} RR * FR \quad [6.26]$$

$$T_{RebCol1} = 387.695 - 9.0 \times 10^{-6} FR \quad [6.27]$$

$$Q_{ConCol2} = -15.777 - 1.1074 FR - 18.3726 RR + 1.0438 \times 10^{-1} FR^2 + 1.0 \times 10^{-6} RR^2 + 3.632 \times 10^{-3} FR * RR \quad [6.28]$$

$$Q_{RebCol2} = 19.968 + 9.4538 FR + 18.3726 RR - 1.0427 \times 10^{-1} FR^2 - 1.0 \times 10^{-6} RR^2 - 3.632 \times 10^{-3} FR * RR \quad [6.29]$$

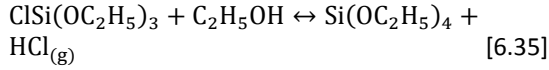
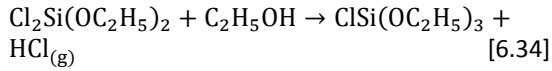
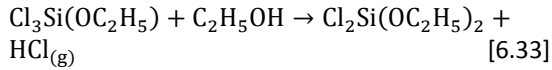
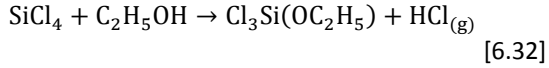
$$T_{ConCol2} = 321.8 - 1 \times 10^{-6} FR \quad [6.30]$$

$$T_{RebCol2} = 346.2 + 1.714 FR - 1.057 \times 10^{-1} FR^2 \quad [6.31]$$

6.2.2.4 RD technology to produce TEOS

The aim to add this technology is to take advantage of the pure SiCl_4 stream for the generation of a high added value product such as TEOS at different purities (98.5-99.0-99.5). The application of the RD technology to produce TEOS in a single unit seems to be an adequate alternative in order to produce high purity tetraethoxysilane.

The reactive distillation columns will be able to produce a wide range of TEOS purities in the same column simply by varying the operating variables. To evaluate the proposed design, the work of Sánchez-Ramírez et al., (2018) the design, the simulation, the evaluation of an economic and environmental framework which considers both the total annual cost and the return on investment as economic index and the Eco-indicator 99 as the environmental index were considered. In addition, Sánchez-Ramírez et al., (2018) work shows the advantages of the intensified process by making a fair comparison with the traditional process (reaction-separation). This scheme was also designed in two stages and evaluated with the same indexes. The chemical reaction sequence is represented in Eqs. (6.32) to (6.35).



In accordance to the Sánchez-Ramírez's et al., (2018) work, all reactive stages were considered under a thermodynamic equilibrium. The model developed in this work is based on the Gibbs free energy minimization which predicts results requiring accurate thermodynamics calculations involving enthalpy and entropy. The reactive distillation was designed in Aspen Plus to cover a wide range of purities. Note that, in a brief comparison between the two systems, the variable that changes is the bottom rate and reboiler heat duty: as the bottom rate increases, smaller purity is obtained. Furthermore, as the reboiler duty decreases so does its purity.

With the previous work, the simulation data in Aspen Plus of the reactive distillation column was collected for each TEOS purity. In this work a superstructure with the three products in parallel is developed. The data show that the SiCl_4 feed is the most important variable to consider in the model, since the column design parameters must be respected to meet the required purity (input and output models). By varying the feed, the dome flows of the column at the bottom of the column were obtained, as well as the thermal load of the condenser and reboiler. The subrogated models for the distillation column reactive for each purity of TEOS that was obtained, are shown in the Eqs. 6.36 to 6.71. Each of the models described below, describes the column to the conditions to produce each of these substances.

Component flow of dome TEOS 0.985:

$$f_{C(\text{SiCl}_4)} = f_{C_{\text{Bottom of the Column (SiCl}_4)}} * 0.48053 \quad [6.36]$$

$$f_{C(\text{C}_2\text{H}_5\text{OH})} = f_{C_{\text{Bottom of the Column (SiCl}_4)}} * 0.000383 \quad [6.37]$$

$$f_{C(\text{SiOC}_2\text{H}_5)} = f_{C_{\text{Bottom of the Column (SiCl}_4)}} * 0.004923 \quad [6.38]$$

$$f_{C(\text{HCl})} = f_{C_{\text{Bottom of the Column (SiCl}_4)}} * 2.06755 \quad [6.39]$$

$$f_{C(\text{N}_2)} = f_{C_{\text{Bottom of the Column (SiCl}_4)}} * 2.3684 \quad [6.40]$$

Component flow of bottom TEOS 0.985:

$$f_{C(\text{SiCl}_4)} = f_{C_{\text{Bottom of the Column (SiCl}_4)}} * 0.00258 \quad [6.41]$$

$$f_{C(\text{C}_2\text{H}_5\text{OH})} = f_{C_{\text{Bottom of the Column (SiCl}_4)}} * 0.00211 \quad [6.42]$$

$$f_{C(\text{SiOC}_2\text{H}_5)} = f_{C_{\text{Bottom of the Column (SiCl}_4)}} * 0.51196 \quad [6.43]$$

$$f_{C(\text{HCl})} = 0 \quad [6.44]$$

$$f_{C(\text{N}_2)} = 0 \quad [6.45]$$

For heat duty of the condenser and reboiler (0.985):

$$Q_{\text{ConRDTEOS98,5}} = f_{C_{\text{Bottom of the Column (SiCl}_4)}} * -78.85959 \quad [6.46]$$

$$Q_{\text{RebrDTEOS98,5}} = f_{C_{\text{Bottom of the Column (SiCl}_4)}} * 63.3406 \quad [6.47]$$

Component flow of dome TEOS 0.99:

$$f_{C(\text{SiCl}_4)} = f_{C_{\text{Bottom of the Column (SiCl}_4)}} * 0.478771924 \quad [6.48]$$

$$f_{C(\text{C}_2\text{H}_5\text{OH})} = f_{C_{\text{Bottom of the Column (SiCl}_4)}} * 0.00065 \quad [6.49]$$

$$f_{C(\text{SiOC}_2\text{H}_5)} = f_{C_{\text{Bottom of the Column (SiCl}_4)}} * 0.00918 \quad [6.50]$$

$$f_{C(\text{HCl})} = f_{C_{\text{Bottom of the Column (SiCl}_4)}} * 2.06479 \quad [6.51]$$

$$f_{C(\text{N}_2)} = f_{C_{\text{Bottom of the Column (SiCl}_4)}} * 2.36847 \quad [6.52]$$

Component flow of bottom TEOS 0.99:

$$f_{C(\text{SiCl}_4)} = f_{C_{\text{Bottom of the Column (SiCl}_4)}} * 0.00503 \quad [6.53]$$

$$f_{C(\text{C}_2\text{H}_5\text{OH})} = f_{C_{\text{Bottom of the Column (SiCl}_4)}} * 0.00461 \quad [6.54]$$

$$f_{C(\text{SiOC}_2\text{H}_5)} = f_{C_{\text{Bottom of the Column (SiCl}_4)}} * 0.50702 \quad [6.55]$$

$$f_{C(\text{HCl})} = 0 \quad [6.56]$$

$$f_{C(N_2)} = 0 \quad [6.57]$$

For heat duty of the condenser and reboiler (0.99):

$$Q_{ConRDTEOS99.0} = f_{C_{Bottom\ of\ the\ Column\ (SiCl_4)}} * -65.52129 \quad [6.58]$$

$$Q_{RebRDTEOS99.0} = f_{C_{Bottom\ of\ the\ Column\ (SiCl_4)}} * 49.56133 \quad [6.59]$$

Component flow of dome TEOS 0.995:

$$f_{C(SiCl_4)} = f_{C_{Bottom\ of\ the\ Column\ (SiCl_4)}} * 0.47715 \quad [6.60]$$

$$f_{C(C_2H_5OH)} = f_{C_{Bottom\ of\ the\ Column\ (SiCl_4)}} * 0.00087 \quad [6.61]$$

$$f_{C(SiOC_2H_5)} = f_{C_{Bottom\ of\ the\ Column\ (SiCl_4)}} * 0.01352 \quad [6.62]$$

$$f_{C(HCl)} = f_{C_{Bottom\ of\ the\ Column\ (SiCl_4)}} * 2.06185 \quad [6.63]$$

$$f_{C(N_2)} = f_{C_{Bottom\ of\ the\ Column\ (SiCl_4)}} * 2.36848 \quad [6.64]$$

Component flow of bottom TEOS 0.995:

$$f_{C(SiCl_4)} = f_{C_{Bottom\ of\ the\ Column\ (SiCl_4)}} * 0.00738 \quad [6.65]$$

$$f_{C(C_2H_5OH)} = f_{C_{Bottom\ of\ the\ Column\ (SiCl_4)}} * 0.00733 \quad [6.66]$$

$$f_{C(SiOC_2H_5)} = f_{C_{Bottom\ of\ the\ Column\ (SiCl_4)}} * 0.50194 \quad [6.67]$$

$$f_{C(HCl)} = 0 \quad [6.68]$$

$$f_{C(N_2)} = 0 \quad [6.69]$$

For heat duty of the condenser and reboiler (0.995):

$$Q_{ConRDTEOS99.5} = f_{C_{Bottom\ of\ the\ Column\ (SiCl_4)}} * -61.69701 \quad [6.70]$$

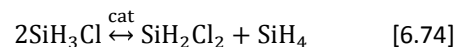
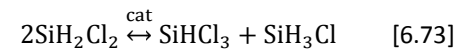
$$Q_{RebRDTEOS99.5} = f_{C_{Bottom\ of\ the\ Column\ (SiCl_4)}} * 45.31013 \quad [6.71]$$

$f_{C(x)}$ is the mol flow of each product in kmol/h; $f_{C_{Bottom\ of\ the\ Column\ (SiCl_4)}}$ is the mol flow of $SiCl_4$ coming from the separation in kmol/h; $Q_{ConRDTEOS}$ is the condenser heat duty of the column; and $Q_{RebRDTEOS}$ is the reboiler heat duty of the column.

6.2.2.5 RD technology to produce silane, monochlorosilane or dichlorosilane

The bottom stream containing $SiHCl_3$ of the distillation columns SiH_2Cl_2 - $SiHCl_3$, will be divided to feed two processes: a reactive distillation column for the production of chlorosilanes and a set of Siemens reactors for the production of polycrystalline silicon. For the RD technology to produce silane, monochlorosilane or dichlorosilane Ramírez-Márquez et al., (2016) proposed a conceptual design of a single reactive distillation column to produce high purity silane, dichlorosilane and monochlorosilane respectively. The relevance of the work of Ramírez Márquez et al., (2016) is that it shows the feasibility to produce pure monochlorosilane and dichlorosilane in the same RD column by simply varying the operative variables. The process for production chlorosilanes should also be economical. Another goal was to provide a low-cost design to carry out the process. The column design considers the benefits of the intensification process, having as a target, besides the recovery of the three products, the reduction of environmental impact. Composition, temperature and cascading control structures were also developed in that work.

The reaction system consists in three simultaneous reactions. In the first one, trichlorosilane ($SiHCl_3$) reacts to dichlorosilane (SiH_2Cl_2) and tetrachlorosilane ($SiCl_4$). Subsequently, dichlorosilane reacts to monochlorosilane (SiH_3Cl) and trichlorosilane. Finally, monochlorosilane is converted to silane (SiH_4) and dichlorosilane. The three reaction steps are shown in Eqs (6.72) to (6.74).



The parameters that were obtained are considered suitable for the RD column. The entire design of the multitasking reactive distillation column was performed using the Aspen Plus process simulator. Note, the SiHCl₃ feed to the RD column was set at 10 kmol/h for the development of the surrogate model based on the work by Ramírez-Márquez et al., (2016). As the previous RD column by varying the feed, the dome flows of the column and the bottom of the column were obtained, as well as the thermal duty of the condenser and reboiler. Based on the process shown by Ramírez-Márquez et al., (2016) the input and output models are shown in the Eqs. 6.75 to 6.110. Note that it is the same reactive distillation column that, when changing the operating conditions, is capable of producing the three different products with high aggregate value (SiH₄, SiH₂Cl₂, and SiH₃Cl). And each of the models described below, simulates the column under the conditions to produce each of these substances.

Component flow of dome silane (SiH₄):

$$\begin{aligned} f_{C(SiHCl_3)} &= 0 & [6.75] \\ f_{C(SiCl_4)} &= 0 & [6.76] \\ f_{C(SiH_2Cl_2)} &= 0 & [6.77] \\ f_{C(SiH_4)} &= f_{C_{Split}(SiHCl_3)} * 2.46 \times 10^{-1} & [6.78] \\ f_{C(SiH_3Cl)} &= f_{C_{Split}(SiHCl_3)} * 3.75 \times 10^{-3} & [6.79] \end{aligned}$$

Component flow of bottom silane (SiH₄):

$$\begin{aligned} f_{C(SiHCl_3)} &= f_{C_{Split}(SiHCl_3)} * 0.0037529 & [6.80] \\ f_{C(SiCl_4)} &= f_{C_{Split}(SiHCl_3)} * 0.74625 & [6.81] \\ f_{C(SiH_2Cl_2)} &= 0 & [6.82] \\ f_{C(SiH_4)} &= f_{C_{Split}(SiHCl_3)} * 0 & [6.83] \\ f_{C(SiH_3Cl)} &= 0 & [6.84] \end{aligned}$$

For heat duty of the condenser and reboiler (SiH₄):

$$\begin{aligned} Q_{ConRDSiH_4} &= f_{C_{Split}(SiHCl_3)} * -55.68329 & [6.85] \\ Q_{RebRDSiH_4} &= f_{C_{Split}(SiHCl_3)} * 58.84151 & [6.86] \end{aligned}$$

Component flow of dome dichlorosilane (SiH₂Cl₂):

$$f_{C(SiHCl_3)} = f_{C_{Split}(SiHCl_3)} * 0.00376 \quad [6.87]$$

$$f_{C(SiCl_4)} = 0 \quad [6.88]$$

$$f_{C(SiH_2Cl_2)} = f_{C_{Split}(SiHCl_3)} * 0.49249 \quad [6.89]$$

$$f_{C(SiH_4)} = 0 \quad [6.90]$$

$$f_{C(SiH_3Cl)} = f_{C_{Split}(SiHCl_3)} * 0.00374 \quad [6.91]$$

Component flow of bottom dichlorosilane (SiH₂Cl₂):

$$f_{C(SiHCl_3)} = f_{C_{Split}(SiHCl_3)} * 1.44911 \times 10^{-5} \quad [6.92]$$

$$f_{C(SiCl_4)} = f_{C_{Split}(SiHCl_3)} * 0.49998 \quad [6.93]$$

$$f_{C(SiH_2Cl_2)} = 0 \quad [6.94]$$

$$f_{C(SiH_4)} = f_{C_{Split}(SiHCl_3)} * 0 \quad [6.95]$$

$$f_{C(SiH_3Cl)} = 0 \quad [6.96]$$

For heat duty of the condenser and reboiler (SiH₂Cl₂):

$$Q_{ConRDSiH_2Cl_2} = f_{C_{Split}(SiHCl_3)} * -82.37442 \quad [6.97]$$

$$Q_{RebRDSiH_2Cl_2} = f_{C_{Split}(SiHCl_3)} * 84.24849 \quad [6.98]$$

Component flow of dome monochlorosilane (SiH₃Cl):

$$f_{C(SiHCl_3)} = 0 \quad [6.99]$$

$$f_{C(SiCl_4)} = 0 \quad [6.100]$$

$$f_{C(SiH_2Cl_2)} = f_{C_{Split}(SiHCl_3)} * 2.93 \times 10^{-3} \quad [6.101]$$

$$f_{C(SiH_4)} = f_{C_{Split}(SiHCl_3)} * 2.07 \times 10^{-3} \quad [6.102]$$

$$f_{C(SiH_3Cl)} = f_{C_{Split}(SiHCl_3)} * 3.28 \times 10^{-1} \quad [6.103]$$

Component flow of bottom monochlorosilane (SiH₃Cl):

$$f_{C(SiHCl_3)} = f_{C_{Split}(SiHCl_3)} * 0.00035 \quad [6.104]$$

$$f_{C(SiCl_4)} = f_{C_{Split}(SiHCl_3)} * 0.6661471 \quad [6.105]$$

$$f_{C(SiH_2Cl_2)} = 0 \quad [6.106]$$

$$f_{C(SiH_4)} = 0 \quad [6.107]$$

$$f_{C(SiH_3Cl)} = 0 \quad [6.108]$$

For heat duty of the condenser and reboiler (SiH₃Cl):

$$Q_{ConRDSiH_3Cl} = f_{C_{Split}(SiHCl_3)} * -45.15792 \quad [6.109]$$

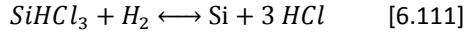
$$Q_{RebRDSiH_3Cl} = f_{C_{Split}(SiHCl_3)} * 47.80694 \quad [6.110]$$

$f_{C(x)}$ is the mol flow of each product in kmol/h; $f_{C_{Split}(SiHCl_3)}$ is the mol flow of SiHCl₃ coming from the split in kmol/h; Q_{ConRD} is the condenser heat duty of the

column; and Q_{RebRD} is the reboiler heat duty of the column.

6.2.2.6 Siemens Reactor

The production polycrystalline silicon is performed in a Siemens reactor, where the polysilicon is deposited on ultrapure silicon electrically heated rods. During the deposition process, which takes from 3 to 5 days, the rods grow continuously until reaching a thickness of 150 mm–80 mm rods (Ramos et al., 2015). As a consequence of the batch nature of the polysilicon deposition, it is necessary to use several deposition reactors operating in parallel with complementary scheduling schemes to reach the required production. Since the production of each Siemens reactor unit is 11.77 kg/h (Ramos et al., 2015), to reach a total production of 15,000 ton/y, 150 Siemens reactor units are required to complete the production. The reactions are showed in Eqs. (6.111) and (6.112) (Del Coso et al., 2008).



The reactor was modeled according to the work by Del Coso and Luque et al., (2008). To model de polysilicon deposition, the second-order reaction is splitted in two reaction systems of first-order. The main variables of the deposition process, including growth rate, deposition efficiency, and power-loss dependence on the gas velocity, the mixture of gas composition, the reactor pressure, and the surface temperature are considered in the model; by providing information regarding the deposition velocity and the polycrystalline silicon quantity obtained.

However, since the model described by Del Coso and Luque et al., (2008) is too complex to be included in the superstructure optimization problem, a surrogate model is developed to estimate the species distribution as a function of the temperature

in the range studied, Eqs. (6.113)-(6.116). It should be noted that the reaction coefficients estimated through Eqs. (6.111) and (6.112) are validated at atmospheric pressure. Consequently, the surrogate model is not able to consider the effect of pressure inside the reactor for values different to atmospheric pressure. The variables of Eqs. (6.113)-(6.116) are the following: X_i is the concentration of the species i (mass fraction) and T is the temperature (K).

$$X_{Si(s)} = -6.220 \times 10^{-7} T^2 + 1.8580059 \times 10^{-3} T - 1.3159371763 \quad [6.113]$$

$$X_{H_2(g)} = 3.9 \times 10^{-9} T^2 - 1.17934 \times 10^{-5} T + 1.47006954 \times 10^{-2} \quad [6.114]$$

$$X_{HCl(g)} = 3.57 \times 10^{-8} T^2 - 1.066805 \times 10^{-4} T + 1.329638743 \times 10^{-1} \quad [6.115]$$

$$X_{SiCl_4(g)} = 1 - X_{Si(s)} - X_{H_2(g)} - X_{HCl(g)} \quad [6.116]$$

The polycrystalline silicon deposition is the largest contributor to the energy consumption of the overall process, resulting in an electrical consumption 60 kWh per kg (Ramos et al., 2015).

6.2.2.7 Auxiliary equipment

All auxiliary equipment such as separators, heat exchangers and pumps, were modeled according to mass and energy balances in steady state. Concerning compressor modeling, polytrophic behavior for all compressors was considered, as well as an efficiency, n_c , of 0.85 (Walas, 1988) The polytrophic coefficient, z , was obtained from Aspen Plus™ offline simulations, having a value of 1.4. Energy balance for compressors was estimated considering Eqs. 6.117 and 6.118.

$$T_{outCompressor} = T_{inCompressor} + T_{inCompressor} \left(\left(\frac{P_{outCompressor}}{P_{inCompressor}} \right)^{\frac{z-1}{z}} - 1 \right) \frac{1}{n_c} \quad [6.117]$$

$$W_{(Compressor)} = F \cdot \left(\frac{R \cdot z \cdot (T_{inCompressor})}{(M_w) \cdot (z-1)} \right) \cdot \frac{1}{n_c} \cdot \left(\left(\frac{P_{outCompressor}}{P_{inCompressor}} \right)^{\frac{z-1}{z}} - 1 \right) \quad [6.118]$$

where, $T_{outCompressor}$ is the out temperature (K); $T_{inCompressor}$ is the entry temperature (K); $P_{outCompressor}$ is the out pressure (kPa); $P_{inCompressor}$ is the entry pressure (kPa); z is a polytrophic coefficient; n_c is the efficiency of the compressor; $W_{(Compressor)}$ is the electrical energy (kW); and R is the constant of ideal gases in SI units.

6.2.3 Solution procedure

The process was formulated as a nonlinear programming (NLP) problem. The model consists of 3,014 equations and 3,716 variables, which are solved to optimize the operating conditions of the Multi-Product Polycrystalline Silicon facility, using a simplified profit objective function, Eq. (6.119). The superstructure includes three reactive distillation columns in parallel for the production of the three TEOS purities, as well as three other reactive distillation columns in parallel for the chlorosilanes. Hence, the main variables of decision are: the temperature of the thermal carboreduction reactor; the temperature, pressure, and $H_2/SiCl_4$ feeding molar ratio of the hydrochlorination reactor, the feeding ratio and the reflux ratio of each distillation column, for the reactive columns the feeding ratio, and the operating temperature of the Siemens Reactor.

The objective function, Eq. (6.119), aims to maximize the process total profit, considering not only the production of the main product (polysilicon), but also the income from by-products (chlorosilanes), deducting the manufacturing cost.

$$\text{OF) } \max z = S_{polycrystalline\ silico} + p SP - b RM - c E \quad [6.119]$$

where, b is the unit cost of each raw material RM ; c is the cost of each utility E ; d MO is the labour cost; p is the price of each by-product SP , and $S_{polycrystalline\ silicon}$ is profit from the sale of the polycrystalline silicon.

Also, a detailed economic evaluation based on the procedure proposed by Turton et al., (2012) was carried out, estimating the equipment cost, production cost, maintenance, administration and manpower. The NLP problem was solved using a multistart initialization approach with CONOPT as the preferred solver.

6.3 Results

Initially the optimization of the model corresponding to the polycrystalline silicon plant and other products of high added value (TEOS at different purities, silane, dichlorosilane and monochlorosilane), was raised with a single scenario. This scenario is to maximize the economic profit of the process and thus be able to reduce the cost of polycrystalline silicon. It is important to mention that in this scenario, all the variables (temperature, pressure, feed ratios, reactive distillation column feed, etc.) were left free, in order to find an optimal profit. During the optimization under the scenario (S1) and to guarantee the maximum economic profit of the process, it was observed that the model tends to produce polycrystalline silicon, silane, dichlorosilane (said production is from the hydrochlorination reactor) and TEOS 99.5 (See Table 1), thus omitting the production of other value-added products such as TEOS 99.0, TEOS 98.5 and monochlorosilane; which becomes obvious since the process seeks maximum profit and this is carried out by producing the compounds with the highest cost of sale. Note that global optimum is not claimed.

Under the argument of having the optimized economic profit in S1, the optimization was pursued using three other scenarios. The second scenario (S2), which guarantees the production of other products with high added value with the same objective function of maximizing profit, specifies the model that produces TEOS 99.0 and any of the chlorosilanes For the above, the scenario was

specified providing a lower bound for the production of SiCl_4 of 10 kmol/h to the reactive distillation column for the production of TEOS 99.0 (so that we can operate over the year with the same column), and for the other two purities of TEOS, the model was forced to stop feeding the RD columns. And in the case of the production of chlorosilanes, the algorithm for the selection of some of the chlorosilanes or, alternatively, the choice of polycrystalline silicon was left free. In a third scenario (S3), the process is intended to produce TEOS 98.5 and some of the chlorosilanes, which guarantee maximum process profit under these circumstances. In the third scenario, the a lower bound for the production of TEOS 98.5 is considered by assuming a feed to the reactive distillation column that produces is of at least 10 kmol/h (for the other two TEOS purities, the model was forced to stop feeding the RD columns); and the SiHCl_3 stream for the production of chlorosilanes or polycrystalline silicon is free of choice. The fourth scenario (S4) requires the process to produce all products with high added value, also guaranteeing a maximum profit in this scenario. For this last scenario, it is sought that TEOS be produced in the same proportion, lower bounds to the feeds to the different alternatives are provided to feed SiCl_4 to the reactive distillation column for the production of TEOS (consequently that we can operate over the year with the same column), in each of the operating conditions suitable for the generation of the three TEOS purities; Likewise, the stream containing high purity SiHCl_3 was forced to divide and at least feed an amount of trichlorosilane to the multitasking reactive distillation column of chlorosilanes in each of the operating conditions, so that it was capable of producing both silane, dichlorosilane and monochlorosilane. It is clear that in each of the scenarios proposed, the operating conditions of each unit will vary, and therefore the energetic and economic costs of the process will vary as well. It must be remembered that to achieve the production

capacity of typical industrial plants of 15,000 ton/y, in the present work a feed of 120 kmol/h of SiO_2 and 240 kmol/h of C is considered in each scenario.

It is important to mention that there is an infinite possibility of scenarios, in which combinations of the products can be produced, that is, a certain amount of TEOS at various purities and chlorosilanes. With the proposed scenarios, it is desired to see the panorama of the process both in profit, as in the final costs of polycrystalline silicon. That is why the choice of feeds to reactive distillation columns, both for the production of TEOS and chlorosilanes, could be higher or lower values, but the only thing that was desired to investigate is the effect of producing such components.

In Table 6.1, the flows of the portfolio of selected products under each of the scenarios is presented. It is evident that under S1 the process obtains its maximum profit (117.94 M\$/y), in addition it can be observed that this is the scenario with the highest production of polycrystalline silicon, resulting in a total of 15,938 ton/y. Scenario S2 produces polycrystalline silicon, TEOS 99.0, dichlorosilane from the hydrochlorination reactor, and silane. In this scenario, the total profit is reduced by 6.67%, due to the fact that the production of polycrystalline silicon is reduced by 9% since the process seeks to produce other value-added products such as silane and TEOS 99.0, which are of lower cost than the products obtained in the previous scenario. This is because the model chooses to produce almost double the silane in S2 compared to S1, which reduces the feed of trichlorosilane to the deposition reactors, and therefore reduces the production of polycrystalline silicon. Something similar occurs with scenarios 3 and 4 (S3 and S4), where the process profit is lower than that in S1. In a specific case of S3, there is a larger profit than scenarios S2 and S4, the profit is larger since the sale price provided by the break-even analysis (Gutierrez and Dalsted,

1990) for polycrystalline silicon is higher than in the other scenarios, this makes the process is with higher profits, but at the cost of increasing the cost of polycrystalline silicon by 5.39% compared to S1. For S4 all possible products in the plant are obtained, said the profit of this last scenario decreases by 6.42%, resulting in a decrease in the sale price of polycrystalline silicon of 2.33% with respect to S1, see Table 6.2

Figure 6.2 clearly shows the product portfolio of the different scenarios. It is clear that both the production of polycrystalline silicon, and the production of each of the high value-added products, both depending on their sale price, are what determine the final profit and the market sale price of polycrystalline silicon.

Table 6.1. Profit [M\$/y], Operating costs [M\$/y], kg of polycrystalline silicon/h, kg of TEOS, and kg of silane of the objective function.

Multi-Product Polycrystalline Silicon Facility				
	S1	S2	S3	S4
Profit [M\$/y]	117.94	110.07	114.09	110.36
Operating costs [M\$/y]	16.09	14.01	15.25	14.05
kg of polycrystalline silicon/h	1875	1708	1768	1656
kg of TEOS (99.5 of purity)/h	26.91	0	0	22.54
kg of TEOS (99.0 of purity)/h	0	22.09	0	20.22
kg of TEOS (98.5 of purity)/h	0	0	147.69	20.34
kg of SiH ₄ /h	4.595	8.73	7.902	9.926
kg of SiH ₂ Cl ₂ /h	2668.694	2656.65	1667.59	2701.57
kg of SiH ₃ Cl/h	0	0	0	164.11

Table 6.2. Price of each Product for all scenarios.

	S1	S2	S3	S4
Price of Polycrystalline Silicon \$/kg	6.86	6.99	7.23	7.02
Price of TEOS 99.5 \$/kg			3.75	
Price of TEOS 99.0 \$/kg			2.50	
Price of TEOS 98.5 \$/kg			1.50	
Price of SiH ₄ \$/kg			88.44	
Price of SiH ₂ Cl ₂ \$/kg			3.67	
Price of SiH ₃ Cl \$/kg			3.0	

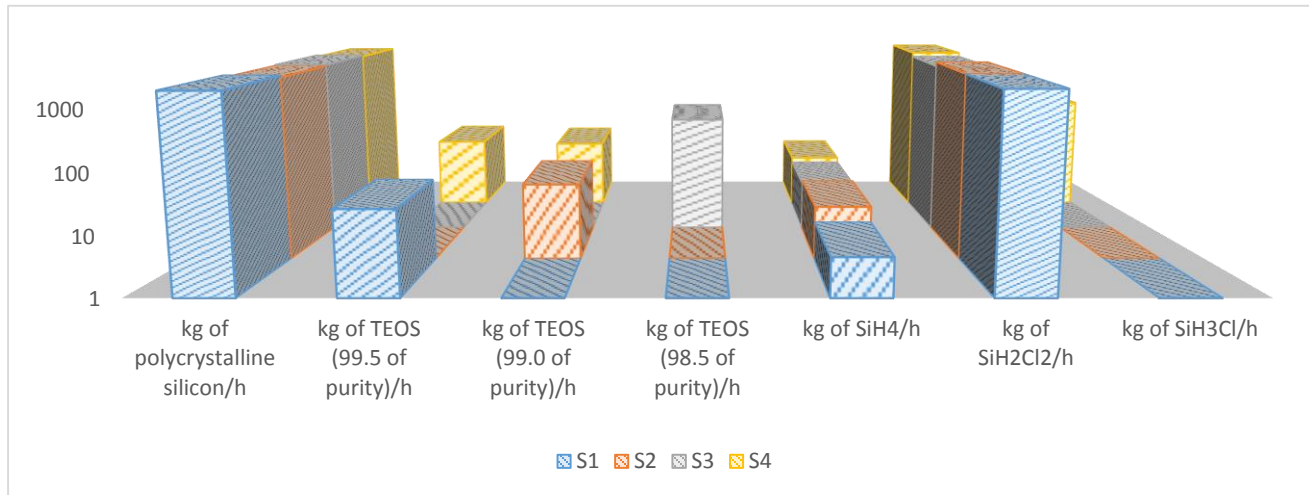


Figure 6.2. Production of polycrystalline silicon and each one of the products of high added value in each proposed scenario.

6.3.1 Main operating parameters

The main operating conditions in the facility are summarized in Table 6.3; where the operating temperature and pressure of each of the major equipment for the production of polycrystalline silicon and several products with high added value are presented. It can be seen that the temperature and pressure of the main units change when the demand for polycrystalline silicon also changes. In the carboreduction reactor it is observed that the larger the production of polycrystalline silicon, the larger the required production of metallurgical silicon; therefore the temperature of the carboreduction reactor is adjusted for the production of metallurgical silicon depending on the scenario. This translates into a metallurgical silicon production capacity in the range of 1400-1600 kg/h for the carboreduction reactor for the four scenarios. In this range, the conditions of the carboreduction reactor are adjusted within the range presented in Section 6.2.2.1, to produce the flow of metallurgical silicon necessary for the chlorosilane production process in the hydrochlorination reactor. In the case of the hydrochlorination reactors, the operating conditions are within the temperature range

of 673-680 K, an operating pressure of 2026 kPa and a feed ratio of $H_2/SiCl_4$ between 1.91 and 5. This is to guarantee the adequate chlorosilanes production ($SiHCl_3$, SiH_2Cl_2 , $SiCl_4$) in each scenario (particularly trichlorosilane being the precursor of polycrystalline silicon). In all scenarios (conventional distillation columns and reactive distillation columns) the variables such as column height and the operating pressure in the installation remain constant across the different capacities. The variables such as the feeding ratio and in the case of conventional columns the reflux ratio are those that suffer variations in the process. These conditions can be observed in Table 6.3; where in the conventional columns there are reflux ratio values from 13.93 to 80 (case of $SiHCl_3$ - SiH_2Cl_2 - $SiCl_4$ separation columns), and reflux ratio values from 60 to 90 in the $SiHCl_3$ - SiH_2Cl_2 separation columns, depending stage. The temperature conditions of Siemens reactors range from 1457 K to 1500 K, ensuring maximum process gain in each scenario.

In particular, it is observed that for S1, the temperature of the carboreduction reactor, 2819 K, is at the point of maximum production of metallurgical silicon which, in synchrony with the conditions of the hydrochlorination reactor with a temperature of 673 K and a

pressure of 2026 kPa, guarantee a high production of trichlorosilane and a not-so-high production of tetrachlorosilane and dichlorosilane. This combination guarantees a high production of polycrystalline silicon and/or chlorosilanes, which therefore makes the process much more profitable. Therefore, a not-so-high reflux ratio value is required in the set of the first conventional columns (where SiCl_4 is separated), and a high reflux ratio value (60.26) is required for the set of the second set of conventional columns, where to guarantee adequate separation and high purity of trichlorosilane, this reflux ratio value is raised. In the case of reactive distillation columns for the production of TEOS, the reflux ratio (1.21) is small and it is consistent for the amount of TEOS 99.5 produced. In the case of the reflux ratio for the reactive distillation column for the production of silicon, it is consistent with the production of silane with respect to the work reported by Ramírez Márquez et al, (2016). For deposition reactors, the temperature of 1500 K is the highest reported in the scenarios, and is consistent with the highest production of polycrystalline silicon reported.

In the case of S2 it can be seen that the conditions of the carboreduction and hydrochlorination reactors, and the conditions of the conventional chlorosilane separation columns are very similar but not equal to those of S1, such conditions do not guarantee the maximum production of trichlorosilane, which ultimately affects the profit of the process significantly. Where there is a difference is in the temperature of the deposition reactor, 50 K with respect to S1), this difference coupled with the fact that when the system is forced to feed at least 10 kmol/h of SiCl_4 , there is a smaller amount of trichlorosilane produced in the hydrochlorination reactor, results in a lower profit scenario. Likewise, trichlorosilane when distributed in the processes of production of chlorosilanes and polycrystalline silicon, in this scenario sends less trichlorosilane to the

deposition reactors and a greater amount to the production of silane, which is reflected in a lower production of polycrystalline silicon. It is because of the above that this scenario does not result in a profit as high as when the system is released, logically this by forcing it to produce products with lower added value, it is also important to mention that the solution is likely to be in a local optimum.

Likewise for S3, Table 6.3 shows an increase in both the temperature of the carboreduction reactor (3029 K) and hydrochlorination (680 K) combined with a high value of H_2/SiCl_4 (5). This combination of operating conditions generates a scenario of high production of both trichlorosilane and tetrachlorosilane, which is compulsory as the system is forced to produce a large amount of TEOS 98.5 and a large amount of polycrystalline silicon to obtain the greatest possible profit. The results show that it is the second process with the highest production of polycrystalline silicon (1768 kg/h) and with a high amount of TEOS 98.5 (147.69 kg/h), which is reflected in a high profit, being the second scenario with higher profit.

In S4 there is the production of all possible products (polycrystalline silicon, TEOS all purities and chlorosilanes), the operating conditions of the whole process remain similar to those of the other scenarios, both the carboreduction and hydrochlorination reactors are helped by high temperatures, as well as adequate pressures for the higher production of metallurgical grade silicon and trichlorosilane and tetrachlorosilane. The above to guarantee a minimum feed of SiCl_4 and SiHCl_3 for the production of TEOS and chlorosilanes. It is evident that the temperature (1479 K) of the deposition reactors also seeks to guarantee the greatest amount of polycrystalline silicon, but has as an impediment that a smaller amount of trichlorosilane is fed and that reduces the amount of polycrystalline silicon produced. By decreasing this amount and the conversion to

polycrystalline silicon being better than to chlorosilanes, the process finds a lower profit.

Table 6.4 shows the energy requirements of each of the equipment under the proposed scenarios. It is clear that the requirements are linked to maximize the profit of each scenario, since it is necessary to find a balance between production and process expenses. The energy requirement values are consistent with those shown in the literature and are shown for each unit in section 6.2 of modeling approach. For the carboreduction reactor the largest energy requirement is found in S3, being the one that requires the largest amount of metallurgical silicon for the production of trichlorosilane and tetrachlorosilane, this is evident in the amount of hydrochlorination reactor energy also being the scenario with larger energy consumption in this area, leading to a balanced production of these two chlorosilanes. In scenarios S1 and S4 the greatest energy requirement is given in the conventional columns. This is due to the large amount of trichlorosilane that these two scenarios are required to produce both chlorosilanes and polycrystalline silicon. The S2 presents a balance between the energy requirements and the quantity of products produced, being the third best scenario in polycrystalline silicon production, but increasing silane production. In S4 a smaller amount of energy is required at the deposition reactors, this is clearly observed by having a smaller amount of polycrystalline silicon produced.

6.3.2 Polycrystalline Silicon Refinery and Other Value-Added Products Cost

Numerous studies in the literature evaluate the effect of expected future investment costs for industrial processes (Sartori, et al., 2014; Policy, 2008). In the case of the polycrystalline silicon refining plant and other products with high added value, the plant

consists of a variety of equipment, such as the carboreduction reactor, the hydrochlorination reactors, and separation equipment (conventional distillation columns), reaction-separation equipment (reactive distillation columns), Siemens deposition reactors, compressors, tanks, exchangers, etc. The process described in Figure 6.1, shows a basic scheme for the positioning of each of the equipment and the function that it performs. In some cases the equipment was doubled or its volumes extended to meet the intended capacity. In the case of carboreduction, only one reactor is sufficient to meet the requirement; in the chlorosilane production section, four reactors are required. Each of these equipments also requires a set of separation columns, with a total of eight conventional distillation columns. For high value-added compounds such as TEOS 99.5, TEOS 99.0, TEOS 98.5, silane, dichlorosilane and monochlorosilane, reactive distillation columns are required independently. For each of the cases, that is TEOS or chlorosilanes, the columns multitask, and for each case with a single column of reactive distillation at different operating conditions, the different products are obtained. In the case of each reactive distillation column for TEOS and for chlorosilanes to ensure adequate production, a pair of reactive distillation columns are required (ie two RD columns for the production of TEOS at different purities, and a pair of RD columns for chlorosilanes). In the case of silicon deposition, 150 Siemens reactors are required to guarantee a production of around 15,000 ton/y. Table 6.5 shows the costs obtained from each unit, reaching a total investment cost of 85.83 M\$ for all scenarios (the same investment cost is used in all scenarios, since the cost of the equipment was made considering the maximum production of each product).

Table 6.3. Operating conditions of each stage of the process.

Max	T[K]	Hy			Separation				Col RD TEOS						Col RD SiH ₄ – SiH ₂ Cl ₂ - SiH ₃ Cl						Siemens T [K]
		T [K]	P [kPa]	H ₂ /SiCl ₄	C1		C2		98.5		99.0		99.5		SiH ₄		SiH ₂ Cl ₂		SiH ₃ Cl		
					FR	RR	FR	RR	RR	P [kPa]	RR	P [kPa]	RR	P [kPa]	DFR	RR	DFR	RR	DFR	RR	
S1	2819	673.2	2026	1.91	2.17	14.94	6.82	60.26	N/A	N/A	N/A	N/A	1.21	101.32	0.25	61.2	N/A	N/A	N/A	N/A	1500.00
S2	2815	674.1	2024.2	1.92	2.17	15.11	6.81	69.13	N/A	N/A	1.37	101.32	N/A	N/A	0.25	61.2	N/A	N/A	N/A	N/A	1457.01
S3	3029	680.5	2026.5	5.00	2.08	13.70	5.45	60.03	1.90	101.32	N/A	N/A	N/A	N/A	0.25	61.2	N/A	N/A	N/A	N/A	1478.61
S4	2799	673.2	2026.5	1.91	2.17	79.99	6.82	90.01	1.90	101.32	1.37	101.32	1.21	101.32	0.25	61.2	0.50	25.8	0.33	24.3	1479.09

* OF= Objective function; TCa=Thermal Carboreduction; Hy=Hydrochlorination Reactor; C1= Column 1; C2= Column 2; Col RD= Reactive distillation Column; T= Temperature; P=Pressure; FR= Feed Ratio; RR= Reflux Ratio; DFR=Distillate to feed ratio; N/A=Not apply.

Table 6.4. Energy requirements and temperatures of each scenario.

Max	TCa Q [kW]	Hy Q [kW]	Separation		Col RD TEOS			Col RD SiH ₄ – SiH ₂ Cl ₂ - SiH ₃ Cl			Siemens Q [kW]
			C1 Q _{Con} /Q _{Reb} [kW]	Column 2 Q _{Con} /Q _{Reb} [kW]	98.5 Q _{Con} /Q _{Reb} [kW]	99.0 Q _{Con} /Q _{Reb} [kW]	99.5 Q _{Con} /Q _{Reb} [kW]	SiH ₄ Q _{Con} /Q _{Reb} [kW]	SiH ₂ Cl ₂ Q _{Con} /Q _{Reb} [kW]	SiH ₃ Cl Q _{Con} /Q _{Reb} [kW]	
S1	33279	4455	-59720/60882	-6085/6284	N/A	N/A	-638/468	-252/266	N/A	N/A	108934
S2	33157	4470	-10912/12044	-5147/5392	N/A	-32/25	N/A	-123/130	N/A	N/A	100480
S3	42104	6049	-10828/11987	-4480/4680	258/208	N/A	N/A	-111/117	N/A	N/A	106079
S4	32754	4341	-54800/55952	-6676/6924	-35/29	-29/23	-31/24	-140./148	-338/345	-679/718	99580

*Comp=Compressors; Exch= Exchanger; St= Steam; Co=Coolant; Q= Heat Duty; Con=Condenser; Reb=Reboiler; W=Work; N/A=Not apply.

Table 6.5. Costs per equipment.

Equipment	Number of equipment	Total Cost (\$USD)	Total Annualized Cost (\$USD/y)
Tanks	8	\$360,307.62	\$72,061.52
Mixers	6	\$1,923,436.73	\$384,687.35
Thermal Carboreduction Reactor	1	\$11,462,274.00	\$2,292,454.80
Melting pot	1	\$630,390.79	\$126,078.16
Conveyor belt	1	\$2,541,800.00	\$508,360.00
Hydrochlorination Reactor	4	\$1,591,515.82	\$318,303.16
Chlorosilanes separator	4	\$898,288.64	\$179,657.73
Compressors	14	\$6,962,313.87	\$1,392,462.77
Heat exchanger	16	\$1,827,836.81	\$365,567.36
Distillation Columns	8	\$16,695,330.43	\$3,339,066.09
RD Column TEOS	2	\$10,730,435.20	\$2,146,087.04
RD Column Chlorosilanes	2	\$6,444,144.76	\$1,288,828.95
Siemens Reactor	150	\$23,864,538.67	\$4,772,907.73
Total		\$85,932,613.34	\$17,186,522.67

* 5 years for the annualization.

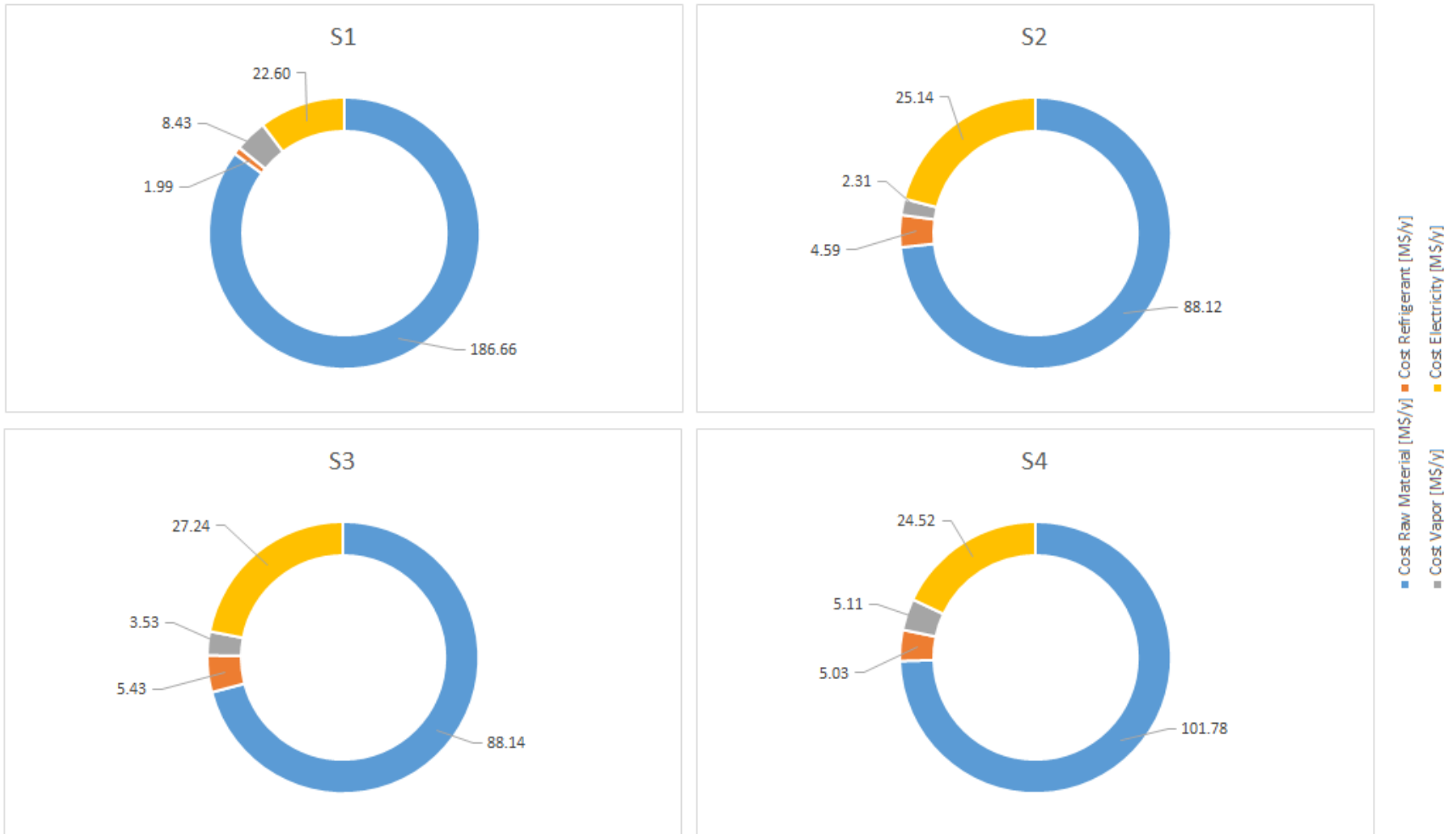


Figure 6.3. Costs of raw material, electricity, steam and refrigerant for each scenario.

The operating costs are also computed. Figure 6.3 shows conclusively the variation in expenses depending on the scenario. It is evident that in S1 shows higher production costs related to the raw material with respect to the other items such as electricity, steam and refrigerants. This fact is linked beforehand to the process with the highest production of polycrystalline silicon. In S3 there is a higher energy and refrigerant consumption than for the other scenarios. In general, it can be observed that in each scenario the costs of each of the items are balanced to guarantee maximum economic profit. In scenarios 2 and 4, a balance between raw material costs and refrigerant costs can be observed, they also have electricity costs in intermediate values with respect to the other two scenarios. In the specific case of S4, vapor cost values are increased due to the use of several distillation columns, both conventional and reactive.

6.3.3 Estimated Price of Polycrystalline Silicon

The average spot polycrystalline silicon price dropped below the 10 \$/kg threshold for the first time in this year, according to PVInsights, (2019). The production analysis in this work say, however, that the polycrystalline silicon refining industry with other high value-added products might lower their production costs to 6.86 \$/kg polycrystalline silicon, a historical

threshold, and still, prices could drop again if the range of high added value products is extended.

Figure 6.4 shows the fluctuation of the price of polycrystalline silicon according to the proposed scenarios. In addition to an estimate of the cost of the polycrystalline silicon process if no additional high added value products were generated in the proposed process. It can be seen that in the 4 scenarios of the process with the generation of high value-added products, the cost of polycrystalline silicon is considerably reduced with respect to the current market scenarios and the scenario without the generation of high value-added products. In the figure it can be seen that the vertices of scenarios 1 and 2 with respect to polycrystalline silicon costs are better in the whole scenario. This indicates that the simultaneous generation of high value-added products such as silane and TEOS at high purities (99.5 and 99.0) and polycrystalline silicon, lead to a substantial reduction in the cost of selling polycrystalline silicon. And finally, the average market spot of polycrystalline silicon price this year can be seen in its best scenario (S1) where the price of silicon can be reduced by 17.64% compared to the same process, but without the generation of other products with high added value such as TEOS or chlorosilanes. There is also a 45.77% (S1) reduction in relation to the market sale price of polycrystalline silicon (per kilogram).

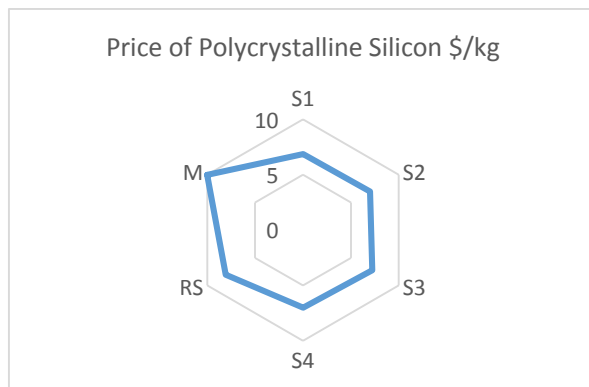


Figure 6.4. Estimated price of polycrystalline silicon in each scenario, without the generation of products with high added value (RS), and the market price according to PVInsights, (2019).

6.4 Conclusions

In this work a superstructure optimization approach is used for the selection of the portfolio of products within a Multi-Product Polycrystalline Silicon Facility. Surrogate models for major units allow selecting the yield and operating conditions. The proposed process is able to meet the same production of polysilicon than current traditional polysilicon facilities do, at a lower production cost since the benefits obtained from selling the high added value by-products obtained increase the profit of the facility. The complete process, and therefore the operating conditions of each unit of the process were optimized under the objective of the maximization profit of the process. The optimal operating conditions of the facility that guarantee a lower energetic consumption, meeting with the required production of polycrystalline silicon require the production of high valuable by-products as TEOS 99.5, and SiH₄, which aid in the economic sustainability of the process. The results after operating expenses, and considering the sale of polycrystalline silicon and the byproducts of the process, have an operational cost of 16.09 M\$/y. The investment for the process is 85.93M\$. Obtaining a competitive production cost for polycrystalline silicon of 6.86 \$/kg, below the commercial price estimated at 10 \$/kg, with the optimal production of 1875 kg/h of Polycrystalline Silicon and the byproducts optimal production of 26.91 kg/h of TEOS 99.5; and 4.595 kg/h of SiH₄.

6.5 Nomenclature

w	Total number of elements in the system
p	Price of each by-product SP [\$/y]
dMO	Cost of manpower [\$/y]

c	Cost of each utility E [\$/y]
b	The unit cost of each raw material RM [\$/y]
a	Factor that considers annual expenses such as maintenance
W	Work exchanged by the system [kW]
Q	Heat exchanged by the system [kW]
z	Polytropic coefficient
x	Mole fraction
X	Amount of the specie [mass fraction]
wt	Weight percent
TAC	Total Annual Cost
T	Temperature [K]
RR	Reflux Ratio
ROI	Return on investment
Rel ratio	H ₂ /SiCl ₄ molar feed ratio
RD	Reactive Distillation
R	Molar gas constant [J/mol K]
PV	Photovoltaic
P	Pressure [kPa]
NLP	Nonlinear program
kW	Kilowatt
K	Kelvin
HCl	Hydrogen chloride
H ₂	Hydrogen
GAMS System	General Algebraic Modeling System
FR	Feed Ratio
FBR	Fluidized Bed Reactor
°C	Celsius
ΔH	Enthalpy variation [kJ/mol]
$W_{(Compressor)}$	Electrical energy [kW]
$T_{outCompressor}$	Out temperature [K]

$T_{inCompressor}$	Entry temperature [K]
T_{RebCol}	Bottom temperature [K]
T_{ConCol}	Top temperature [K]
$S_{polycrystalline\ silico}$	Profit from the sale of the polycrystalline silicon
Q_{RebCol}	Reboiler heat duty [kW]
Q_{ConCol}	Condenser heat duty [kW]
$P_{outCompressor}$	Out pressure [kPa]
p^o	Standard-state pressure (100 kPa);
$P_{inCompressor}$	Entry pressure [kPa]
I_F	Fixed annualized investment
y_i	Molar fraction of species i

6.6 Acknowledgements

The authors acknowledge CONACyT (Mexico), Universidad de Guanajuato and PSEM3 at Universidad de Salamanca.

6.7 References

Brage, F. J. P., 2003. Contribución al modelado matemático de algunos problemas en la metalurgia del silicio (Doctoral dissertation, Universidade de Santiago de Compostela).

Ceccaroli, B., & Lohne, O., 2003. Solar grade silicon feedstock. Handbook of photovoltaic science and engineering, 153-204.

Chamness L. & Tracy D., 2011. Polysilicon Manufacturing Trends. Issue 4 and Volume 2011. <https://www.renewableenergyworld.com/2011/08/01/polysilicon-manufacturing-trends/#gref>

Ciftja, A., 2008. Refining and recycling of silicon: a review.

Darling, S. B., You, F., Veselka, T., & Velosa, A., 2011. Assumptions and the levelized cost of energy for photovoltaics. *Energy & Environmental Science*, 4(9), 3133-3139.

Del Coso, G., Del Canizo, C., & Luque, A., 2008. Chemical vapor deposition model of polysilicon in a trichlorosilane and hydrogen system. *Journal of the Electrochemical Society*, 155(6), D485-D491.

Ding, W. J., Yan, J. M., & Xiao, W. D., 2014. Hydrogenation of silicon tetrachloride in the presence of silicon: thermodynamic and experimental investigation. *Industrial & Engineering Chemistry Work*, 53(27), 10943-10953.

Enríquez-Berciano, J.L., Tremps-Guerra, E., Fernández-Segovia, D. and de Elío de Bengy, S., 2009. Monografías sobre Tecnología del Acero. Parte III: Colada del acero. Universidad Politécnica de Madrid.

EPIA, 2011. EPIA Sustainability Working Group Fact Sheet. <http://www.epia.org/news/fact-sheets/>.

Gutierrez, P. H., & Dalsted, N. L., 1990. Break-even method of investment analysis. *Farm and ranch series. Economics; no. 3.759*.

IEA, 2012. Trends in Photovoltaic Applications: Survey Report of Selected IEA Countries between 1992 and 2011. Report IEA-PVPS1-21:2012, International Energy Agency. http://www.iea-pvps.org/index.php?id=92&elD=dam_fronternd_push&docID=1239.

Martín, M., 2016. Industrial Chemical process. Analysis and Design. Elsevier Oxdord.

Mints, P., 2018. Photovoltaic Manufacturer Capacity, Shipments, Price & Revenues 2017/2018. SPV Market Work.

Payo, M. J. R., 2008. Purificación de triclorosilano por destilación en el proceso de obtención de silicio de grado solar (Doctoral

dissertation, Universidad Complutense de Madrid).

Policy, U., 2008. Guide to cost-benefit analysis of investment projects. *The EU*.

PVinsights, 2019. PVinsights Grid the world. United States of America Publishing. Recovered from <http://pvinsights.com/>

Ramírez-Márquez C., Martín-Hernández E., Martín M., Segovia-Hernández J.G., 2019. Optimal Design of a Multi-Product Polycrystalline Silicon Facility. *AIChE Annual Meeting, November 10-15, 2019*. Hyatt Regency, Orlando.

Ramírez-Márquez, C., Contreras-Zarazúa, G., Martín, M., & Segovia-Hernández, J. G., 2019. Safety, Economic, and Environmental Optimization Applied to Three Processes for the Production of Solar-Grade Silicon. *ACS Sustainable Chemistry & Engineering*, 7(5), 5355-5366.

Ramírez-Márquez, C., Otero, M. V., Vázquez-Castillo, J. A., Martín, M., & Segovia-Hernández, J. G., 2018. Process design and intensification for the production of solar grade silicon. *Journal of cleaner production*, 170, 1579-1593.

Ramírez-Márquez, C., Sánchez-Ramírez, E., Quiroz-Ramírez, J. J., Gómez-Castro, F. I., Ramírez-Corona, N., Cervantes-Jauregui, J. A., & Segovia-Hernández, J. G., 2016. Dynamic behavior of a multi-tasking reactive distillation column for production of silane, dichlorosilane and monochlorosilane. *Chemical Engineering and Processing: Process Intensification*, 108, 125-138.

Ramos, A., Filtvedt, W. O., Lindholm, D., Ramachandran, P. A., Rodríguez, A., & Del Cañizo, C., 2015. Deposition reactors for solar grade silicon: A comparative thermal analysis of a Siemens reactor and a fluidized bed reactor. *Journal of Crystal Growth*, 431, 1-9.

Rubber & Plastics News Report, 2016. Wacker to build silica plant in Tenn. <https://www.rubbernews.com/article/20161214/NEWS/161219980/wacker-to-build-silica-plant-intenn>.

Sánchez-Ramírez, E., Ramírez-Márquez, C., Quiroz-Ramírez, J. J., Contreras-Zarazúa, G., Segovia-Hernández, J. G., & Cervantes-Jauregui, J. A., 2018. Reactive Distillation Column Design for Tetraethoxysilane (TEOS) Production: Economic and Environmental Aspects. *Industrial & Engineering Chemistry Work*, 57(14), 5024-5034.

Sartori, D., Catalano, G., Genco, M., Pancotti, C., Sirtori, E., Vignetti, S., & Del Bo, C., 2014. Guide to cost-benefit analysis of investment projects. *Economic appraisal tool for Cohesion Policy*, 2020.

Turton R., Bailie R. C., Whiting W.B., Shaeiwitz J.A., Bhattacharyya D., 2012. Analysis, Synthesis and Design of Chemical Processes. Pearson Education.

Wai C. M. & Hutchison S. G., 1989. Free energy minimization calculation of complex chemical equilibria: Reduction of silicon dioxide with carbon at high temperature. *Journal of Chemical Education*, 66 (7), 546.

Walas, S. M., 1988. Chemical process equipment; selection and design (No. 660.28 W3).

Yue, D., You, F., & Darling, S. B., 2014. Domestic and overseas manufacturing scenarios of silicon-based photovoltaics: Life cycle energy and environmental comparative analysis. *Solar Energy*, 105, 669-678.

7 Conclusions

7 Conclusions

The work aims at improving solar silicon production by synthesizing a novel process and optimizing the operating conditions following a systematic approach. The manuscript is divided into five stages that cover design, synthesis, multiobjective optimization and multiproduct portfolio optimization towards sustainable and profitable production.

The conclusions of the work presented are:

- We performed a stochastic global optimization for the design of processes for $\text{Si}_{(\text{SG})}$ production to improve and compare their cost.
- The Siemens process is the base case, but it has been optimized, and two novel processes have been developed and optimized, an intensified process based on the one Union Carbide is using, where we substitute the distillation columns by a reaction distillation column and a Hybrid one combining Siemens and Union Carbide processes.
- The results shows than the Siemens process presented the smallest TAC, but with the lowest production of $\text{Si}_{(\text{SG})}$. The Intensified FBR Union Carbide Process, showed the largest TAC due to the capital cost of the equipment and the heat duty for $\text{Si}_{(\text{SG})}$ purification.
- The Hybrid Process exhibited a large production of $\text{Si}_{(\text{SG})}$, with a TAC between the one of the Siemens process and that of the Intensified FBR Union Carbide. Evaluating the TAC vs production of $\text{Si}_{(\text{SG})}$, it turned out that the Hybrid Process was the best of the three from the economic point of view.
- The Hybrid Process shows the largest profit from the sale of the multiple products resulting, with earnings of \$40.47 M/y. However, the environmental impact measured by the Eco-Indicator 99 showed that the Siemens process is the one with the lowest impact. The Hybrid process is the second best. It is expected that with this type of research can be made more competitive the technology based on $\text{Si}_{(\text{SG})}$, lowering the costs of the process and generating new research routes to be carried out for the industry of solar panels.
- We present the evaluation of three processes for obtaining Si_{SG} , according to properties of safety, profitability and environmental impact. The optimal parameters of each process were obtained by means of multiobjective optimization by the DETL method. Through the Pareto Fronts, the solutions with the best values of each objective function were found.
- The inclusion of safety principles in the design of the three processes leads to the development of one of the main approaches that must be taken into account in the birth of any process.
- The results show the Siemens Process as the best process in terms of the three objectives. However, it has to be considered that Si_{SG} production is very low (25% of that obtained from the Hybrid Process) and that current markets demand higher production, so the choice of ROI as an economic index did not turn out to be the adequate. Taking into account the above and considering that the Hybrid Process results with a safety index very similar to that of the Siemens Process, it can be the best option for its industrial implementation.
- The Intensified FBR Union Carbide Process proved to be the least safe process of the three, although with better performance in environmental terms than the Hybrid Process. It was concluded that one of the factors that most affect safety in the Intensified FBR Union Carbide Process is the inclusion of SiH_4 in the production of Si_{SG} , that increases greatly the frequency and the affectation probability of some accident in the process.

- The approach presented here is an effort to include safety as part of process design, and in particular it can be extended to other systems that also present substances that represent a hazard.
- The PRHI has been tested on three processes for Si_{SG} production, in accordance to the case study results, type of compounds, and the several operating conditions that play a key role in determining the level of inherent occupational health hazards. The compound boiling points and the equipment operating conditions (Temperature and Pressure) are two parameters that disrupt the value of the index. Moreover, the number of reactions involved in the processes also have a huge impact on the PRHI values. The index assessed in the three processes for polycrystalline silicon production proves that it is possible to attempt a quantification of inherent occupational health hazards in the initial stages of process design.
- According to the presented comparison of the different processes, the Siemens Process is hypothetically the healthiest, most profitable, safest and most environmentally friendly. That is, the process that best follows the concept of inherent occupational health hazards, but it is also the least productive. For superior Si_{SG} production, the Hybrid Process is the best suitable option.
- The surrogate based optimization of a polycrystalline silicon production process based on the hybridization of the Siemens and the Union Carbide processes developed in previous works (Ramirez-Marquez et al., 2018 & 2019) is performed. Each unit has been modeled in detail. The entire process, and therefore the operating conditions of each unit of the process were optimized under three objective functions: the maximization of the production of polycrystalline silicon, the maximization profit of the process, and the minimization of operating costs.
- The advantage of evaluating the process under the three objective functions is to determine the effect of the operating conditions under each objective function showing that the maximum production of the target compound does not always guarantee a lower selling price. The optimal operating conditions of the facility that guarantee a lower energetic consumption, meeting with the required production of polycrystalline silicon require the production of high valuable by-products which aid in the economic sustainability of the process.
- The results of each objective function present advantages and disadvantages. For a large production of polycrystalline silicon, operating costs increase. If operating costs are minimized, the production of polycrystalline silicon is low. By maximizing the profit of the process, a trade-off between the last two objective functions is achieved.
- For this scenario, the results after operating expenses, and considering the sale of polycrystalline silicon and the byproducts of the process, are an operational cost of 6.48 M\$/y. The investment for the process is 9.97M\$. Obtaining a competitive production cost for polycrystalline silicon of 8.93 \$/kg, below the commercial price estimated at 10 \$/kg. Also, a decrease in the price of polycrystalline silicon is observed if the production size of the polycrystalline silicon plant is increased, the price was reduced by 1.03 \$/kgSi_{Poly}, increasing production 10 times.
- Additionally, the advantages of optimizing the development of customize optimization methods, in contrast with the use of generic equipment models in the previous works developed in the Aspen Plus software has been shown.
- A superstructure optimization approach is used for the selection of the portfolio of products within a Multi-Product Polycrystalline Silicon Facility. Surrogate models for major units allow selecting the yield and operating conditions. The proposed process is able to meet the same production of polysilicon than current traditional polysilicon facilities do, at a lower

production cost since the benefits obtained from selling the high added value by-products obtained increase the profit of the facility.

- The complete process, and therefore the operating conditions of each unit of the process were optimized under the objective of the maximization profit of the process. The optimal operating conditions of the facility that guarantee a lower energetic consumption, meeting with the required production of polycrystalline silicon require the production of high valuable by-products as TEOS 99.5, and SiH_4 , which aid in the economic sustainability of the process.
- The results after operating expenses, and considering the sale of polycrystalline silicon and the byproducts of the process, have an operational cost of 16.09 M\$/y. The investment for the process is 85.93M\$. Obtaining a competitive production cost for polycrystalline silicon of 6.86 \$/kg, below the commercial price estimated at 10 \$/kg, with the optimal production of 1875 kg/h of Polycrystalline Silicon and the byproducts optimal production of 26.91 kg/h of TEOS 99.5; and 4.595 kg/h of SiH_4 .

8 Curriculum Vitae

8 Curriculum Vitae

César Ramírez Márquez

Academic trajectory:

2016-2019 Doctor's degree /PhD

University of Guanajuato,
Division of Natural Sciences,
Department of Chemical Engineering,
PhD in Chemical Engineering,
Guanajuato, Gto.

- Name of the thesis: "Refinery for the Production of Solar Grade Silicon and Different Products of High Value Added" PhD in Chemical Engineering, University of Guanajuato. (Thesis to be defended on February, 2020) Directed by Dr. Juan Gabriel Segovia Hernández, in collaboration with Prof. Mariano Martín of the University of Salamanca (Spain).

2014-2015 Master

University of Guanajuato,
Division of Natural Sciences,
Department of Chemical Engineering,
Master Chemical Engineering (Process Integration),
Guanajuato, Gto.

- Name of the thesis: "Design and Control of a Multi-Tasking Reactive Distillation Column for Production of Silane, Dichlorosilane and Monochlorosilane" Degree in Master Chemical Engineering, University of Guanajuato. (Thesis defended on January 25, 2016) Directed by Dr. Juan Gabriel Segovia Hernández; receiving *cum laude* distinction.

2008- 2013 Undergraduate/University

University of Guanajuato,
Division of Natural Sciences.
Department of Chemical Engineering.
Degree in Chemical Engineering.
Guanajuato, Gto.

- Name of the thesis: "Dynamic Behavior of Alternative Separation Processes for Ethanol Dehydration by Extractive Distillation." Degree in Chemical Engineering, University of Guanajuato. (Thesis defended on September 11, 2013) Directed by Dr. Juan Gabriel Segovia Hernández, in collaboration with Prof. Massimiliano Errico of the University of Cagliari (Italy); receiving *cum laude* distinction.

Honors and Awards:

- Best average out of 26 students in my generation.
- *Cum laude* recognition.
- Recognition "**University Merit for High Academic Achievement**" in the 2009-2010 school year.
- Recognition "**University Merit for High Academic Achievement**" in the 2014-2015 school year.
- Laureate Master Degree work.
- Recognition "**University Merit for High Academic Achievement**" in the 2017-2018 school year.
- Recognition "**University Merit for High Academic Achievement**" in the 2018-2019 school year.

Academic events:

- University of Guanajuato 2012 Summer Scientific Research with the subject "Strategies for SMEs competitiveness".
- Creativity and Innovation Contest for its projects of social, technological, environmental, cultural and artistic impact. The project received 2nd. place in the category: POSTGRADUATE LEVELED INVENTION. Project: Smart Investment. Student Responsible: César Ramírez Márquez, Doctorate in Sciences in Chemical Engineering. Advisors: Juan Gabriel Segovia Hernández, Nelly Ramírez Corona, Jorge A. Cervantes Jáuregui. Assignment: Division of Natural and Exact Sciences Campus Guanajuato.

Professional experience:

- Academic stay in the Company JRI located in Santiago de Chile from August 2012 through January 2013.
- Collaboration as Staff Member in AMIDIQ XXXV National Meeting, Puerto Vallarta, Jalisco.
- Collaboration as Staff Member in AMIDIQ XXXVI National Meeting, Cancun, Quintana Roo.
- Collaboration as Staff Member in AMIDIQ XXXIX National Meeting, San Jose de los Cabos, Baja California Sur.
- Sessions on Statistics in Social Sciences from August through December 2015.
- Sessions in the Master's degree in Applied Linguistics of English Teaching, August-December 2015.
- Predoctoral stay at the University of Salamanca, Spain from January 2017 through June 2018.
- Predoctoral stay at the University of Salamanca, Spain from May 2018 through October 2018.
- Sessions on Design and Simulation of Processes and Products in Chemical Engineering, August-December 2017-2019.
- Sessions on the subject Physical Chemistry in Chemical Engineering from January through July 2019.
- Sessions on Probability and Statistics in Chemical Pharmaceutical Biology from August through December 2019.

Further training

- Course "(Bio) Reactive and Hybrid Separations". Taught by Professor Andrzej Gorak in the Department of Chemical Engineering, University of Guanajuato, Campus Guanajuato., Guanajuato, Gto., July 2013, with a curricular value of 20 hours.
- Course "Process Design- Applications in Biorefineries". Taught by Professor Álvaro Orjuela Londoño in the Department of Chemical Engineering, University of Guanajuato, Campus Guanajuato., Guanajuato, Gto., January 2013, with a curricular value of 20 hours .
- Symposium "Alternative Energies in Mexico." Taught at the Department of Chemical Engineering, University of Guanajuato, Guanajuato Campus, Guanajuato, Gto., August 2014, with a curricular value of 8 hours.
- Course "The evolution of distillation sequencing: from simple to complex configurations". Taught by Professor Massimiliano Errico in the Department of Chemical Engineering, of the University of Guanajuato, Guanajuato Campus, Guanajuato, Gto., January 2015, with a curricular value of 20 hours.
- Course "Process Design and Optimization Using Renewable Sources". Taught by Professor Mariano Martín in the Department of Chemical Engineering, University of Guanajuato, Campus Guanajuato., Guanajuato, Gto., August 2015, with a 20-hour curricular value .
- Course "Achieving more sustainable solutions through process". Taught by Professor Rafiqul Gani in the Department of Chemical Engineering, University of Guanajuato, Guanajuato Campus, Guanajuato, Gto., January 2016, with a curricular value of 4 hours.
- Course "Process intensification through dynamic operation". Taught by Professor Oscar Andrés Prado Rubio in the Department of Chemical Engineering, University of Guanajuato, Campus Guanajuato., Guanajuato, Gto., August 2017, with a curricular value of 40 hours.
- Course "Taller de habilidades orales y escritas en inglés técnico (cómo redactar un artículo y hacer una presentación oral en inglés técnico)"- ["Workshop of oral and written skills in technical English (how to write an article and make an oral presentation in technical English)"]. Taught by Professors Irasema Mora-Pablo and Troy Crawford. in the Department of Chemical Engineering, University of Guanajuato, Campus Guanajuato., Guanajuato, Gto., August 2019, with a curricular value of 20 hours.
-

Publications in International Journals

- **Ramírez – Márquez, C.**, Segovia - Hernández, J.G., Hernández, S., Errico, M., Rong, B.G., 2013, Dynamic Behavior of Alternative Separation Processes for Ethanol Dehydration by Extractive Distillation Industrial & Engineering Chemistry Research, 52, 17554 – 17561. (ISSN: 15205045)
- Segovia - Hernández, J.G., Vázquez – Ojeda, M., Gómez – Castro, F.I., **Ramírez – Márquez, C.**, Errico, M., Tronci, S., Rong, B.G., 2014, Process Control Analysis for Intensified Bioethanol Separation Systems, Chemical Engineering and Processing: Process Intensification, 72, 119 – 125. (ISSN: 0255-2701)
- Errico, M., **Ramírez – Márquez, C.**, Torres – Ortega, C.E., Rong, B.G., Segovia - Hernández, J.G., 2014, Design and Control of an Alternative Distillation Sequence for Bioethanol Purification, Journal of Chemical Technology & Biotechnology, Volume 90, Issue 12, pages 2180–2185. (ISSN: 1097-4660)
- Acosta-Solórzano, A. D., Guerrero-Farfán, O., **Ramírez-Márquez, C.**, Gómez-Castro, F. I., Segovia-Hernández, J. G., Hernández, S., & Briones-Ramírez, A., 2016, Controllability Analysis of Distillation Sequences for the Separation of Bio-Jet Fuel and Green Diesel Fractions. Chemical Engineering & Technology, 39(12), 2273-2283. (ISSN: 1521-4125)
- Sánchez-Ramírez, E., Alcocer-García, H., Quiroz-Ramírez, J. J., **Ramírez-Márquez, C.**, Segovia-Hernández, J. G., Hernández, S., & Castro-Montoya, A. J., 2016, Control properties of hybrid distillation processes for the separation of biobutanol. Journal of Chemical Technology and Biotechnology, 92(5), 959-970. (ISSN: 1097-4660)
- Lucero-Robles, E., Gómez-Castro, F. I., **Ramírez-Márquez, C.**, & Segovia-Hernández, J. G., 2016, Petlyuk Columns in Multicomponent Distillation Trains: Effect of Their Location on the Separation of Hydrocarbon Mixtures. Chemical Engineering & Technology, 39(12), 2207-2216. (ISSN: 1521-4125)
- **Ramírez-Márquez, C.**, Cabrera-Ruiz, J., Segovia-Hernández, J. G., Hernández, S., Errico, M., & Rong, B. G., 2016, Dynamic behavior of the intensified alternative configurations for quaternary distillation. Chemical Engineering and Processing: Process Intensification, 108, 151-163. (ISSN: 0255-2701)
- **Ramírez-Márquez, C.**, Sánchez-Ramírez, E., Quiroz-Ramírez, J. J., Gómez-Castro, F. I., Ramírez-Corona, N., Cervantes-Jauregui, J. A., & Segovia-Hernández, J. G., 2016, Dynamic behavior of a multi-tasking reactive distillation column for production of silane, dichlorosilane and monochlorosilane. Chemical Engineering and Processing: Process Intensification, 108, 125-138. (ISSN: 0255-2701)
- Alcántara-Avila, J. R., Tanaka, M., **Ramírez Márquez, C.**, Gómez-Castro, F. I., Segovia-Hernández, J. G., Sotowa, K. I., & Horikawa, T., 2016. Design of a Multitask Reactive Distillation with Intermediate Heat Exchangers for the Production of Silane and Chlorosilane Derivates. Industrial & Engineering Chemistry Research, 55(41), 10968-10977. (ISSN: 15205045)
- Contreras-Zarazúa, G., Vázquez-Castillo, J. A., **Ramírez-Márquez, C.**, Segovia-Hernández, J. G., & Alcántara-Ávila, J. R., 2016, Multi-objective optimization involving cost and control properties in reactive distillation processes to produce diphenyl carbonate. Computers & Chemical Engineering, 105, 185-196. (ISSN: 0098-1354)
- Martínez-Gomez, J., **Ramírez-Márquez, C.**, Alcántara Avila, J. R., Segovia-Hernández, J. G., & Ponce-Ortega, J. M., 2016, Intensification for the Silane Production Involving Economic and Safety Objectives. Industrial & Engineering Chemistry Research, 56(1), 261-269. (ISSN: 15205045)
- Contreras-Zarazúa, G., Vázquez-Castillo, J. A., **Ramírez-Márquez, C.**, Pontis, G. A., Segovia-Hernández, J. G., & Alcántara-Ávila, J. R., 2017, Comparison of intensified reactive distillation configurations for the synthesis of diphenyl carbonate. Energy, 135, 637-649. (ISSN: 0360-5442)
- **Ramírez-Márquez, C.**, Otero, M. V., Vázquez-Castillo, J. A., Martín, M., & Segovia-Hernández, J. G., 2018, Process design and intensification for the production of solar grade silicon, Journal of Cleaner Production, 170, 1579-1593. (ISSN: 0959-6526)
- Sánchez-Ramírez, E., **Ramírez-Márquez, C.**, Quiroz-Ramírez, J. J., Contreras-Zarazúa, G., Segovia-Hernández, J. G., & Cervantes-Jauregui, J. A., 2018, Reactive Distillation Column Design for Tetraethoxysilane (TEOS) Production: Economic and Environmental Aspects. Industrial & Engineering Chemistry Research, 57(14), 5024-5034. (ISSN: 15205045)
- Torres-Ortega, C. E., **Ramírez-Márquez, C.**, Sánchez-Ramírez, E., Quiroz-Ramírez, J. J., Segovia-Hernandez, J. G., & Rong, B. G., 2018, Effects of intensification on process features and control properties of lignocellulosic bioethanol separation and dehydration systems. Chemical Engineering and Processing-Process Intensification. 128, 188-198. (ISSN: 0255-2701)
- Cabrera-Ruiz, J., **Ramírez-Márquez, C.**, Hasebe, S., Hernández, S., & Alcántara Avila, J. R., 2018, Outlook of the dynamic behavior of closed-loop control through open-loop analysis for intensified separation processes. Industrial & Engineering Chemistry Research, 57(49), 16795-16808. (ISSN: 15205045)
- Palma-Barrera, J. P., Sánchez-Ramírez, E., **Ramírez-Márquez, C.**, Cervantes-Jauregui, J. A., & Segovia-Hernández, J. G., 2018, Reactive Distillation Column Design for Tetraethoxysilane (TEOS) Production. Part II: Dynamic Properties and Inherent Safety. Industrial & Engineering Chemistry Research, 58(1), 259-275. (ISSN: 15205045)

- Sánchez-Ramírez, E., Quiroz-Ramírez, J. J., Hernández, S., Hernández, J. G. S., Contreras-Zarazúa, G., & **Ramírez-Márquez, C.**, (2019). Synthesis, design and optimization of alternatives to purify 2, 3-Butanediol considering economic, environmental and safety issues. *Sustainable Production and Consumption*, 17, 282-295.
- **Ramírez-Márquez, C.**, Contreras-Zarazua, G., Martín, M., & Segovia-Hernández, J. G. (2019), Safety, Economic and Environmental Optimization Applied to Three Processes for the production of solar grade silicon, *ACS Sustainable Chemistry & Engineering*, 7(5), 5355-5366. (ISSN 2168-0485)
- **Ramírez-Márquez, C.**, Contreras-Zarazúa, G., Vazquez-Castillo, J. A., López-Caamal, F., Hernández-Escoto, H., Alcantara-Avila, J. R., & Segovia-Hernández, J. G, 2019, Operability and PI Control of Reactive Distillation Configurations, *Industrial & Engineering Chemistry Research*. (ISSN: 15205045)

Publications in International Journals Under Review

- **Ramírez-Márquez C.**, Martín-Hernández E., Martín M., Segovia-Hernández J. G. Surrogate based optimization of a process of polycrystalline silicon production. *Computers & Chemical Engineering*.
- **Ramírez-Márquez C.**, Villicaña-García E., Cansino-Loeza B., Segovia-Hernández J. G., María Ponce-Ortega J. M. Inherent Occupational Health Hazards In The Production Of Solar Grade Silicon. *Process Safety and Environmental Protection*
- Sánchez-Ramírez E., **Ramírez-Márqueza C.**, Quiroz-Ramírez J.J., Angelina-Martínez A. Y., Vicente-Cortazar V., Segovia-Hernández J. G. Improving Sustainability in Dividing Wall Columns for Quaternary Mixtures. *Chemical Engineering & Processing: Process Intensification*
- Villicaña-García E., **Ramírez-Márquez C.**, Segovia-Hernández J.G., Ponce-Ortega J.M. Planning production of solar grade silicon to yield solar panels involving behavior of population. *AIChE Journal*
- Hernández-Pérez L. G., **Ramírez-Márquez C.**, Segovia-Hernández J. G., Ponce-Ortega J. M. Simultaneous Structural and Operating Optimization of Process Flowsheets Combining Process Simulators and Metaheuristic Techniques: The Case of Solar-Grade Silicon Process. *Computers & Chemical Engineering*

National Conferences

- *“Comportamiento dinámico de procesos de separación alternativos para la deshidratación del etanol por destilación extractiva”* (“Dynamic behavior of alternative separation processes for dehydration of ethanol by extractive distillation”), in poster format (ID 16), XXXV National Meeting AMIDIQ, Puerto Vallarta, Jalisco.
- *“Análisis de control de nuevos sistemas intensificados de destilación para la configuración de una columna de pared divisoria cuaternaria”* (“Control analysis of new intensified distillation systems for the configuration of a quaternary dividing wall column”), in poster format (ID 47), XXXVI National Meeting AMIDIQ, Cancun, Quintana Roo.
- *“Comportamiento dinámico de una columna de destilación reactiva multitarea para la producción de silano, diclorosilano y monoclorosilano”* (“Dynamic behavior of a multitasking reactive distillation column for the production of silane, dichlorosilane and monochlorosilane”), in poster format (ID 34), XXXVII National Meeting AMIDIQ, Puerto Vallarta, Jalisco.
- *“Optimización de un proceso integrado reaccion-separacion para producción de biobutanol”* (“Optimization of an integrated reaction-separation process for biobutanol production”), in oral format (ID 95), XXXVII National Meeting AMIDIQ, Puerto Vallarta, Jalisco.
- *“Propiedades de control de procesos de destilación híbridos para la purificación de biobutanol”* (“Hybrid distillation process control properties for biobutanol purification”), in poster format, National Congress of Renewable Energy Students CNEER-2016, Temixco, Morelos.
- *“Sintonización de Controladores Tipo PI por el Método Híbrido de Evolución Diferencial con Lista Tabu”* (“Tuning of Type PI Controllers by the Hybrid Method of Differential Evolution with Tabu List”), in oral format, XXXVIII National Meeting AMIDIQ, Ixtapa-Zihuatanejo, Guerrero, Mexico.
- *“Diseño sustentable para la producción de silicio de grado solar”* (“Sustainable design for the production of solar grade silicon”), in oral format (ID 477), XXXIX National Meeting AMIDIQ, San José de los Cabos, Baja California Sur.

- “Análisis Dinámico de Columnas de Doble Pared Dividida Novedosas para Separaciones Cuaternarias” (“Dynamic Analysis of Novel Divided Double Wall Columns for Quaternary Separations”), in oral format (ID 84), XXXIX National Meeting AMIDIQ, San José de los Cabos, Baja California Sur.
- “Optimización Simultánea de los Parámetros de Diseño y Control para la Zona de Reacción en la Bioproducción de Furfural” (“Simultaneous Optimization of the Design and Control Parameters for the Reaction Zone in Furfural Bioproduction”), in oral format (ID 77), XL National Meeting AMIDIQ, Huatulco, Oaxaca, Mexico.
- “Optimización de Rentabilidad, Seguridad y Ambiental Aplicada a Tres Procesos para la Producción de Silicio de Grado Solar” (“Optimization of Profitability, Safety and Environmental Applied to Three Processes for the Production of Solar Grade Silicon”), in oral format (ID 33), XL National Meeting AMIDIQ, Huatulco, Oaxaca, Mexico.

International Conferences

- “Diseño de una columna de destilación reactiva multitarea para la purificación de silanos” (“Design of a multitasking reactive distillation column for silane purification”), International energy conference 2015 (IEC 2015), Mexico, DF.
- “Dynamic Behavior of a Multi-Tasking Reactive Distillation Column for Production of Silane, Dichlorosilane and Monochlorosilane”, International. **Ramírez – Márquez , C.**, Segovia - Hernández J.G., Ramírez - Corona, N., Cervantes - Jáuregui J.A., Jiménez – Gutiérrez, A., 2016, , In the Proceedings of European Symposium on Computer Aided Process Engineering - 26 (ESCAPE), Edited by Zdravko Kravanja and Miloš Bogataj, Elsevier (ISBN: 978-0-444-63873-1), UK, 307 - 312.
- “Novel Reactive Distillation Processes to produce Diphenyl Carbonate: Multi-Objective Optimization involving Cost and Controllability Criteria”, International. G. Contreras-Zarazúa, J.A. Vázquez-Castillo, **C. Ramírez-Márquez** , J. G. Segovia-Hernández, R. Alcantara- Avila, 2017, , Proceedings of the 27th European Symposium on Computer Aided Process Engineering – ESCAPE 27. October 1st - 5th, 2017, Barcelona, Spain © 2017 Elsevier B.V.
- “Tuning of PI controllers by Differential Evolution with Tabu List method”, International. **César Ramírez-Márquez**, Erick Yair Miranda-Galindo, Juan Gabriel Segovia-Hernández and Salvador Hernández, 2017, Proceedings of the 27th European Symposium on Computer Aided Process Engineering – ESCAPE 27. October 1st - 5th, 2017, Barcelona, Spain © 2017 Elsevier B.V.
- “Alternative processes for obtaining solar grade silicon”, International. **César Ramírez-Márquez**, E Otero, M. V., Vázquez-Castillo, J. A., Martín, M., & Segovia-Hernández, J. G., 2018, Proceedings of the 28th European Symposium on Computer Aided Process Engineering – ESCAPE 28. June 10-13, 2018, Graz, Austria © 2018 Elsevier B.V.
- “Processes Separation to Furfural, Design and Optimization Involving Economical, Environmental and Safety Criteria”, International. G. Contreras-Zarazua, E. Sánchez-Ramírez, J.A. Vázquez-Castillo, **C. Ramírez-Márquez**, J.G. Segovia-Hernández, 2018, Proceedings of the 28th European Symposium on Computer Aided Process Engineering – ESCAPE 28. June 10-13, 2018, Graz, Austria © 2018 Elsevier B.V.
- “Simultaneous design and controllability optimization for the reaction zone for furfural bioproduction”, International. A.G. Romero-García, O.A. Prado-Rúbio, G. Contreras-Zarazúa, **C. Ramírez-Márquez**, J.G. Segovia-Hernández, 2019, Proceedings of the 29th European Symposium on Computer Aided Process Engineering – ESCAPE 29. June 16-19, Eindhoven, Holanda © 2019 Elsevier B.V.
- “Optimal Design of a Multi-Product Polycrystalline Silicon Facility”, International. **C. Ramírez-Márquez**, E. Martín-Hernández, M. Martín, J.G. Segovia-Hernández, 2019, 2019 AIChE Annual Meeting, November 10-15, 2019 Hyatt Regency, Orlando.

Book Chapters

- Pandu, R. G., & Shivom, S. (Eds.). (2017). Differential Evolution In Chemical Engineering: Developments And Applications (Vol. 6). World Scientific, Chapter 9: “Optimization of Intensified Separation Processes using Differential Evolution with Tabu List.” Eduardo Sánchez-Ramírez, Juan José Quiroz-Ramírez, **César Ramírez-Márquez**, Gabriel Contreras-Zarazúa, Juan Gabriel Segovia-Hernández, and Adrián Bonilla-Petriciolet. Pp 260-288.
- Segovia-Hernández, J. G., & Gómez-Castro, F. I. (2017). Stochastic Process Optimization using Aspen Plus®. CRC Press, Chapter 7: “Using External User-Defined Block Model in Aspen Plus®”. Eduardo Sánchez-Ramírez, Juan José Quiroz-Ramírez, and **César Ramírez-Márquez**. Pp 125-139.

- Segovia-Hernández, J. G., & Gómez-Castro, F. I. (2017). Stochastic Process Optimization using Aspen Plus®. CRC Press, Chapter 10: “*Optimization of a Silane Production Process**”. **César Ramírez-Márquez**, Eduardo Sánchez-Ramírez and Juan José Quiroz-Ramírez. Pp 193-218.
- Segovia-Hernández, J. G., & Gómez-Castro, F. I. (2017). Introduction to Software for Chemical Engineers, Chapter 12: “*Modular Process Simulators*”. Rubén Ruiz-Femenia, **César Ramírez Márquez**, Luis G. Hernández-Pérez, José A. Caballero, Mariano Martín, José María Ponce-Ortega, Juan Gabriel Segovia.

Patent Request

- Mexican Institute of Industrial Property, divisional patent management, regional office of Bajío. Application file MX / a / 2017/003086, as of March 9, 2017. Folio MX / E / 2017/017977. Representative: University of Guanajuato. Inventors: **César Ramírez Márquez**, Juan Gabriel Segovia Hernández.
- Mexican Institute of Industrial Property, divisional patent management, regional office of Bajío. Application file MX / a / 2018/011311, as of September 18, 2018. Folio MX / E / 2018/070159. Representative: University of Guanajuato. Inventors: **César Ramírez Márquez**, Juan Gabriel Segovia Hernández, Eduardo Sánchez Ramírez, Juan José Quiroz Ramírez.
- Mexican Institute of Industrial Property, divisional patent management, regional office of Bajío. Application file MX / a / 2019/003382, as of March 25, 2019. Folio MX / E / 2019/018569. Representative: University of Guanajuato. Inventors: **César Ramírez Márquez**, Juan Gabriel Segovia Hernández, Eduardo Sánchez Ramírez, Jorge A. Cervantes Jáuregui.

Human Resource Training

Co-director

- Palma Barrera Juan Pablo, Name of the Thesis: “*Diseño de un Proceso Sustentable para la Producción de Tetraetoxisilano Usando Destilación Reactiva*” (“*Design of a Sustainable Process for the Production of Tetraethoxysilane Using Reactive Distillation*”). Degree in Chemical Engineering, University of Guanajuato. (Work defended on November 29, 2018).
- Romero García Ana Gabriela, Name of the Thesis: “*Optimización de la Zona de Reacción en el Proceso de Producción de Furfural a Partir de Biomasa*” (“*Optimization of the Reaction Zone in the Furfural Production Process from Biomass*”). Master in Chemical Engineering (Process Integration). University of Guanajuato. (Work defended on January 15, 2019).